Glucose induced toxicity to cells: Protective effects of *Momordica charantia*

ALI OMAR ALJOHI

A Thesis submitted in partial fulfilment of the requirements of the Manchester Metropolitan University for the degree of Doctor of Philosophy

School of Healthcare Sciences

Manchester Metropolitan University

2014

Table of contents

List of figures

List of tables

Abstract

Increased advanced glycation endproducts (AGEs) formation and oxidative stress are believed to underlie the pathogenesis of diabetic vascular complications including the impairment of the wound healing. In most developing countries, diabetic treatment is expensive and plants provide a cheap potential natural source of anti-diabetic remedies. Several studies have examined the beneficial effects of using *Momordica charantia* (MC) because of its hypoglycaemic properties in diabetic subjects. Here, for the first time, the anti-glycation and antioxidant properties of aqueous extracts of *Momordica charantia* pulp (MCP), flesh (MCF) and charantin were assessed *in vitro*. Since wound-healing is one of the most costly complications and affecting 15% of diabetic patients, the potential angiogenic activities of MCP, MCF and charantin in the presence or absence of AGEs were investigated.

Lysozyme was glycated using either glucose or methylglyoxal in the presence or absence of 5 to 15 mg/ml of *Momordica charantia* extracts in 0.1 M sodium phosphate buffer (pH 7.4) at 37°C for three days. The formation of glucose or methylglyoxal-derived AGE crosslinks was assessed using sodium dodecyl sulphate-polyacrylamide gel electrophoresis followed by Coomassie blue staining. A non-competitive ELISA method was used to investigate the effect of *Momordica charantia* extracts on carboxymethyllysine (CML) concentrations. Antioxidant activities of all extracts of *Momordica charantia* were evaluated using the stable free radical 1,1-diphenyl-2-picrylhydrazyl (DPPH) and hydroxyl radical-scavenging activity, metal chelating activity and reducing power. The phenolic, flavonols and flavonoid contents of all extracts were also measured. *In vitro* angiogenic assays including cell proliferation, migration and endothelial tube formation in Matrigel™ were used to assess the potential angiogenic effects of the natural extracts. By Western blotting, the angiogenic signalling pathways induced by AGEs and potentially modulated by MCP, MCF and charantin were also investigated. Furthermore, the neutralization of the receptor for AGEs (RAGE) was

performed using a monoclonal anti-RAGE antibody to highlight the role of RAGE in the modulation of AGE-induced signalling pathways followed addition of MCP, MCF and charantin.

All extracts inhibited the formation of MG-derived AGEs in a dose-dependent manner and the MCF extract showed the most potent inhibitory effect on both AGE and CML formation. Antioxidant capacity of MCF was significantly higher than MCP based upon the DPPH and hydroxyl radical-scavenging activity ($p < 0.005$); however, MCP shows higher metal-chelating activity in comparison to other extracts. The content of phenolic compounds was expressed in gallic acid equivalents (GAE), whereas flavonols and flavonoid contents were expressed in rutin equivalents (RE). In addition, all *Momordica charantia* extracts increased bovine aortic endothelial cell (BAEC) proliferation, migration and tube formation with induction of p-ERK1/2 expression through RAGE. Moreover, these natural extracts decreased the anti-angiogenic effects of high concentration of BSA-AGEs.

Momordica charantia does not only have established hypoglycaemic effects but this study shows that crude extracts are capable of preventing MG-derived cross-linked AGEs and Glyoxalic acid-derived CML at least *in vitro*. This anti-glycation activity might be due to their antioxidant properties from their phenolic content. Furthermore, because of its pro-angiogenic effects and its ability to reduce the AGEs-induced anti-angiogenic effect, *Momordica charantia* presents a promising natural product for the development of a new strategy to accelerate wound-healing especially in diabetic foot. Thus, use of *Momordica charantia* deserves more attention in particular its ability to reduce AGE formation and oxidative stress in diabetic subjects and as a pro-angiogenic therapy.

Declaration

I hereby declare that this work has been composed by myself, and has not been accepted for any degree before and is not currently being submitted in candidature for any degree other than the degree of Doctor of Philosophy of the Manchester Metropolitan University.

ALI ALJOHI

Acknowledgement

No project can be carried out by only one individual. Special thanks to almighty Allah who is the source and origin of all knowledge.

I fell highly privileged to express my heartiest gratitude to my worthy and kind supervisor Dr. Nessar Ahmed for his dynamic supervision, constructive criticism and affectionate behaviour throughout this study. His wide knowledge and logical way of thinking have been of great value for me. In addition, his intensive and creative comments have helped me step by step throughout this project.

I am also forever grateful to my supervisor, Prof. Mark Slevin for his approachability; optimism and fortitude has been invaluable. Thank you for your practical support and insight. His wisdom and generosity will not be forgotten.

My supervisor, Dr. Sabine Matou-Nasri was always there to listen and give advice. I would like to express my deep and sincere gratitude to her for understanding and personal guidance in the lab.

Thank you for your practical and writing support. Her wisdom and generosity will not be forgotten.

I am also forever grateful to my wonderful mother and my exceptional father for their encouragement with prayers and best wishes. To all my beloved brothers and sisters, thank you for putting my degree into perspective when it seemed all-consuming.

I owe my loving thanks to my wife, Manal, my children Omar, Aliyah and Galiyah. They have lost a lot due to my research study. Without their encouragement and understanding, it would have been impossible for me to finish this work.

I would like to thank my colleagues at the School of Healthcare Science who shared great research ideas during my time at Manchester Metropolitan University.

I would also like to extend my greatest thanks to my sponsor (Ministry of Higher Education in Saudi Arabia). Thank you for the financial and moral support throughout my course, without you this work could not have been possible.

List of abbreviations

ADA	American Diabetes Association
AG	Aminoguanidine
AGEs	Advanced glycation endproducts
ANF	Anti-nuclear antibodies
ANOVA	Analysis of variance
AR	Aldose reductase
BAEC	Bovine aortic endothelial cells
BSA	Bovine serum albumin
CAM	Chick chorioallantoic membrane
CML	Carboxymethyllysine
DM	Diabetes mellitus
DMEM	Dulbecco's Modified Eagle's Medium
DMSO	Dimethyl sulfoxide
DNA	Deoxyribonucleic acid
DPPH	1,1-Diphenyl-2-picryl-hydrazyl
ECM	Extracellular matrix
EDTA	Ethylenediaminetetraacetic acid
ELISA	Enzyme-linked immunosorbent assay
eNOS	Endothelial nitric oxide synthase
ERK	Extracellular signal-regulated kinases
FBS	Foetal bovine serum
FGF-2	Fibroblast growth factor-2
FN3K	Fructosamine-3-kinase

GAE	gallic acid equivalents
GC/MS	Gas chromatography–mass spectrometry
GLUT1	Glucose transporter 1
GSH	Gluthathione
HbA_{1c}	Haemoglobin A_{1c}
HPLC	High-performance liquid chromatography
IDDM	Insulin-dependent diabetes mellitus
IDF	International Diabetes Federation
IFCC	International Federation of Clinical Chemistry and Laboratory Medicine
JNK	Jun N-terminal kinases
LDL	Low density lipoprotein
MALDI-TOF-MS	Matrix-assisted laser desorption ionisation time-of-flight mass spectrometry
MAPK	Mitogen-activated protein kinases
MC	*Momordica charantia*
MCF	*Momordica charantia* flesh
MCP	*Momordica charantia* pulp
mRNA	Messenger ribonucleic acid
NADPH	Reduced nicotinamide adenine dinucleotide phosphate
NF-kB	Nuclear factor kappa light chain enhancer of activated B cell
NIDDM	Non-insulin-dependent diabetes mellitus
NO	Nitric oxide
PBS	Phosphate buffer saline
PPAR-α	Peroxisome proliferator-activated receptor alpha

PSG	Pencillin, streptomycin and L-glutamine
RAGE	Receptor for advanced glycation endproducts
RE	Rutin equivalents
RIPA	Radioimmunoprecipitation assay
RNA	Ribonucleic acid
ROS	Reactive oxygen species
SD	Standard deviation
SDS	Sodium dodecyl sulphate
SDS-PAGE	Sodium dodecyl sulphate-polyacrylamide gel electrophoresis
SPM	Serum-poor medium
sRAGE	Soluble receptor for advanced glycation endproducts
TEMED	N, N, N′, N′-tetramethylethylenediamine
VCAM-1	Vascular cell adhesion protein 1

Publications

Ali Aljohi, Sabine Matou-Nasri and Nessar Ahmed. Antiglycation and antioxidant properties of *Momordica charantia*. (Submitted).

Ali Aljohi, Sabine Matou-Nasri, Manal Abudawood, Mark Slevin and Nessar Ahmed.

Momordica charantia extracts promote angiogenesis effects in endothelial cells *in vitro.* (In preparation).

Ali Aljohi, Sabine Matou-Nasri, Manal Abudawood, Mark Slevin and Nessar Ahmed.

Momordica charantia extracts *and* charantin reduce advanced glycation end-products mediated anti-angiogenic effects *in vitro.* (In preparation).

Emhamed Boras, Mark Slevin, Yvonne Alexander, **Ali Aljohi**, William Gilmore, Jason Ashworth, Jerzy Krupinski, Lawrence A Potempa, Ibrahim Alabdulkareem, Adila Elobeid and Sabine Matou-Nasri (2014). Monomeric C-reactive protein and Notch-3 co-operatively increase angiogenesis through PI3K signalling pathway. *Cytokine.* (Accepted on May, 2014)

Ali Aljohi, Mark Slevin, Sabine Matou-Nasri and Nessar Ahmed (2012). Antiglycation and antioxidant properties of *Momordica charantia*. 2nd Prize Poster Presentation Award. Poster presented at Annual Research Student Conference, 20 April, Manchester Metropolitan University, UK.

Ali Aljohi, Mark Slevin, Sabine Matou-Nasri and Nessar Ahmed (2012). Antiglycation and antioxidant properties of *Momordica charantia*. Presented at the 11th International Symposium on the Maillard reaction, 16-20 September, Nancy, France.

Chapter 1. Introduction

1.1 Diabetes Mellitus

Diabetes mellitus (DM) is a metabolic multiple aetiology disease associated with high blood sugar concentration. When untreated, it may lead to a number of medical complications including chronic hyperglycaemia and disturbances in the metabolism of proteins, fats and carbohydrates (Al-Hassan, 2003; Patel *et al*, 2012). The elevated blood sugar of a patient suffering from diabetes mellitus occurs due to the pancreas' failure to produce adequate levels of insulin. In addition, it also can occur because the patient's cells prove unresponsive to any insulin produced. It is consequently possible to observe abnormal insulin synthesis and incorrect manifestation of its properties during onset of the disease (ADA, 2009).

DM has become increasingly prevalent in recent years. The massive incidence of DM in the world is believed to have been a result of several factors, such as increased consumption of calorie-rich diets, increases in the ageing population, lifestyles and obesity (ADA, 2014; Romao and Roth, 2008). As a very common chronic disease, DM was considered the fifth leading cause of death (Malik, 2014). DM caused 1.5 million (2.7%) deaths in 2012, up from 1.0 million (2.0%) deaths in 2000. International Diabetes Federation (IDF) has predicted that the worldwide number of patients with diabetes will increase by the year 2035 to 592 million, with figures for 2013 standing at approximately 382 million (IDF, 2013).

DM is divided into three types. Type 1 diabetes, also known as insulin-dependent diabetes mellitus (IDDM) (ADA, 2010), is observed when the body fails to generate insulin. In particular, insulin deficiency is detected when the pancreas loses insulin-generating beta cells located in the islets of Langerhans. In this case, the patient is required to wear a specialised insulin pump or inject insulin on a daily basis. In contrast, type 2 diabetes is diagnosed

because of insulin resistance. It is most commonly observed in adults and is therefore often known as 'adult-onset diabetes'. This condition is characterised by the cells' inability to interact efficiently with insulin. In certain cases, type 2 diabetes is observed in conjunction with absolute insulin deficiency. This type of diabetes is known as non-insulin-dependent diabetes mellitus (NIDDM). However, a decision was made to abolish the NIDDM and IDDM acronyms because of their confusing natures. Thus, diabetic patients are now classified according to the observed pathogenesis of their diseases rather than according to their treatment (ADA, 2010). The third type of diabetes is known as gestational hyperglycaemia. This condition is described as a patient's intolerance towards carbohydrates during pregnancy even if the patient has a pre-existing diabetic condition (Nakata *et al*, 2013). Hyperglycaemia is a common condition during diabetes mellitus. It is associated with a range of diabetic complications.

1.2 Hyperglycaemia and diabetic complications

The biomedical field defines hyperglycaemia as a condition during which an elevated quantity of sugar is present in the blood. According to ADA diagnosis criteria, fasting plasma glucose (FPG) $\geq$ 7 mmol/l and HbA1c $\geq$ 6.5 % can be diagnosed as diabetic (ADA, 2013). However, initial hyperglycaemic symptoms are observed at concentrations ranging from 15–20 mmol/l (Cox *et al.*, 2005).

Diabetic complications can be either microvascular or macrovascular. Microvascular complications refer to a range of pathological functional changes that take place at the microvascular level. Increased blood sugar levels lead to microvascular damage and conditions such as retinopathy, neuropathy, nephropathy and cardiomyopathy (Nathan *et al.*, 2005). Microvascular complications develop within 10–15 years in diabetic patients. They are typical chronic complications associated with lowered life expectancy and considerable

morbidity (Ali *et al.*, 2010). In the context of diabetes, the notion of macrovascular complications was conceived to describe a range of pathological changes taking place in all main blood vessels resulting in structural and functional alterations. Chronic hyperglycaemia leads to chemical changes occurring in the inner walls of blood vessels. These changes result in endothelial dysfunctions, increased arterial wall stiffness and lowered compliance of the vascular system, thus promoting macrovascular complications. A common macrovascular complication is atherosclerosis. It is believed to be responsible for the elevated risk of stroke, peripheral vascular pathologies and myocardial infarction (Laakso, 2010).

1.3 Protein glycation (Maillard reaction)

Glycation is the addition of sugars, such as fructose or glucose, to lipids or proteins. This non-enzymatic reaction, which takes place between protein amino groups and reduces sugars, leads to the formation of complex, brown-coloured pigments as well as protein-protein covalent bonds. Glycation was discovered and investigated by Louis Maillard (1912). Compared to other reducing sugars, glucose is the least reactive; thus, it was speculated that glucose was chosen during evolution as the main free sugar present *in vivo*. Nevertheless, similar to other carbohydrates, it reacts with free amino acid lysine ε-amino and arginine groups, which leads to the formation of a Schiff base. As shown in Figure 1, a C=O aldehyde group is converted into an imine C=N group during the formation of this base (Ulrich and Cerami, 2001).

Maillard indicated that the reaction he discovered could potentially play a vital role in diabetes, but this idea was too radical for his time. The technology available in the early 1900s made it impossible to support or reject this presumption. However, the practical significance of the process was soon realised by food chemists, as they were able to explain

the brown colour and the loss of certain protein properties during cooking or food storage (Ulrich and Cerami, 2001).

The Maillard reaction's clinical significance was realised in the mid-1970s. Initial investigations were concerned with the reaction between sugars and haemoglobin A_{1c} (HbA_{1c}). This form of haemoglobin is minor, but its quantity in blood is elevated exclusively in diabetics. Additionally, HbA_{1c} formed via the addition of glucose molecules to amino groups located on haemoglobin β-chains. This reaction was believed to proceed via a non-enzymatically obtained Schiff structure. The fact that Schiff bases were usually thermodynamically unstable presented a major argument against this assumption. Further investigations showed that Schiff bases were only intermediate structures and led to an Amadori rearrangement. The final product, a carbohydrate fragment, is attached to the HbA_{1c} molecule as a 1-deoxy-1-fructosyl fragment (Figure 1.1) (Ulrich and Cerami, 2001).

It was suggested that the Maillard reaction was important in the pathogenesis of diabetic complications and the promotion of aging (Brownlee, 1992). Subsequently, proteins containing Amadori products in the main polypeptide chain were called glycated proteins. The term was coined to distinguish them from glycosylated proteins, which were obtained with the aid of enzymes. In turn, the process during which Amadori products form was called glycation. Cross-links and complex pigments formed during the course of the Maillard reaction from glycated proteins were referred to as advanced glycation end-products (AGE) (Ahmed, 2005; Bucala and Vlassara, 1995).

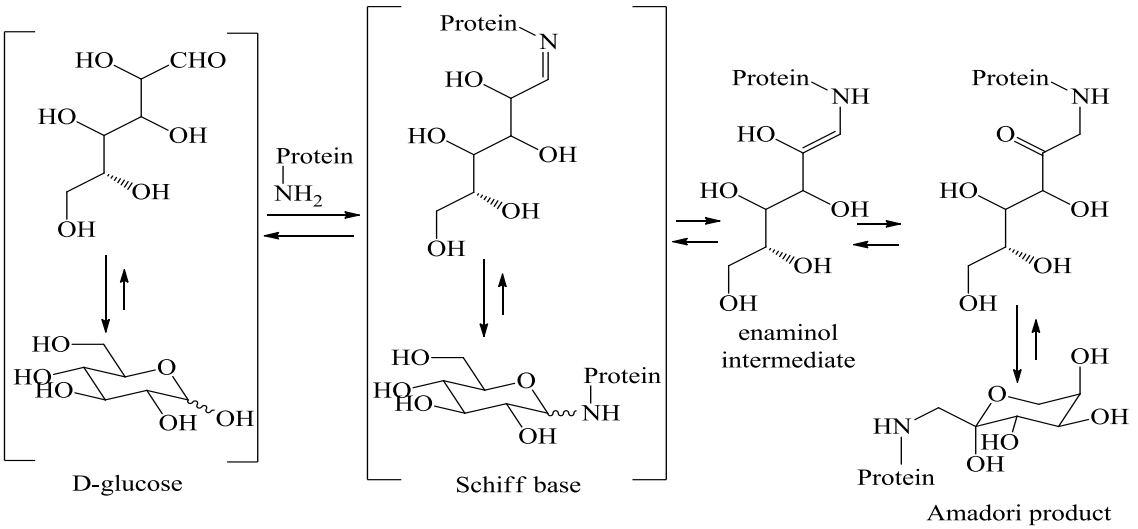

Figure 1.1: Formation of a Schiff base and subsequent Amadori rearrangement (Ulrich and Cerami, 2001)

1.4 Chemistry of protein glycation

1.4.1 Protein glycation: early stage

The kinetics of the early stage depend extensively on water activity, media temperature (Davies *et al.*, 1998; Wang *et al.*, 2013), the carbonyl carbon electrophilicity and the quantity of sugar present in blood in the acyclic form (Yaylayan *et al.*, 1994). It was also suggested that the pK_a of protein, the amino groups and their location within the molecule influences protein glycation's early stage (Spiro, 2002). Early stage protein glycation is represented in Figure 1.1.

1.4.2 Protein glycation: intermediate stage

The intermediate stage of protein glycation begins with deoxyosone degradation via dehydration of the Heyns and Amadori products. The primary deoxyosones are identified and their structures are presented in Figure 1.2.

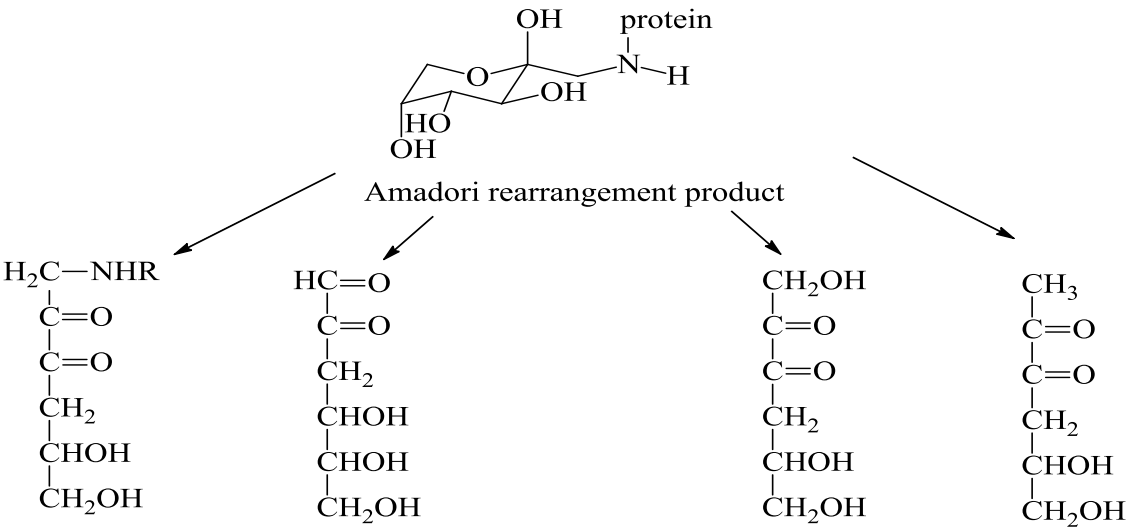

Figure 1.2: Deoxyosones obtained from Amadori products (Dills, 1993)

Formation of the deoxyosones (Figure 1.2) is considered to proceed via 2, 3 or 1, 2-enolisation of the sugar residue under acidic conditions (Yaylayan *et al.*, 1994). The deoxyosones' chemistry presumes an array of possible transformations taking place with the amino-carbonyl group (Figure 1.3). The initial enolisation leads to the formation of reductose, which undergoes cyclisation to the corresponding aminoacetyl furan (Leonil *et al.*, 1997).

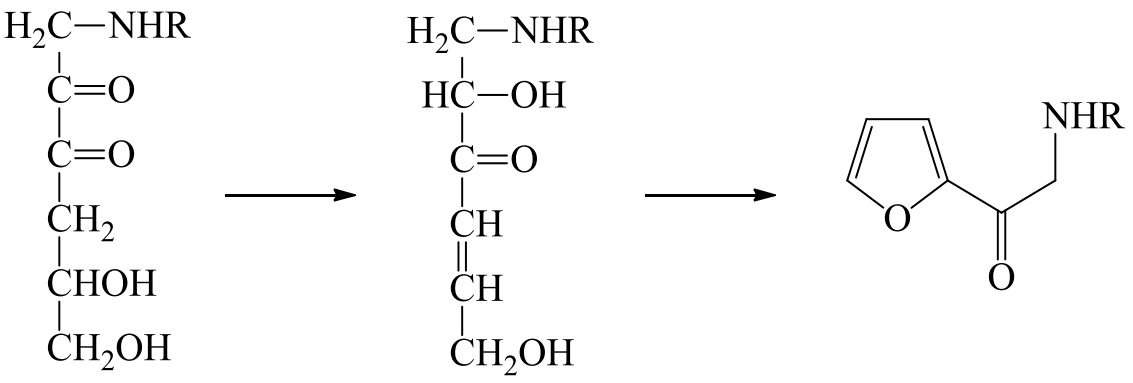

Figure 1.3: Formation of 1-amino-1,4-dideoxyosones from deoxyosones (Dills, 1993).

1.4.3 Protein glycation: advanced stage

The advanced stage of protein glycation is characterised by the formation of AGEs. AGEs present a heterogeneous group of organic molecules obtained from the protein glycation products formed during the intermediate stages of glycation. For instance, deoxyosones can undergo intra- and inter-molecular transformations leading to the formation of pyrraline and pentosidine (Figure 1.4) (Dills, 1993). AGEs can be fluorescent or non-fluorescent and cross-linked or non-cross-linked.

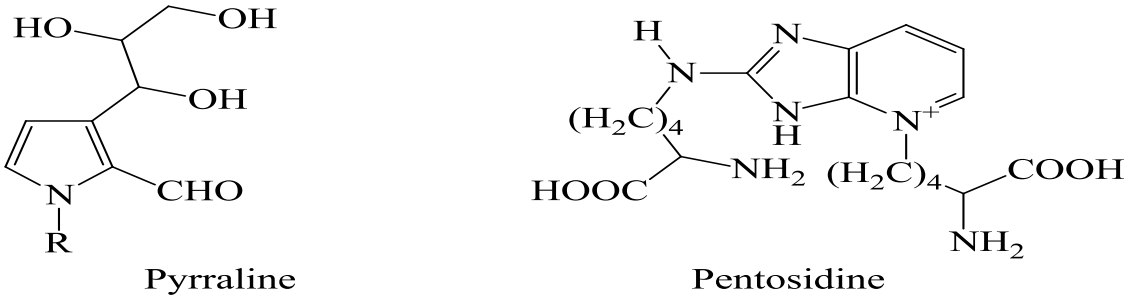

Figure 1.4: Pyrraline and pentosidine (Dills, 1993)

1.5 Glycation and oxidation reaction (other pathways for AGE formation)

1.5.1 Autoxidative glycation (Wolf pathway)

The autoxidation of monosaccharides is a non-enzymatic reaction between the α-hydroxycarbonyl group of sugar and oxygen. The main products of the process are α-oxoaldehydes and hydrogen peroxide. This reaction was discovered by Wolf and co-workers in 1984 (Wolff and Dean, 1987). It was suggested that free radicals play a key role in this process and the reaction was started by the enolisation of the initial monosaccharide. Subsequently, the formed enediol was dehydrated to a dicarbonyl compound. These reactions are a part of the Wolf autoxidation pathway (Figure 1.5).

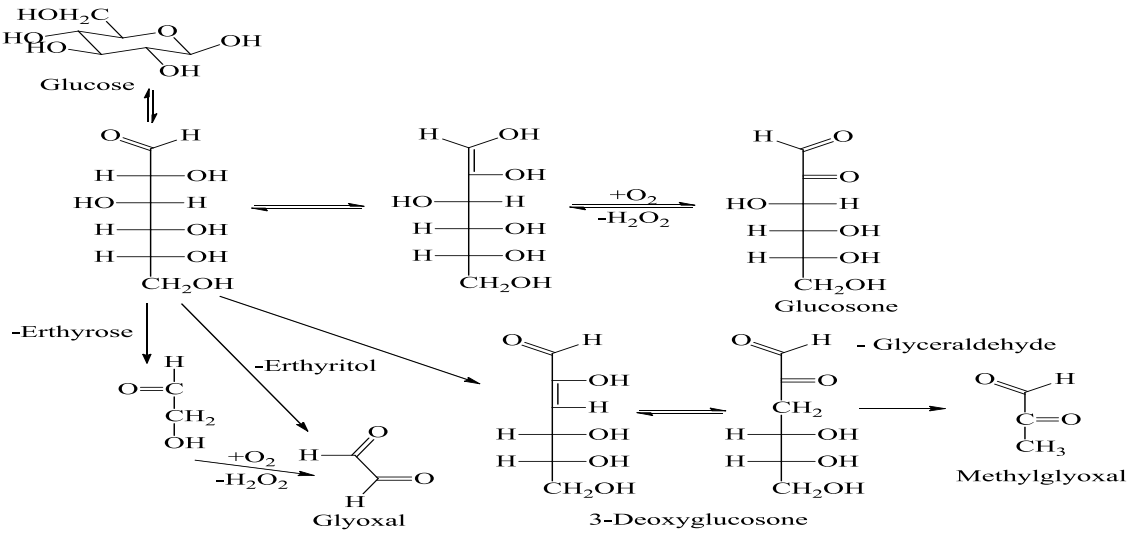

Figure 1.5: Autoxidative glycation (Wolf pathway)

Along with dicarbonylic compounds, glucosone and a range of additional AGE products are formed. Thus, the glucose molecules lose either erythrose or erythritol to give glyoxal and 3-deoxyglucosone, which react with the production of glyceraldehyde and methylglyoxal (Monnier, 2003).

1.5.2 Schiff base fragmentation (Namiki pathway)

In certain cases, the Schiff base does not enter the Amadori rearrangement but undergoes a series of elimination reactions leading to the production of AGEs. These elimination reactions lead to the release of a primary amine and a range of unstable dialdehydes, such as methylglyoxal, glucosone and glyoxal (Ferreira *et al.*, 2003). These products and the corresponding reaction pathway were initially described by Namiki and Hayashi (1983) (Figure 1.6).

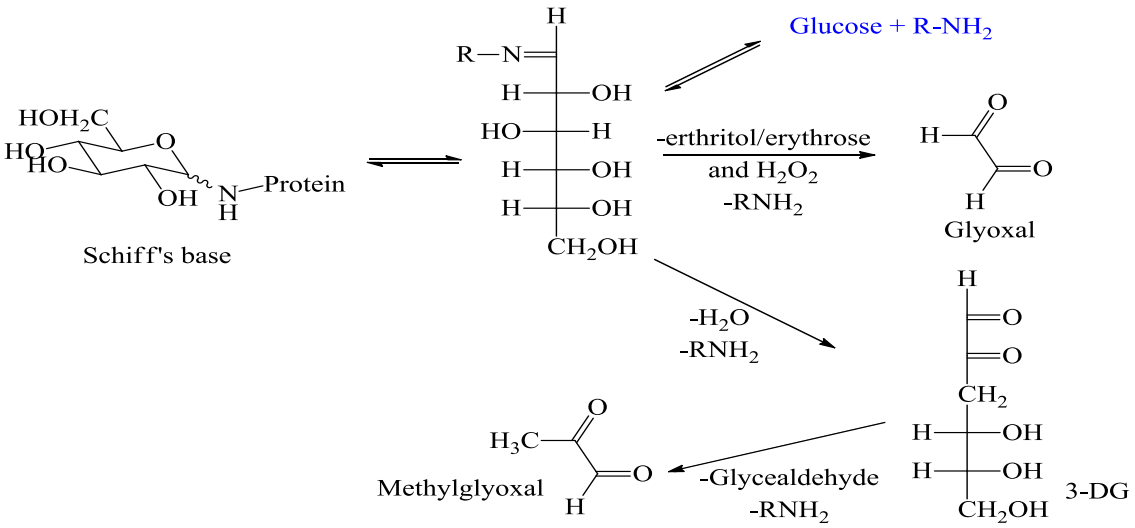

Figure 1.6: The Namiki pathway of AGE formation (Baynes, 2001)

1.5.3 Glycoxidation reactions

The term 'glycoxidation products' was originally introduced in order to characterise products formed by sequential glycation and oxidation reactions; however, it is commonly utilised to describe the autoxidation of Amadori products (Thorpe and Baynes, 2003). Glucose can participate in oxidation reactions via a free carbonyl group present in its open chain form. If the reaction media contains oxygen, glucose has the ability to auto-oxidise and generate active oxygen compounds, such as peroxy radicals. These radicals form covalent bridges between proteins, thus altering their functions. The resultant production of glycation-derived free radicals is believed to play an essential role in the pathogenesis of diabetic complications (Giacco and Brownlee, 2010).

In the human body, unbound metal ions promote glycoxidation and subsequent AGE formation. During this process, the hydroxyl radical is a key intermediate. This type of radical takes part in lipid peroxidation and formation of *meta*- and *ortho*-tyrosine (Figure 1.7). Both tyrosine intermediates are unnatural and form exclusively in the presence of

hydroxyl radicals (Huggins *et al.*, 1993). These radicals are generated in the presence of active metal ions, such as Cu^{+} or Fe^{2+} (M^{n+}), from hydrogen peroxide (Figure 1.8).

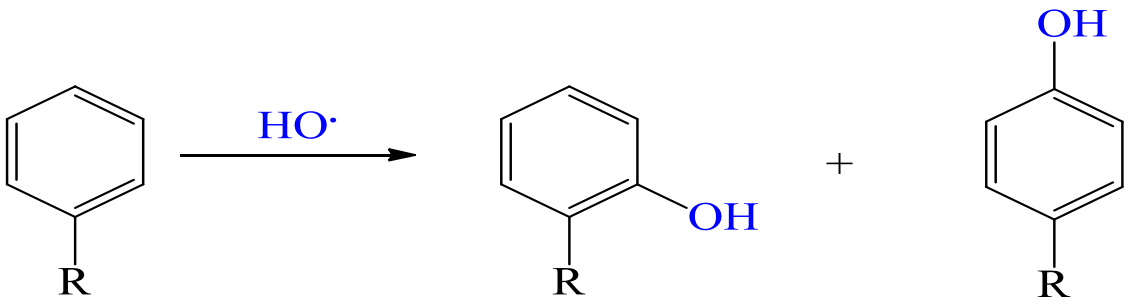

Figure 1.7: Hydroxyl radical glycoxidation (Huggins *et al*., 1993)

$$M^{n+} + H_2O_2 \longrightarrow M^{n+-1} + HO\cdot + HO^{-}$$

Figure 1.8: Formation of hydroxyl radicals (Kaur and Halliwell, 1994).

1.6 Factors affecting glycation

Protein glycation was identified as leading to diabetic complications and a range of age-related conditions (Brownlee, 2000). For this reason, factors affecting this reaction should be given a considerable amount of attention. The kinetics of the initial nucleophilic attack between the amino groups of proteins and the carbonyl group of reducing sugars ultimately depends on pH, oxygen, metal ions and the electrophilicity of the sugar carbonyl carbon (Bunn and Higgins, 1981). It was suggested that only a certain, small percentage of lysine groups enter the glycation reaction (Thorpe and Baynes, 1996). Low pK_a in this region promotes initial glycation of this protein (Lin *et al.*, 1998). Additionally, Amadori rearrangement was influenced by the presence of adjacent histidine groups, carboxylate

groups and negatively charged ions, such as phosphates, present in the reaction media. All these factors promote the chemical transformations the formed Amadori products undergo (Venkatraman *et al.*, 2001).

The formation of glycated proteins *in vivo* has been found to be dependent upon the inherent reactivity of specific amino groups, the half-life of the protein and the degree and duration of hyperglycaemia (Ahmed, 2005; Wautier and Schmidt, 2004).

1.7 Characterisation of AGEs

The glycation reaction leads to a series of compounds manifesting considerable structural diversity. Nevertheless, all AGEs can be classified into four groups based on their cross-linking and fluorescent properties (yellowish-brown fluorescent colour) (Bousova *et al.*, 2005).

1.7.1 Fluorescent cross-linked AGEs

Reactions between basic groups of amino acids or Amadori intermediates and compounds containing α-dicarbonyls result in a series of cross-linked AGEs, as shown in Figure 1.9.

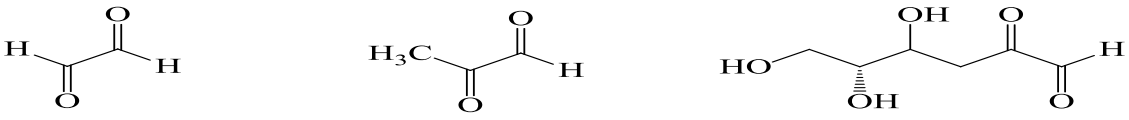

Figure 1.9: α-dicarbonyl derivatives obtained during the course of glycation (Thornalley *et al.*, 1999)

The cross-links between proteins formed by the structures (Figure 1.9) are believed to be responsible for the adverse effects by AGEs during aging-related processes and diabetes.

Fluorescence and the ability to produce cross-links are the most important features of this class of compounds. The formation of cross-linked fluorescent AGEs is shown in Figure 1.10.

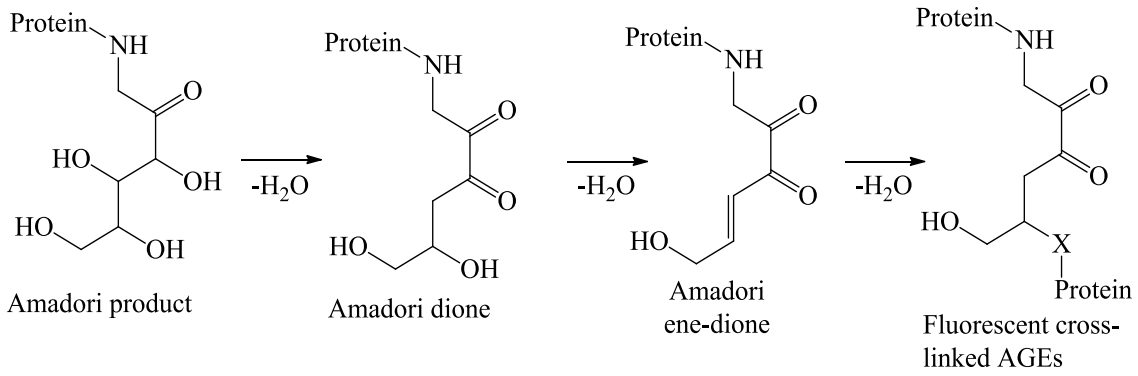

Figure 1.10: Formation of fluorescent cross-linked AGEs (Thornalley *et al.*, 1999)

The first isolated and characterised fluorescent cross-linked AGE, pentosidine, was obtained from collagen. The synthesis of this compound is possible through a reaction between arginine and lysine residues with most carbohydrates (Sell *et al.*, 1999). Pentosidine is not the only natural fluorescent cross-linked AGE; additional examples are presented in Figure 1.11.

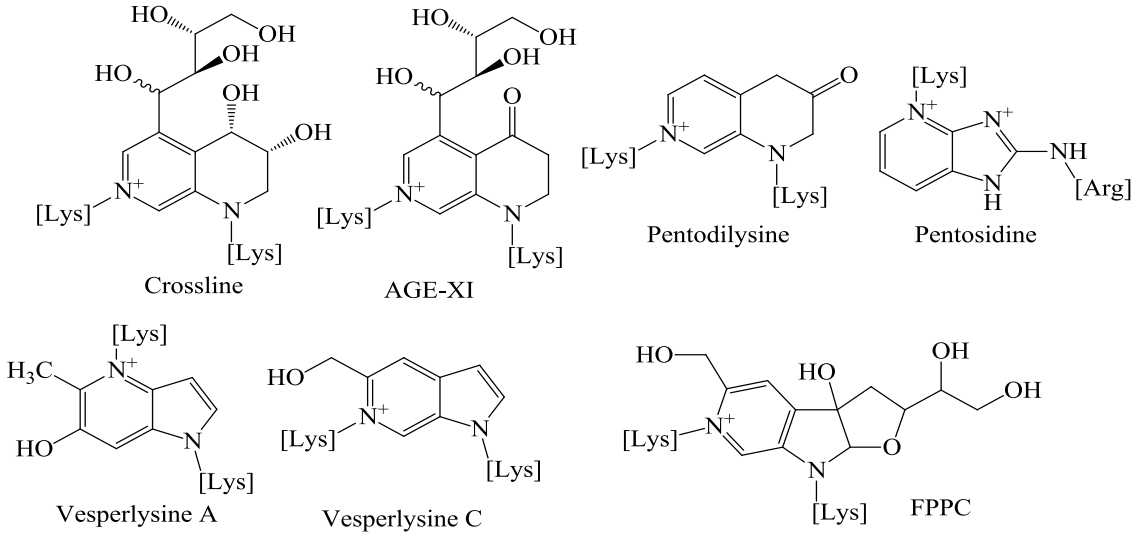

Figure 1.11: Examples of fluorescent cross-linked AGEs (Ulrich and Cerami, 2001)

1.7.2 Non-fluorescent cross-linked AGEs

The highest proportion of AGEs is non-fluorescent AGEs with protein-protein cross-linking *in vivo* (Ahmed, 2005). The main AGE-structures belonging to this group are imidazolium dilysine cross-links also known as glyoxal-lysine dimer (GOLD) or methylglyoxal-lysine dimer (MOLD) cross-links (Chellan and Nagaraj, 1999). Examples of non-fluorescent cross-linked AGEs are shown in Figure 1.12.

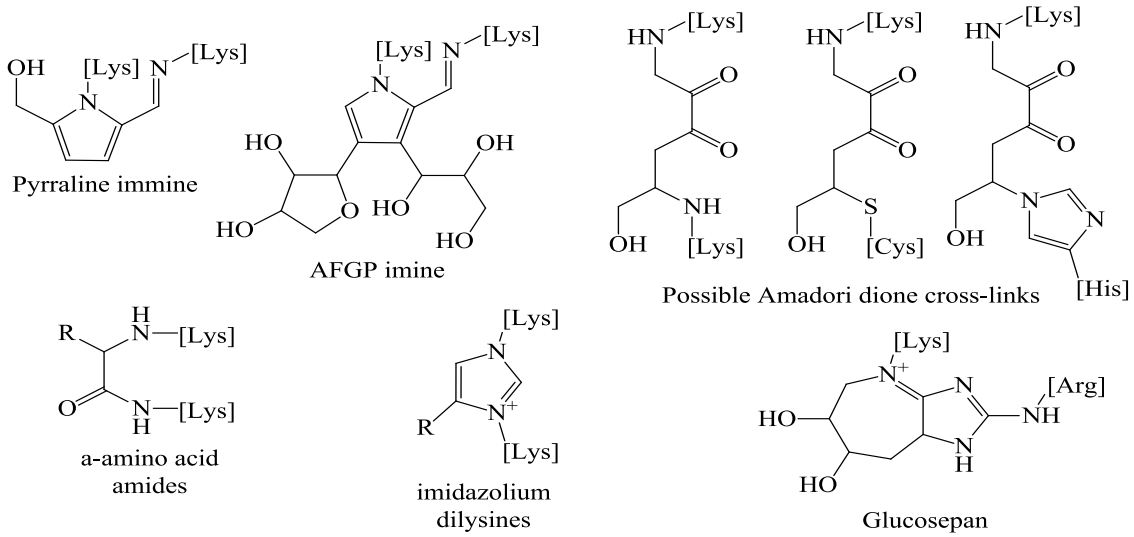

Figure 1.12: Examples of non-fluorescent cross-linked AGEs (Ulrich and Cerami, 2001)

1.7.3 Fluorescent non-cross-linked AGEs

In addition to cross-linked AGEs, which can considerably influence the function and structure of proteins, a range of fluorescent non-cross-linked AGEs are detected in the blood of diabetic patients. These compounds may have adverse effects on possible protein cross-linking. They also play the role of biological receptors promoting a variety of undesired changes at tissue and cellular levels (Niwa, 1999). The backbone of the organic linking fragment is similar to fluorescent cross-linked AGEs. The only exception is that one of the bonds connecting the heterocyclic part with the amino acid is substituted by the N-H bond (Figure 1.13).

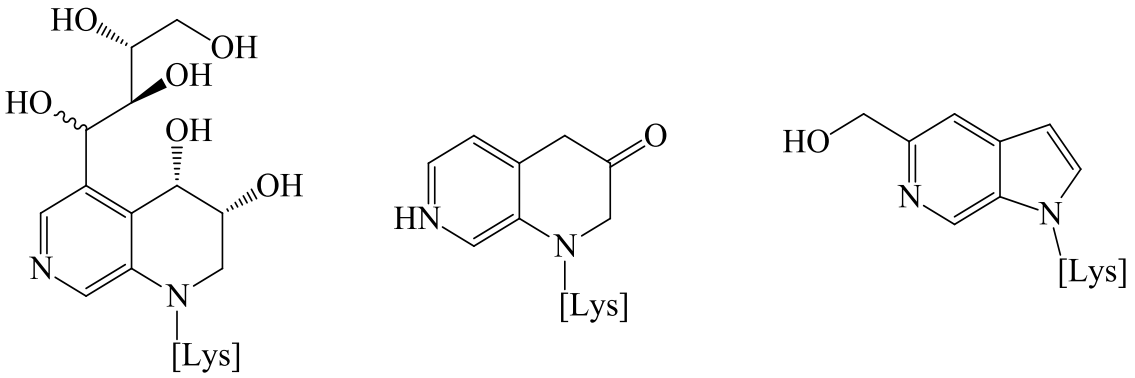

Figure 1.13: Examples of fluorescent non-cross-linked AGEs (Niwa, 1999)

1.7.4 Non-fluorescent non-cross-linked AGEs

A number of non-fluorescent, non-cross-linked AGE structures arising from protein glycation have been described under physiological conditions. Carboxymethyllysine (CML) carboxyethyllysine (CEL), pyrraline and imidazolones (Paul *et al.*, 1998) are the classical types within this group (Figure 1.15). Of the aforementioned AGEs, CML (Ikeda *et al.*, 1996) and pentosidine are of particular importance *in vivo* and can be used as AGE accumulation markers throughout life and in diabetes (Dyer *et al.*, 1993; McCance *et al.*, 1993).

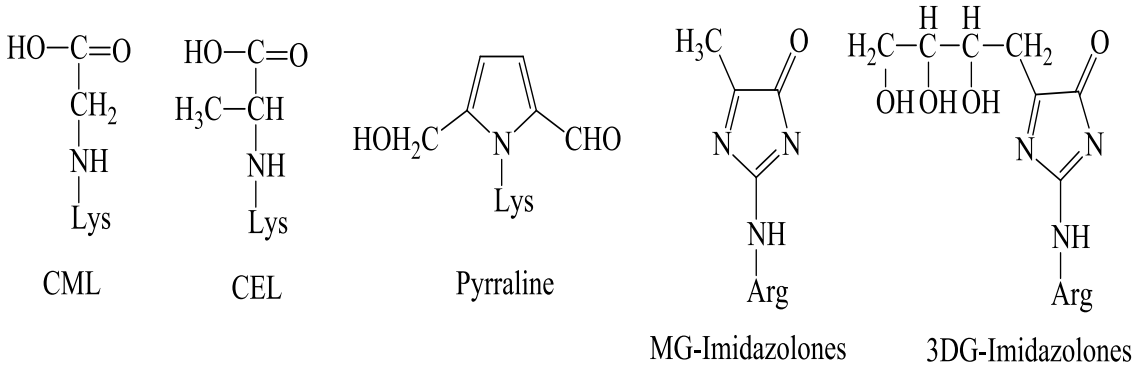

Figure 1.14: Examples of non-fluorescent, non-cross-linked AGEs (Bailey, 2001)

1.8 Intracellular glycation and AGE formation

The extent of intracellular glycation and subsequent AGE formation correlate inversely with a series of diabetic complications (Schalkwijk and Miyata, 2012). AGEs are generated via either lipid peroxidation or the oxidation of Amadori compounds. The dicarbonyl compound methylglyoxal generates via non-oxidative glyceraldehyde-3-phosphate fragmentation and generates the most important AGEs in the intracellular environment (Brownlee, 2005). Thiamine and benfotiamine play an important role during intracellular glycation. Thiamine is a highly powerful AGE inhibitor and benfotiamine, a thiamine pro-drug soluble in lipids, lowers the formation of AGEs (Balakumar *et al.*, 2010; Hammes *et al.*, 1999).

Initially, it was believed that AGEs were only able to form exclusively on extracellular long-lived macromolecules. This was because the rate of glycation was slow, and intracellular proteins simply would not occur within the time necessary to accumulate any measurable quantity of AGEs (Giardino *et al.*, 1996). The extent of AGE production in endothelial cells that are the main location for hyperglycaemia damage is more significant. For instance, Giardino *et al.* (1994) established that after one week of culturing cells in media rich with glucose, the concentration of AGEs in endothelial cells increased 14-fold. This significant, rapid rate of AGE synthesis likely correlates with the hyperglycaemia-promoted formation of intracellular sugars. Compared with glucose, these sugars are much more reactive and include glyceraldehyde-3-phosphate, glucose-6-phosphate, methylglyoxal and fructose (Goldin *et al.*, 2006).

Diabetes-related hyperglycaemia leads to a range of chemical alterations in intracellular metabolites, thus resulting in a series of diabetic complications (Cade, 2008). These alterations are reversible, but the damage done to the tissues and internal organs is not

(Bucala *et al.*, 1993; Sakata *et al.*, 2001). In addition, AGEs also enter the body through a range of exogenous sources, such as foods and cigarettes.

1.9 Exogenous sources of AGEs

Curing tobacco leaves was suggested as a source of chemicals that considerably increase the *in vivo* concentration of AGEs. Glycotoxins obtained from cigarettes readily enter the alveoli where they penetrate lung cells and spread throughout the body via the blood stream. Glycotoxins interact with glycation products, thus contributing to overall AGE formation (Cerami *et al.*, 1997). Similar conclusions were drawn in other studies indicating that tobacco smoke was a well-known and considerable source of AGEs (Peppa *et al.*, 2003). Thus, the combustion of pre-AGEs found in tobacco smoke led to the formation of toxic and reactive AGEs in the human body. Consequently, it was established that AGE concentration was significantly elevated in the blood of smokers. As a result, diabetic smokers were reported to manifest higher AGE concentrations in their ocular lenses and arteries (Peppa *et al.*, 2003).

Heat is used worldwide for food treatment to improve its taste, bioavailability and safety. Along with a range of positive effects, overheating food can result in protein degradation as well as deteriorative, undesired reactions (Faist and Erbersdobler, 2001; Jaeger *et al.*, 2010). In certain cases, heat treatment promotes the Maillard reaction, thus adding desired aromas, colours and flavours to food products. In particular, this reaction is widely exploited in baking bread, roasting coffee and the production of caramel. In addition, a range of Maillard reaction products is added to juices, sodas and other industrial products (Luevano-Contreras and Chapman-Novakofski, 2010; O'Brien and Morrissey, 1990).

Unfortunately, the common Western diet has an increasing, exogenous source of AGEs (Richard *et al.*, 2010). The overall content of these compounds in food products depends on the composition of nutrients in them. Thus, foods rich in fats and proteins present a higher

AGE content (Goldberg *et al.*, 2004; Uribarri *et al.*, 2010). The formation of AGEs is accelerated by elevating the time and extent of exposure to the increased temperature. Additionally, by using enzyme-linked immunosorbent assays (ELISA), it was established that nearly 10% of ingested AGEs enter the blood and circulate within the body. Two-thirds of this quantity remains covalently incorporated in tissues and organs. The remaining one-third leaves the body via the kidneys (Koschinsky *et al.*, 1997).

Most of Maillard reaction products that synthesise *in vivo* and enter the human body with food remain uncharacterised. Nevertheless, some of these compounds are dicarbonyl derivatives as well as pyrralines and furfurals derivatives (Ames, 2008). It was also established that regardless of AGE diversity, CML (N-epsilon-carboxymethyl-lysine) was the most abundant AGE. During analytical investigations of foods, CML is always among the first characterised AGEs. This compound is particularly abundant in milk and milk-containing products. For this reason, CML was chosen as an AGE marker in food (Ames, 2008).

Regardless of whether AGEs form *in vivo* or enter the body via food or tobacco smoke, they express their biological properties via interaction with the receptor for advanced glycation end-products (RAGE).

1.10 Biological effects of AGEs (receptor-dependent effects)

RAGE is a compound belonging to the immunoglobulin group of receptors. In humans, the gene responsible for the expression of RAGE is located on the sixth chromosome, which is situated between Class II and III of the histocompatibility complex genes. The gene consists of 11 exons, and typical variations of this gene have been described (Hudson and Schmidt, 2004).

The mass of a typical RAGE molecule is 45-kDa. A significant part of this molecule is located within the cellular wall; however, an extracellular element is also present. The extracellular part of a RAGE molecule is composed of a variable (V-type) domain, which is followed by two constant (C-type) domains. The V-type domain is similar to the one found in immunoglobulin. RAGE possesses a single domain that runs from one side of the membrane to the other. The V-type domain has proven highly important in binding with organic ligands, and the constant domain cytosolic tail is crucial for RAGE-mediated signalling (Srikanth *et al.*, 2011). In addition to full-length normal RAGE molecules, a series of truncated variations are found. The existence of these variations is explained by the presence of splice variants in the mitochondrial RNA. For instance, an N-truncated protein type does not possess the V-type segment, but it is similar to normal RAGE proteins in all other features and is not excluded from the cell membrane (Basta, 2008). A schematic representation of RAGE is given in Figure 1.15.

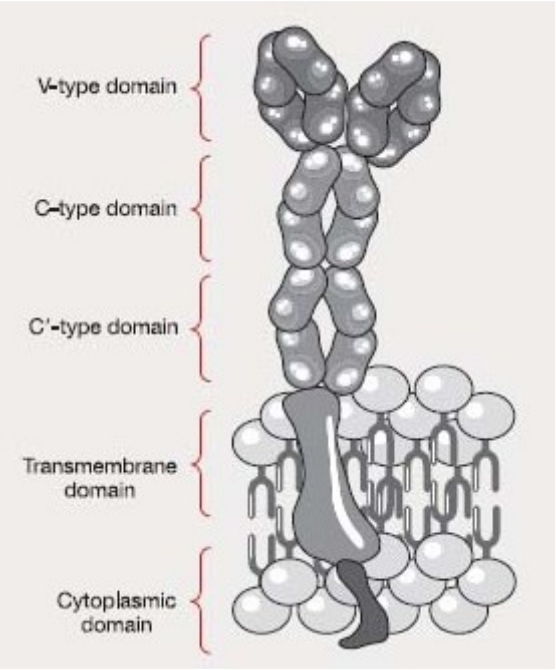

Figure 1.15: Schematic representation of RAGE (Basta, 2008).

RAGE molecules are formed in a series of organs and tissues, but their highest concentration is in the skeletal muscles, the lungs and the heart. Additionally, this type of protein can be found in lymphocytes and macrophages. In vessels, RAGE is located in smooth muscle cells and endothelium (Koyama *et al.*, 2007). AGE receptors play a critical role in the development of diabetes complications (Win *et al.*, 2012). This conclusion was supported by investigations on experimental models. For instance, RAGE activation was shown to contribute to axonal sprouting, which is an accompanying development of the central nervous system. On the other hand, RAGE inhibition leads to depression of sciatic nerve functions and its regeneration (Huttunen *et al.*, 2000).

The most significant outcome of AGE-RAGE interaction is the activation of a series of biological mechanisms resulting in oxidative stress. The biological consequences of the AGE-RAGE interaction are summarised in Figure 1.16.

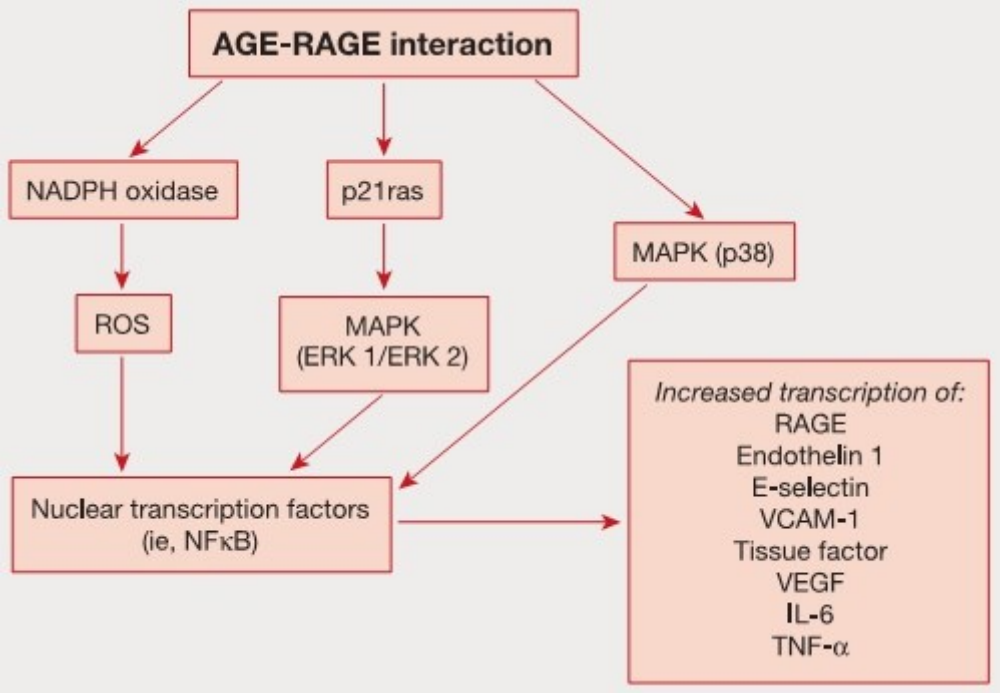

Figure 1.16: Biological effects of AGE-RAGE interaction (Marchetti, 2009)

The interactions of interest result in the promotion of prolonged inflammation as a direct result of the expression of pro-inflammatory chemokines and cytokines (Figure 1.16). The expression of both compounds is RAGE dependent. The first biological effect of the AGE-RAGE interaction is the promotion of the reactive oxygen species (ROS). The first stages of ROS formation are influenced by the NAD(P)H-oxidase system. A recent investigation indicated that alterations in the sequence of amino acids responsible for RAGE formation result in alterations of the signal transmitted by the molecule inside the cell. Furthermore, the duration and intensity of the signal resulted in different signalling pathways employed by RAGE. These pathways and the corresponding outcomes are represented in Figure 1.16 (Marchetti, 2009).

Interaction with RAGE as well as AGE metabolism results in the formation of ROSs. These species are of paramount importance in promoting oxidative stress and further diabetic complications.

1.11 Oxidative stress, free radicals and glycation

Free radicals and oxidative stress are associated with a range of pathological conditions including atherosclerosis, Alzheimer's disease, chronic inflammation and diabetes. In all these processes, ROSs are of paramount importance (Brieger *et al.*, 2012; Rahbar and Figarola, 2003). Thus, oxidative stress is characterised by considerable imbalance between the formation of free radicals and their deactivation by natural defence mechanisms. This mechanism exists in all organisms and executes in order to prevent tissue damage and dysfunction. The excess quantity of free radicals is generated by cytochrome p450, mitochondria respiration, xanthine oxidase functions and RAGE-mediated processes (Lander *et al.*, 1997).

It is being suggested that ROSs induce signalling in pathophysiological and physiological conditions. For instance, ROS production within certain biological boundaries is critical to sustained homeostasis (Rahbar and Figarola, 2003). Regardless where ROSs are produced and the conditions of their production, an elevated concentration of powerful oxidants has two outcomes: the activation of specific signalling mechanisms and damage to all cell components (Hensley *et al.*, 2000; Kvietys and Granger, 2012). ROSs include a variety of chemicals, including hypochlorous acid (HOCl), hydroxyl radical (HO•), peroxyl radical (ROO•), alkoxyl radical (RO•), hydrogen peroxide (H_2O_2) and superoxide anions (O2•–) (Hensley *et al.*, 2000; Rahbar and Figarola, 2003).

Glycation presents one of the major sources of active α-dicarbonyl active intermediates and ROSs generated via non-oxidative and oxidative glycation pathways (Rahbar and Figarola, 2003).

The role of methylglyoxal in promoting the formation of free radicals is extensively documented. Thus, during the glycation reaction, methylglyoxal induces the synthesis of superoxide radicals, peroxynitrite, hydrogen peroxide and many other substances responsible for oxidative damage. Additionally, methylglyoxal is responsible for the increase in activity of pro-oxidant enzymes, such as p38 MAPK and NADPH oxidase, as well as the elevated expression of PPAR-α and JNK (Desai and Wu, 2008).

Elevated concentrations of nitric oxide (NO) result in the extensive formation of peroxynitrite (ONOO·). This ROS is a strong nitrating agent and a powerful oxidant. Generated during glycation, peroxynitrites have the ability to damage proteins and DNA molecules due to their oxidising properties. They also promote a range of diseases, including diabetes (Pacher *et al.*, 2007).

AGEs promote oxidative stress through a range of mechanisms. First, AGEs catalyse the formation of growth factors and cytokines. In addition, these compounds are able to bind with their corresponding receptors (RAGE) and increase ROS generation. Furthermore, oxidative stress occurs because of the imbalance between ROS production and antioxidant defences (Tan *et al.,* 2007). In endothelial cells, AGEs catalyse the synthesis of vascular cell adhesion molecules and intercellular adhesion molecules, and they elevate the activity of NF-kB, which leads to increased oxidative stress (Kikuchi *et al.*, 2003).

1.12 Diabetic complications and glycation

Generally, complications associated with diabetes are of two types: macrovascular and microvascular. Although numerous studies have been conducted on this topic, the cause for the majority of diabetic complications is unclear. However, one possible cause is AGEs and their build-up on long-lived proteins. On the other hand, vascular complications of diabetes can be reduced through glycaemia management, which eventually lessens AGE formation (Ahmed and Thornalley, 2007; O'Sullivan and Dinneen, 2009).

1.12.1 Advanced glycation end-products and microvascular complications

The formation of AGEs can increase diabetic microvascular complications in animals and humans (McCance *et al*, 1993; Wada and Yagihashi, 2005). Features found in conditions with microvascular complications, which are pervasive, are an increase of vascular permeability and prothrombosis, coagulation of the basement membrane and a reduction in blood flow (Huebschmann *et al.*, 2006). However, diabetes mellitus is largely responsible for microvascular complications with unsuccessful treatment (Karachalias *et al.*, 2003). Moreover, conditions such as retinopathy, nephropathy and neuropathy (Peppa and Vlassara, 2005) are microvascular diseases that develop in diabetes over periods greater than 10–15 years.

1.12.1.1 Diabetic retinopathy

Diabetic retinopathy is the main microvascular complication found in diabetes, and it can cause the loss of vision. Over a period of 20 years, all patients with type 1 diabetes suffer from retinopathy to a certain extent, while about 60% of patients with type 2 diabetes suffer from retinopathy (Fong *et al.*, 2004). A number of *in vivo* and *in vitro* studies suggest that the main reason for the growth and expansion of retinopathy might be increased intracellular and extracellular AGEs in diabetes (Anitha *et al.*, 2008; Sato *et al.*, 2006). Moreover, AGEs exhibit a growth inhibitory action on pericytes thereby leading to pericyte loss, which is the earliest histological hallmark of diabetic retinopathy. This, in turn, induces basement membrane thickening, which significantly contributes to the breakdown of the inner blood-retinal barrier (Assero *et al.*, 2001; Stitt and Curtis, 2005). In addition, AGE formation can lead to abnormal proliferative reactions in retinal microvascular endothelial cells, which may result in the abnormal expression of endothelial nitric oxide synthase (eNOS) (Giacco and Brownlee, 2010; Hogan *et al.*, 1992).

1.12.1.2 Diabetic cataract

Cataract is a major cause of visual impairment and blindness worldwide and is characterised by opacification of the lens. Furthermore, cataractogenesis can be caused by chronic hyperglycaemia (Crabbe, 1998; Franke *et al.*, 2003). However, the mechanism responsible for diabetic cataract formation is unknown. Currently, the glycation theory is widely accepted as playing a key role in cataract development in the lens. Several studies report that the formation of AGEs on lens crystalline may cause protein oxidation cross-linking, and formation of high molecular weight aggregates responsible for cataract formation (Cheng *et al.*, 2006; Linetsky *et al.*, 2008). In addition, the development of a diabetic cataract can be caused by the glycation of channel proteins and sodium-potassium pump (Na/K-ATPase) (Gallicchio and Bach, 2010; Stevens, 1998).

1.12.1.3 Diabetic nephropathy

Of diabetic patients, 40–50% suffer from diabetic nephropathy (Berger *et al.*, 2003; Wolf, 2004). This complication involves the coagulation of glomerular and tubular basement membranes along with the enlargement of the mesangial layer, which eventually leads to vascular occlusion, microvascular damage and fibrotic changes, thus causing glomerulosclerosis (Coughlan *et al.*, 2005). This disease is responsible for death and morbidity in diabetic patients and often leads to end-stage renal disease (Mima, 2013; Yamagishi *et al.*, 2007). Furthermore, animal and other clinical studies have shown that AGE formation interferes with renal destruction, which is related to hyperglycaemia (Brownlee *et al.*, 1988; Forbes *et al.*, 2005). However, nephropathy patients have increased AGEs, which could be due to decreased clearance in the kidney rather than increased production by glycation (Shimoike *et al.*, 2000). Moreover, several studies with human subjects show higher levels of pentosidine (Hashimoto *et al.*, 2010; Monnier *et al.*, 2005) and CML (Beisswenger *et al.*, 2013; Mao *et al.*, 2003; Miura *et al.*, 2003) in diabetic patients' renal tissues regardless of end-stage renal diseases.

1.12.1.4 Diabetic neuropathy

Diabetic neuropathy occurs when the peripheral sensory and autonomic nervous systems are damaged (Magalhães *et al.*, 2008). The formation of AGEs is regarded as the main biochemical pathway related to diabetic neuropathy (Fowler, 2008; Sugimoto *et al.*, 2008; Zochodne, 2007). Furthermore, the AGE-modified peripheral nerve myelin is vulnerable to phagocytosis by macrophages, which leads to segmental demyelination (Shi *et al.*, 2013). In addition, damaged regenerative activity in diabetic neuropathy due to glycation of the extracellular matrix proteins collagen and laminin alters the electrical charges and coagulates the nerve capillary basement membrane (Monnier *et al.*, 1984; Tomlinson and Gardiner, 2008).

Increasing evidence suggests the interaction of AGEs with RAGE is involved in nerve dysfunction, which may play an inflammatory role in peripheral nerve damage, although their precise role remains unknown (Huijberts *et al.*, 2008). Moreover, AGEs change the expression levels of the inducible form of nitric oxide synthase (iNOS), which in turn reduces blood flow in the nerve and induces hypoxia in the peripheral nerve (Jack and Wright, 2012; Wada and Yagihashi, 2005).

1.12.2 Advanced glycation end-products and macrovascular complications

Macrovascular complications in diabetes involve a broad spectrum of pathological changes affecting major blood vessels leading to structural and functional abnormalities. The glycation of wall components and functional changes initiate endothelial dysfunction and make artery walls harder or decrease vascular compliance, which leads to structural amendments. Moreover, atherosclerosis is believed to be fundamentally responsible for the high incidence of vascular diseases such as stroke, myocardial infarction and peripheral vascular disease (Rahman *et al.*, 2007).

1.12.2.1 Diabetes and atherosclerosis

Atherosclerosis is known to be a chronic inflammatory disease caused by the contraction of arteries and the gradual development of lesions (Christian and Heidi, 2011). According to several studies, atherosclerosis develops in diabetic patients due to AGE formation (Jandeleit-Dahm and Cooper, 2008; Schmidt and Stern, 2000; Vlassara and Palace, 2002; Yamagishi *et al.*, 2005). Moreover, abnormal lipoprotein metabolism, protein cross-linking and matrix component changes may assist AGEs in accelerating the atherosclerosis process (Ahmed *et al.*, 2009; Goh and Cooper, 2008). AGEs may induce atherosclerosis by oxidising low density lipoprotein (LDL). Moreover, glycated LDL uptake by macrophages contribute to the development of foam cell formation (Basta *et al.*, 2004; Brown *et al.*, 2005; Chang *et al.*, 2011). Furthermore, AGEs promote vasoconstriction by quenching NO (Pandolfi and De

Filippis, 2007). In addition, AGEs may also inhibit vascular repair after injury (Crauwels *et al.*, 2000; Guo and Dipietro, 2010), increased endothelial dysfunction through interaction with RAGE (Hallam *et al.*, 2010; Smit and Lutgers, 2004; Tan *et al.*, 2002), neointimal proliferation along with more plaque destabilisation (Burke *et al.*, 2004; Raposeiras-Roubin *et al.*, 2013). Moreover, the interaction of AGEs with RAGE may also act as an essential element in the formation of atherosclerosis in diabetic patients (Jandeleit-Dahm *et al.*, 2008; Yamagishi *et al.*, 2005). Considering this, the activation of NF-kB and activator protein-1 transcription factors in vascular cells by AGEs may contribute to the elevated expression of a range of genes associated with atherosclerosis, including VCAM-1, endothelin-1, inflammatory cytokines and PAI-1 (Inagaki *et al.*, 2003; Laakso, 2010).

1.13 Diabetes and impaired wound-healing (Angiogenesis)

Angiogenesis can be defined as the process of forming novel capillary blood vessels (Egginton, 2010). In adults, the rate of this process is usually very low compared with other types of tissues. Physiological exceptions are found during wound healing and in the female reproductive system, where angiogenesis is strictly regulated (Egginton, 2010). Uncontrolled angiogenesis results in juvenile haemangioma, rheumatoid arthritis and diabetic retinopathy (Liekens *et al.*, 2001).

The proliferation of endothelial cells takes place during angiogenesis. A range of factors in the microenvironment surrounding forming blood vessels controls this process. These factors include influence from cytokines, the adjacent extracellular matrix and neighbouring cells. The complex interactions of these factors results in signals allowing the dividing cells to produce the required architecture (Nelson and Chen, 2003).

The migration of endothelial cells is of paramount importance in angiogenesis. A range of factors, including mechanotactic stimuli, heptotactics and chemotactics, regulates this

process. Additionally, extracellular matrix degradation is necessary to enable further progression of the blood cells. Endothelial migration of cells involves three main mechanisms: chemotaxis, or the directed movement in the direction of a soluble chemoattractants gradient; haptotaxis, or a shift in the direction of an immobilised ligands gradient; and mechanotaxis, or the migration in the direction determined by external mechanical forces (Delgado *et al.*, 2011; Lamalice *et al.*, 2007).

Following cell proliferation and migration, the newly formed endothelial cell outgrowth needs to organise into an adequate, three-dimensional, tube-shaped structure. This outgrowth is called primary capillary plexus, and its reorganisation leads to the formation of blood vessels. This process can be modulated and assessed *in vivo* by allowing endothelial cells to produce tubes on fibrin clots or collagen (Cai, 2012).

As mentioned before, angiogenesis takes place during wound healing and tissue repair. The process of wound healing can be defined as the complete replacement of damaged or destroyed tissue by living tissue. It consists of two main components: repair and regeneration. Wound healing consists of four overlapping phases: initial bleeding, inflammation, cell proliferation and tissue remodelling (Bainbridge, 2013).

During the wound-healing process, the bleeding phase is usually the shortest phase. The magnitude depends on the wound but is essential and normal. Large numbers of chemicals inhibit the following inflammatory phase. Inflammation expands rapidly within hours but resolves gradually over several weeks. The repair material generates during the proliferation stage. The onset is rapid, but it takes several weeks for the process to reach its full magnitude (Reinke and Sorg, 2012). The final stage of the wound-healing process is remodelling the produced tissue. It overlaps with the proliferation stage and begins 1–2 weeks after the injury (Culav, 1999; Guo and Dipietro, 2010).

Patients with DM suffer from impaired wound healing (Kolluru *et al*., 2012). Wound healing in diabetic patients is characterised by defective formation or deposition of the healing matrix (Lerman *et al.*, 2003). In humans, diminished perfusion due to arterial diseases and peripheral neuropathy are known to contribute to impaired wound healing. During the normal wound-healing process, apoptosis plays a critical role in the removal of granulation tissue as well as fibroblasts and minor blood vessels in the tissue. In contrast, the extent of apoptosis related process is increased in diabetic patients as a direct result of the elevated glucose concentration in the blood (Bao *et al.*, 2009). In addition, increased glucose levels alter the properties of messenger RNA (mRNA), which leads to the formation of lower quantities of collagen, fibronectin and plasminogen activator inhibitor that results in delayed cell replication and excessive cell death (Baumgartner-Parzer *et al.*, 1995).

A growth factor is a natural chemical able to promote cell growth. In turn, fibroblast growth factor (FGF-2) plays a role in angiogenesis and wound healing via the regulation of cell differentiation and the proliferation of newly formed cells and their migration. FGF-2 binds to the surface of the cell and promotes the dimerisation of FGF receptors with the subsequent activation of tyrosine kinase receptors and autophosphorylation of the cognate receptors (Boilly *et al.*, 2000).

1.14 Measurement of glycation reaction products

The determination of protein modification has always provided a challenge for biochemists. The complex nature of glycation combined with the fact that AGEs are a mixture of different structures has led to difficulty measuring them; the lack of internal standards leaves assays open to error, as they require a high degree of accuracy and reproducibility for each sample (Smit and Lutgers, 2004).

Various tests have been conducted qualitatively and quantitatively to determine the level of AGEs; some utilise a vital mechanism known as fluorescence spectroscopy *in vitro* and *in vivo* (Meerwaldt *et al.*, 2008). In addition, immunochemical techniques, such as ELISA, are another means to describe AGE structures, which use specific polyclonal and monoclonal antibodies for AGEs (Lin *et al.*, 2002). A method that has been extensively used in recent studies is mass spectrometry. Moreover, utilising matrix-assisted laser desorption ionisation time-of-flight mass spectrometry (MALDI-TOF-MS) peptide mapping is considered a useful technique to determine particular protein glycation products *in vitro* and *in vivo* (Kislinger *et al.,* 2004; Niwa, 2006). Nonetheless, a separation assay method, such as SDS-PAGE, is used during the course of glycation research (Ahmad *et al.*, 2007; Xie *et al.*, 2011).

1.14.1 Measurement of early glycation products

The measurement of early-stage glycation products (Amadori products) is used in order to evaluate metabolic control in diabetic patients. The two parameters commonly used are glycated haemoglobin (HbA_{1c}) and fructosamine.

1.14.1.1 Glycated haemoglobin

The number of methods employed in measuring HbA_{1c} is ion exchange chromatography by High-performance liquid chromatography (HPLC), affinity chromatography (relies on the distinction of structure), immunochemical assays and spectroscopic methods (Kislinger *et al.*, 2004). However, the measurement of HbA_{1c} is normally utilised to monitor glycaemia in diabetes. In addition, the International Federation of Clinical Chemistry and Laboratory Medicine (IFCC) has provided an approved reference method for measuring HbA_{1c} in humans (Groche *et al.*, 2003; Lai, 2008). The percentage of HbA_{1c} molecules is a valuable diagnostic marker and accordingly reflects the extent of exposure to glucose 4–8 weeks before testing.

1.14.1.2 Glycated serum proteins

A colorimetric technique is generally employed by clinicians to measure fructosamine (Lapolla *et al.*, 2005). The measurement of glycated serum proteins (fructosamine) is gaining acceptance as a procedure for time-averaged control of glycaemia in diabetic patients. Unlike HbA_{1c}, fructosamine levels reflect the blood glucose concentration over the preceding 10–20 days, thus responding more quickly to changes in diabetic therapy (Guillausseau *et al.*, 1990).

1.14.2 Measurement of intermediate glycation products

Several studies show that people suffering from diabetes may have increased concentrations of plasma glyoxal and methylglyoxal as compared to non-diabetics (Brown *et al.*, 2013; Khuhawar *et al.*, 2006). In addition, the plasma of people suffering from diabetes have elevated levels of 3-deoxyglucosone (Niwa, 1999). In addition, the formation of AGEs found in diabetics increases along with rising levels of dicarbonyl compounds such as glyoxal, methylglyoxal and 3-deoxyglucosone (Ahmed and Thornalley, 2003). With the use of mass-spectrometric methods, dicarbonyl compounds are quantitatively demonstrated. The estimation of dicarbonyl compounds is of interest in terms of evaluating oxidation processes occurring in glycated proteins.

1.14.3 Measurement of AGEs

Advanced glycation end-products were initially measured by spectroscopic and fluorimetric methods. However, these methods are not very specific and can only provide mere indications on the general trend of the glycation process (Brownlee *et al*, 1988). More recently, various investigators have developed ELISA methods using polyclonal and monoclonal antibodies (Cheng *et al.*, 2005; Monnier *et al.*, 2005). The limitation of this current methodology is, however, that no absolute AGE standard for quantitative analysis exists (Singh *et al.*, 2001). AGEs are currently being identified as biomarkers for specific disease processes. In addition, CML and pentosidine are discovered *in vivo* (Ni *et al.*, 2009).

CML and pentosidine levels found in diabetic patients were originally evaluated by GC/MS; however, the ELISA method has recently been used to measure the level of CML with anti-CML monoclonal antibodies (Hartog *et al.*, 2007). Furthermore, diabetic patients with nephropathy were found to have elevated levels of pentosidine (Kerkeni *et al.*, 2012). Likewise, the high level of serum CML was discovered in patients with diabetes who also have retinopathy and/or nephropathy, in contrast to patients without these conditions (Jakus and Rietbrock, 2004; Vinik, 2011).

1.15 Natural defence mechanisms against glycation

The human body developed a range of cellular mechanisms to protect the body against glycation and the accumulation of AGEs. These mechanisms employ glyoxalase systems (I and II), glutathione and aldose reductase to detoxify reactive dicarbonyl compounds and to sequentially reduce AGE formation (Gomes *et al.*, 2005; Thornalley, 1998). Additionally, a novel group of enzymes called Amadoriases catalyses the deglycation of Amadori products, thus defending against glycation (Gerhardinger *et al.*, 1995; Kousar *et al.*, 2012).

Human FN3K (fructosamine-3-kinase) was shown to phosphorylate fructoselysine groups situated on glycated proteins and transform it into fructoselysine-3-phorphate. This compound breaks down spontaneously, thereby reversing the glycation reaction in its early stage (Lapolla *et al.*, 2013; Szwergold *et al.*, 2001). In addition, macrophages possess receptors, which enable them to identify and remove glycated proteins by endocytosis (Matsumoto *et al.*, 2002; Vlassara *et al.*, 1988).

1.16 Natural glycation inhibitors

Although many different natural compounds are currently under extensive study and analysis *in vivo*, few have successfully entered clinical trials. However, none of these compounds has so far been approved for clinical use. Recently, several studies have specified that dietary

supplementation with combined anti-glycation and anti-oxidant nutrients may be a safe and simple complement to traditional therapies aiming to prevent and target diabetic complications (Ahmad *et al.*, 2007; Babu *et al.*, 2006). For example, polyphenol compounds including garcinol from *Garcinia indica* fruit (Yamaguchi *et al.*, 2000), Luobuma tea (Yokozawa and Nakagawa, 2004), and crisilineol from *Thymus vulgaris* (Morimitsu *et al.*, 1995) have shown to be potent inhibitors of AGE formation. In addition, rutin from tomato paste was found to inhibit glycation (Kiho *et al.*, 2004) and autoxidative reactions (Cervantes-Laurean *et al.*, 2006). Moreover, a number of anti-oxidant nutrients have been reported to have anti-glycation properties *in vitro*. For instance, the extract of green tea contains large amounts of tannins (flavonoids), which have been reported to inhibit AGE formation (Babu *et al.*, 2007). Additionally, ranges of other AGE inhibitors were extracted from natural sources. These compounds include epigallocatechin-3-gallate, caffeic acid and chlorogenic acid, which are all commonly extracted from coffee beans and green tea. Examples of natural inhibitors also include capsaicin, hesperidin and quercetin (Popova *et al.*, 2010). The chemical structures of these inhibitors are presented in Figure 1.17.

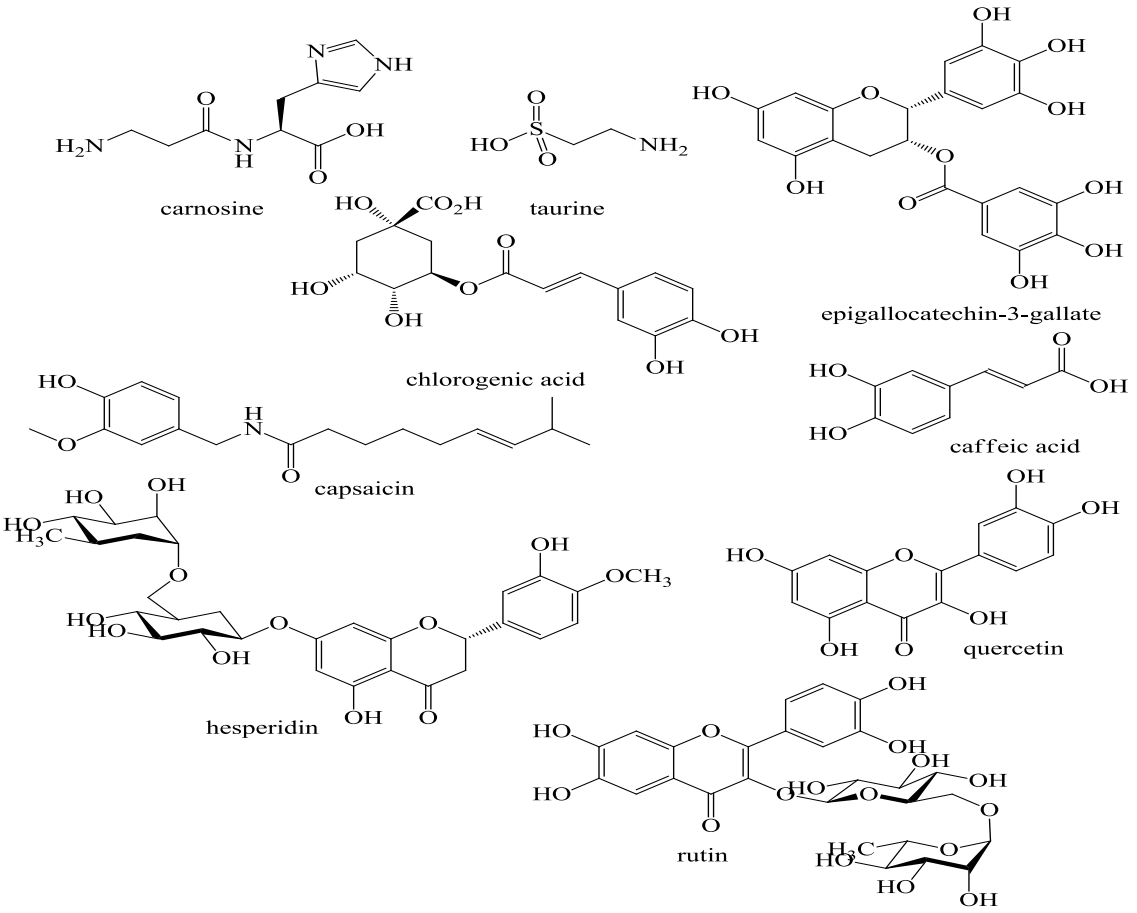

Figure 1.17: Naturally occurring glycation inhibitors (Popova *et al.*, 2010)

These compounds are not the only inhibitors found in nature. Historically, it was established that salicylate-based treatment had a positive effect on reducing the glycosuria manifested by diabetic patients. Moreover, N-acetyllysine and lysine proved to be beneficial in lowering albuminuria occurring during diabetes. Nevertheless, the first compound extensively studied in *in vivo* and *in vitro* experiments was aminoguanidine (AG). Originally, Chang *et al.* (2003) established that AG had the ability to inhibit fluorescence and cross-linking of aortic collagen. Later, the compound was demonstrated to mitigate a range of diabetic complications including vasculopathy, neuropathy and nephropathy (Thornalley, 2003). This compound did not affect hyperglycaemia but was able to deactivate reactive dialdehyde intermediates produced during glycation, thus demonstrating inhibitory properties

(Thornalley *et al.,* 1999). In addition to being an excellent AGE inhibitor, AG was also found to deactivate ROSs, such as nitric oxide radicals. Nevertheless, AG had a range of side effects including anaemia and the elevated possibility of anti-nuclear antibody (ANF) development. Higher rates of renal-neoplastic and pancreatic tumours were detected in diabetic patients treated with aminoguanidine. As a result, complications associated with this compound forced the cessation of aminoguanidine treatments (Rahbar and Figarola, 2003). Along with natural glycation inhibitors, a range of their synthetic counterparts was developed (Figure 1.18).

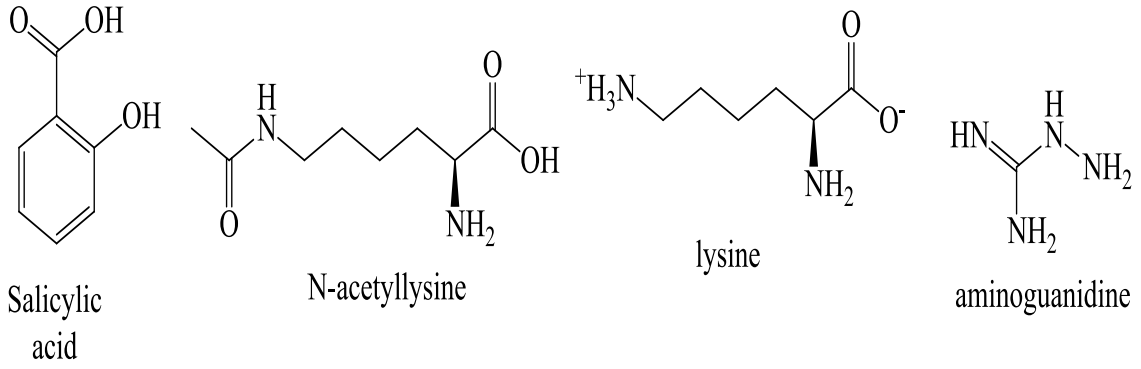

Figure 1.18: Salicylic acid, N-acetyllysine, lysine and aminoguanidine (Rahbar and Figarola, 2003)

Moreover, dipeptide carnosine discovered by Vladimir Gulevich a Russian scientist. It is been found in animal muscles and brain tissues. Several studies shows that carnosine might have an effective anti-glycating agent (Hipkiss *et al.*, 1995; Hobart *et al.*, 2004; Argirova & Argirov, 2003). The dipeptide has been shown to inhibit formation of protein carbonyls and cross-links induced by reducing sugars and other reactive aldehydes such as. Methylglyoxal and malondialdehyde (Hipkiss, 2005).

1.17 *Momordica charantia*

Momordica charantia (MC) is a vegetable and medicinal plant belonging to the Cucurbitaceae family that grows in the subtropical and tropical regions. This plant is also known as bitter melon, bitter gourd, balsam pear or karela (Grover and Yadav, 2004; Joseph and Jini, 2013). The bitter taste is common for all areas of this vegetable plant. A raw fruit, produced by the plant, presents an elongated, cucumber-shaped object. Initially, the fruit is dark green and gradually turns yellow-orange as it ripens. At maturity, it splits into several irregular parts pointing upwards or sideways (Figure 1.19). Seeds are released from the lowest part of the fruit (Lee *et al.,* 2009).

Figure 1.19: development stages of *Momordica charantia* (A)-Raw; (B)-Mature; (C)-Ripe (Lee *et al*., 2009)

Usually, fruits are collected from the MC when they are still immature. They are used extensively in traditional medicine to mitigate diabetes symptoms and to improve general

well-being. According to Lee *et al*. (2009), MC presents a highly promising plant with anti-diabetic properties. In addition, MC demonstrates a range of other pharmacological and biological activities.

The properties of MC have been investigated since the 1960s. Ranges of metabolites were extracted from the fruit of this plant and the seeds it releases. From the chemical point of view, primary metabolites present in the bitter melon are triterpenes, glycosides, phenolic acids, flavonoids, essential oils, minerals, soluble dietary fibres, crude proteins and fats. Additionally, raw fruits contain elevated doses of Vitamins A and C (Chen *et al.*, 2009). Cucurbitane triterpenoids are the most important secondary metabolites present in MC. These substances, as well as aglycones, produce a range of beneficial biological effects, which are particularly important in obesity and diabetes. Additionally, cucurbitane triterpenoids have anti-oviposition, anti-feedant, anti-diabetic and anti-cancer properties (Baby and Jini, 2013).

MC demonstrated anti-diabetic properties in diabetic rats by decreasing glucose concentrations and anti-hyperlipidemic effects (Kameswararao *et al*., 2003). Furthermore, a reviewer's evaluation showed MC's hypoglycemic effects in humans, although two studies did not show any effect on glucose levels (Deng, 2012). The existing investigations in this area were not consistent due to poor study design. Moreover, the exact nature of the anti-diabetic compound has not been established yet.

1.18 Charantin

Charantin is one of the triterpenoids obtained from MC. This substance presents a typical triterpenoid of the cucurbitane type and has pronounced anti-diuretic properties. Pitipanapong *et al.* (2007) demonstrated that charantin could be used in diabetes treatment and could potentially replace conventional treatment. Charantin presents a mixture of two chemicals, namely stigmasteryl glucoside and steryl glucoside (Figure 1.20).

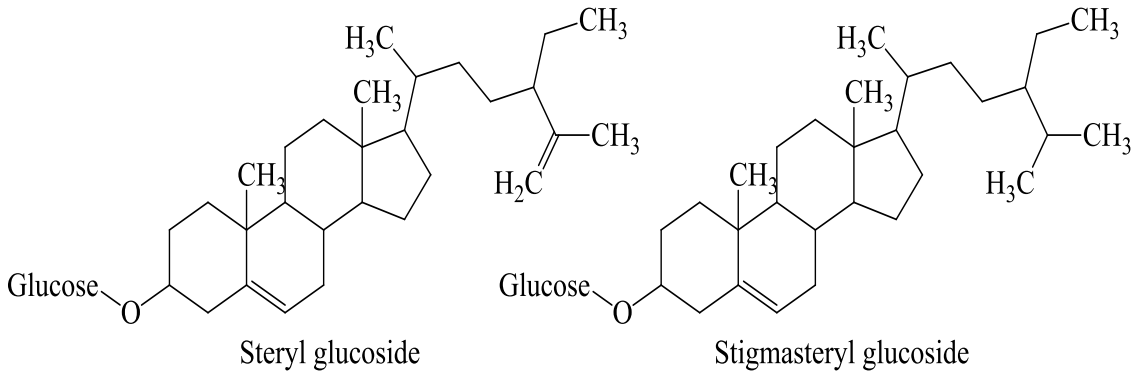

Figure 1.20: Chemical structures of charantin (Pitiphanpong *et al.*, 2007)

Pitiphanpong *et al*. (2007) established that the most efficient way of obtaining the charantin chemicals mixture was to use the pressurised liquid extraction method (PLE). However, HPLC has been suggested as a possible alternative. Using this approach, it is possible to extract charantin along with other substances from small or large dried MC fruit (Lee *et al.,* 2009).

Anti-diabetic properties of the individual chemicals forming charantin were also investigated. The charantin mixture was separated and identified as stigmastadienol and sitosterol glycosides. These compounds were separately tested for *in vivo* hypoglycemic effects, but neither compound exhibited any notable effects on the glucose concentration. For this reason, it can be concluded that charantin, along with the two glycosides, may be formed by other unidentified components responsible for charantin activity (Baby and Jini, 2013).

1.19 Aims of the study

Ths aims of the study were:

- To confirm and evaluate the antioxidant activities of MCP, MCF extracts and charantin *in vitro*.
- To investigate and compare the effect of MCP, MCF and charantin extracts on the formation of AGEs *in vitro*.
- To examine the effects of BSA-AGEs and MCP, MCF extracts and charantin on angiogenesis using BAEC *in vitro*.

Chapter 2 Materials and Methods

2.1 Materials

- 1,1-Diphenyl-2-picryl-hydrazyl (Sigma, UK)
- 24-well, 48-welland96-well plates (Scientific Laboratory Supplies, UK)
- 2-Mercaptoethanol (Sigma, UK)
- Acetic acid (Fisher Scientific International, UK)
- Acrodisc 32 mm syringe filter with 0.2 µm membrane (Pall Corporation, UK)
- Acrylamide/Bis solution 40% (Bio-Rad Laboratories, Germany).
- Aluminium trichloride (Fluka, UK)
- Ammonium persulphate (Sigma, UK)
- Antibiotics: Pencillinand Streptomycin solution containing L-glutamine (PSG) in 0.9% NaCl (Sigma, UK)
- Ascorbic acid (Sigma, UK)
- BIO-RAD protein estimation kit (Bio-Rad laboratories, UK)
- Blotting papers (Schleicher and Schuell, UK)
- Bovine aortic endothelial cells, secondary cell line (Cell and Molecular Biology Research Laboratory, Manchester Metropolitan University, UK)
- Bovine serum albumin (Sigma, UK)
- Carboxymethyllysine antibody; Rabbit polyclonal antibodies to CML (Bioscience, UK)
- Charantin (Xi'an Day Natural Tech, China)
- Cheese cloth (Scientific Laboratory Supplies, UK)
- ColorBurst™ Electrophoresis Marker for SDS-PAGE (Sigma, UK)
- Coomassie brilliant blue (Sigma, UK)

- Cryotubes (Scientific Laboratory Supplies, UK)
- Detoxi-gel endotoxin removal columns (Thermo Scientific, USA)
- D-glucose (BDH, UK)
- Dialysis tube size 3 (Visking, UK)
- Dimethyl sulfoxide, DMSO (Sigma, UK)
- Dulbecco's modified Eagle's medium, DMEM (Lonza SPRL, Belgium)
- ECL_1 and ECL_2 kits (Amersham Biosciences, UK).
- Eppendorf tubes (Scientific Laboratory Supplies, UK)
- Ethanol (Fisher Scientific International, UK)
- Ethylene diamine tetra acetic acid (Sigma, UK)
- E-toxate kit for endotoxin measurement (Sigma, UK)
- Ferric chloride (Sigma- Aldrich, UK)
- Ferrous chloride (Sigma- Aldrich, UK)
- Ferrous sulphate (Sigma- Aldrich, UK)
- Ferrozine (3-(2-pyridyl)-5, 6-bis (4-phenyl-sulfonic acid)-1, 2, 4-triazine (Fluka, UK)
- Fibroblast growth factor-basic, bFGF or FGF-2 (R & D Systems, USA)
- Foetal bovine serum, FBS (Lonza, Belgium)
- Folin-Ciocalteau reagent (Sigma, UK)
- Fresh *Momordica charantia* (Local store, Manchester, UK)
- Gallic acid (Sigma- Aldrich, UK)
- Gelatine, 0.1% w/v (Sigma- Aldrich, UK)
- Glycerol (BDH, UK)
- Glycine (BDH, UK)
- Glyoxalic acid (Fisher Scientific, UK)
- Goat anti-Rabbit Immunoglobulin G (IgG) (Dako, UK)

- Hydrochloric acid (Sigma, UK)
- Hydrogen peroxide (Sigma, UK)
- IgG1 Isotype Control from murine myeloma (Sigma, UK)
- Isopropanol (Sigma,UK)
- ISOTON® II Diluent (Bekman Coulter, UK)
- Lysozyme (Sigma, UK)
- Mannitol (Sigma, UK)
- Matrigel Basement Membrane matrix 10 ml (vWR, UK)
- Methanol (Fisher Scientific International, UK)
- Methylene blue stain (Sigma, UK)
- Methylglyoxal (Sigma, UK)
- N, N, N′, N′-tetramethylethylenediamine (Sigma, UK)
- Nitrocellulose membrane (Scientific Laboratory Supplies, UK)
- OxiSelect N-Epsilon CML Elisa Kit (Bioscience, UK)
- Parafilm (Scientific Laboratory Supplies, UK)
- Paraformaldehyde (Sigma, UK)
- Phosphate buffer saline (Lonza, UK)
- Plate sealers (R & D systems, USA)
- Potassium ferricyanide (Sigma, UK)
- Potassium phosphate mono- and di-basic anhydrous (Sigma, UK)
- Protease Inhibitor Cocktail (Sigma, UK)
- Rabbit anti-Mouse (Murine) IgG Mouse (Dako, UK)
- Rabbit IgG secondary antibody, Goat polyclonal to Rabbit IgG (Abcam, UK)
- Radioimmunoprecipitation assay buffer (Sigma, UK)
- RAGE (E-1), Monoclonal Antibody (Insight, UK)

- Razor blades (Kratos analytical, UK)
- Rutin (Sigma-Aldrich, UK)
- Skimmed milk powder (Local store, Manchester, UK)
- Sodium azide (Sigma, UK)
- Sodium bicarbonate (Sigma, UK)
- Sodium chloride (Sigma, UK)
- Sodium cyanoborohydride (Fluka, UK)
- Sodium deoxycholate (Sigma, UK)
- Sodium dihydrogen orthophosphate anhydrous (BDH, UK)
- Sodium dodecyl sulphate (BDH, UK)
- Sodium hydroxide (BDH, UK)
- Sodium salicylate (Sigma-Aldrich, UK)
- Sterile needle (BD Plastipak, UK)
- Thermanox plastic cover slips, 13mm diameter (Scientific Laboratory Supplies, UK)
- Tissue culture flasks (T-25, and T-75) (Scientific Laboratory Supplies, UK)
- Trichloroacetic acid (Sigma, UK)
- Tris (hydroxymethyl) methylamine (BDH, UK)
- Trypsin-10X (Sigma, UK)
- Tween 20 solution (Sigma, UK)
- VectaSpin 3 centrifuge tube filters (Sigma, UK)

2.2 Equipment and software

- Adobe illustrator CS4
- Adobe Photoshop 7.0
- Analytical balance (Sartorius Machatronics Ltd, UK)
- Automated cell counter (Bio-rad, UK)

- Autovortex mixer SA1 (Stuart Scientific Co, UK)
- Blender for fresh *Momordica charantia* (Kenwood limited, UK)
- Blotter (Hoefer Semi-Phor) (Amersham Pharmacia Biotech, UK)
- CE-4400 UV-VIS double beam scanning spectrophotometer (Cecil Instruments, UK)
- Centaur 2 MSE centrifuge (Fisons Scientific Equipment, UK)
- Centrifuge S415D (Eppendorf, Germany)
- Class II microbiological safety cabinet (Walker safety cabinet Ltd, UK)
- CO_2 incubator for cell culture use (Lab Impex Research, UK)
- Cross power 500 for electrophoresis (Atto, Japan).
- Digital multi-channel pipettes (Eppendorf, Germany)
- Dual gel casting electrophoresis chambers (Atto, Japan)
- Eppendorf Centrifuges 5415 D (Eppendorf, Germany)
- Fuji S2 Pro camera
- G Box Chem HR 16 (gel documentation and analysis system) (Syngene, UK)
- Gene tool image analyzer (Syngene, UK)
- Grant-bio shaker POS-300 (Grant Instruments Ltd, UK)
- Ice maker (P & S Refrigeration, UK)
- Image J software analyzer (free on line software)
- Inverted phase contrast microscope (Nikon TMS, Japan)
- Laboratory freezer Bio cold (Scientific Laboratory Supplies, UK)
- Laboratory fridge (Scientific Laboratory Supplies, UK)
- Laboratory pH/mV/temperature meter AGB-75 (Medical Scientific Instruments, England).
- LTE IP 30 incubator for glycation samples (Scientific Laboratory Supplier, UK)
- Luminescence spectrometer model LS 30 (Perkin Elmer LAS Ltd, UK).

- Magnetic stirrer hotplate (Stuart Scientific Co, UK).
- Media card reader (MISCO, UK)
- Micro flow biological safety cabinet (Bioquell Ltd, UK)
- Microplate reader, 96-well (Spectramax, Finland)
- Microsoft office Excel 2003 (Microsoft, USA)
- Mini-protein tetra system (Bio-rad, UK)
- Multiskan Go plate reader (Thermo, UK)
- Rotary evaporator RE100 (BUCHI, UK)
- Rotatest shaker R100 (Luckman Ltd, UK)
- Sigma laboratory centrifuge 3K10 for cell culture use (Howe, Germany)
- Single threshold coulter counter (Beckman Coulter, UK)
- Trans-blot SD semi-dry transfer cell (Bio-Rad Laboratories, Germany).
- TC10 Automated cell counter (Bio-Rad Laboratories, Germany)
- Ultrospec 2000 UV–VIS spectrophotometer (Pharmacia Biotech Ltd, UK)
- Water bath for cell culture use Grant JB series (Scientific Laboratory Supplies, UK)
- Water de-ionizer (Millipore, UK)

2.3 Solutions

- Preparation of 30% acrylamide solution **(solution A)** for SDS-PAGE: Acrylamide (29.2 g) and N, N´-methylene-bis-acrylamide (0.8 g) were dissolved in 100 ml of distilled water.
- Preparation of 10% ammonium persulphate (**solution D)** for SDS-PAGE: Ammonium persulphate (100 mg) was dissolved in 1 ml of distilled water.
- Preparation of 1 mg/ml Bovine serum albumin (BSA) standard solution for the Bio-rad protein assay: BSA (20 mg) was dissolved in 20 ml of distilled water.
- Preparation of blocking buffer (1% BSA-TBST): BSA (1g) was dissolved in 100 ml

of Tris-buffered saline and tween-20 (TBST). The pH was adjusted to 7.4.

- Preparation of destaining solution for SDS-PAGE: Methanol (250 ml) was added to acetic acid (70 ml) and the volume was made up to 1 L with distilled water.
- Preparation of revelation solution for Western blotting membrane: Mixture in equal volume of ECL_1 solution and ECL_2 solution.
- Preparation of electrode buffer (running buffer) for SDS-PAGE and Western blotting: Tris-base (12.02 g), SDS (4 g) and glycine (57.68 g) were dissolved in 2 L of distilled water. The buffer was stored at room temperature.
- Preparation of 5% milk-TBST used as blocking buffer for Western blotting: Skimmed milk (5 g) was dissolved in 100 ml of TBST buffer. The pH was adjusted to 7.4.
- Preparation of sample buffer for Western blotting: Tris-base (1.51 g), glycerol (20 ml), SDS (4 g), 2-mercaptoethanol (10 ml) and bromophenol blue (0.004 g) were dissolved in 100 ml of distilled water. The pH was adjusted to 6.8 and stored at -20°C.
- Preparation of sample treatment buffer for SDS-PAGE: Sodium dodecyl sulphate (0.1 g), 2-mercaptoethanol (0.1 ml) and glycerol (2 ml) were added to 1 ml of solution C and the volume was made up to 10 ml with distilled water.
- Preparation of separating solution for Western blotting analysis: Tris-base (45.5 g) and SDS (1 g) were dissolved in distilled water. The pH was adjusted to 8.8. The final volume of the buffer was made up to 250 ml with distilled water.
- Preparation of separating gel solution for 10% SDS-PAGE: Solution A (6 ml) and solution B (4.5 ml) were added to distilled water (7.5 ml) and mixed. Then, ammonium persulphate (80 µl) was added to the mixture. Gel polymerization was initiated by adding TEMED (10 µl) and allowed to set for 45 – 60 minutes.
- Preparation of separating gel (12.5%) for Western blotting: Separating solution (2.5 ml) was added to distilled water (4.2 ml) and mixed with 40 % acrylamide/bis-

acrylamide solution (3.3 ml). Then, ammonium persulphate (100 µl) was added to the mixture. Gel polymerization was initiated by adding TEMED (10 µl) and allowed to set for 20 – 25 minutes.

- Preparation of (0.05, 0.1 and 0.2 M) sodium phosphate buffer solution (pH 7.4): the acid component of the buffer (sodium dihydrogen phosphate) and the basic component (sodium hydroxide) were weighed out in a certain ratio according to the Henderson Hasselbalch equation. The desired volume was then accordingly adjusted with distilled water and the solution was mixed. The pH was adjusted to 7.4. Sodium azide (3 mM) was added to the mixture to prevent any bacterial growth. The buffer was stored at 4 °C.
- Preparation of stacking gel (4.5%) for SDS-PAGE: Solution A (0.9 ml) and solution C (1.5 ml) were added to distilled water (3.6 ml) and mixed. Then, ammonium persulphate (20 µl) was added to the mixture. Polymerization was initiated by adding TEMED (10 µl). The gel was allowed to set for 30 minutes.
- Preparation of stacking solution used for Western blotting: Tris-base (15 g) and SDS (1 g) were dissolved in distilled water. The final volume of the buffer was made up to 250 ml with distilled water. The pH was adjusted to 6.8.
- Preparation of staining solution for SDS-PAGE: Coomassie brilliant blue (2.5 g) was dissolved in methanol (500 ml) and acetic acid (100ml). The volume was made up to 1 L with distilled water and then filtered.
- Preparation of TBST buffer: Tris-base (2.422 g), NaCl (16.36 g), and Tween 20 (2 ml) were dissolved in 2 L of distilled water. The pH was adjusted to 7.4.
- Preparation of Towbin buffer: Tris-base (1.51 g), glycine (7.2 g) and SDS (0.167 g) were dissolved in 425 ml distilled water and 75 ml of methanol. The pH was adjusted to 8.3. Preparation of tracking dye solution for SDS-PAGE: Bromophenol blue (1 mg)

was dissolved in glycerol (0.1 ml) and mixed with 0.9 ml of distilled water.

- Preparation of 0.5 M Tris-HCl buffer (**solution C)** for SDS-PAGE: Tris (hydroxymethyl) aminomethane (6.1 g), SDS (0.4 g) and HCl (4.2 ml) were dissolved in distilled water up to 1 L. The pH was adjusted to 6.8.
- Preparation of 1.5 M Tris-HCl buffer (**solution B)** for SDS-PAGE: Tris (hydroxymethyl) aminomethane (18.2 g), SDS (0.4 g) and HCl (2 ml) were dissolved in distilled water. The pH was adjusted to 8.8.
- Preparation of tubing dialysis: Appropriate length of tubing was cut and boiled in distilled water for 10 minutes. The tubes were stored at 4 °C in distilled water containing few drops of chloroform to prevent any bacterial growth.
- Reconstitution of FGF-2: Sterile phosphate-buffered saline was added to the vial in order to prepare a working stock solution (100 μg/ml). The carrier-free protein was immediately used upon reconstitution to avoid loss in activity. FGF-2 aliquots were stored at -20 °C.

2.4 Methods

2.4.1 Preparation of extracts

Aqueous MC flesh and pulp extracts were prepared according to a modified method previously described (Virdi *et al.*, 2003). Flesh and pulp of MC (130 mg) were extracted using methanol in a ratio of 1:10. The homogenization was done in a blender at the highest speed set with one minute burst for a sum of 12 minutes. The homogenized extract was filtered through cheesecloth. A rotary evaporator was used to evaporate methanol and any remaining methanol was evaporated using a water bath at 100 °C.

2.4.2 Preparation of AGEs

Briefly, either BSA or lysozyme (10 mg/ml) was incubated at 37 °C with glucose (0.05-0.5 M) or methylglyoxal (0.1 M) in sodium phosphate buffer (0.1 M, pH 7.4) containing 3 mM sodium azide for different time intervals (Mashilipa *et al.*, 2011). The prospective inhibitors of AGE formation such as MCP extract, MCF extract and charantin were introduced into the incubation mixture simultaneously. Control sample was incubated under the same conditions without the addition of sugars or inhibitors. All incubations were carried out in triplicate. After incubation, un-reacted sugar was removed by dialysis against distilled water for 2 days at 4ºC. The aliquots were removed immediately and stored at -20ºC until analysis. Markedly, the removal of endotoxin from the glycated and non-glycated solutions was achieved using Detoxi-gel resin columns. BSA-AGE formation was assessed by measuring the absorbance at 585 nm with a fluorescence spectrophotometer. The endotoxin level of the solution of BSA-AGEs was estmated with an E-toxate kit based on *Limulus Amebocyte* lysate assay and was found to be below the detection limit (< 0.125 EU/mL). Moreover, BSA-AGEs were dissolved in DMEM and were accordingly filtered with the use of a sterile 0.2 μm filter. The endotoxin-free BSA-AGE solution was kept at -20°C.

2.4.3 Preparation of carboxymethyllysine (CML)

Carboxymethyllysine (CML)-modified protein was prepared based on an established method described by (Reddy *et al.*, 1995). In brief, BSA (100 mg) was incubated at 37ºC for 24 hours with Glyoxalic acid (3 mg) as well as $NaCNBH_3$ (10 mg) in 0.2 M sodium phosphate buffer (10 ml, pH 7.8). To remove unbound sugars, the sample was dialysed against distilled water. Different concentrations (5-15 mg/ml) of MCP, MCF as well as charantin extracts were added to the mixture. After incubation, the aliquots were stored at -20ºC until analysis.

2.4.4 Protein dialysis

The removal of unbound sugars following glycation was achieved using dialysis against distilled water. Samples of protein were delivered into the tubing of the dialysis system and dialysed against 2 litres of distilled water. The samples were stirred at 4ºC with 4–5 changes implemented over a two-day period. Following dialysis, samples were stored at -20 ºC.

2.4.5 Protein estimation using Bio-Rad protein assay

BSA was used at 1 mg/ml (1 µg/µl) as a standard protein for calibration. Protein lysate (10 µl) was mixed with distilled H_2O (90 µl) in a bijoux tube. Bio-Rad protein assay (2 ml) was added to each tube. Absorbance of the protein solution was measured at 595 nm with a spectrophotometer. An example of standard curve established for protein estimation is shown below.

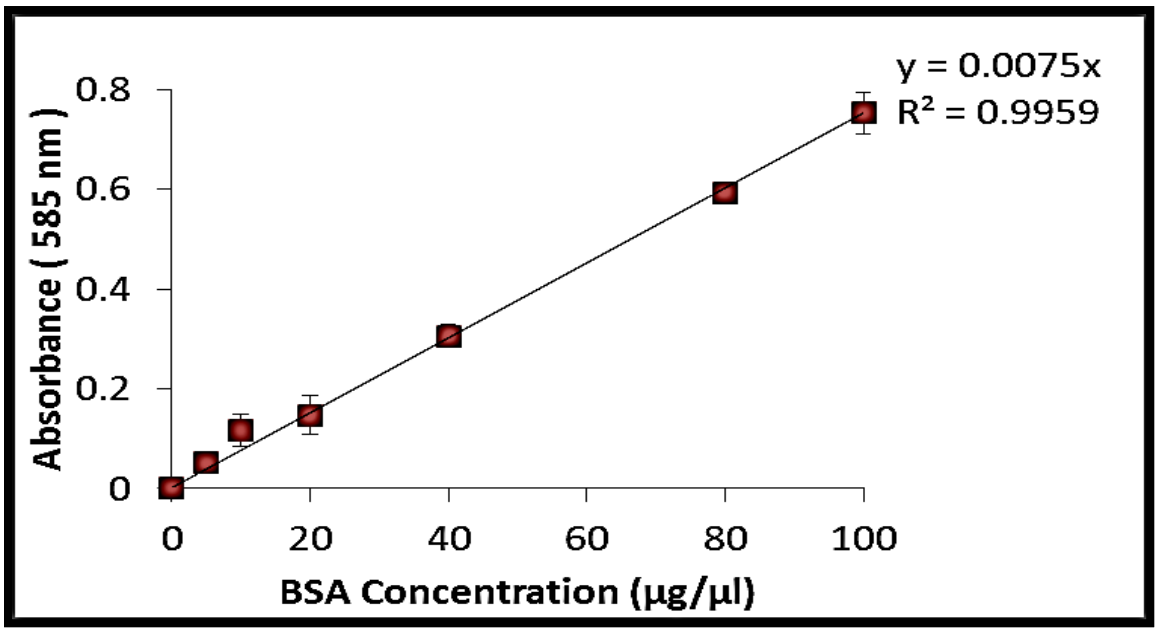

Figure 2.1: Calibration graph for protein measurement using the Bio-Rad method.

Each value represents the mean ± SD (n = 3).

2.4.6 Endotoxin removal from BSA-AGEs and extracts

The Detoxi-gel resin column underwent regeneration through wash cycles with five resin-bed volumes of 1% sodium deoxycholate, and subsequently by 3-5 resin-bed volumes of basal DMEM. Bovine serum albumin-AGEs or natural extracts were diluted in DMEM containing red phenol (used a tracking dye) then added to the column. The flow of column was ceased when the samples filled the resin-bed from top to bottom. Following, incubation was carried out for 60 minutes at room temperature prior to samples being collected. In an attempt to achieve greater efficiency with a gravity-flow column, the samples emerged from the column after the void volume was collected.

2.4.7 Determination of endotoxin content in BSA – AGE solutions

BSA-AGE solutions were analysed to detect the remaining endotoxin content using E-toxate kit. Samples, water and endotoxin standards (100 µl) were added to the endotoxin-free glass test tubes. Subsequently, E-toxate working solution (100 µl) was added to each tube by inserting a pipette to just above the contents, and the lysate was then allowed to flow down the side of the tube. The tubes were mixed gently and covered with parafilm®, and incubated for 1 hour at 37 °C. Following incubation, the tubes were gently inverted 180°C and observed for evidence of gelation. The formation of a hard gel was considered to be a positive test. All other results including soft gels, turbidity, and increased viscosity or clear liquid were considered to be negative tests. Notably, the amount of endotoxin level (EU/ml) was calculated using the following formula:

Endotoxin (EU/ml) =1/ (Highest dilution of sample found positive) X Lowest concentration of Endotoxin standard found positive

2.4.8 Detection of AGE's

2.4.8.1 Measurement of cross-linked AGEs by SDS-PAGE

Integrity and cross-linking of glycated proteins were determined by the extent of dimer and polymer formation in protein samples removed from cross-linking assays carried out in the presence of MCP, MCF and charantin extracts. The cross-linking efficiency was assessed using 10 % SDS-PAGE according to the method of Laemmli (1970). Protein samples were diluted 1:10 in 0.5 M Tris-HCl buffer, pH 6.8 containing 1 % (w/v) SDS, 1 % (v/v) 2-mercaptoethanol and 20% (v/v) glycerine and then boiled for 5 minutes. Samples containing 1–2 mg/ml of protein and standard molecular weight marker were loaded into the wells followed by 2–3 µl of bromophenol blue and then subjected to electrophoresis using the mini-Protean® 3 apparatus. Gels were stained in a solution containing 0.25 % (w/v) Coomassie brilliant blue R, 50 % (v/v) methanol and 10 % (v/v) acetic acid. Gels were destained in a solution containing 25 % (v/v) methanol and 7 % (v/v) acetic acid.

2.4.8.2 Image analysis of SDS-PAGE gels

The gels were photographed using Gene snap programme from G Box Chem HR16 imaging system. Bands were compared within the same gel. Integrated Density (I.D) was measured to analyse the one dimensional electrophoretic gels and the percentage inhibition of cross-linked AGEs was calculated using the following formula:

% inhibition = 100 x (I.D without inhibitor – I.D with inhibitor) / I.D without inhibitor

2.4.8.3 Measurements of fluorescent AGEs

The formation of AGEs was assessed by their characteristic of fluorescence emission spectra at 420 nm after excitation at 350 nm. Glycated samples (10 mg/ml) were thawed at room temperature and 0.2 ml of each sample were diluted in 1.8 ml of distilled water to give a solution with a final concentration of 1 mg/ml. Fluorescent measurements were carried out

using a fluorimeter. Fluorescence intensity standards were used to calibrate with quinine sulphate (1 ng/ml) in H_2SO_4 and monitor the performance of the instrument. Distilled water solution was used as a blank to zero the spectrophotometer. The fluorescence of AGEs was expressed in arbitrary units (AU) per mg of protein.

2.4.8.4 Detection of CML using ELISA

Samples (100 µl) were transferred to 96-well plates and incubated overnight at 4 °C, and wells were rinsed twice with 250 µl of PBS. Add 200 µl of assay diluent to the wells, plates were left for 2 hours at room temperature on an orbital shaker, and were then washed 3 times using 1X washing buffer. Diluted primary antibody (1:1000) of anti-CML-antibody (100 µl) was added to the wells and plates were left at room temperature for 1 hour incubation on an orbital shaker. Any unbound antibody was removed by washing the wells 3 times with 1X washing buffer. Diluted HRP conjugated-secondary antibody (1:1000) was added to the wells and plates were left at room temperature for 1 hour incubation on an orbital shaker. Any unbound secondary antibody was removed by washing 3 times with 1X washing buffer. A warm HRP substrate solution (100 µl) was added to the wells and the plate was left for 20 minutes at room temperature. The enzyme reaction was stopped by adding a stop solution (100 µl) to each well and the absorbance was determined at 450 nm using a microplate reader.

2.4.9 Methods for antioxidant activity of *Momordica charantia*

2.4.9.1 DPPH radical scavenging capacity

1, 1-diphenyl-2-picryl-hydrazyl (DPPH) free radical-scavenging activity of extracts was calculated according to a modified version of an established procedure (Tang *et al.*, 2004). Different extracts of (15 mg/ml) MCP, MCF extracts and charantin were mixed with 0.5 ml of methanolic solution that includes DPPH radicals (0.1 mM) and kept at room temperature

for 30 minutes in the dark. The absorbance was measured at 517 nm with a spectrophotometer. Ascorbic acid was utilized as a positive control and the distilled water was used as a blank to zero the spectrophotometer. Free radical-scavenging activity (FRSA) was computed as [(A-B)/B*100] where:

A= the absorbance of 0.5 ml of the extracts mixed with 0.5 ml of DPPH solution.

B= the absorbance of 0.5 ml of the extracts mixed with 0.5 ml of methanol.

2.4.9.2 Metal chelating activity

The ability of MCP, MCF extracts and charantin to chelate ferrous ions (Fe^{2+}) was assessed according to a modified version of an established procedure (Loizzo *et al.*, 2012). Briefly, the reaction mixture was composed of 500 µl of extracts (5–15 mg/ml), 50 µl of $FeCl_2$ (2 mM) and 600 µl of deionized water. The mixture was shaken well and incubated at room temperature for 10 minutes. A volume of 100 µl of 5 mM ferrozine was then added, mixed and left for another 5 minutes to complex the residual Fe^{2+}. The absorbance with the Fe^{2+} ferrozine complex was measured at 562 nm with a spectrophotometer. Ethylene diamine tetra acetic acid solution (EDTA) was used as a positive control and the distilled water was used as a blank to zero the spectrophotometer. The chelating activity of the extract for Fe^{2+} was calculated from the following formula: Chelating rate = [1 – (absorbance of the sample) / (absorbance of control)] ×100 %

2.4.9.3 Hydroxyl radical scavenging activity

The hydroxyl radical scavenging activity of MCP, MCF extracts and charantin were tested based on a modified approach previously described (Kubola and Siriamornpun, 2008). Hydroxyl radical trapping property was assessed by monitoring the hydroxylation of salicylate by the Fe^{3+}-salicylate-H_2O_2 system. The reaction mixture was composed of 1 ml of $FeSO_4$ (1.5 mM), 0.7 ml of H_2O_2 (6 mM), 0.3 ml of sodium salicylate (20 mM) and 1 ml of

extracts (5-15 mg/ml) and incubated for 1 hour at 37ºC. The absorbance was measured at 562 nm with a spectrophotometer. Mannitol was used as a positive control and the distilled water was used as a blank to zero the spectrophotometer. The scavenging activity of hydroxyl radicals was calculated as follows:

Scavenging activity (%) = $[1 – (A_1 – A_2)/A_0] \times 100$

Where A_0 was the absorbance of the control, A_1 was the absorbance of the extract and A_2 was the absorbance without sodium salicylate.

2.4.9.4 Measurement of reducing power

The reducing power of the MCP, MCF extracts and charantin were measured using a modified version of an established procedure described by Tsai *et al.*, (2006). In brief, a volume of 2.5 ml of extracts (15 mg/ml) were mixed with 2.5 ml of 0.2 M sodium phosphate buffer (pH 6.6) and 2.5 ml of 1% $K_3Fe(CN)_6$. The mixture was incubated for 30 minutes at 50 ºC. A volume of 2.5 ml of 10 % TCA (w/v) was added and the samples were centrifuged at 1000 rpm for 10 minutes. The supernatant (2.5 ml) was mixed with 2.5 ml of distilled water and 0.5 ml of 0.1% of $FeCl_3$. The absorbance was measured at 700 nm. Blanks were prepared using distilled water without extracts to zero the spectrophotometer. Ascorbic acid was used as positive control.

2.4.9.5 Measurement of total phenolic compounds

The amount of total phenolic compounds in MCP, MCF extracts and charantin were estimated according to a modified version of an established procedure described by (Miliauskas et al., 2004). Briefly, aliquots of 1 ml of the ethanolic MCP, MCF and charantin extracts (10 g/l) were mixed with 5 ml of folin-ciocalteau reagent (diluted 10-fold), mixed and incubated for 3 minutes at room temperature. A volume of 5 ml of 10% Na2CO3 solution was added, and the mixture was incubated for 1 hour at room temperature. The standard

curve was prepared using (0 - 0.3 mg/ml) ethanolic gallic acid solution. The absorbance was measured at 760 nm and the final results were expressed as mg/g of gallic acid equivalents (GAE). A standard curve required is shown below. A phenolic compound in Momordica charantia extracts in gallic acid equivalents (GAE) was calculated as follows: C= c * v / m

Where: C total content of phenolic compounds, mg/g plant extracts, in GAE

c: the concentration of Gallic acid established from the calibration curve (mg/ml)

v: the volume of extracts (ml)

m: the weight of pure plant extracts (g)

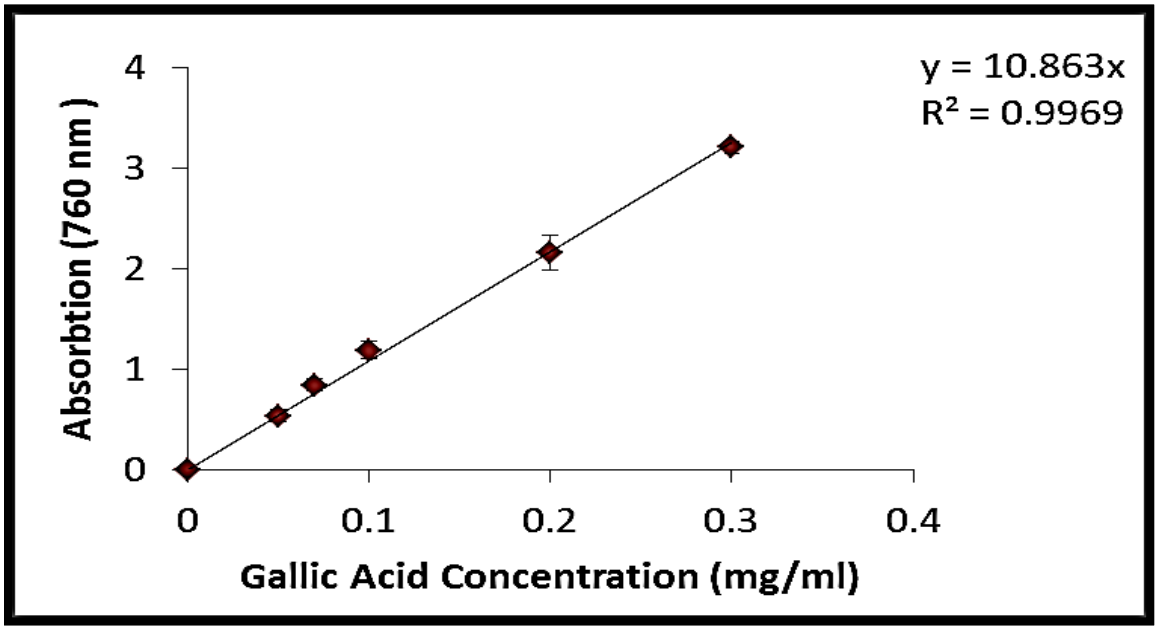

Figure 2.2: The standard curve using ethanolic gallic acid solution

Gallic acid (0 - 0.3 mg/ml) was used as a standard solution for phenolic contents. Each value represents the mean ± SD (n = 3).

2.4.9.6 Measurement of total flavonols

The content of flavonols was determined by a colorimetric method according to a modified version described by Miliauskas *et al*. (2004). Briefly, Aliquots of 1 ml of ethanolic MCP, MCF extracts and charantin (10 g/l) were mixed with 1 ml $AlCl_3$ in ethanol (20 g/l) and 3 ml (50 g/l) sodium acetate ethanol, the mixture was incubated for 1 hour at 20 ºC. The absorbance was measured at 440 nm. Blank sample were prepared without the extract. The standard curve was prepared using (0 - 0.5 mg/ml) rutin ethanolic solutions. Flavonols contents had been expressed in milligrams of rutin comparable per gram of extract. Total flavonols compound in *Momordica charantia* extracts in Rutin equivalents (RE) was calculated as follows: $X= C*V/m$

Where: X total content of flavonols compound, mg/g plant extracts, in RE

c: the concentration of Rutin established from the calibration curve (mg/ml)

v: the volume of extracts (ml)

m: the weight of pure plant extracts (g)

2.4.9.7 Measurement of total flavonoid

The content of Flavonoid was determined by a colorimetric method according to a modified version described by Miliauskas *et al*. (2004). Briefly, a volume of 1 ml of ethanolic MCP, MCF extracts and charantin (10 g/l) was mixed with equal volumes of 2 % $AlCl_3$ in ethanol (20 g/l). The mixture was shaken and incubated for 40 minutes at 20 ºC. The absorption was measured at 415 nm with a spectrophotometer. Blank sample was prepared without the extracts. Flavonoid contents were expressed in milligrams of rutin is equivalent per gram of extract. Total flavonoid compound in *Momordica charantia* extracts in Rutin equivalents (RE) was calculated as follows: $X = (A*m_0*10)/ (A_0*m)$

where: X—flavonoid content, mg/g plant extract in (RE)

A—the absorption of plant extract solution

A_0—the absorption of standard rutin solution

m—the weight of plant extract, g

m_0—the weight of rutin in the solution,

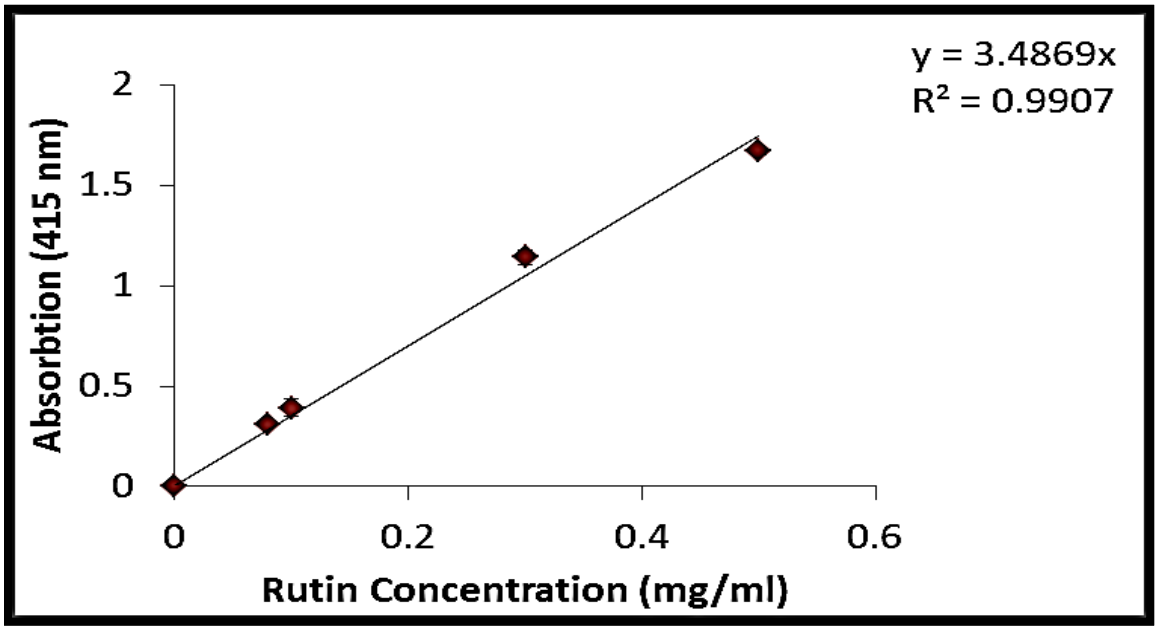

Figure 2.3: The standard curve using ethanolic Rutin solution

Rutin (0 - 0.5 mg/ml) was used as a standard solution for flavonoid and flavonols contents. Each value represents the mean ± SD (n = 3).

2.4.10 Methods for cell culture

2.4.10.1 Thawing of cells

Cryotubes containing the frozen bovine aortic endothelial cells (BAEC) were taken from a liquid nitrogen container, and were carefully cleaned with 70% ethanol. The frozen cells were in a freezing medium containing 10% DMSO and 90% FBS. During the thawing process, the

medium was thawed until became liquid but still cold to prevent any cell toxicity effect of the DMSO, a cryo-protector agent. The cell suspension was transferred to a universal tube containing a cold complete 15% FBS medium. The suspension was centrifuged at 1300 rpm for 5 minutes. The supernatant was then discarded and the cell pellet was re-suspended in 1 ml of warm fresh complete medium. Subsequently, cells were seeded in T-75 flasks and incubated at 37°C in a humidified atmosphere of 95% air and 5% CO_2-incubator.

2.4.10.2 Heat inactivation of foetal bovine serum (FBS)

Frozen FBS bottle (previously stored at -20°C) was incubated in a water bath (at a temperature of 37°C) until the serum was totally thawed. The heat-inactivation of the foetal bovine serum proteins occurred for 30-45 minutes in the water bath at 56°C. Notably, every 10 minutes, the bottle would be turned. Following this period, the bottle was taken out from the water bath and allowed to settle until it reached room temperature. Aliquots of heat-inactivated serum (50 ml Falcon tubes) were stored at - 20°C.

2.4.10.3 Preparation of complete medium supplemented with 15% FBS

In order to prepare 500 ml of complete medium supplemented with 15% FBS, the following reagents were mixed as described in Table 2.1:

Table 2.1: Preparation of culture medium supplemented with 15% FBS.

Reagent	Volume of medium (500ml)
DMEM	420 ml
FBS	75 ml
PSG	5 ml

2.4.10.4 Preparation of serum-poor medium supplemented with 2.5% FBS

Serum-poor medium (SPM) containing 2.5% FBS was prepared by diluting 15% FBS with DMEM (in 100 ml) as indicated in Table 2.2.

Table 2.2: Preparation of culture medium supplemented with 2.5% FBS.

Reagents	2.5% FBS
DMEM with PSG (0% medium)	83.34 ml
15% FBS	16.66 ml

2.4.10.5 Culture of bovine aortic endothelial cells

Bovine aortic endothelial cells (BAEC) were given by Dr. Sabine Matou-Nasri (Cell and Molecular Biology Research Laboratory, Manchester Metropolitan University). The endothelial cells were previously characterised by the presence of the von Willebrand factor. In tissue culture T-75 flasks coated with 0.1% gelatine, BAEC were cultured in complete medium composed of 15% FBS-DMEM supplemented with 2 mM L-glutamine, 100 U/ml penicillin and 100 μg/ml streptomycin. The culture flasks were put at 37°C in a humidified atmosphere of 95% air and 5% CO_2-incubator.

2.4.10.6 Trypsinization and sub-culture of cells:

Upon confluence being reached, the medium was removed and discarded from the T-75 flask. Then, the cells were washed with 10 ml of sterile PBS and incubated with 5–10 ml of 1X trypsin solution for 2-5 minutes at 37°C. When cell detachment was achieved by the enzymatic action of the trypsin, 5 ml of complete medium were added to the flask to counteract the activity of the trypsin. The cell suspension was centrifuged at 1300 rpm for a

period of 5 minutes at room temperature. After discarding the supernatant, the cell pellet was re-suspended in fresh complete medium, and then split at a ratio 1:2 before being seeded in new T-75 flasks for sub-culture, which corresponded to a new passage. Throughout all the studies, the cells were used between passage 4 and 12.

2.4.10.7 Preparation of freezing medium:

Freezing medium was composed of 90% FBS and 10% DMSO. For example, for 25 ml of freezing medium, 2.5 ml of sterile DMSO were added to cold FBS (22.5ml). To avoid any risk of contaminations, the freezing medium was filtered and stored at -20°C. Fresh freezing medium was defrosted shortly before use.

2.4.10.8 Freezing of cells:

Two cryotubes with an estimated 5 x 10^5 cells in freezing medium per cryotubes were prepared from the same confluent flask and stored at –20°C for a period of half-an-hour. Subsequently, they were either stored overnight at –80°C or stored for 1 hour in liquid nitrogen. The cells were subsequently moved into liquid nitrogen for long-term storage.

2.4.10.9 Cell counting

Cells were counted using a Beckman-Coulter counter and repeated three times for accuracy. Briefly, the cell suspension (0.05 ml) was diluted in isotonic solution (10 ml) in a counting chamber. Each cell count was based on the aspiration of 0.5 ml of cell suspension. Therefore, the cell concentration was calculated as follows:

Cell number / ml = mean of three cell counts x dilution factor (200) / 0.5 ml

2.4.10.10 Assessment of cell proliferation using the Coulter counter

BAEC (2.5 x 10^4 / ml) were seeded in complete medium in 24-well plates (0.5 ml / well). The cells were incubated for approximately 4 hours, the time to adhere to the bottom of the well. Then, the complete medium was discarded and the cells were washed gently 3 times with

PBS. Fresh media supplemented with 2.5% FBS, defined as serum-poor medium (SPM), was added to each well. Different concentrations of BSA-AGEs, native BSA, MCP, MCF and charantin extracts were added to the wells for 72 hours incubation. MCP, MCF and charantin extracts were also tested in the presence of BSA-AGEs. FGF-2 (25 ng/ml), a pro-angiogenic growth factor, was used as positive control. Control wells with untreated cells cultured in complete medium were also included in the experiments. After 72 hours incubation, the cells were washed 3 times with PBS and trypsinized. The number of cells was counted using the Beckman-Coulter counter. Each experiment was carried out in triplicate, and repeated at least three times independently.

2.4.10.11 Assessment of cell viability using automated cell counter

BAEC ($2.5x10^4$ / ml) were seeded in complete medium in 24-well plates (0.5 ml / well). After 4 hours incubation, the complete medium was discarded and the cells were washed gently with PBS (3 times). Fresh SPM was poured into each well. Different concentrations of BSA-AGEs, BSA, MCP, MCF and charantin extracts were added to the wells. FGF-2 (25 ng/ml) was used as positive control. Control wells with untreated cells cultured in complete medium were included. After 72 hours incubation, the cells were washed 3 times with PBS and trypsinized. Cell sample (10 µl) was mixed in equal volume with trypan blue (10 µl), a cell viability dye excluded by live cells and took up by dead cells. The cell viability was assessed using TC10, an automated cell counter. Each experiment was carried out in triplicate, and repeated at least three times independently.

2.4.10.12 Assessment of cell migration (wound healing assay)

Sterilized Thermanox plastic coverslips were placed into each well of a 24-well plate. BAEC (1×10^5 /ml) were seeded in complete medium on each coverslip (0.5 ml / well). After 24 hours incubation, at pre-confluence, the complete medium was replaced with SPM for a further 24-48 hour-incubation. Attached to the coverslip, the cell monolayer was washed with

PBS (3-4 times) then wounded on each side of the central area with a sterile razor blade producing straight edged cuts. The wounded cell monolayer was washed with PBS to remove cellular debris or dislodged cells then placed in a new 24-well plate containing fresh SPM. Different concentrations of BSA-AGEs, native BSA, MCP, MCF and charantin extracts were added to the wells. MCP, MCF and charantin extracts were also tested in the presence of BSA-AGEs. FGF-2 (25 ng/ml) was used as positive control. Control wells with untreated cells cultured in SPM were included in the experiments. After 18-24 hours incubation, the coverslips were rinsed 3 times with PBS, fixed in 100% ethanol for 5 minutes, and allowed to air-dry. Cells were stained with methylene blue for 5 minutes and excess stain was removed with distilled water. The plates were left to air-dry. Pictures of 5 random areas of each coverslip with straight edged cuts were taken using phase contrast microscopy (10X magnification). The migration of the cells into the cell denuded area was quantified by counting the numbers and the distance of migrated cells in each field of view. The distance of migration was determined using Image J software (http://rsbweb.nih.gov/ij/indix.html). Each experiment was carried out in triplicate, and repeated at least three times independently.

2.4.10.13 Assessment of cell differentiation (Matrigel™ tube formation assay)

Endothelial cell differentiation to form vascular tube-like structures is the final and key step of angiogenesis. About 24 hours before the experiment, the Matrigel™ matrix (a reconstituted basement membrane and reduced in growth factors) was transferred from the freezer to the fridge to thaw. Sterile yellow tips were placed in the freezer to avoid the gel polymerization. Matrigel™ and sterile Eppendorf tubes were placed on ice. After trypsinization of the cells and centrifugation, cells were re-suspended in 1 ml of complete medium. Then, 32 µl of BAEC (1 x 106/ml) were mixed with a volume of 8 µl of BSA-AGEs, native BSA, MCP, MCF and charantin extracts at various concentrations and 40 µl of Matrigel™ at 4°C, on ice. MCP, MCF and charantin extracts were also tested in the presence

of BSA-AGEs. The addition of 8 µl of complete medium and FGF-2 (25 ng/ml) to the cells were used as control and positive control, respectively. The final mixture (80 □l) was equally poured under a spot shape into two wells (35 µl / well) of a 48-well plate per each condition. The Matrigel™ was allowed to polymerise for 1 hour incubation. Following polymerization, 500 µl of complete medium were added in order to cover each (un) treated cell/Matrigel™ spot. After 24 hours incubation, the cells were washed twice with PBS and then fixed with 4% paraformaldehyde for 15 minutes. Using a phase contrast microscopy (100X magnification), the photomicrographs were taken with a digital camera.

2.4.11 Western blotting

2.4.11.1 Cell treatment and cell lysis for Western blot

BAEC (3 x 10^5/ml) were seeded in complete medium in a 24-well plate (0.5 ml /well). After 24 hours incubation, at pre-confluence, the medium was discarded, and the cells were washed with PBS (3 times). Fresh SPM was added to each well for further 24 hours incubation. MC extracts (10 µg /ml) were added to the cells for 10 minutes incubation. Promptly, at the end of the incubation, the medium was discarded, and the cells were rinsed with 500 µl of cold PBS. Ice cold radioimmunoprecipitation assay (RIPA) buffer (100 µl) was added to lyse the untreated cells (control) and cells treated with FGF-2 (positive control) or MC extracts. Gently the plate was shaken on ice for a few minutes, cells were scraped using a cell scraper. The total cells lysates were transferred to cold Eppendorf tubes on ice and stored at -20°C until used.

2.4.11.2 Western blot

The acrylamide gel was prepared by mixing 40% bis-acrylamide (3.3 ml) with distilled water (4.2 ml) and separating buffer (2.5 ml) in a universal tube. Ammonium persulphate (APS) solution (10%, 100 µl) was added followed by 10 µl TEMED solution and the separating gel

was left to polymerise for 25 minutes. A few drops of isopropanol were added on top of the mixture. Isopropanol was removed after 25 minutes and rinsed with plenty of distilled water. As much as possible, distilled water was removed using a piece of Whatman® filter paper and then the stacking solution was prepared in a second universal tube, by mixing 40% bis-acrylamide (1.45 ml) with distilled water (6.1 ml), and stacking buffer (2.5 ml). As previously, 10% APS (100 µl) was added followed by TEMED solution (10 µl) and the stacking gel was left to polymerise for 15 minutes. The combs, clamps, and gaskets were then removed carefully to avoid damaging the wells and the gel plates were inserted into the electrophoresis chamber. The chamber was subsequently filled with electrode buffer (25 mM Tris, 192 mM glycine, 0.1% SDS, pH 8.3) in the space between the two sets of glass plates. Protein samples, sample buffer and molecular weight marker were taken out from the freezer and left to thaw at room temperature. The amount of proteins of each sample was determined by Bio-Rad protein assay and was fixed at 15 µg for equal protein loading into the wells. Equal volume of protein samples and 2X sample buffer were mixed in Eppendorf tubes. The tubes were placed in the boiling water for 15 minutes. The molecular weight marker (10 µl) and the protein samples (around 20 µl) were gently loaded. The sample buffer (20 µl) was added to the first and the last well while in the second well, the molecular weight marker was added. The syringe was washed after loading the marker and after each sample. Samples containing (15 µg) protein (up to 20 µl solution), along with pre-stained molecular weight markers, were separated by SDS-PAGE (10% w/v) at 60V for 45-60 minutes, until the samples tracked with the bromophenol blue (from the sample buffer) reached the top of the separating gel. Then during the protein separation, the voltage was increased up to 200V for 30-45 minutes, until the dye reached the bottom of the separating gel.

2.4.11.3 Blotting of gel

Two nitrocellulose membranes and 12 pieces of blotting paper were soaked for 2 minutes in Towbin buffer, the transfer buffer. Stacking gels were removed from the separation gels and discarded. The gels were sandwiched separately. The sandwich was performed in an electro-blotter for each gel in the following order: three pieces of blotting paper, one piece of nitrocellulose membrane, gel and at the top 3 pieces of blotting papers. Any bubbles within the sandwiches were removed by rolling a clean 5 ml tip over the sandwich. Proteins were transferred from the gel to the membrane with a current fixed at 40 mA for 1 gel or 90 mA for 2 gels, for one hour.

2.4.11.4 Blocking the nitrocellulose membranes

Membranes were blocked with 1% BSA-TBS Tween (pH 7.4) for 1 hour at room temperature on rotating shaker. The blocking buffer was discarded and 10 ml of primary antibody solution (1:1000) such as rabbit polyclonal anti-ERK1/2 and mouse monoclonal anti-p-ERK1/2 antibodies were poured onto each nitrocellulose membrane, then left on a rotating shaker overnight at 4°C. The membranes were subsequently washed five times for 10 minutes in TBS-tween at room temperature. Then, each membrane was immersed in 10 ml of mouse anti-rabbit or rabbit anti-mouse horseradish peroxidase-conjugated secondary antibody solution (1:1000) diluted in TBS-tween containing 5% (w/v) de-fatted milk for ERK1/2 and p-ERK1/2, respectively. After 1 hour at room temperature on the rotating shaker, the secondary antibody solutions were discarded and the membranes were washed five times for 10 minutes in TBS-tween.

2.4.11.5 Development of nitrocellulose membranes

In a dark room, the nitrocellulose membranes were immersed in enhanced chemiluminescence (ECL) solution. To prepare the ECL solution, 1 ml of solution-A was added to 1 ml of solution-B and kept in the dark room for five minutes at room temperature.

Then the reactive ECL solution (1 ml) was poured onto the membrane for one minute and the excess of the reagent was drained off from the membrane. To avoid the membranes drying out and to protect them from light, they were quickly wrapped in cellophane films and kept in a black box. The box containing the nitrocellulose membranes was taken to the G-Box for image analysis and the fluorescence intensities of the bands were quantified using image J analysis software. The results were semi-quantitative and compared to the control.

2.4.12 RAGE neutralization

2.4.12.1 Cell culture for Western blot

BAEC (3 x 10^5 /ml) were seeded in complete medium in a 24-well plate (0.5 ml / well). When they reached pre-confluence, the medium was discarded, and the cells were washed with PBS. Fresh SPM was added to each well, and then 20 µg/ml of mouse polyclonal anti-RAGE antibody or 20 µg/ml of its isotype control (IgG1) were added to the medium. After 2 hours incubation, the cells were treated with BSA-AGEs, MCF, MCP and charantin extracts for 10 minutes incubation. The medium was subsequently discarded, and each well was rinsed with 500 µl of cold PBS. RIPA buffer (100µl) was added to each wells and kept on ice. Gently the plate was shaken on ice for a few minutes and the cells were scraped using a cell scraper. The total cells lysates were transferred to cold Eppendorf tubes on ice and stored at –20°C until used.

2.4.12.2 Assessment of cell differentiation after RAGE neutralization

Matrigel™ and sterile Eppendorf tubes were placed on ice. T-75 flasks were washed with PBS then the cells were scraped to maintain intact the structure of transmembrane protein RAGE. After centrifugation, cells were re-suspended in 1 ml of complete medium. BAEC (1 x 10^6 /ml) were mixed with 20 µg/ml of anti-RAGE antibody or with 20 µg/ml of isotype control (IgG1) and kept on ice for 1 hour. Then, the cells were handled in the absence or

presence of FGF-2, BSA-AGEs and natural extracts according to the Matrigel™ tube formation assay's method as previously described (2.4.3.13).

2.4.13 Statistical analysis

Statistical analysis was made through using Microsoft Office Excel 2007. The results of each experiment are expressed as mean ± Standard Deviation. Data were analysed for statistical significance using Student *t*-test and ANOVA. Variations with p values ≤ 0.05 were considered statistically different. Each experiment was performed at least three times and some illustrated data were shown in representative model.

Chapter 3. Antioxidant activities of *Momordica charantia* extracts

3.1 Introduction

Oxidative stress is the most important risk factor of the beginning of diabetes and its complications. Over the last decade, it has been proved that there is a strong relationship between oxidative stress and diabetes (Rains and Jain, 2011). It has been known that oxidative stress increased in insulin-dependent (type 1) and non-insulin-dependent diabetes (type 2) (Rahimi *et al.*, 2005). Oxidative stress is increased by reactive oxygen species (ROS) with the free radical formation, also considered as key indicator of oxidative stress (Tabatabaei-Malazy *et al.*, 2013). Glutathione and catalase are antioxidant enzymes mainly produced by the liver to counteract the effects of these reactive oxygen species. Moreover, natural antioxidant compounds can be extracted from external sources such as natural products (Okayama *et al.*, 2006). It has been proposed earlier that antioxidant compounds found in MC extract exert a strong activity against oxidative stress (Mahomoodally *et al.*, 2012). In this chapter, the antioxidant activity of several MC extracts was assessed using different *in vitro* antioxidant assays. The content of flavonols, flavonoids and phenolic compound in various MC extracts was also determined *in vitro* leading to the establishment of the link between antioxidation activities and antiglycation of MC extracts.

3.2 Aims and objectives

The aim of the present study is to investigate and compare the antioxidant activities of MCP, MCF extracts and charantin *in vitro*.

3.3 Methods

Antioxidant activities of all MCP, MCF extracts and charantin were assessed using the DPPH as described in section (2.4.9.1). Hydroxyl radical-scavenging activity was assessed as

mentioned in section (2.4.9.3). Metal chelating activity of MCF, MCP and charantin was measured as explained in section (2.4.9.2). Reducing power of all extracts was also measured as described in section (2.4.9.4). The phenolic, flavonols and flavonoid contents of all extracts were also determined using methods as explained on sections (2.4.9.5), (2.4.9.6) and (2.4.9.7).

3.4 Results

3.4.1 Effect of MCP, MCF extracts and charantin on DPPH radicals:

In the presence of MCP, MCF as well as charantin, the particular changes in colour from deep-violet to light-yellow and succeeding drop in absorbance of the constant DPPH radical were calculated at 517 nm on spectrophotometer. The percentage inhibitions were used to evaluate the protective effect of 15 mg/ml of MCP, MCF and charantin extracts on major DPPH search activity *in vitro*. All extracts were showed a significant ($p< 0.001$). Inhibition compared to control, MCF have more scavenging activity (Figure 3.1).

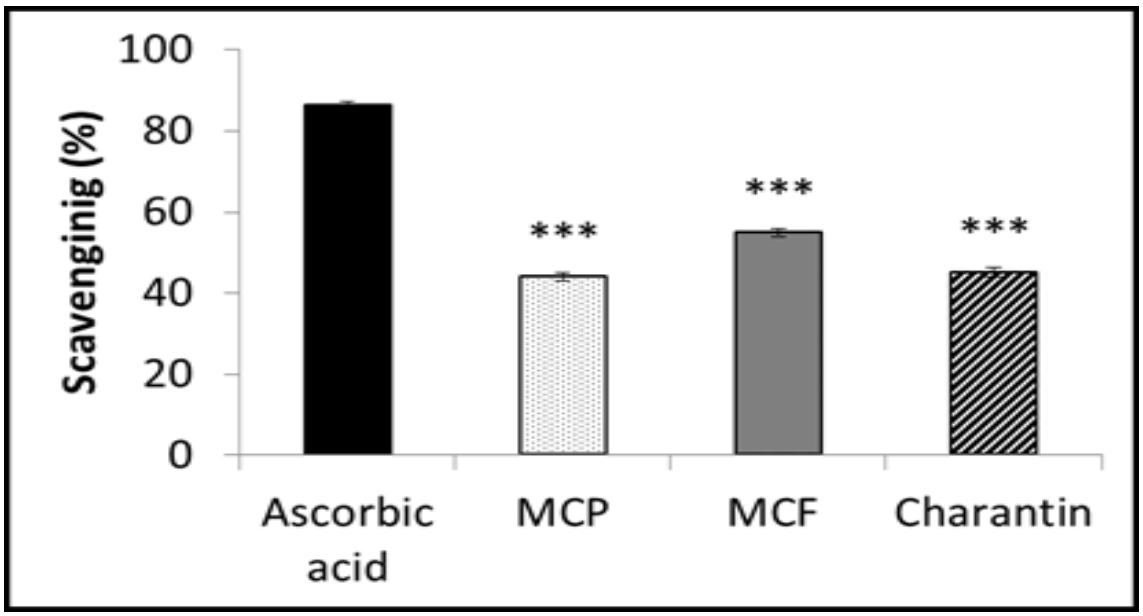

Figure 3.1: Effect of MCP, MCF extracts and charantin on DPPH radical scavenging activity. The bar graph shows the effect of 15 mg/ml of MCP, MCF and charantin on DPPH radicals. 1,1-Diphenyl-2-picryl-hydrazyl radicals were prepared by dissolving DPPH in methanol. This solution was mixed with an equal volume of 15 mg/ml of MCP, MCF and charantin. The samples were kept in the dark for 15 minutes at room temperature and the decrease in absorption was measured at 517 nm. Ascorbic acid was used as positive control. Results are presented as mean ± SD (n=3). *** $p < 0.0001$

3.4.2 Effect of MCP, MCF extracts and charantin on metal chelating activity:

The ability of MCP, MCF and charantin to chelate transition metal ions has been screened by simply examining Fe^{2+}-ion chelation. The metal chelating power of all extracts has been examined towards ferrous ions. In this assay, almost all extracts showed variable chelating activity since confirmed by simply their effectiveness within lowering ferrozine complex in dose dependent manner ($p < 0.001$). MCP possesses much more chelating activity in comparison to other extracts (Figure 3.2).

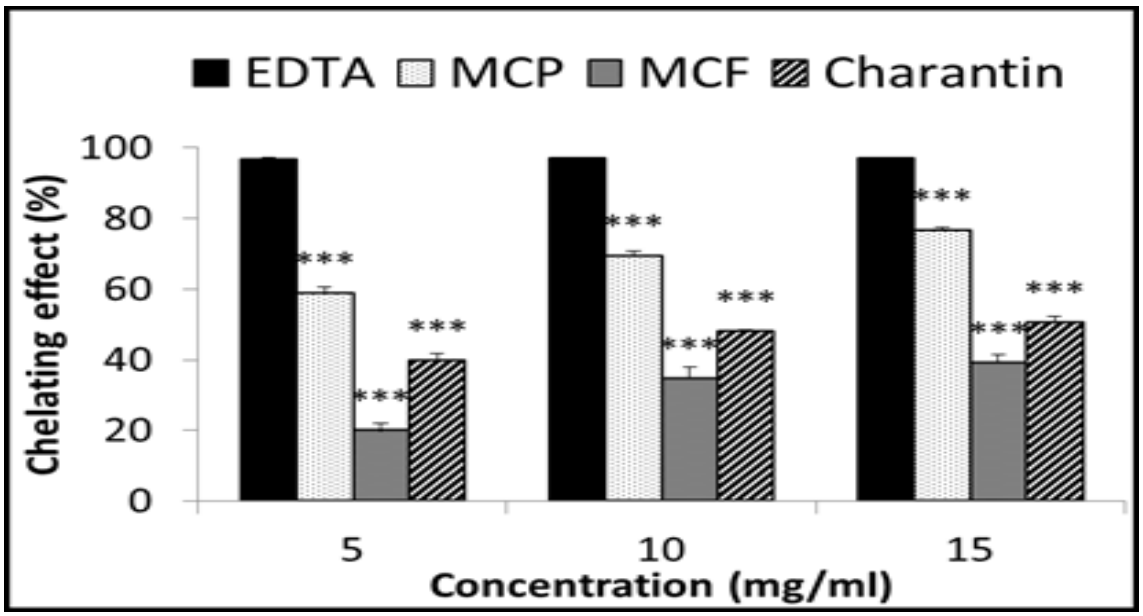

Figure 3.2: Metal chelation activity of MCP, MCF extracts and charantin. The bar graph shows the effects of different concentrations (5-15 mg/ml) of MCP, MCF extracts and charantin on metal chelation. Ethylene diamine tetra acetic acid was used as a positive control. Results are presented as mean ± SD (n=3). *** $p < 0.0001$

3.4.3 Effect of MCP, MCF extracts and charantin on hydroxyl radical scavenging activity:

The actual scavenging abilities of MCP, MCF and charantin extracts on hydroxyl radical reserve from the 2- deoxyribose corrosion method. The results usually are mentioned as a percentage inhibition. All three extracts raise hydroxyl radical hunt in a dependent mode of dose. MCF had highest scavenging than other extracts but lesser than ascorbic acid (Figure 3.3).

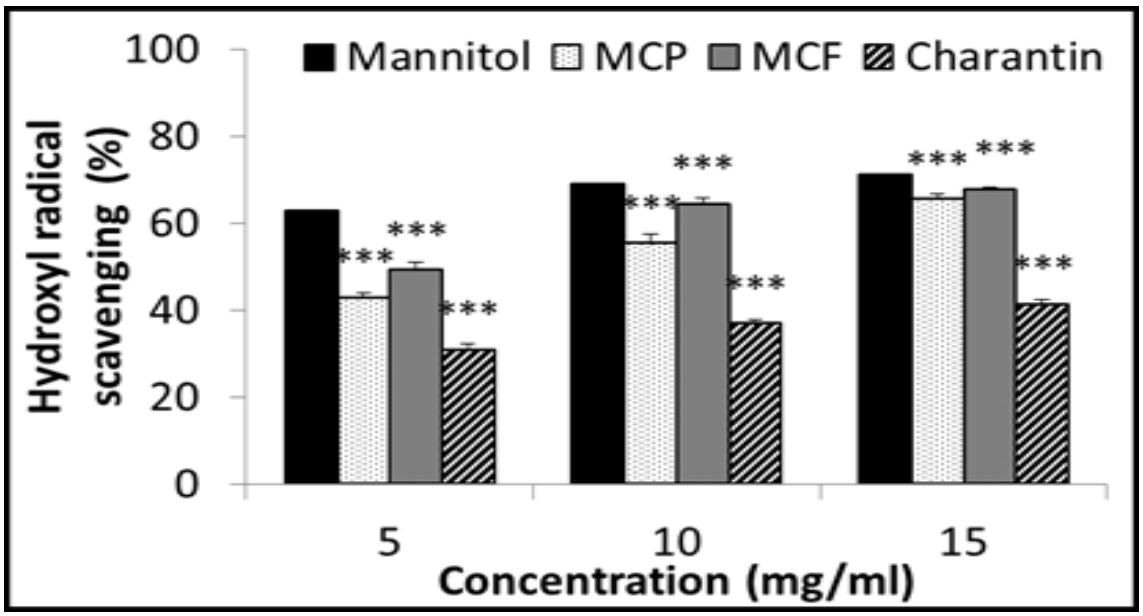

Figure 3.3: Hydroxyl radical scavenging activity of MCP, MCF extracts and charantin. The bar graph shows the effect of different concentrations (5-15 mg/ml) of MCP, MCF extracts and charantin on hydroxyl radicals. Mannitol was used as a positive control. Results are presented as mean ± SD (n=3). *** $p < 0.0001$

3.4.4 Effect of MCP, MCF extracts and charantin on reducing power:

MCP, MCF and charantin at the concentration of 15 mg/ml showed significant reducing power as demonstrated by their effectiveness in reducing ferric ions to ferrous ions. The results clearly indicate that MCP, MCF and charantin extract have high reducing power compared to the control (Ascorbic acid) (Figure 3.4). In contrast, the lowest reducing activity was found in MCP with 83% of inhibition when tested at the same concentration.

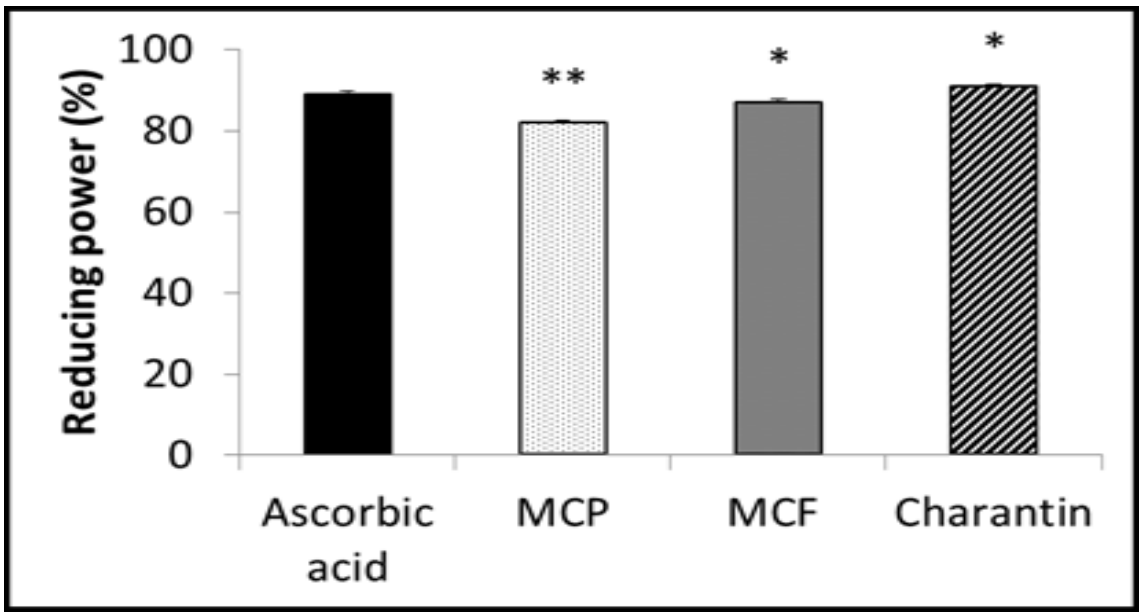

Figure 3.4: Reducing power of MCP, MCF extracts and charantin. The bar graph shows the effect of 15 mg/ml of MCP, MCF extract and charantin on reducing power. Ascorbic acid was used as a positive control. Results are presented as mean ± SD (n=3). * $p < 0.05$, **$p < 0.01$

3.4.5 Total phenolic content of MCP, MCF extracts and charantin:

The substances of phenolic compounds (mg/g) in MC extracts were articulated in gallic acid corresponding (GAE). The results demonstrated that this overall phenolic amount in every component different significantly, the contents of total phenols in all extract as measured by Folin-Ciocalteau reagent in terms of gallic acid equivalent. The highest amount was found in MCF extract with a value of 175.33 ± 2.30 mg/g whereas for MCP extract was 134.66 ± 1.15 mg/g, and the lowest amount was found in charantin extract with 81±1.51 (Figure 3.5).

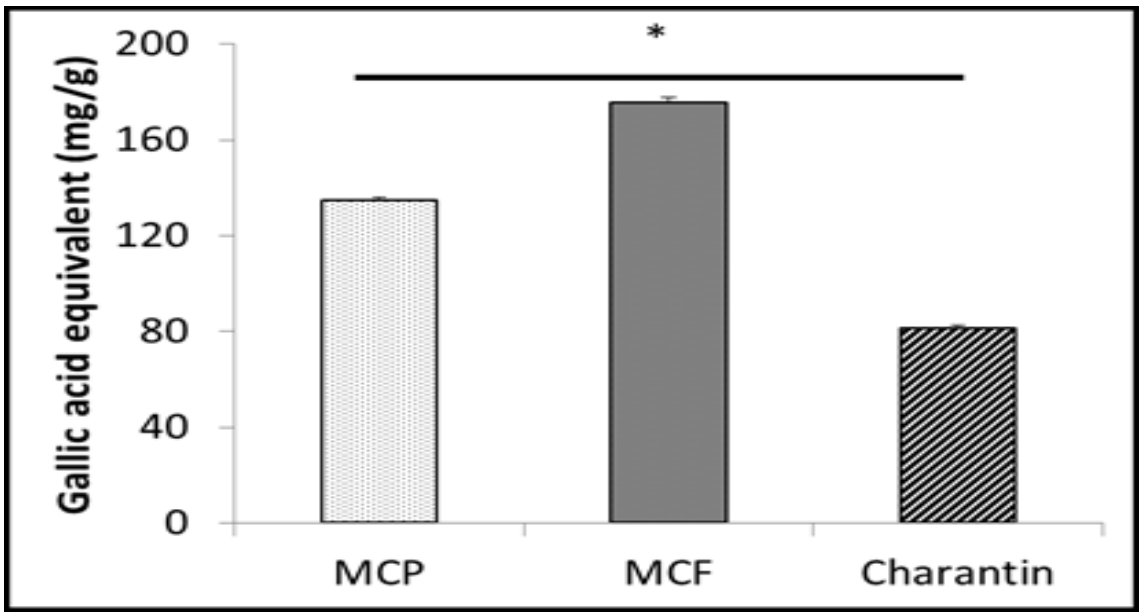

Figure 3.5: Total amount of phenolic compound in MCP, MCF extracts and charantin.

The content of phenolic compounds in 10g/l ethanolic MCP, MCF and charantin were expressed in gallic acid equivalents (GAE). Results are presented as mean ± SD (n=3). * $p < 0.05$

3.4.6 Total Flavonols content of MCP, MCF extracts and charantin:

The content of flavonols compounds (mg/g) in MC extracts were resolute and articulated in rutin equivalents. The concentration of flavonols mixed in a smaller amount as resemble with total phenolic and flavonoid. The highest amounts were found in MCP extract with a value of 47.86± 0.91 mg/g, whereas for MCF extract was 41.11 ± 1.38 mg/g and charantin was found to be the lowest with a value of 30.33±1.90 (Figure 3.6).

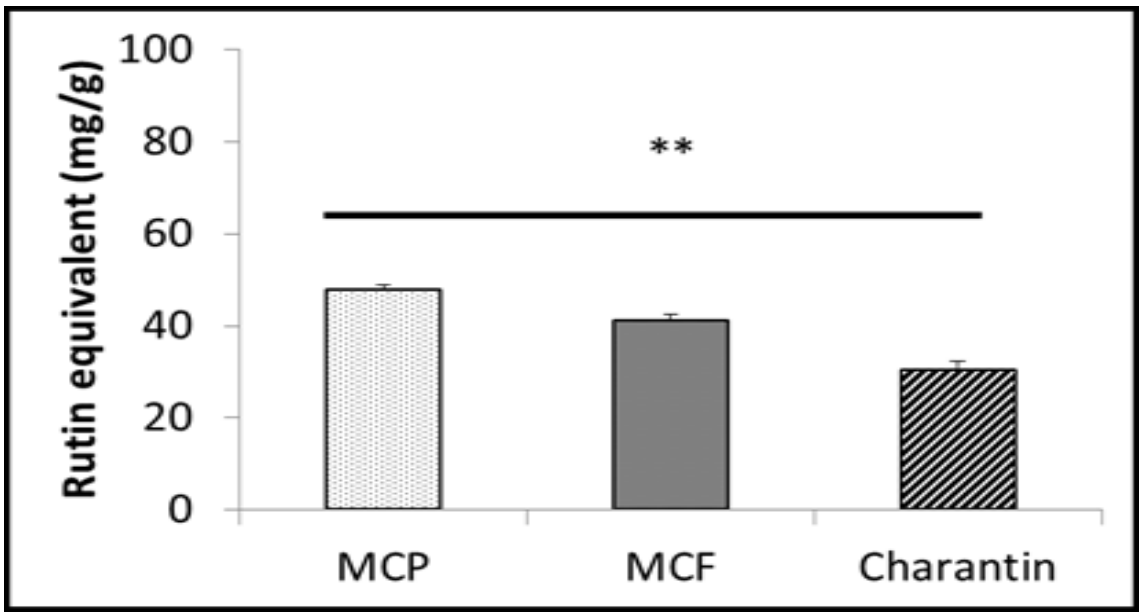

Figure 3.6: Total amount of Flavonols content in MCP, MCF extracts and charantin. The content of flavonols in (10g/l) ethanolic MCP, MCF and charantin were expressed in rutin equivalents. Results are presented as mean ± SD (n=3). **p < 0.01

3.4.7 Total Flavonoid content of MCP, MCF extracts and charantin:

The total of flavonoid substance of MCP, MCF and charantin mixture were moreover equivalent to rutin. This result, as presented in, showed that total flavonoid contents ranges from 134.67 ± 1.89 mg/g – 64.55 ± 2.03 mg/g. The flavonoid content in MCF extract was notably ($p < 0.05$) more than that in MCP and charantin extracts (Figure 3.7).

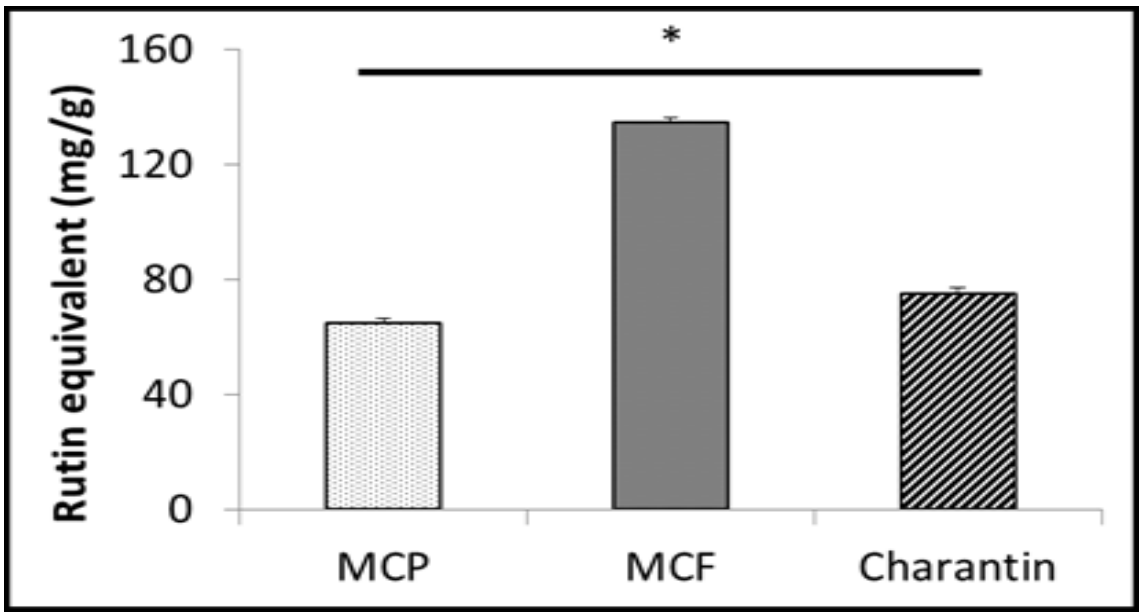

Figure 3.7: Total amount of flavonoid content in MCP, MCF extracts and charantin. The content of flavonoid in (10g/l) ethanolic MCP, MCF and charantin were expressed in rutin equivalents. Results are presented as mean ± SD (n=3). * $p < 0.05$

3.5 Discussion

In the present study, all extracts found to have antioxidant properties against DPPH radical with MCF have the most potent. These results supported the finding by Lin *et al*., (2011). The DPPH radical scavenging activity of phenolic compounds in MC extracts is because of their redox properties, which closely depends upon the chemical structure of the compound, the number of hydroxyl groups and the substitution pattern of hydroxyl groups (Roy *et al.,* 2007). In a previous similar finding, MC extract has been shown to chelates Cu^{2+} ions and protects against LDL oxidation (Hsieh *et al*., 2005). The chelation activities of ferrous ions by MC extracts were assessed by measuring the absorption of ferrozine-ferrous complex. In the presence of ferrous chelating agents; the complex formation is disrupting and lead to the reduction of the red colour of the complex. Therefore, measurement of colour reduction

reflects an index of metal chelation activity of coexisting chelators (Chua *et al*., 2008). The hydroxyl radical is a strong reactive free radical produced in biological systems and has the power to damage the majority of biomolecules in living cells (Sim and Sil, 2008). The present study has revealed that all extracts can scavenge hydroxyl radicals *in vitro* in a dose dependent manner. Furthermore, MCF extract has better scavenger when compared with MCP and charantin extracts. It has been established that the reducing power might be linked with a polyphenol chemical substances, which were proven to apply antioxidant properties by donating a hydrogen atom (Kubola and Siriamornpun, 2008, Kumaran and Karunakaran, 2007). The results of this study indicate that MCF and charantin extracts reduce ferricyanide complex to ferrous ions more efficiently when compared with MCP (Krishnaiah *et al*., 2011). The small antioxidant compounds of molecular weight, for instance polyphenols, flavonoids and flavonols, were found in MC (Gogi *et al*., 2010, Krishnaiah *et al*., 2011, Shan *et al*., 2012). The results of the present study show that MCF extract which contains the maximum amount of phenolic substances show greatest antioxidant activity. Furthermore, MC may have antioxidant activities due to ascorbic acid (Vitamin C), Vitamin A and Vitamin E (Behera, 2005). The findings from these results confirmed that antioxidants properties correlate with antiglycation activities in some plants (Ahmad and Ahmed, 2006), in this regards, antiglycation activities of MC extracts were investigated in the next chapter.

Chapter 4. Antiglycation properties of *Momordica charantia* extracts

4.1 Introduction

High glucose levels in the body cause more AGE formation (Hsu and Zimmer, 2010). Over the past decade, there has been considerable interest in glycation and its role in the development of diabetic complications. The formation and accumulation of AGEs has been shown to play an important essential role in the pathogenesis of diabetic complications through (Jack and Wright, 2012). Therefore, in order to prevent diabetic complications, inhibitors of AGE formation may have an important role for future therapy. The uses of many plant-based preparations as oral hypoglycaemic agents have been subjected to scientific evaluation (Keter and Mutiso, 2012) including MC also known as the bitter gourd. MC is used for the management of several diseases including hypertension and diabetes. A number of researchers have examined the anti-diabetic properties of MC (Singh *et al*., 2011) and hypoglycaemic properties (Joseph and Jini, 2013). However, the antiglycation activity of MC has not been investigated yet.

In this chapter, several methods were performed *in vitro* to compare the effects of MCP, MCF, and charantin on the formation of cross-linked AGEs. In addition, fluorescence measurement was used to identify and characterize the formation of fluorescent AGEs. To detect the effects of different MC extracts on inhibition of protein cross-linking, lysozyme dimerization by methylglyoxal followed by SDS-PAGE analysis was used. ELISA assay was used to examined antiglycation properties of MC extracts on a specific AGE like CML.

4.2 Aims and objectives

The aim of this study is to investigate and compare the effect of MCP, MCF and charantin extracts on the formation of AGEs *in vitro*.

The objectives of this study are:

- To identify and compare the effects of different concentrations of sugars and different period of incubations on fluorescent AGEs and formation of cross-linked AGEs *in vitro.*
- To investigate and compare the ability of MCP, MCF and charantin extracts to inhibit the formation of cross-linked AGEs *in vitro*.
- To study and validate the effect of MCP, MCF and charantin extracts on the formation of a named AGE ie CML *in vitro* using ELISA.

4.3 Methods

Lysozyme was glycated by incubating with different concentration of sugars in the presence / absence of MC extracts (section 2.4.2). The formation of fluorescent AGEs was assessed by their characteristic fluorescence (section 2.4.8.3). Cross-linked AGEs were assessed using sodium dodecyl sulphate polyacrylamide gel electrophoresis (SDS-PAGE) followed by Coomassie blue staining as described previously in section (2.4.8.1). CML was detected using ELISA as mentioned in section (2.4.8.4).

4.4 Results

4.4.1 Effect of different glucose concentrations on florescent AGE formation *in vitro*

Effect of varying concentrations of glucose (0.05 – 0.5 M) on glycation of lysozyme *in vitro* was found by determining the intensity of fluorescence. Figure 4.1 illustrates the effect of

different concentrations of glucose on fluorescent AGE formation over 14 days. Subsequent analysis was made by using 0.5 M glucose. As shown in Figure 4.1, the fluorescence intensity of lysozyme incubated with glucose increased significantly ($p < 0.01$) as compared with the control. Magnitude of this effect depended on the concentration of glucose. The effect determined for lysozyme being incubated for 14 days with 0.5 M glucose was more than 9.2-fold greater as compared to control and 1.5-fold greater than the effect observed in case of 0.05 M glucose.

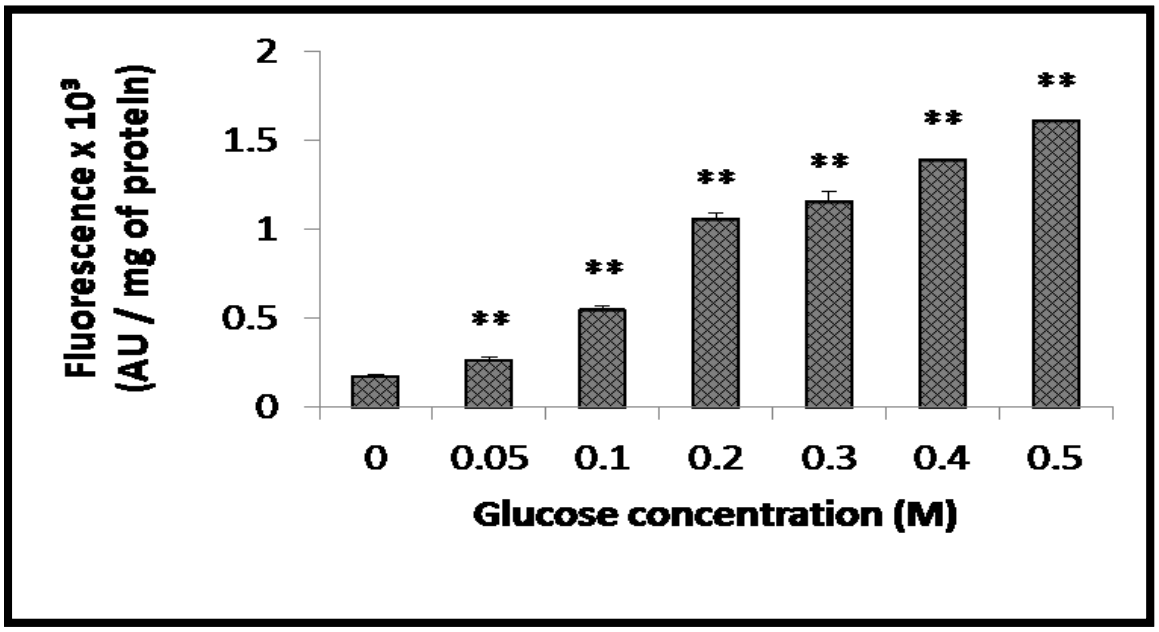

Figure 4.1: The effect of different glucose concentration on fluorescent AGE formation in the lysozyme-glucose system. The bar graph shows the effect of different concentrations of glucose on fluorescent AGE formation. Lysozyme (10 mg/ml) was incubated with different concentrations of glucose (0 – 0.5 M) in 0.1 M sodium phosphate buffer of pH 7.4 at 37 °C for 14 days. Each value represents the mean ± SD (n = 3), **p < 0.01.

4.4.2 Effect of period of incubation on fluorescent AGE formation *in vitro*

It has been determined during the study that the fluorescence intensity, an indicator of AGE production, increased gradually during incubation and reached its optimum level on 15th day. A significantly ($p < 0.01$) lesser intensity of fluorescence was demonstrated by the control lacking glucose as compared to the intensity determined in the presence of glucose from 3rd day to the last day of incubation. Fluorescence obtained in case of lysozyme incubation with glucose for 15 days was more than 12.1-folds greater as compared to control and 2-folds greater than the starting time of incubation (Figure 4.2).

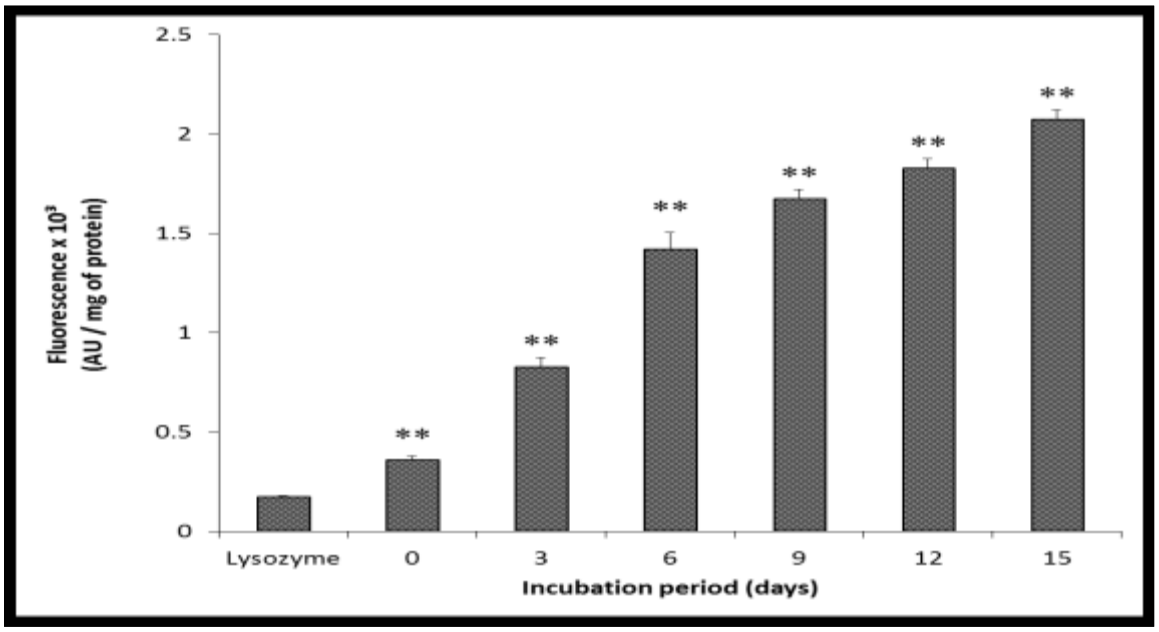

Figure 4.2: The effect of different incubation time on fluorescent AGE formation in the lysozyme-glucose system. The bar graph shows the effect of different incubation times on fluorescent AGE formation. Lysozyme (10 mg/ml) was incubated with glucose (0.5 M) in 0.1 M sodium phosphate buffer of pH 7.4 at 37 °C for 15 days. Each value represents the mean ± SD (n = 3), **p < 0.01.

4.4.3 Effect of different glucose concentration on cross-linked AGE formation *in vitro*

The influence of different concentrations of glucose incubated with lysozyme on the cross-linked AGE production over 15 days of incubation at 37ºC is shown in Figure 4.3. When glucose is incubated with lysozyme, cross-linked AGEs are produced that cause formation of dimers having a molecular weight of approximately 28 kDa as indicated by molecular weight markers (Figure 4.3, lane a). Decreased electrophoretic mobility with higher M_r as compared to control was observed with varying concentrations of glucose (Figure 4.3, lane c to h).

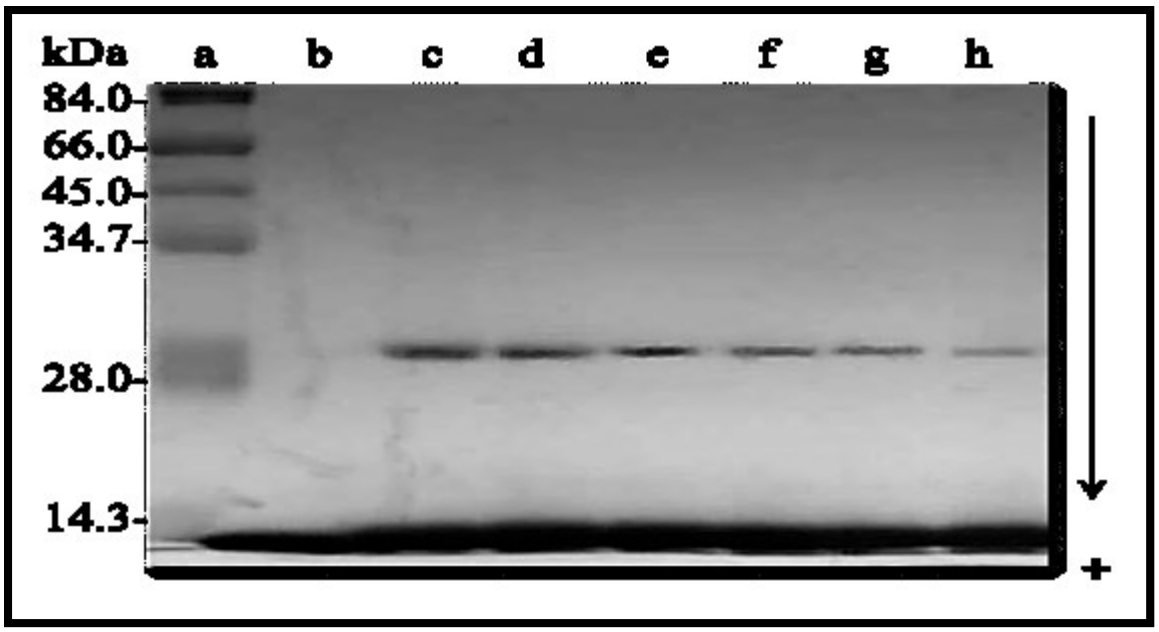

Figure 4.3: The effect of different glucose concentration on cross-linking AGE formation in the lysozyme-glucose system. Gel showing lysozyme (10 mg/ml) incubated alone (lane b) or in the presence of different glucose concentrations (c) 0.5 M, (d) 0.4 M, (e) 0.3 M, (f) 0.2 M, (g) 0.1 M and (h) 0.05 M in 0.1 M sodium phosphate buffer of pH 7.4 at 37 °C for 15 days. The cross-linked AGEs were analysed using SDS-PAGE and stained with Coomassie blue. The result is a representative figure of at least three independent experiments.

The formation of cross-linked AGEs upon lysozyme incubation with glucose demonstrated significant ($p< 0.05$) increase in comparison with control as illustrated in Figure 4.4. This influence also depended on the dose of glucose. The cross-linked AGE formation was more than 24-fold greater when lysozyme was incubated for 15 days with 0.5 M glucose as compared to the control and 3.9-fold greater when 0.1 M glucose was used.

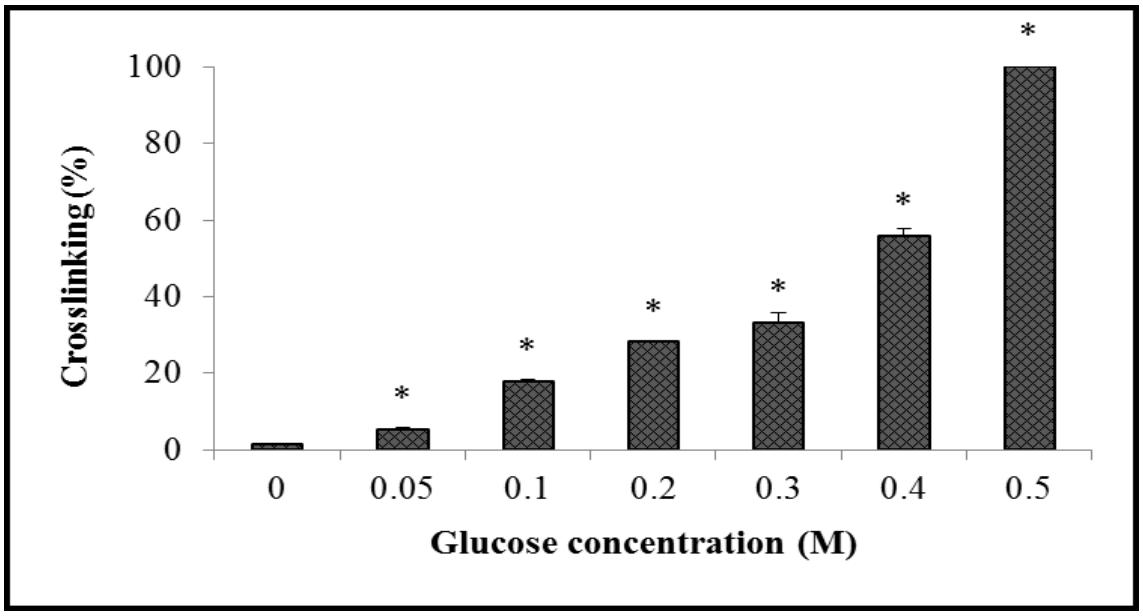

Figure 4.4: The effect of different glucose concentration on cross-linked AGE formation in the lysozyme-glucose system. The bar graph shows the scanning of SDS-PAGE gel to show the effect of Lysozyme (10 mg/ml) with different concentrations of glucose (0 – 0.5 M) in 0.1 M sodium phosphate buffer of pH 7.4 at 37 °C for 15 days. Each value represents the mean ± SD (n = 3), * $p < 0.05$.

4.4.4 Effect of period of incubation on cross-linked AGE formation *in vitro*

Adequate quantity of cross-linked AGEs was produced when lysozyme was allowed to react with glucose for varying incubation periods. The control sample contained lysozyme only (Figure 4.5, lane b). In comparison with the control, decreased electrophoretic mobility due to

greater relative molecular weight (M_r) was demonstrated by glycated lysozyme at different times during incubation as shown in Figure 4.5, lane c to h.

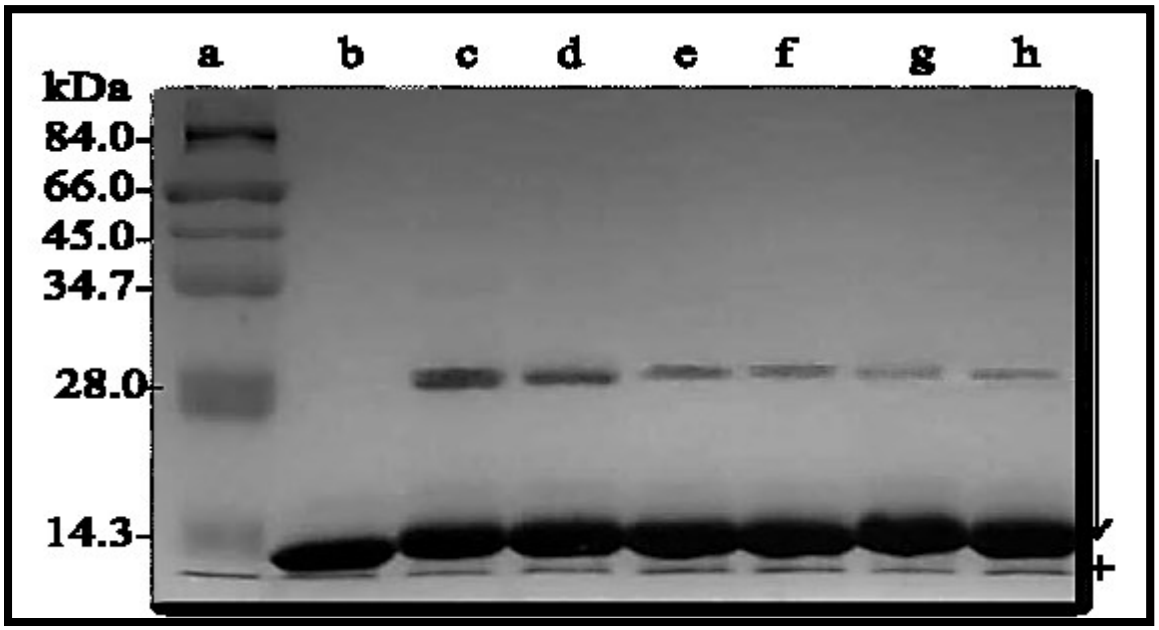

Figure 4.5: The effect of different incubation time on cross-linking AGE formation in the lysozyme-glucose system. Gel showing lysozyme (10 mg/ml) incubated alone (lane b) or in the different incubation time (c) 15 days, (d) 12 days, (e) 9 days, (f) 6 days, (g) 3 days and (h) 0 day with glucose in 0.1 M sodium phosphate buffer of pH 7.4 at 37 °C for 15 days. The cross-linked AGEs were analysed using SDS-PAGE and stained with Coomassie brilliant blue solution. The result is a representative figure of at least three independent experiments.

It is evident from the scanning of this gel as shown in Figure 4.6 that the formation of cross-linked AGEs was significantly ($p< 0.05$) increased in comparison with control sample and this occurred in a dose dependent manner as earlier. The formation of cross-linked AGEs was more than 60 folds greater when lysozyme was incubated with glucose for 15 days as compared to control and 4.67 folds greater when incubated for 0 day.

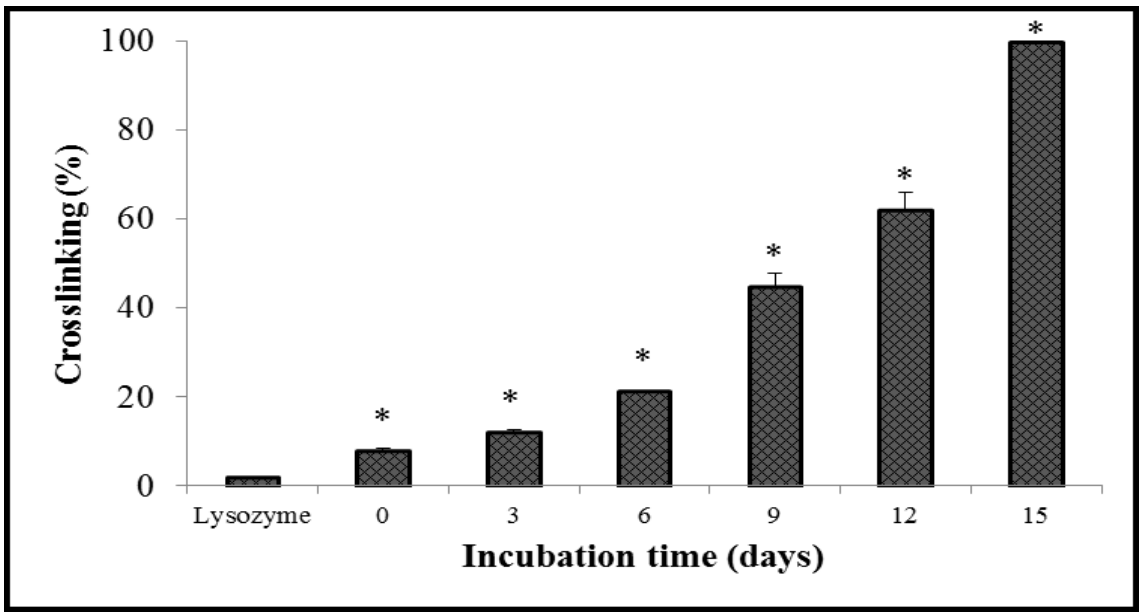

Figure 4.6: The effect of different incubation time on cross-linking AGE formation in the lysozyme-glucose system. The bar graph shows scanning of SDS-PAGE gel to show the effect of lysozyme (10 mg/ml) with glucose at different incubation times (0 – 15 days) in 0.1 M sodium phosphate buffer of pH 7.4 at 37 °C. Each value represents the mean ± SD (n = 3), * $p < 0.05$.

4.4.5 Effect of MCP on methylglyoxal-derived AGEs:

Methylglyoxal reacts with lysozyme at a faster rate compared to glucose leading to production of adequate amount of cross-linked AGEs within 3 days of incubation and causes the formation of trimers as well (Figure 4.7, lane b). Varying concentrations of MCP (5-15 mg/ml) were used for the assay. Since the formation of dimers was inhibited by MCP during the assay, the quantity of dimerized lysozyme was decreased in a dose- dependent manner (Figure 4.7, lanes c to e).

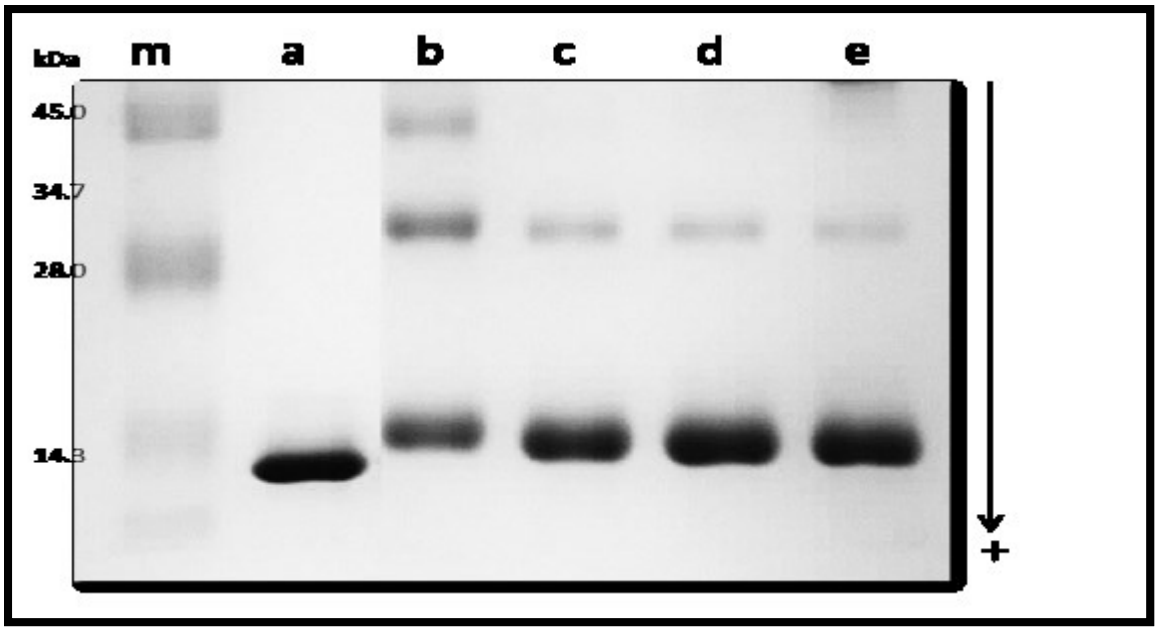

Figure 4.7: Gel showing the effect of MCP on methylglyoxal-derived AGEs. Lysozyme (10 mg/ml) incubated alone (lane a) or in the presence of 0.1 M methylglyoxal (lane b) in 0.1 M sodium phosphate buffer of pH 7.4 at 37 °C for 3 days. The inhibition of dimer formation was determined using different concentrations of MCP (c) 5 mg/ml, (d) 10 mg/ml and (e) 15 mg/ml. The cross-linked AGEs were analysed using SDS-PAGE and stained with Coomassie brilliant blue solution. The result is a representative figure of at least three independent experiments.

A significant ($p < 0.001$) inhibition of cross-linked AGE formation was demonstrated by MCP extract *in vitro* when compared to the control. This inhibition depended on the concentration of MCP extract as the highest inhibition (49%) was determined in reaction mixtures having 15 mg/ml of MCP extract (Figure 4.8).

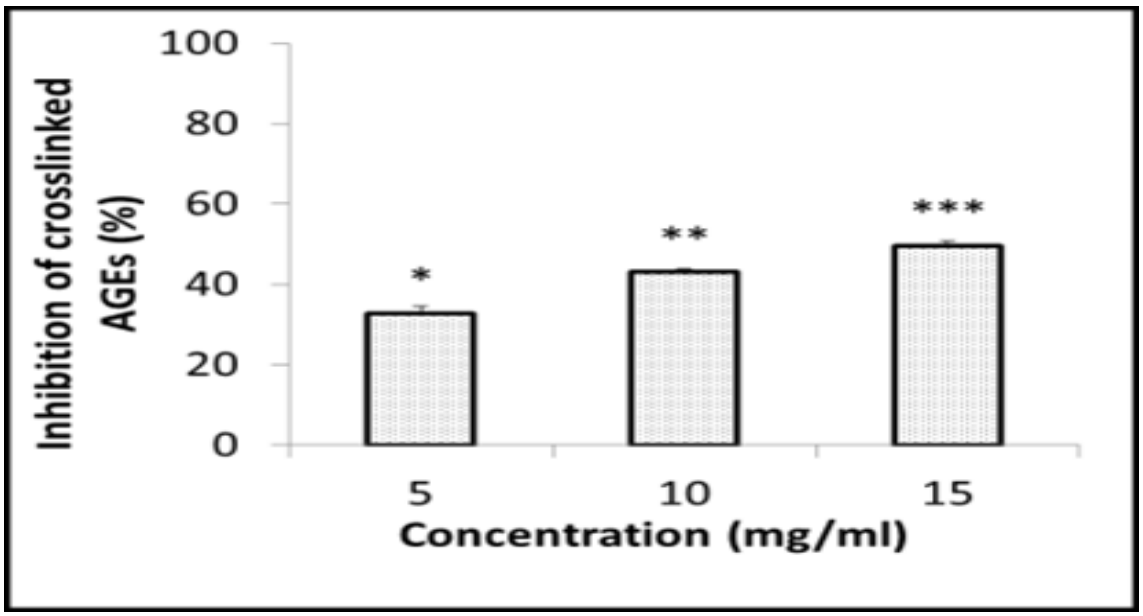

Figure 4.8: The effect of MCP on methylglyoxal-derived AGE formation. The bar graph shows scanning of SDS-PAGE gel to show the effect of MCP on crosslinked AGE. Lysozyme (10 mg/ml) was incubated with methylglyoxal (0.1 M) in 0.1 M sodium phosphate buffer of pH 7.4 at 37 °C for 3 days. The percentage inhibition of methylglyoxal-derived AGE formation was determined using different concentrations of MCP. Each value represents the mean ± SD (n = 3), * $p < 0.05$, **$p < 0.01$, *** $p < 0.0001$.

4.4.6 Effect of MCF on methylglyoxal-derived AGEs:

The glycation mixture was incubated with varying concentrations of MCF for three days. Generation of dimers was inhibited substantially depending on the concentration of MCF. 40%, 55% and 88% inhibition was caused by 5, 10 and 15 mg/ml of MCF respectively as shown in Figure 4.9, lanes c to e. A reaction mixture containing methylglyoxal and lysozyme was taken as a positive control in which dimers and trimers were generated in the absence of MCF (Figure 4.9, lane b).

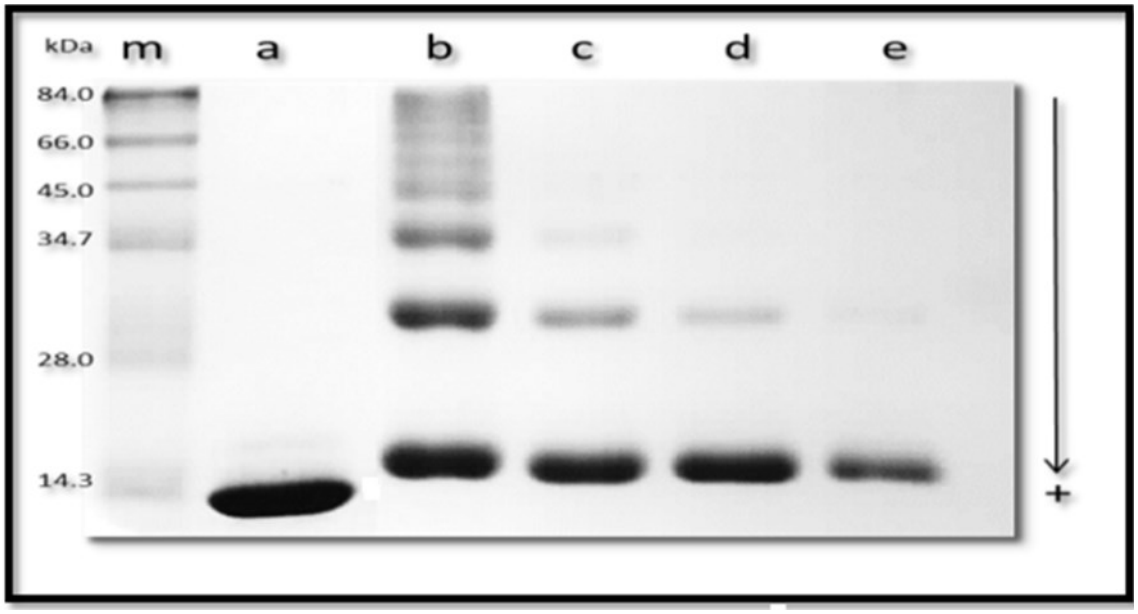

Figure 4.9: Gel showing the effect of MCF on methylglyoxal-derived AGEs. Lysozyme (10 mg/ml) incubated alone (lane a) or in the presence of 0.1 M methylglyoxal (lane b) in 0.1 M sodium phosphate buffer of pH 7.4 at 37 °C for 3 days. The inhibition of dimer formation on protein cross-linking was determined using different concentrations of MCF (c) 5 mg/ml, (d) 10 mg/ml and (e) 15 mg/ml. The cross-linked AGEs were analysed using SDS-PAGE and stained with Coomassie brilliant blue solution. The result is a representative figure of at least three independent experiments.

Formation of cross-linked AGEs *in vitro* was significantly ($p < 0.01$) inhibited by MCF extract as compared to the control sample and this inhibition was dependent on MCF concentration as optimum (88%) inhibition was observed in the sample with 15 mg/ml of MCF extract (Figure 4.10).

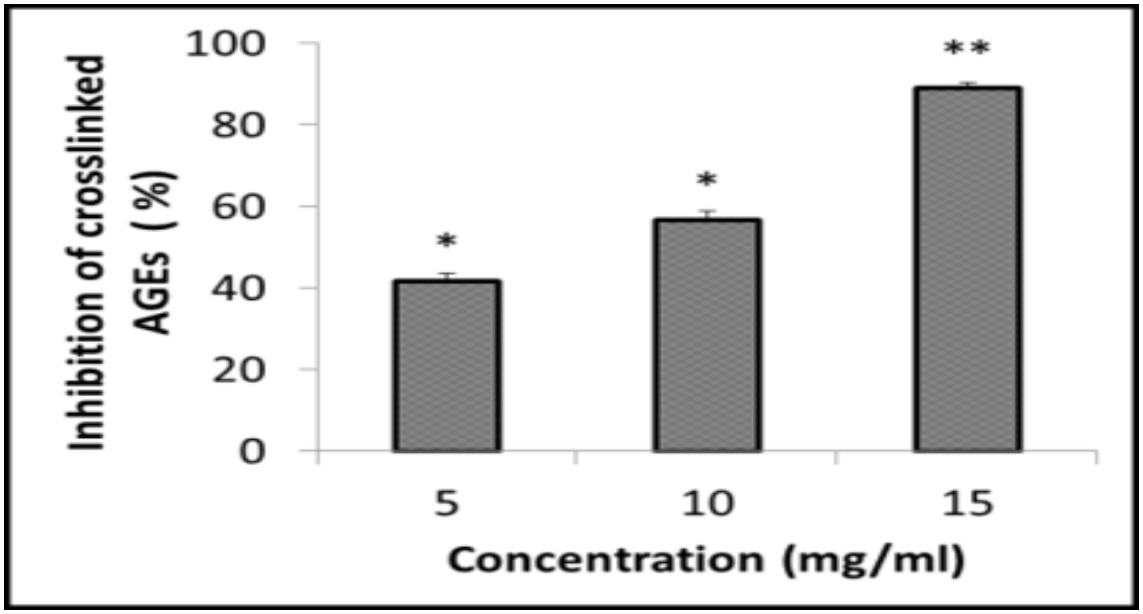

Figure 4.10: The effect of MCF on methylglyoxal-derived AGE formation. The bar graph shows the effect of MCF on cross-linked AGE. Lysozyme (10 mg/ml) was incubated with methylglyoxal (0.1 M) in 0.1 M sodium phosphate buffer of pH 7.4 at 37 °C for 3 days. The percentage inhibition of methylglyoxal-derived AGE formation was determined using different concentrations of MCF. Each value represents the mean ± SD (n = 3), * $p < 0.05$, **$p < 0.01$.

4.4.7 Effect of charantin on methylglyoxal-derived AGEs:

The impact of varying concentrations of charantin (5-15 mg/ml) on the generation of cross-linked AGEs is shown in Figure 4.11. When 0.1 M methylglyoxal was incubated with lysozyme (14 kDa, lane b), a considerable quantity of cross-linked AGEs were generated within 3 days.

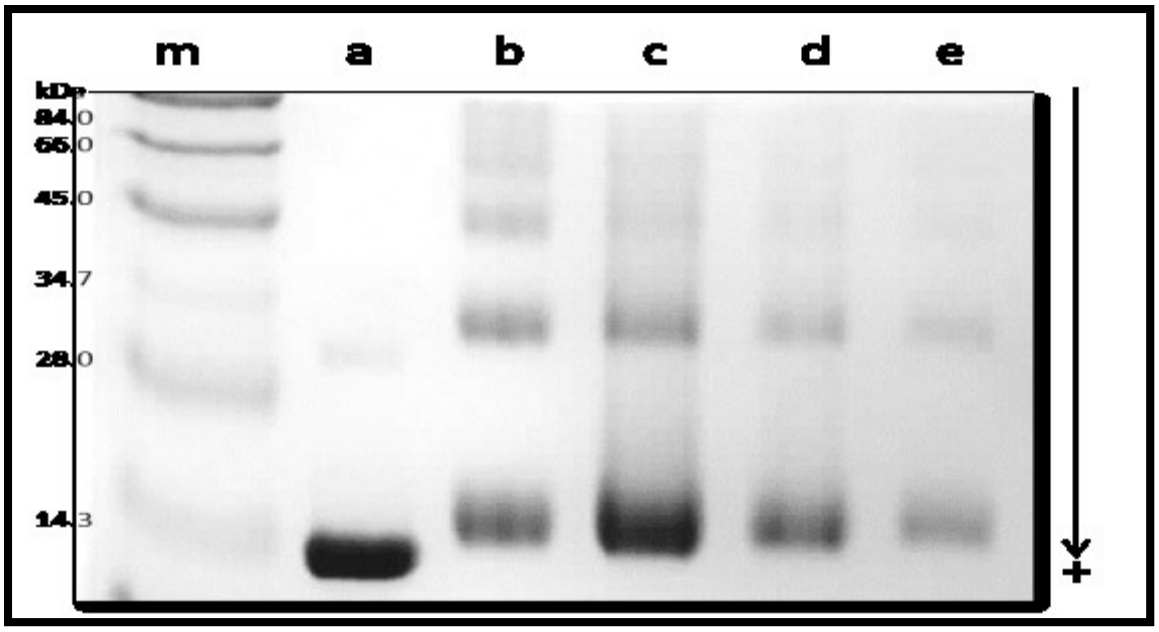

Figure 4.11: Gel showing the effect of charantin on methylglyoxal-derived AGEs. Lysozyme (10 mg/ml) incubated alone (lane a) or in the presence of 0.1 M methylglyoxal (lane b) in 0.1 M sodium phosphate buffer of pH 7.4 at 37 °C for 3 days. The inhibition of dimer formation on protein cross-linking was determined using different concentrations of charantin (C) 5 mg/ml, (d) 10 mg/ml and (e) 15 mg/ml. The cross-linked AGEs were analysed using SDS-PAGE and stained with Coomassie brilliant blue solution. The result is a representative figure of at least three independent experiments.

The inhibitory effect of charantine on generation of cross-linked AGEs was found to be dependent on concentration of charantin and the optimum inhibition (55%) was caused by 15mg/ml charantine extract as shown by Figure 4.12.

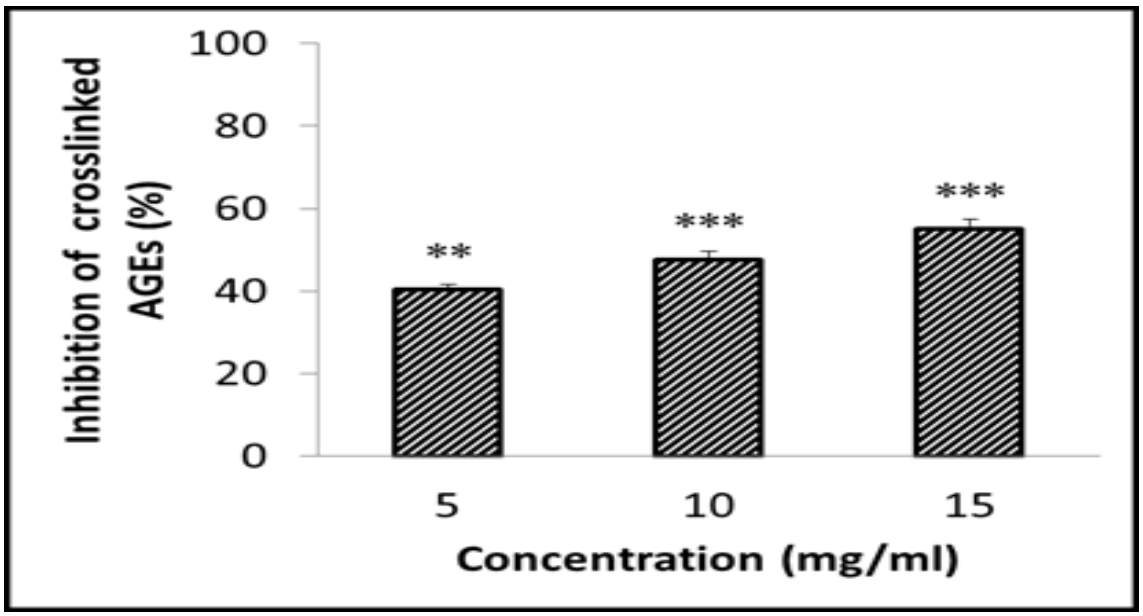

Figure 4.12: The effect of charantin on methylglyoxal-derived AGE formation. The bar graph shows scanning of SDS-PAGE gel to show the effect of charantin on cross-linked AGE. Lysozyme (10 mg/ml) was incubated with methylglyoxal (0.1 M) in 0.1 M sodium phosphate buffer of pH 7.4 at 37 °C for 3 days. The percentage inhibition of methylglyoxal-derived AGE formation was determined using different concentrations of charantin. Each value represents the mean ± SD (n = 3), **p < 0.01, *** p < 0.0001.

4.4.8 Effect of MCP, MCF and charantin on CML levels using ELISA:

Compared to the control containing BSA-CML, significant inhibition (p< 0.01) was demonstrated by all of the extracts with maximum inhibition by the MCF extract. Moreover, the inhibition depended on the concentration of extracts (Figure 4.13). MCF at the concentration of 5 and 15 mg/ml significantly inhibited CML formation by 37% and 61% respectively. MCP at the same concentration 5 and 15 mg/ml decreased CML formation by 26% and 53% respectively. Charantin also inhibited CML formation by 23% and 45% respectively.

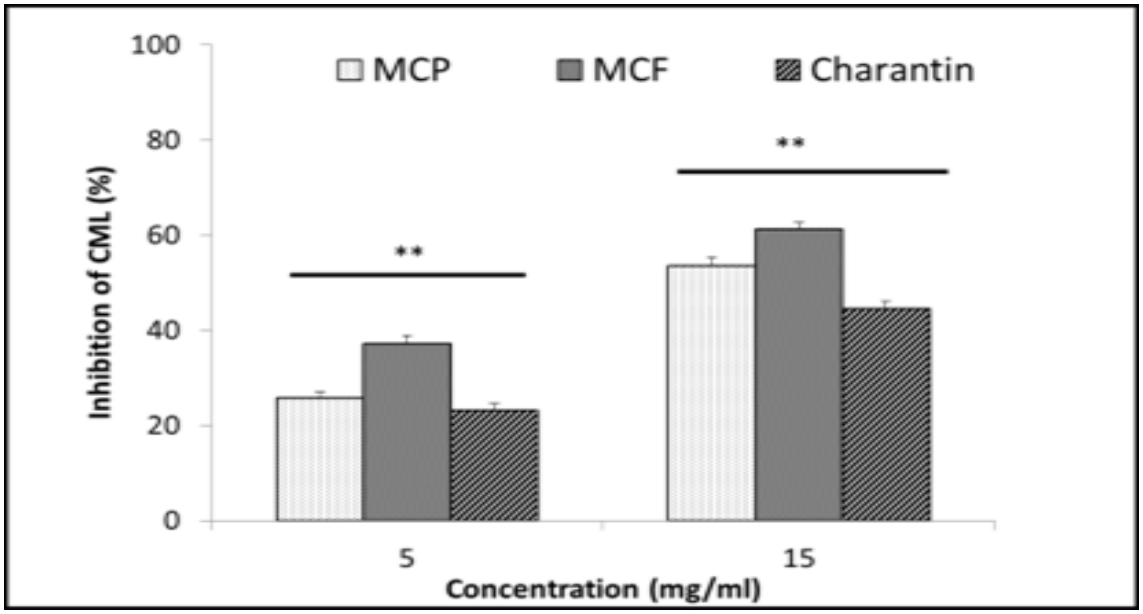

Figure 4.13: The effect of MCP, MCF and charantin on CML formation as measured by ELISA. The bar graph shows the inhibition effect of MCP, MCF and charantin on CML levels were determined in the presence of different concentrations (5 and 15 mg/ml) of MCP, MCF and charantin extracts. Results are presented as mean ± SD (n=3), **$p<0.01$.

4.4 Discussion

DM is one of fastest growing diseases in the world. It is been reported that up to one-third of diabetes patients use alternative medicines. MC is one of the most popular plant using as anti-diabetic agent (Joseph and Jini, 2013). Protein glycation *in vitro* was investigated in the current study by incubating proteins with sugars at physiological pH; however, non-physiological concentrations of sugars were also employed to increase the rate of formation of AGEs in a shorter time period. Lysozyme serves to be an efficient protein model for determination of cross-linked AGE generation since oligomerisation occurs readily and can be measured conveniently following scanning of SDS-PAGE gels. Numerous earlier studies have also explored glycation of lysozyme *in vitro* (Kislinger *et al*., 2004). In this chapter, the findings show that increase cross-linked AGEs correlate with glucose concentration and the period of incubation. It is believed that the accumulation of cross-linked AGEs in tissues and

plasma is thought to be responsible for the long-term complications related to diabetes and ageing (Brownlee, 1995, Nimbalkar *et al*., 2012). The measurements of fluorescence to study the effects of different glucose concentrations and different period of incubation on AGE formation also supported the previous finding with SDS-PAGE gels. Methylglyoxal (α-dicarbonyl) was chosen to complete the other experiments because it is highly reactive and contain the carbonyl groups (aldehyde/ketone). In addition, methylglyoxal has the ability to bind with sulfhydryl, amino, lysine, arginine and guanidine functional groups in proteins (Goldin *et al*., 2006). This study showed for the first time that MCP, MCF and charantin extracts have significant potential inhibition to the formation of AGEs in a dose-dependent manner *in vitro*. The most common AGE generated by oxidation reactions and glycation is carboxymethyllysin (CML) (Fujiwara *et al*., 2011). Animal and human tissues have increased concentrations of CML in skin collagen in diabetes and aging (Dyer *et al*., 1993, Kamata *et al*., 2009). The current study established that CML formation inhibited by MCP, MCF and charantin extracts with the MCF extract having the most potent effect. Several studies showed that MC significantly lowers the glucose level in diabetic patients and diabetic rats (Joseph and Jini, 2013, Waheed *et al*., 2006). In this regards, MC could stop AGE formation by lowering the glucose level. Numerous studies established that MC comprises of several amino acids that could decrease the generation of AGEs by blockage of carbonyl groups (Kim, 2009, Mahomoodally *et al*., 2012). Moreover, it is indicated that the abilities to inhibit the formation of AGE is linked to the plant extracts antioxidant properties to scavenge radicals formed during the Maillard reaction which forms the basis of glycation (Boo *et al*., 2012, Shan *et al*., 2012). In the present study, extracts, which were found to have antioxidant properties against free radical activity, were also seen to possess antiglycation potential. Indeed, this protection against glycation-induced crosslinking may be due to the ability to chelate transition metals thus preventing autoxidative glycation and glycoxidation reactions.

In previous studies, MC extract has been shown to chelates Cu^{2+} ions and protects against LDL oxidation (Hsieh *et al*., 2005). The small antioxidant compounds of molecular weight, for instance polyphenols, flavonoids and flavonols, were found in MC (Gogi *et al*., 2010, Shan *et al*., 2012). The results of the present study show that MCF extract, which contains the maximum amount of phenolic substances, shows greatest antioxidant activity, therefore, could stop glycation.

Chapter 5. Pro-angiogenesis effect of *Momordica charantia*

5.1 Introduction

Angiogenesis refers to the process of a new blood vessels formation from existing blood vessels and is essentially important for physiological and pathophysiological situations such as female of the reproductive cycle, embryogenesis and wound healing (Ferrara and Kerbel, 2005; Giuliano and Pagès, 2013). It had been established earlier that the generation of advanced glycation endproducts (AGEs) plays a crucial role in causing diabetic vascular complications. Moreover, numerous research studies have determined that wound-healing can be impaired due to the accumulation of AGEs (Huijberts *et al*., 2008). In this connection, MC is known for its potential to speed up, improve the wound healing process (De Nardo *et al*., 2013), and increase beta cells proliferation (Ahmed *et al*., 1998). All the main steps of angiogenesis can be simulated *in vitro* by studying endothelial cells in basic angiogenic assays including tube formation, cell proliferation and migration assays. Thus, bovine aortic endothelial cells (BAEC) were cultured and treated with either BSA-AGEs and MC extracts or both. The receptor for AGEs (RAGE) was neutralized to demonstrate whether MC extracts kept its angiogenic effects.

5.2 Aims and objectives

The aim of this work was to examine the effects of BSA-AGEs with *Momordica charantia* extracts on angiogenesis using BAEC *in vitro*.

The objectives of this study were:

- To investigate the effect of native BSA, BSA-AGEs and MC extracts on BAEC proliferation using the Coulter counter.

- To investigate the effect of MC extracts on anti-angiogenic effect of AGEs on BAEC proliferation using the Coulter counter.
- To determine the cytotoxicity effects of BSA-AGEs or MC extracts on BAEC using automated cell counter (Bio-Rad, UK).

- To identify the potential effect of native BSA, BSA-AGEs and *Momordica charantia* extracts on BAEC migration and tube formation using wound healing and the Matrigel™ assay

- To identify the potential effect of MC extracts combined with BSA-AGEs on BAEC migration and tube formation using wound healing and the Matrigel™ assay, respectively.

- To investigate the angiogenic signalling pathways induced by *Momordica charantia* extracts by Western blotting and after RAGE neutralization using anti-RAGE antibody.

5.3 Methods

BAEC were used to investigate the effect of MC extracts in the presence or absence of BSA-AGEs on cell proliferation as described in section (2.4.3.11). Cell viability was assessed using automated cell counter as mentioned earlier in section (2.4.3.12). In addition, the effect of MC extracts in the presence or absence of BSA-AGEs on cell migration was determined using the wound-healing assay described in detail in section (2.4.3.13). Cell differentiation was assessed using Matrigel™ tube formation assay as described in section (2.4.3.14). MC-induced signalling pathway was investigated using Western blotting as mentioned in section (2.4.4) and after RAGE neutralization as described in section (2.4.5).

5.4 Results

5.4.1 Effects of BSA, BSA-AGEs, MCP, MCF and charantin on BAEC proliferation.

Effects of different concentrations (10 – 75 μg/mL) of MCP, MCF and charantin extracts were studied on BAEC proliferation after a treatment for 72 hours (Figures 5.1-5.5). To check the cell response, FGF-2 was used as positive control and induced a significant increase in the cell number by 67% (p =0.0252), compared to the untreated control cells (Figures 5.1-5.5). The addition of increasing concentrations of MC extracts and charantin significantly enhanced BAEC proliferation in a dose-dependent manner, with a peak of stimulation at 50 μg/mL (Figure 5.1-5.3). Briefly, at 10, 50 and 75 μg/mL, MCP increased BAEC proliferation of cells by 76% (10 μg/mL, p = 0.0240), 125% (50 μg/mL, p = 0.0259) and 83% (75 μg/mL, p = 0.0281), respectively, compared to untreated control cells (Figure 5.1). At the same concentrations, MCF increased the cell growth by 69% (10 μg/mL, p = 0.0251), 117% (50 μg/mL, p = 0.0277) and 81% (75 μg/mL, p = 0.0261), compared to the control (Figure 5.2). Similarly, charantin increased cell proliferation by 43% (10 μg/mL, p = 0.0254), 103% (50 μg/mL, p = 0.0273) and 50% (75 μg/mL, p = 0.0197) when compared to the control (Figure 5.3). On the contrary, 50 μg/ml BSA-AGEs increase the cell number (32%, p =0.0215), while 75 μg/ml BSA-AGEs caused (11%, p = 0.04) inhibition of cell proliferation as shown in Figure 5.4 while native BSA had no effect (Figure 5.5).

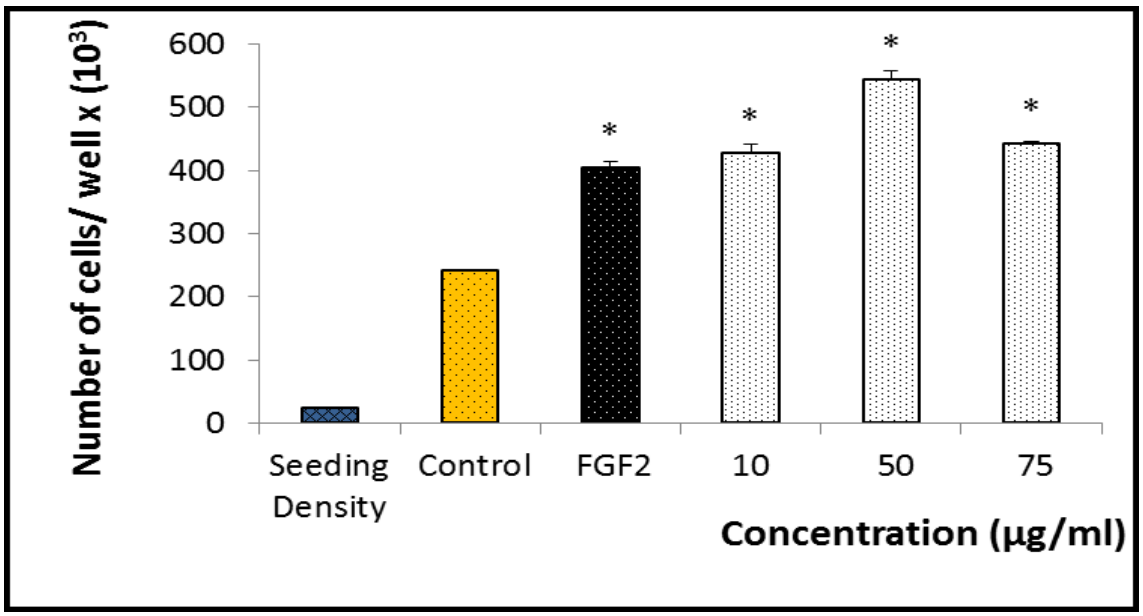

Figure 5.1: Effect of different concentrations of MCP extract on BAEC proliferation. Bovine aortic endothelial cells (2.5 x 10^4 / ml) were seeded in 24-well plates and incubated with different concentrations of MCP extract (10 – 75 µg/ml) for 72 hours. Fibroblast growth factor-2 (25 ng/ml) was used as a positive control. Results are presented as mean ± SD (n=3). * $p < 0.05$.

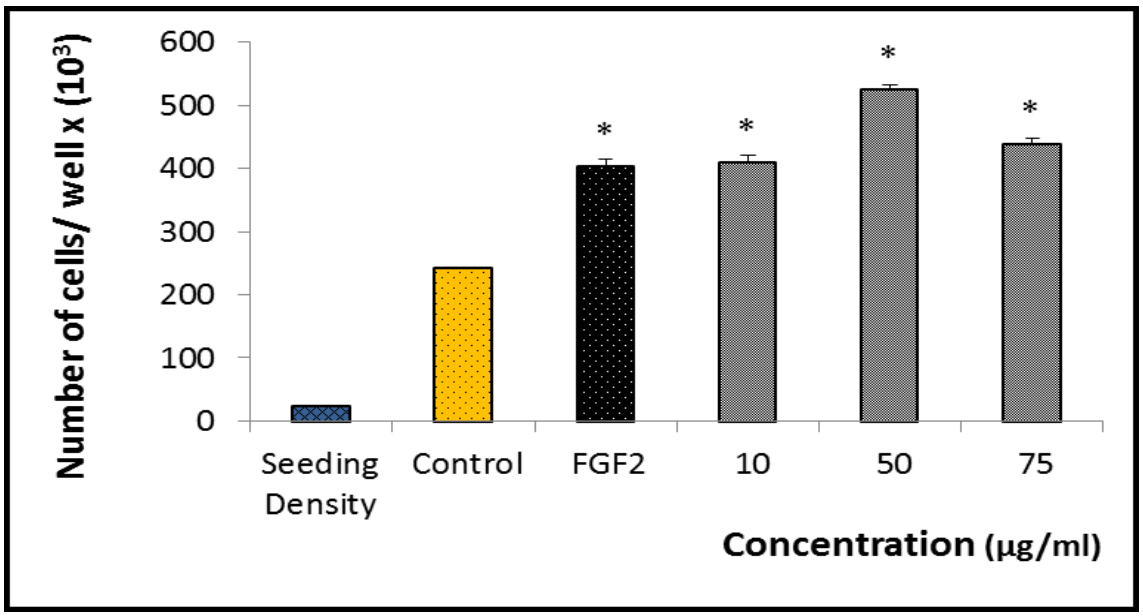

Figure 5.2: Effect of different concentrations of MCF extract on BAEC proliferation. Bovine aortic endothelial cells (2.5 x 10^4 / ml) were seeded in 24-well plates and incubated with different concentrations of MCF extract (10 – 75 µg/ml) for 72 hours. Fibroblast growth factor-2 (25 ng/ml) was used as a positive control. Results are presented as mean ± SD (n=3). * $p < 0.05$.

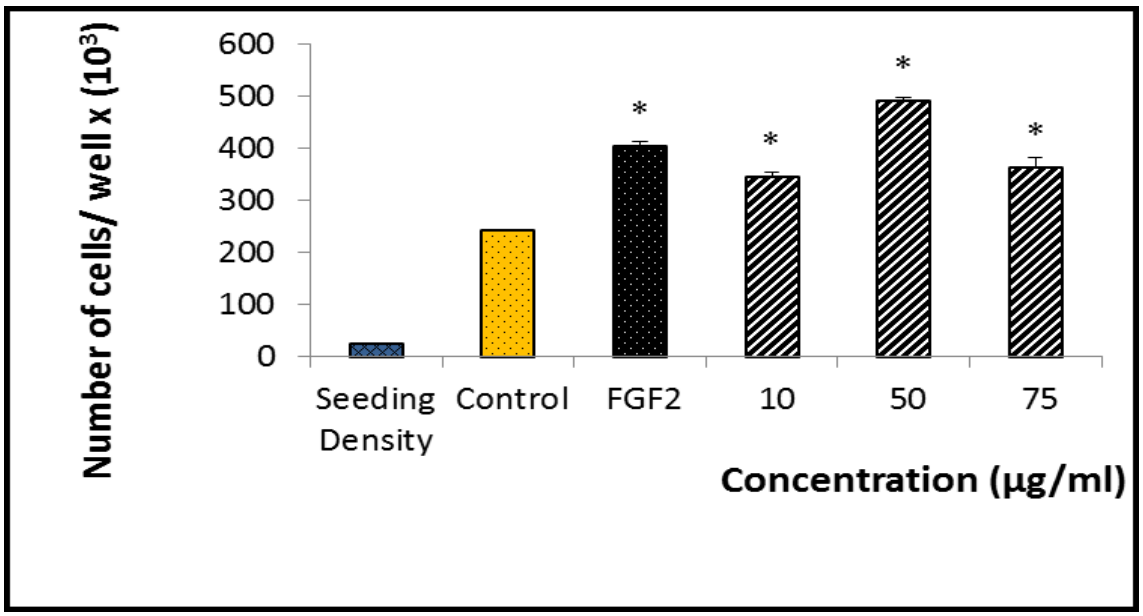

Figure 5.3: Effect of different concentrations of charantin extract on BAEC proliferation. Bovine aortic endothelial cells (2.5 x 10^4 / ml) were seeded in 24-well plates and incubated with different concentrations of charantin extract (10 – 75 µg/ml) for 72 hours. Fibroblast growth factor-2 (25 ng/ml) was used as a positive control. Results are presented as mean ± SD (n=3). * $p < 0.05$.

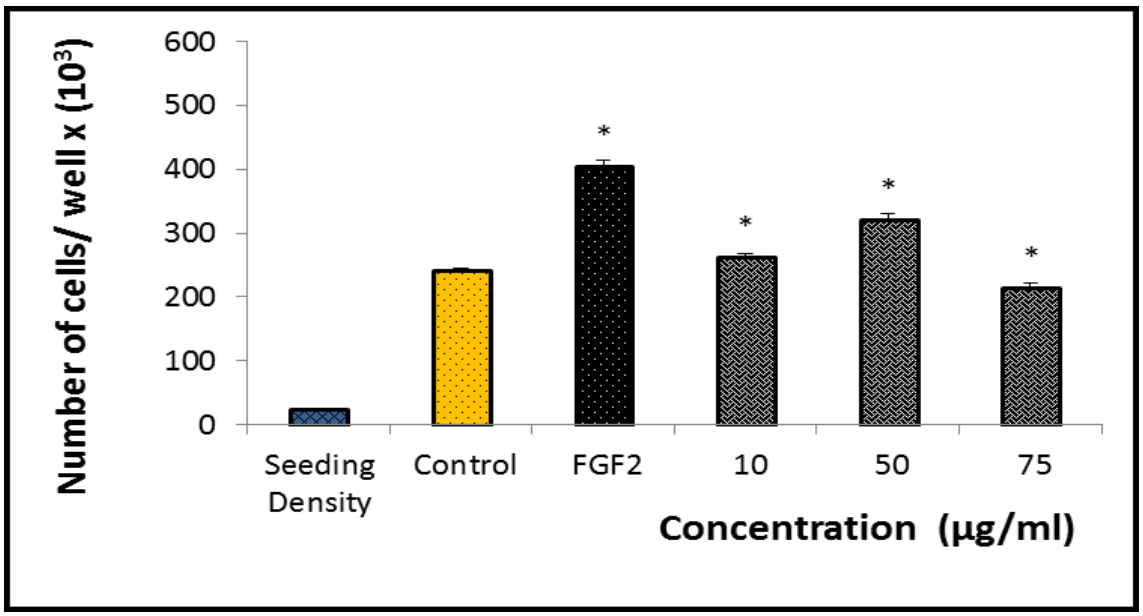

Figure 5.4: Effect of different concentrations of BSA-AGEs on BAEC proliferation. Bovine aortic endothelial cells (2.5 x 10^4 / ml) were seeded in 24-well plates and incubated with different concentrations of BSA-AGEs (10 – 75 µg/ml) for 72 hours. Fibroblast growth factor-2 (25 ng/ml) was used as a positive control. Results are presented as mean ± SD (n=3). * $p < 0.05$.

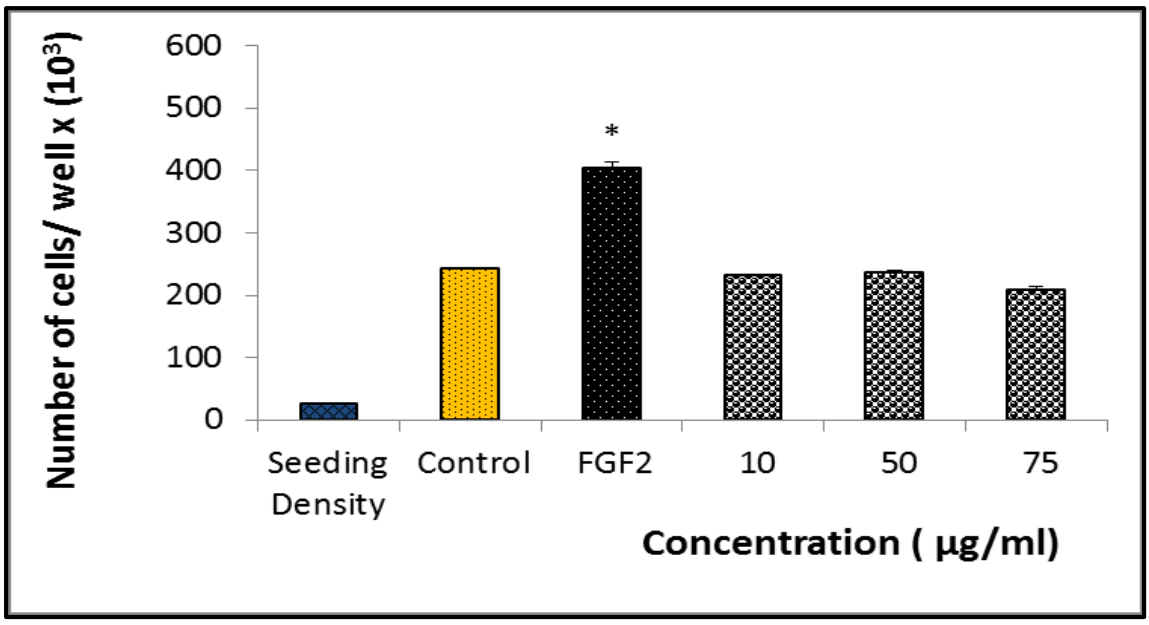

Figure 5.5: Effect of different concentrations of BSA on BAEC proliferation. Bovine aortic endothelial cells (2.5 x 10^4 / ml) were seeded in 24-well plates and incubated with different concentrations of BSA (10 – 75 µg/ml) for 72 hours. Fibroblast growth factor-2 (25 ng/ml) was used as a positive control. Results are presented as mean ± SD (n=3).

5.4.2 Effects of MC and charantin extracts on AGE-induced inhibition of endothelial cell proliferation

BSA-AGEs were studied in the presence or absence of MC and charantin extracts (10 µg/ml) on BAEC proliferation using the Coulter counter (Figure 5.6). First, the cell response with the pro-angiogenic growth factor FGF-2, the positive control, which significantly increased the cell number by 2.2-fold (p = 0.007), compared to the untreated control cells. High concentration of BSA-AGEs (250 µg/ml) inhibited cell proliferation by 0.5-fold (p = 0.008) when compared to the untreated control cells (Figure 5.6). The addition of MC extracts to BSA-AGEs reduced by 1.9-fold (p = 0.0068) the inhibitory effect of BSA-AGEs on the proliferation of BAEC treated with the addition of MCP extract and by 1.7-fold (p = 0.009) the inhibitory effect of BSA-AGEs on the proliferation of BAEC treated with the addition of MCF extract or charantin (Figure 5.6).

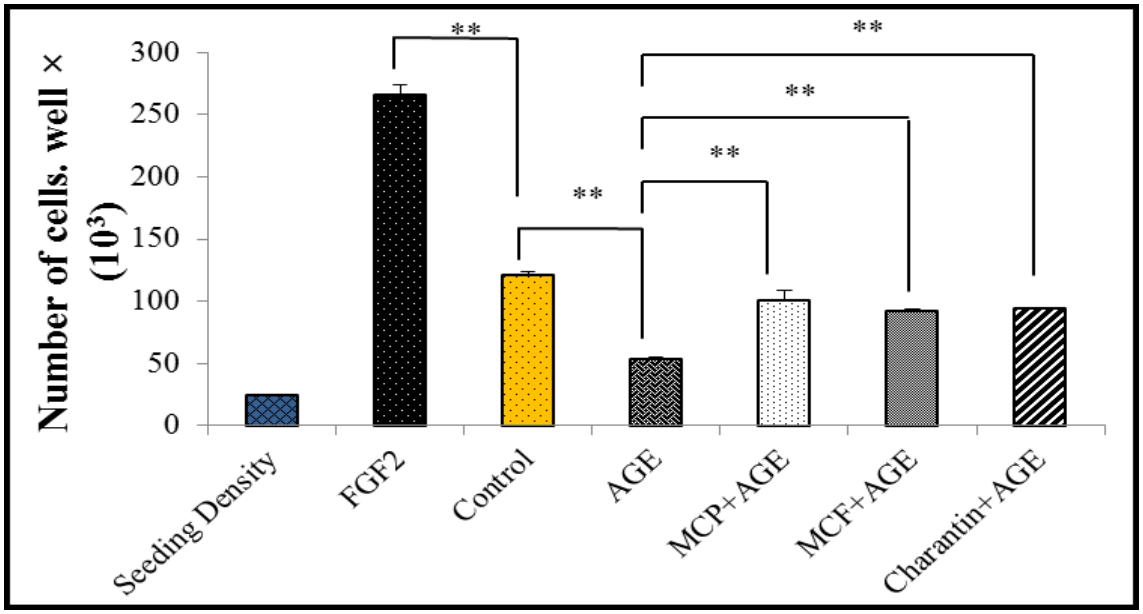

Figure 5.6: Effects of the MC and charantin extracts on AGE-induced inhibition of endothelial cell proliferation. Bovine aortic endothelial cells (2.5 x 10^4 / ml) were seeded in 24-well plates and incubated with 10 µg/ml of *Momordica charantia* extracts and 250 µg/ml BSA-AGEs for 72 hours. Fibroblast growth factor-2 (25 ng/ml) was used as a positive control. Results are presented as mean ± SD (n=3). ** $p < 0.01$.

5.4.3 Effects of BSA, BSA-AGEs, MCP, MCF and charantin on BAEC migration (wound-healing assay)

Since cell migration is an essential process for angiogenesis (Vestweber, 2007), it was important to evaluate the effects of BSA-AGEs, BSA, MCP, MCF and charantin on BAEC migration using an *in vitro* denudation injury model such as the wound-healing assay (Figure 5.7). Representative photomicrographs of cell migration in untreated condition (Figure 5.7, A), or treated conditions either with FGF-2 (Figure 5.7, B), BSA-AGEs (Figure 5.7), BSA (Figure 5.8), MCP (Figure 5.9), MCF (Figure 5.10) and charantin (Figure 5.11) were shown. FGF-2 (25 ng/mL), used as a positive control, significantly increased the distance of cell migration by 26.5% (p = 0.0282) and the number of migrated cells by 47% (p = 0.0284), when compared to untreated control cells (Figure 5.7, B). BSA-AGEs at a concentration of

75 μg/ ml significantly reduced the distance of BAEC migration into the denuded area by 5% ($p < 0.05$). In addition, the number of migrated cells was inhibited by 13% ($p < 0.05$), compared to the control (Figure 5.7). Furthermore, BSA at the same concentration did not change the number of migrated cells and 9% reduction of the distance of migration was observed, compared to the control (Figure 5.8). At 10 μg/mL, MCP significantly increased BAEC migration at a similar level to FGF-2 with an enhancement of the distance of migration by 27% ($p = 0.0284$) and the number of migrated cells by 43% ($p = 0.0284$) when compared to untreated control cells. MCP increased the distance of migration significantly by 16.7% (50 μg/ml, $p = 0.0289$) and 11.8% (75 μg/ml, $p = 0.0282$). MCP increased the number of migrated cells by 33% (50 μg/ml, $p = 0.0288$) and decreased 14% (75 μg/ml, $p = 0.0229$), respectively (Figure 5.9). At the concentration of 50 μg/ ml, MCF (Figure 5.10) and charantin (Figure 5.11) significantly increased the migrated cell number by 45% (50 μg/ml, $p = 0.0281$) and 40% (50 μg/ml, $p = 0.0286$), respectively. Furthermore, MCF at the concentration of 75 μg/ ml increased the distance of migration by 22% (75 μg/ ml, $p = 0.0292$), while charantin at the concentration of 10 μg/ ml increased the distance of migration by 18% (10 μg/ ml, $p = 0.0277$). Briefly, a significant decrease of the migrated cell number was observed by 7% ($p = 0.0313$) by the addition of 10 μg/ ml MCF, then to reach a peak of 45% ($p = 0.0281$) at 50 μg/ ml, compared to the control (Figure 5.10). The number of migrated cells slightly increased by 25% ($p = 0.0295$) in the presence of 75 μg/ ml MCF (Figure 5.10). At all concentrations used, charantin increased the number of migrated cells reaching a peak of 45% (50 μg/ ml, $p = 0.0286$), compared to untreated control cells (Figure 5.11).

(a)

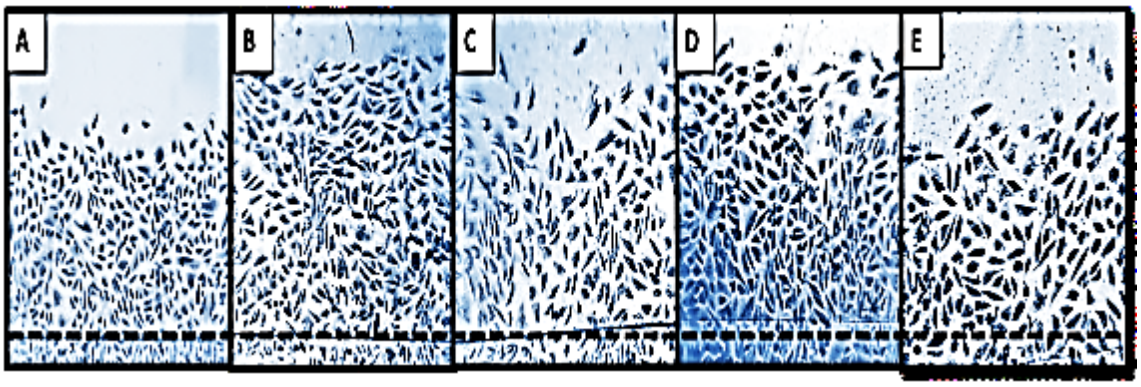

(b)

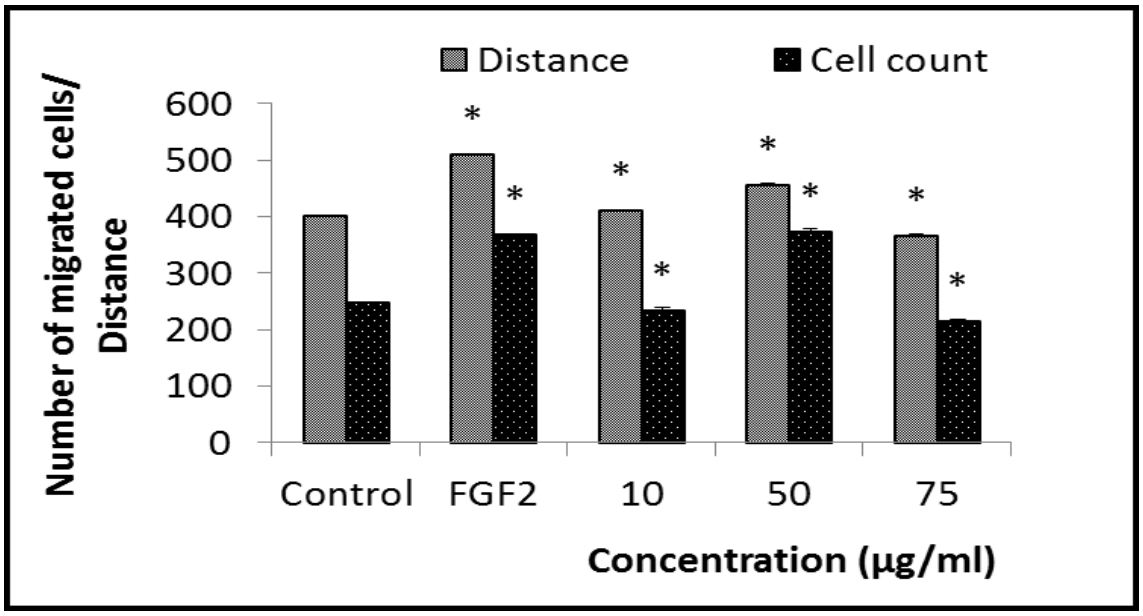

Figure 5.7: Representative photomicrographs and bar graph showing the effects of BSA-AGEs on BAEC migration using wound-healing assay. (a) A representative photomicrographs shows the effect of (A) Control (B) FGF-2 (25ng /ml) (C) BSA-AGE (10 µg/ml) (D) BSA-AGE (50 µg/ml) (E) BSA-AGE (75 µg/ml) for 24 hours. The numbers of migrated cells in the denuded area were counted (original magnification X40, scale bar = 100 µm). Experiments were performed in triplicate wells and repeated three times. A representative example is shown. (b) The bar graph shows the effects of BSA-AGE on BAEC migration. Graph shows the mean ± S.D. * $p < 0.05$

(a)

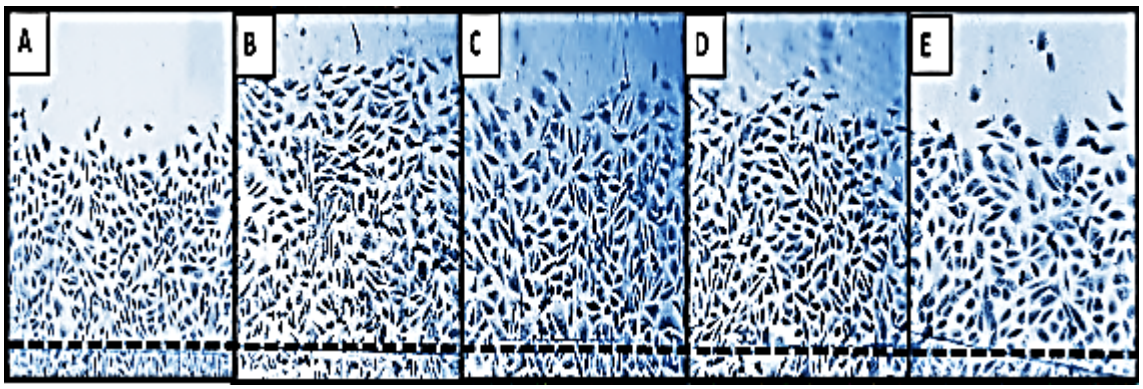

(b)

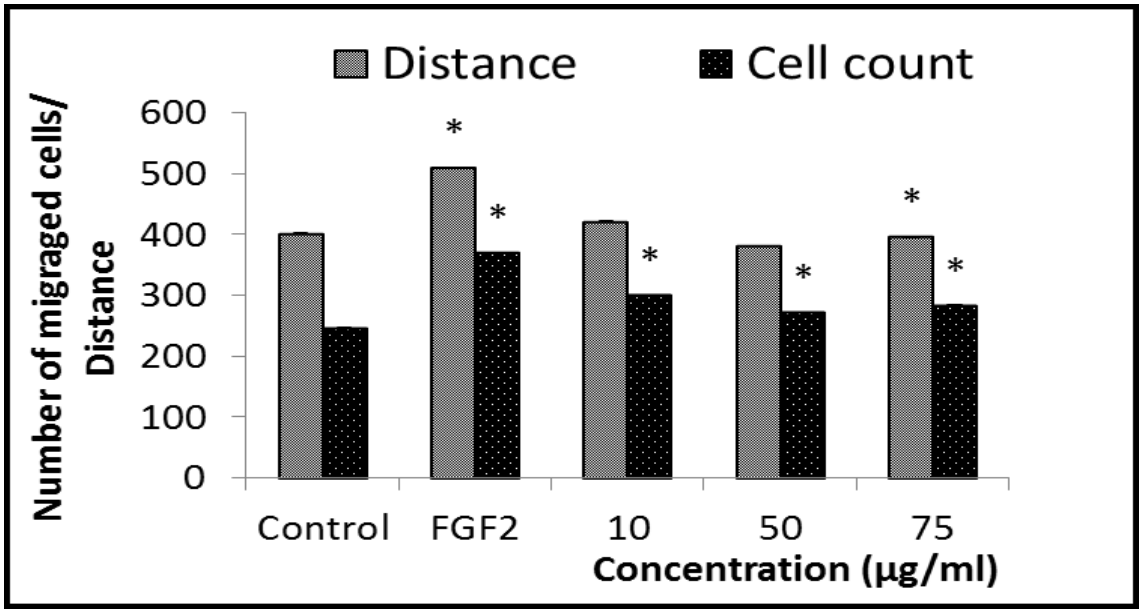

Figure 5.8: Representative photomicrographs and bar graph showing the effects of BSA on BAEC migration using wound-healing assay. (a) A representative photomicrographs shows the effect of (A) Control, (B) FGF-2 (25ng /ml), (C) BSA (10 µg/ml), (D) BSA (50 µg/ml) and (E) BSA (75 µg/ml) for 24 hours. The numbers of migrated cells in the denuded area were counted (original magnification X40, scale bar = 100 µm). Experiments were performed in triplicate wells and repeated three times. A representative example is shown. (b) The bar graph shows the effects of BSA on BAEC migration. Graph shows the mean ± S.D (n=3). * $p < 0.05$

(a)

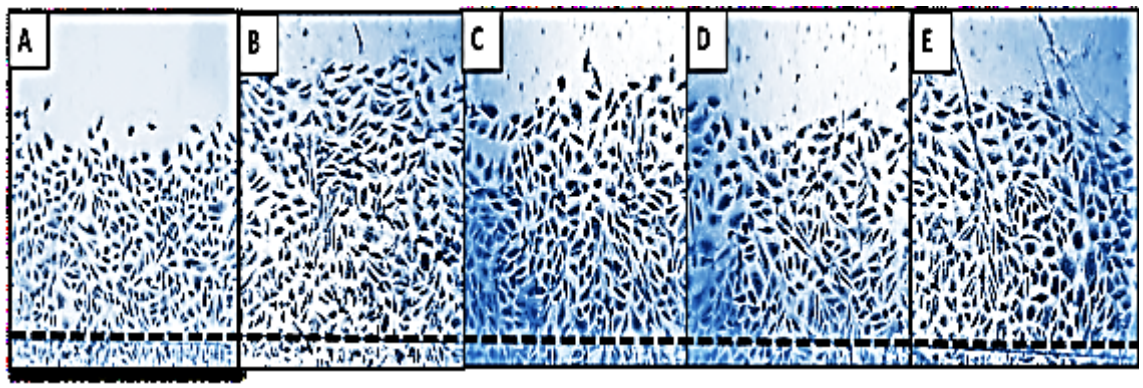

(b)

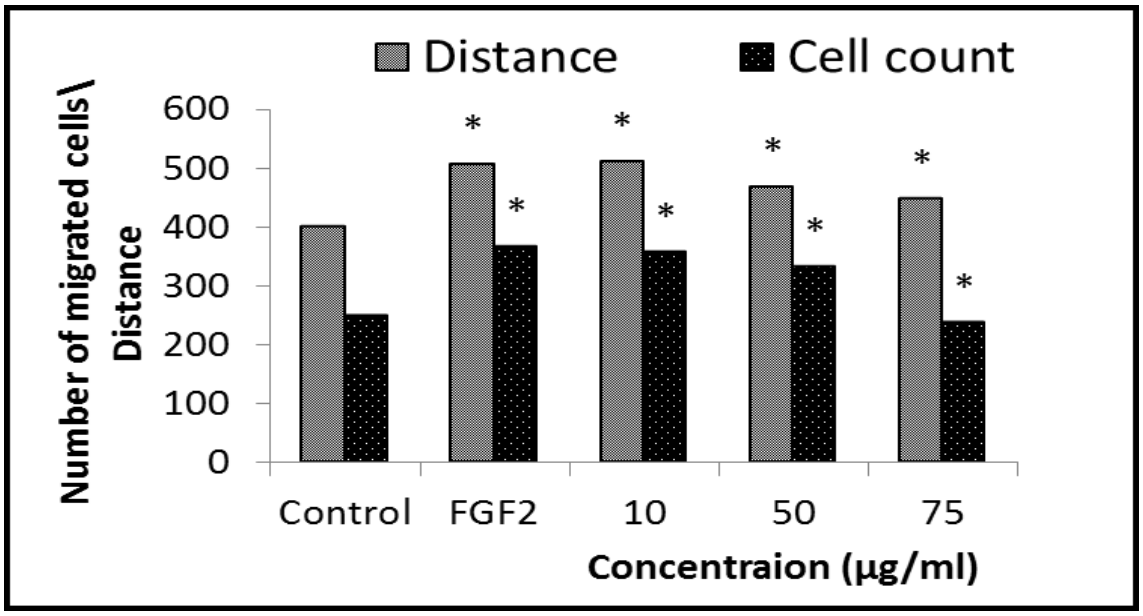

Figure 5.9: Representative photomicrographs and bar graph showing the effects of MCP on BAEC migration using wound-healing assay. (a) A representative photomicrographs shows the effect of (A) Control (B) FGF-2 (25ng /ml) (C) MCP (10 µg/ml) (D) MCP (50 µg/ml) (E) MCP (75 µg/ml) for 24 hours. The numbers of migrated cells in the denuded area were counted (original magnification X40, scale bar = 100 µm). Experiments were performed in triplicate wells and repeated three times. A representative example is shown. (b) The bar graph shows the effects of MCP on BAEC migration. Graph shows the mean ± S.D. * $p < 0.05$

(a)

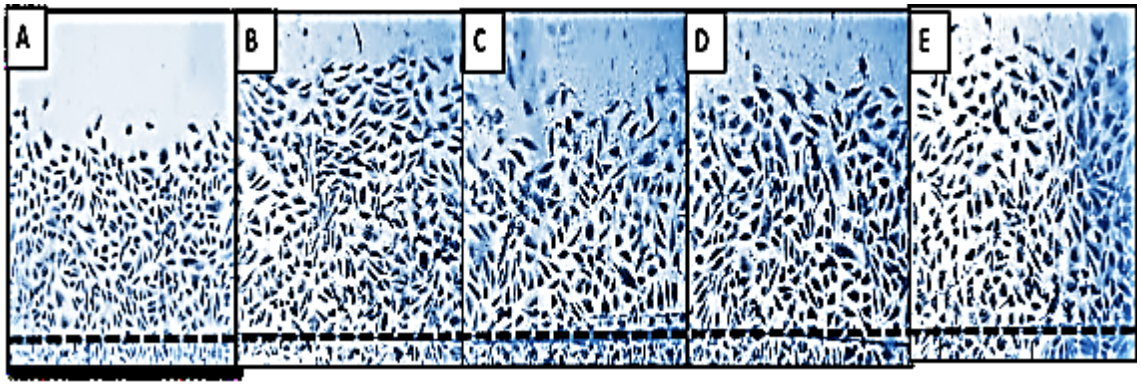

(b)

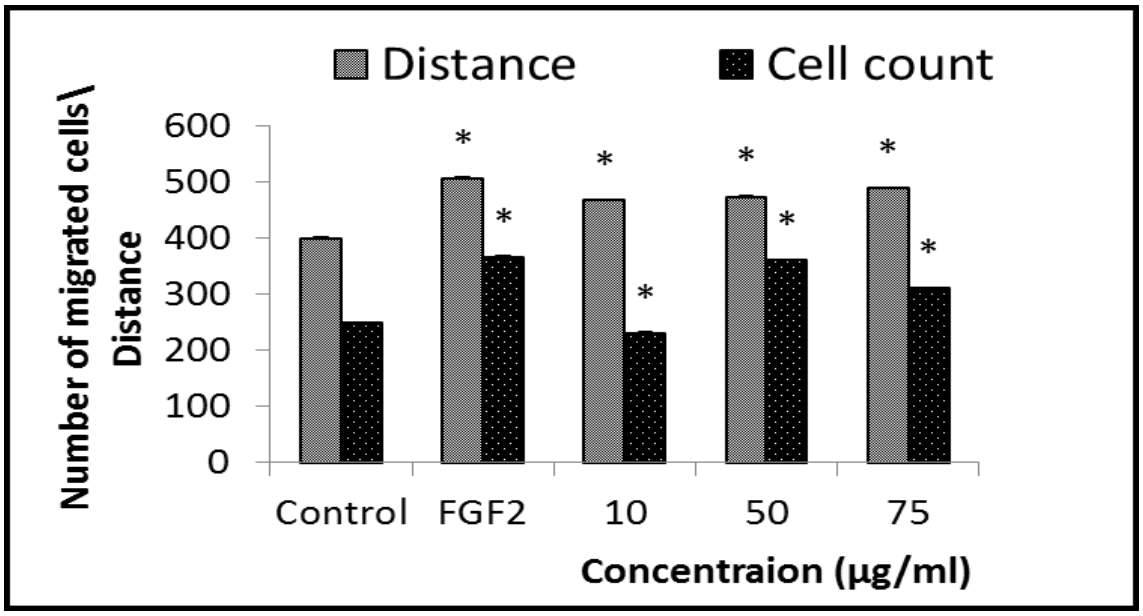

Figure 5.10: Representative photomicrographs and bar graph showing the effects of MCF on BAEC migration using wound healing assay. (a) A representative photomicrographs shows the effect of (A) Control, (B) FGF-2 (25ng /ml), (C) MCF (10 µg/ml), (D) MCF (50 µg/ml) and (E) MCF (75 µg/ml) for 24 hours. The numbers of migrated cells in the denuded area were counted (original magnification X40, scale bar = 100 µm). Experiments were performed in triplicate wells and repeated three times. A representative example is shown. (b) The bar graph shows the effects of MCF on BAEC migration. Graph shows the mean ± S.D. * $p < 0.05$.

(a)

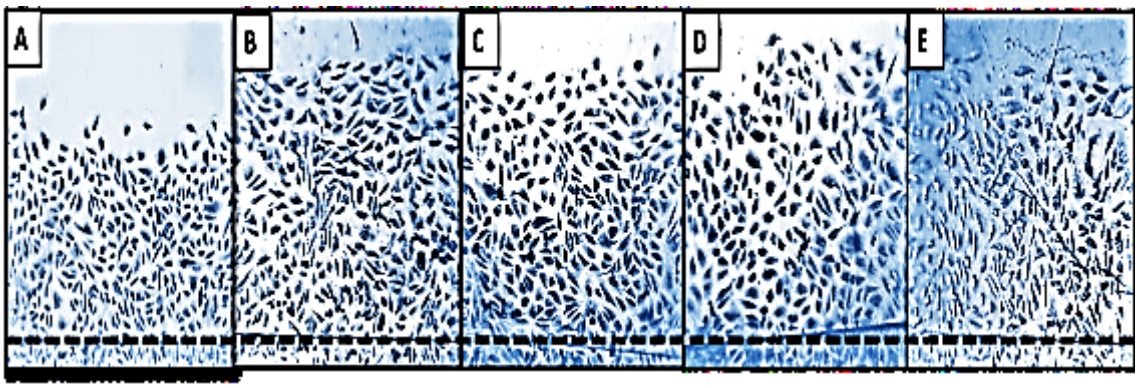

(b)

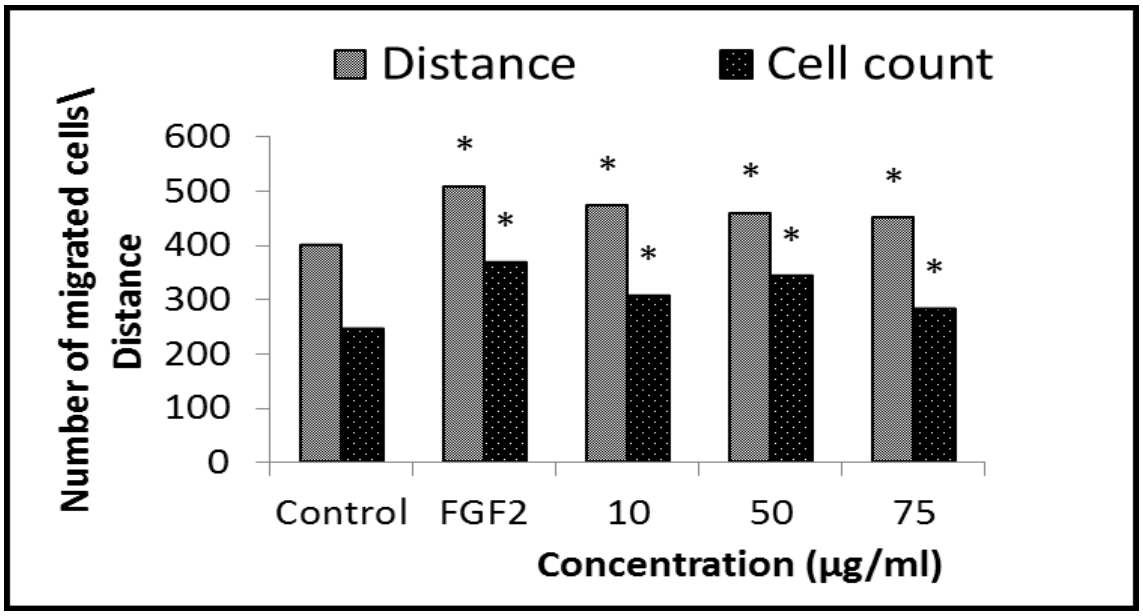

Figure 5.11: Representative photomicrographs and bar graph showing the effects of charantin on BAEC migration using wound healing assay. (a) A representative photomicrographs shows the effect of (A) Control, (B) FGF-2 (25ng /ml), (C) charantin (10 µg/ml), (D) charantin (50 µg/ml) and (E) charantin (75 µg/ml) for 24 hours. The numbers of migrated cells in the denuded area were counted (original magnification X40, scale bar = 100 µm). Experiments were performed in triplicate wells and repeated three times. A representative example is shown. (b) The bar graph shows the effects of charantin on BAEC migration. Graph shows the mean ± S.D. * $p < 0.05$

5.4.4 Effect of MC and charantin extracts on AGE-induced inhibition of endothelial cell migration using wound-healing assay

To assess the effect of high concentration of BSA-AGEs (250 µg/ml) on the migration of BAEC, the cells were subjected to a wound-healing assay followed by a 24-hour treatment in the presence or absence of 10 µg/mL MCP, MCF extracts and charantin (Figure 5.12, a). Representative photomicrographs of cell migration in untreated condition (Figure 5.12, A), or treated conditions either with FGF-2 (Figure 5.12, B), BSA-AGEs (Figure 5.12, C) or BSA-AGEs combined with MCP (Figure 5.12, D), MCF (Figure 5.12, E) or with charantin (Figure 5.12, F) were shown. FGF-2, used as a positive control, significantly increased the distance of cell migration by 1.37-fold (p = 0.031) and the number of migrated cells by 1.5-fold (p = 0.028), compared to untreated control cells. The cell treatment with high concentration of BSA-AGEs decreased the cell migration by 0.5-fold (p = 0.028) the distance of migration and by 0.58-fold (p = 0.026) the number of migrated cells. The addition of MCP extract to high concentration of BSA-AGEs reduced the inhibitory effect of BSA-AGEs on BAEC migration by about 1.45-fold (p = 0.03) the distance of migration and by about 1.6-fold (p = 0.028) the number of migrated cells, compared to BSA-AGEs treated cells. MCF extracts reduced the inhibitory effect of BSA-AGEs on cells by 1.67-fold (p = 0.029) the distance of migration and by 1.64-fold (p = 0.029) the number of migrated cells. Charantin was also reduce the inhibitory effect of BSA-AGEs by 1.28-fold (p = 0.035) the distance of migration and by about 1.29-fold (p = 0.025) the number of migrated cells.

(a)

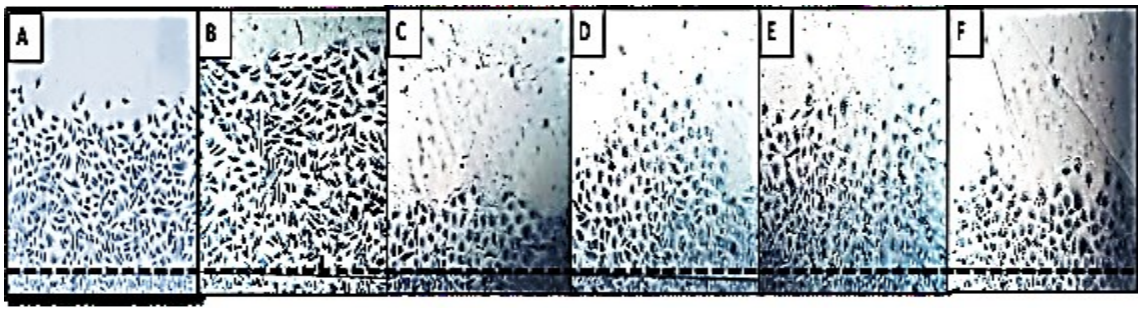

(b)

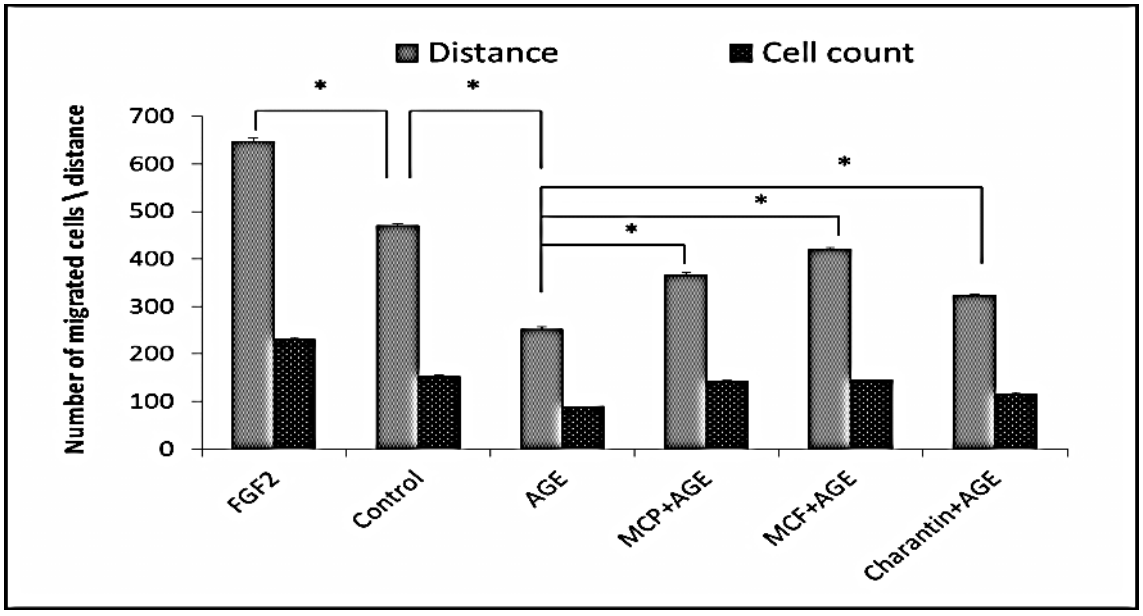

Figure 5.12: Representative Photomicrographs and bar graph showing the effects of MC and charantin extracts on AGE-induced inhibition of endothelial cell migration. (a) A representative photomicrographs shows the effect of (A) control, (B) FGF-2 (25 ng /ml), (C) BSA-AGEs at 250 µg/ml, (D) BSA-AGEs combined with 10 µg/ml MCP, (E) BSA-AGEs combined with 10 µg/ml MCF and (F) BSA-AGEs combined with 10 µg/ml charantin, for 24 hours incubation. The numbers of migrated cells in the denuded area were counted and the distance of migration measured using image J software (original magnification, 40X, scale bar = 100 µm). Experiments were performed in triplicate and repeated three times. (b) The graph shows the effects of combination of BSA-AGEs (250 µg/ml) with *Momordica charantia* extracts on BAEC migration. The bar graph shows the mean ± S.D. * $p < 0.05$.

5.4.5 Effects of BSA, BSA-AGEs, MCP. MCF and charantin on BAEC cell viability using automated cell counter

Figure 5.13 shows no cytotoxic effect of BSA-AGEs when used at 10 and 50 µg/ml, while a significant (p =0.00002) cytotoxic effect causing 28% decrease of cell viability was detected by the presence of 75 µg/ml BSA-AGEs, compared to the untreated control cells, after 72 hours incubation (Figure 5.14). In addition, all MCP, MCF and charantin extracts had no cytotoxic effect on BAEC (Figures 5.15, 5.16, 5.17).

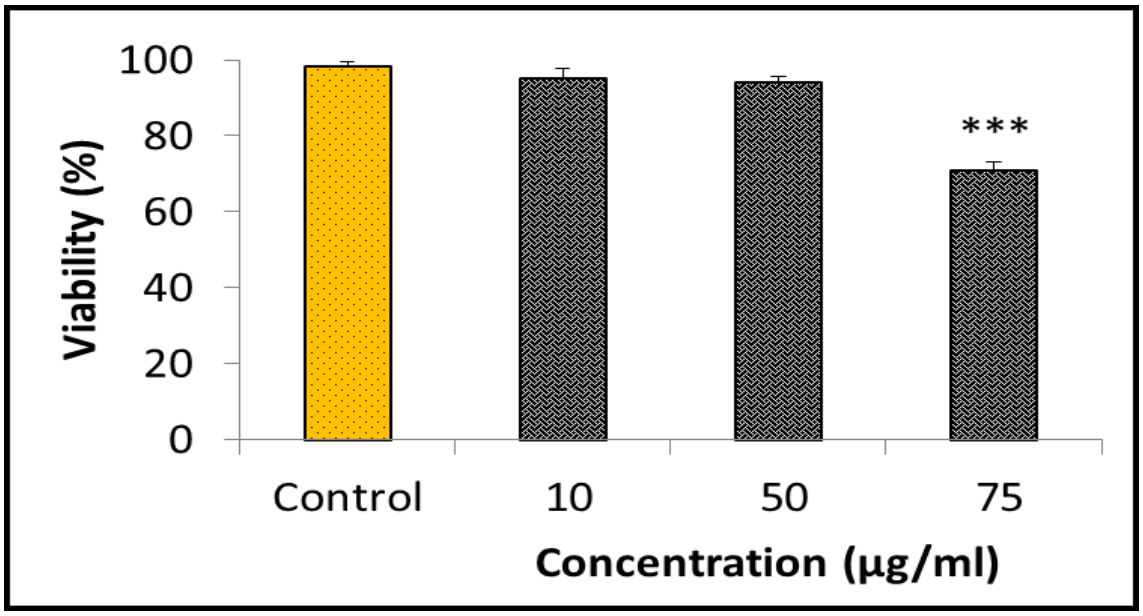

Figure 5.13: Effect of BSA-AGEs on BAEC viability using trypan blue assay. Bovine aortic endothelial cells (2.5 x 10^4 / ml) were seeded in 24-well plates and incubated with different concentrations of BSA-AGEs (10 – 75 µg/ml). After 72 hours incubation, the cell suspension (10 µl) was mixed with trypan blue dye (10 µl) and cell viability was assessed by automated cell counter. Results are expressed as mean ± SD (n = 3) of three independent experiments *** $p < 0.0001$.

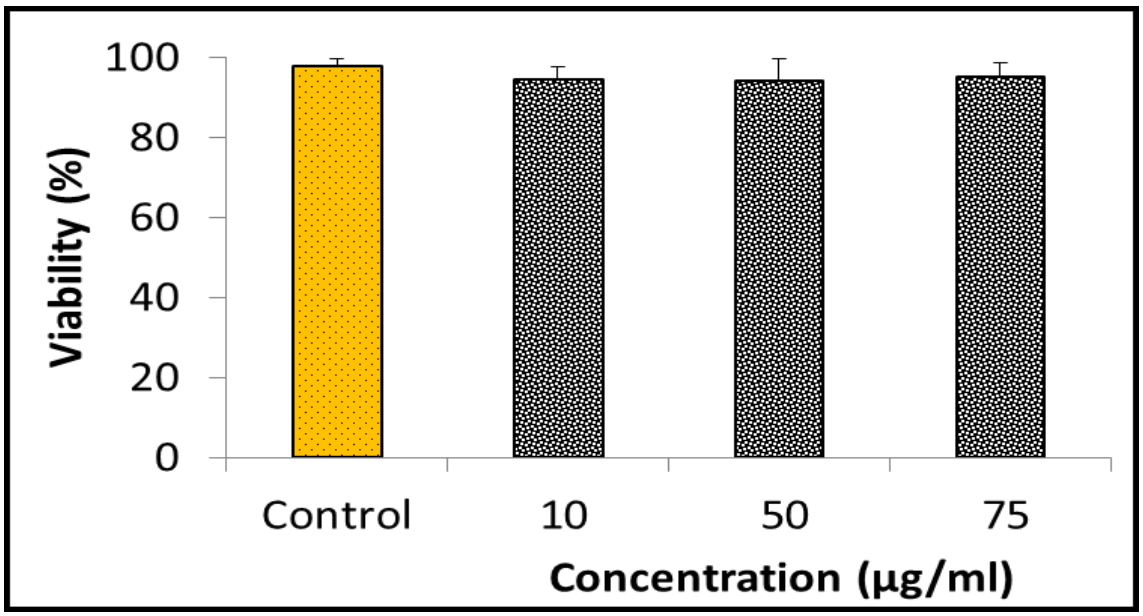

Figure 5.14: Effect of BSA on BAEC viability using trypan blue assay. Bovine aortic endothelial cells (2.5 x 10^4 / ml) were seeded in 24-well plates and incubated with different concentrations of BSA (10 – 75 µg/ml). After 72 hours incubation, the cell suspension (10 µl) was mixed with trypan blue dye (10 µl) and cell viability was assessed by automated cell counter. Results are expressed as mean ± SD (n = 3) of three independent experiments.

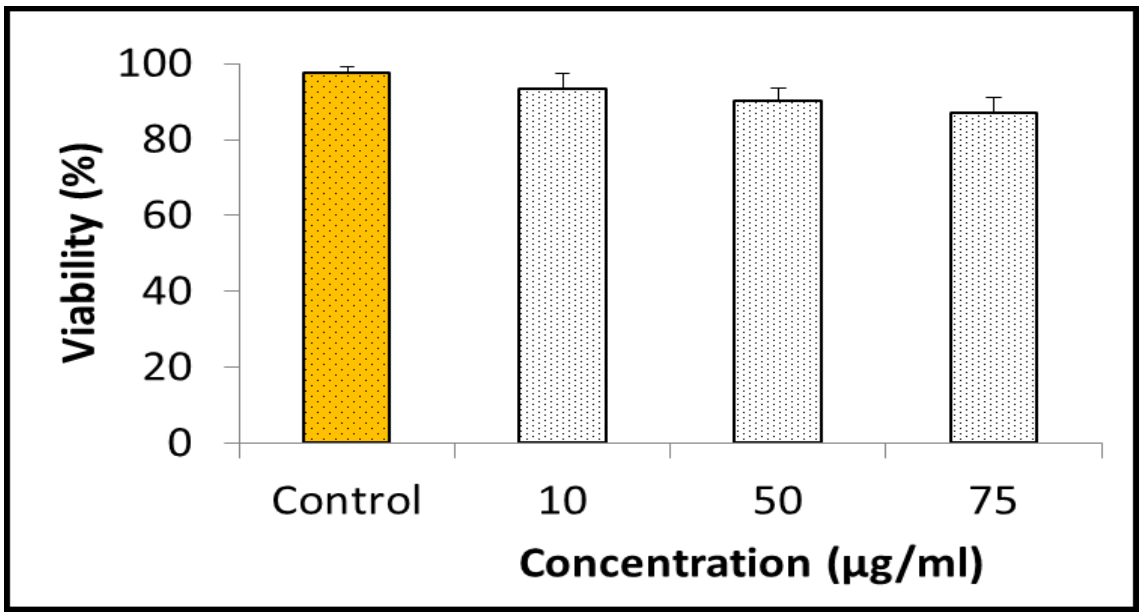

Figure 5.15: Effect of MCP on BAEC viability using trypan blue assay. Bovine aortic endothelial cells (2.5 x 10^4 / ml) were seeded in 24-well plates and incubated with different concentrations of MCP (10 – 75 µg/ml). After 72 hours incubation, the cell suspension (10 µl) was mixed with trypan blue dye (10 µl) and cell viability was assessed by automated cell counter. Results are expressed as mean ± SD (n = 3) of three independent experiments.

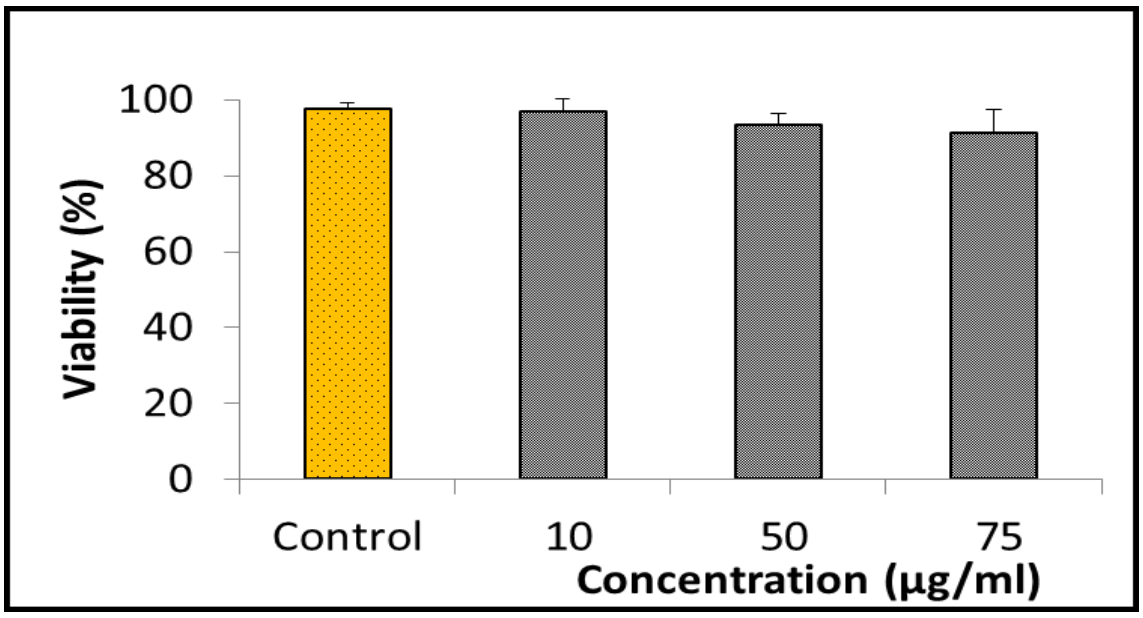

Figure 5.16: Effect of MCF on BAEC viability using trypan blue assay. Bovine aortic endothelial cells (2.5 x 10^4 / ml) were seeded in 24-well plates and incubated with different concentrations of MCF (10 – 75 µg/ml). After 72 hours incubation, the cell suspension (10 µl) was mixed with trypan blue dye (10 µl) and cell viability was assessed by automated cell counter. Results are expressed as mean ± SD (n = 3) of three independent experiments.

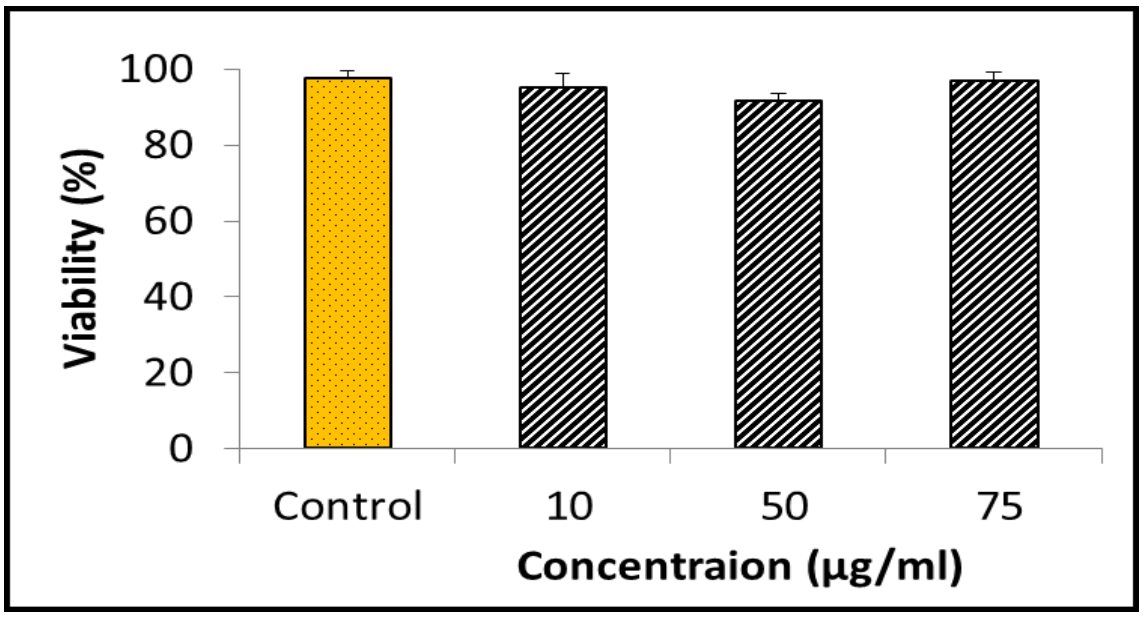

Figure 5.17: Effect of charantin on BAEC viability using trypan blue assay. Bovine aortic endothelial cells (2.5 x 10^4 / ml) were seeded in 24-well plates and incubated with different concentrations of charantin (10 – 75 µg/ml). After 72 hours incubation, the cell suspension (10 µl) was mixed with trypan blue dye (10 µl) and cell viability was assessed by automated cell counter. Results are expressed as mean ± SD (n = 3) of three independent experiments.

5.4.6 Effects of BSA, BSA-AGEs, MCP, MCF and charantin on BAEC differentiation using tri-dimensional Matrigel ™ culture

Within 24 hours incubation, activated endothelial cells differentiated, aligned to form tubes organized in a capillary-like network (Figure 5.18, a). Representative photomicrographs of cell differentiation/ tube formation in untreated condition (Figure 5.18, A), or treated conditions either with FGF-2 (Figure 5.18, B), or 10 µg/ml (Figure 5.18, C), 50 µg/ml (Figure 5.18, D), and 75 µg/ml (Figure 5.18, E), of BSA-AGEs (Figure 5.18), BSA (Figure 5.19), MCP (Figure 5.20), MCF (Figure 5.21) or of charantin (Figure 5.22) were shown. Treated with FGF-2 (Figure 5.18, B), the positive control, the stimulated cells formed a capillary-like network with a significant increase of the network density by 42% (p = 0.0058)

compared to the untreated control cells which formed a few tube-like structures (Figure 5.18, A). At 10 and 50 µg/ml, BSA-AGEs significantly ($p < 0.01$) increased tube formation by 119% and 169%, respectively, while at 75 µg/ml, the tube formation was significantly ($p = 0.012$) inhibited by 14% of control, compared to the untreated control cells (Figure 5.18). BSA at the same concentration showed no effect on tube formation compared to untreated cells (Figure 5.19). While no effect was noticed at the lowest concentration of MCP, in the presence of 50 and 75 µg/ml MCP, the tube formation significantly increased by 74% ($p = 0.0093$) and 42% ($p = 0.0086$), respectively, compared to the control (Figure 5.20). At all concentrations used, MCF significantly enhanced tube formation by 162% ($p = 0.0082$) at 10 µg/ml, 197% ($p = 0.0078$) at 50 µg/ml and 182% ($p = 0.0079$) at 75 µg/ml, compared to the control (Figure 5.21). In addition, charantin significantly enhanced endothelial tube formation with increased concentrations (Figure 5.22). Indeed, charantin significantly increased the number of closed areas by 57% ($p = 0.0096$) at 10 µg/ml, by 149% ($p = 0.0076$) at 50 µg/ml and by 219% ($p = 0.0079$) at 75 µg/ml, compared to the control (Figure 5.22).

(a)

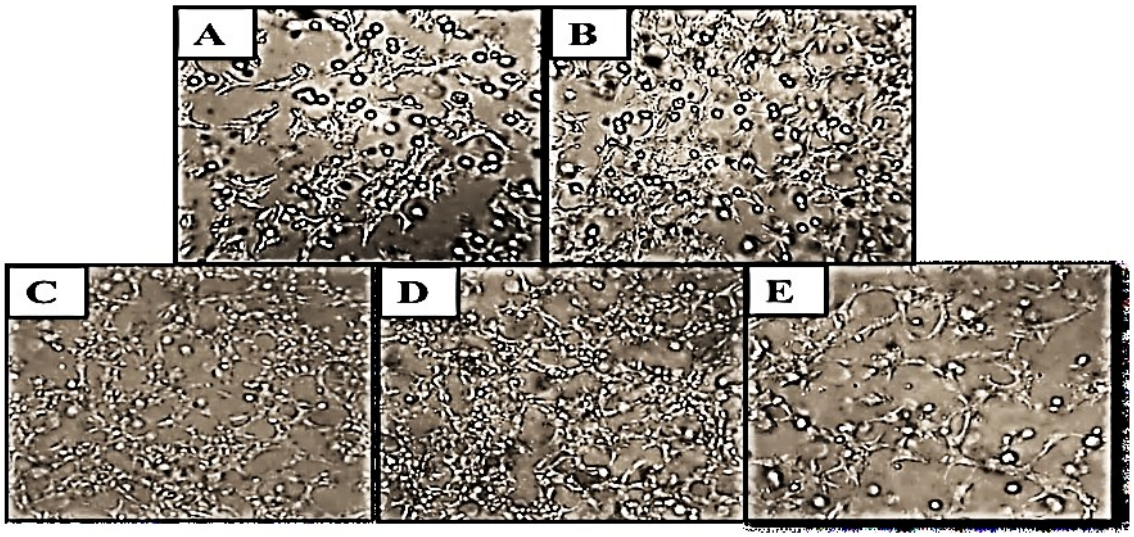

(b)

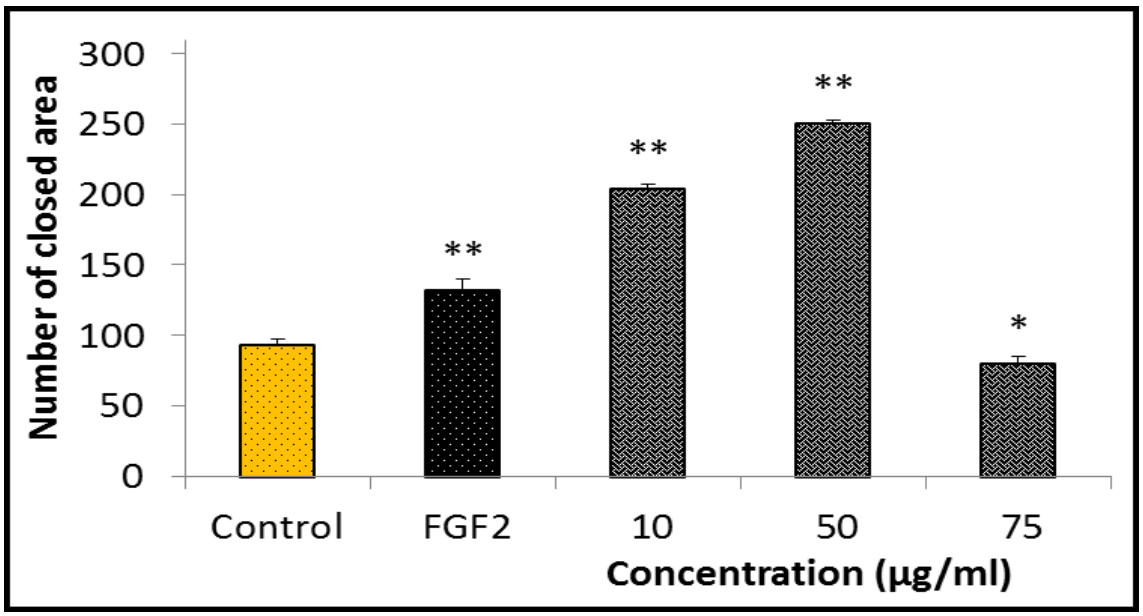

Figure 5.18: Effect of BSA-AGE on BAEC tube formation assay. (a) Representative photomicrographs showing the effect of (A) control, (B) FGF2 (25 ng/ml), (C) AGE (10 µg/ml), (D) AGE (50 µg/ml) and (E) AGE (75 µg/ml) on BAEC differentiation (original magnification, 40X). (b) The graph shows the effects of BSA-AGEs on BAEC tube formation. The bar graph shows the mean ± S.D. * $p < 0.05$, ** $p < 0.01$.

(a)

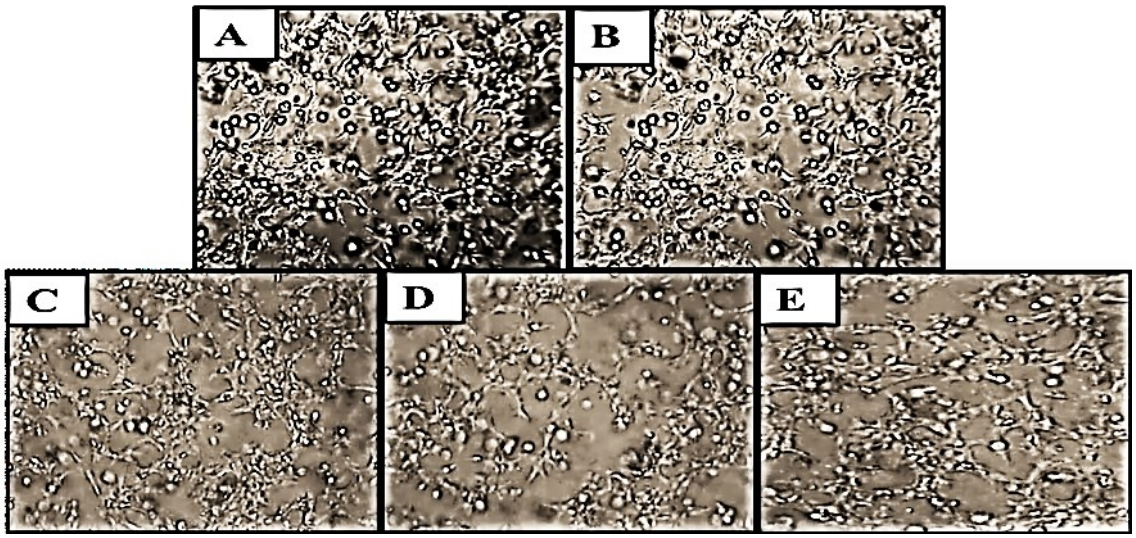

(b)

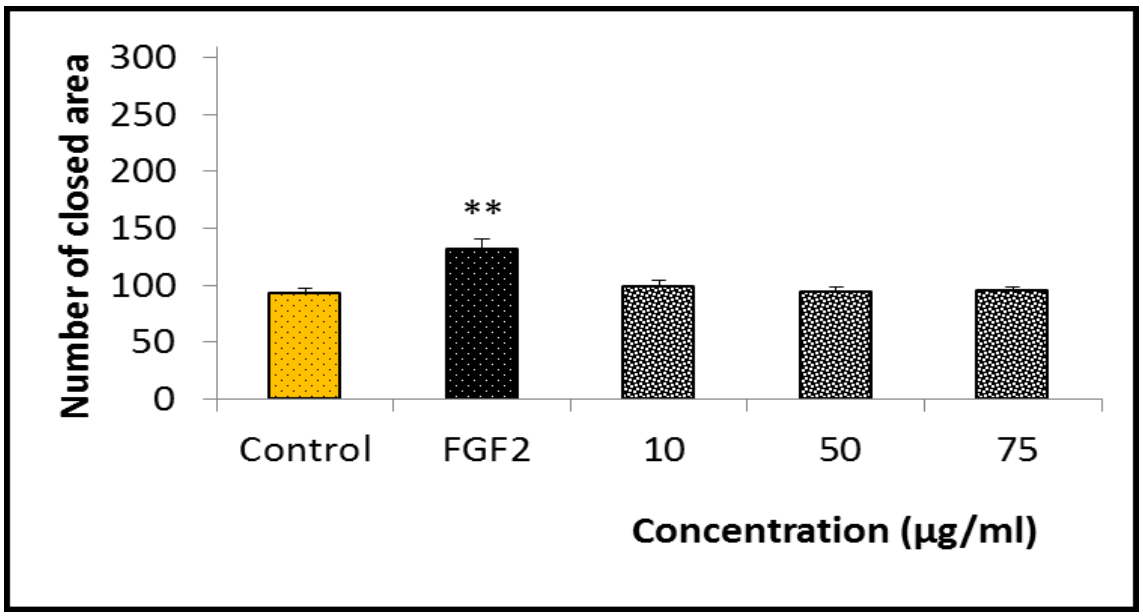

Figure 5.19: Effect of BSA on BAEC tube formation assay. (a) Representative photomicrographs showing the effect of (A) control, (B) FGF2 (25 ng/ml), (C) BSA (10 µg/ml), (D) BSA (50 µg/ml) and (E) BSA (75 µg/ml) on BAEC differentiation (original magnification, 40X). (b) The graph shows the effects of BSA on BAEC tube formation. The bar graph shows the mean ± S.D. $^{**}p < 0.01$.

(a)

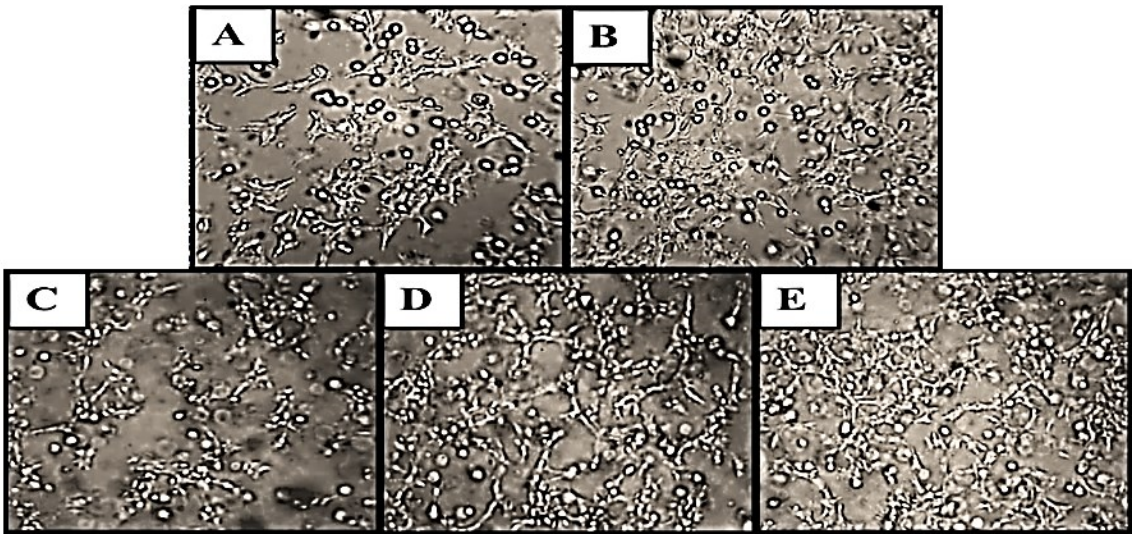

(b)

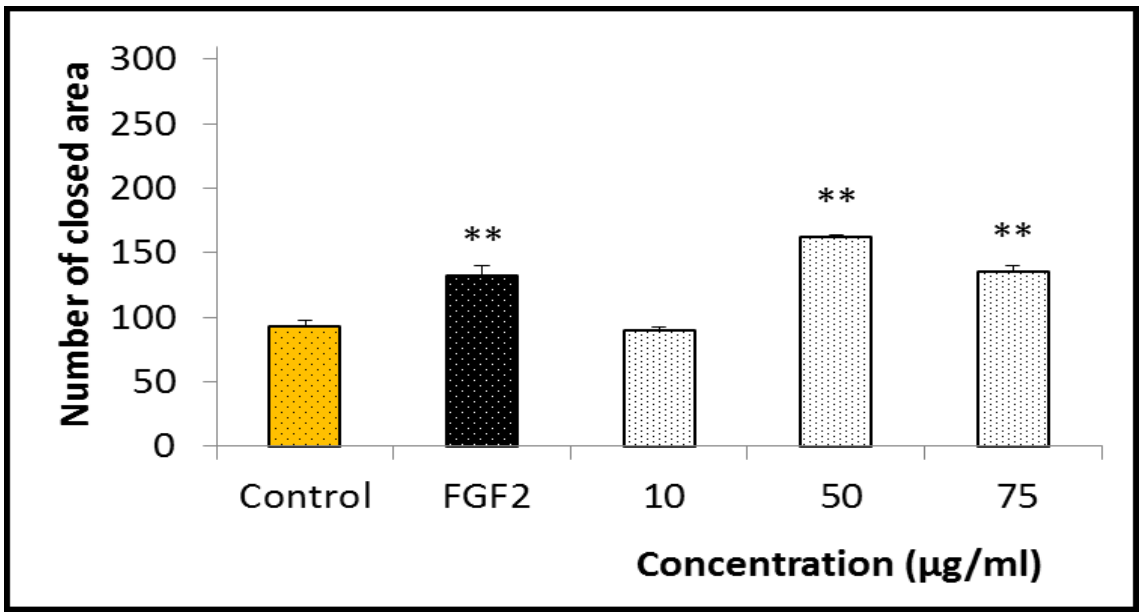

Figure 5.20: Effect of MCP on BAEC tube formation assay. (a) Representative photomicrographs showing the effect of (A) control, (B) FGF2 (25 ng/ml), (C) MCP (10 µg/ml), (D) MCP (50 µg/ml) and (E) MCP (75 µg/ml) on BAEC differentiation (original magnification, 40X). (b) The graph shows the effects of MCP on BAEC tube formation. The bar graph shows the mean ± S.D. $^{**}p < 0.01$.

(a)

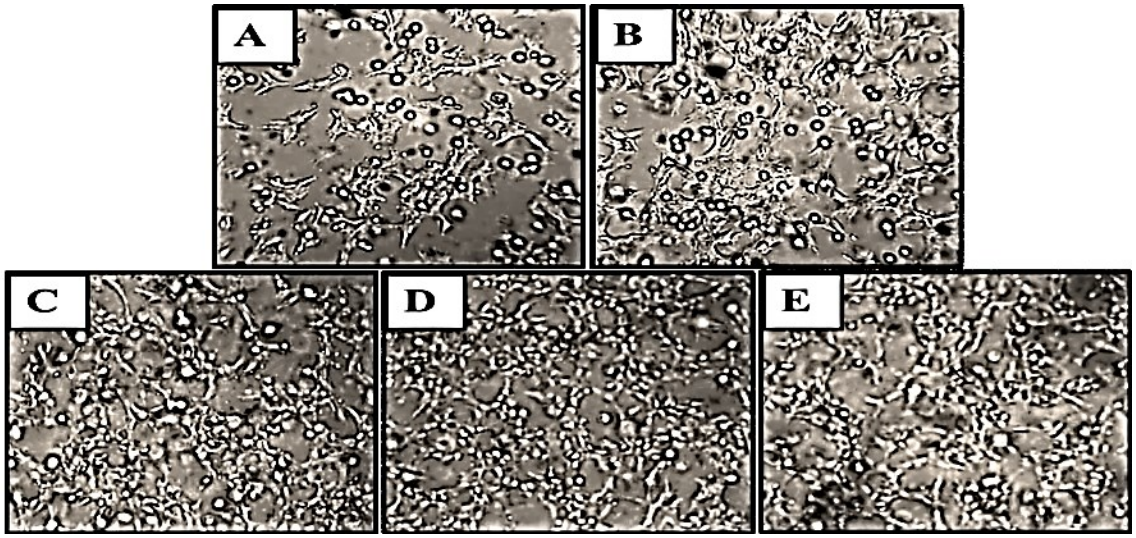

(b)

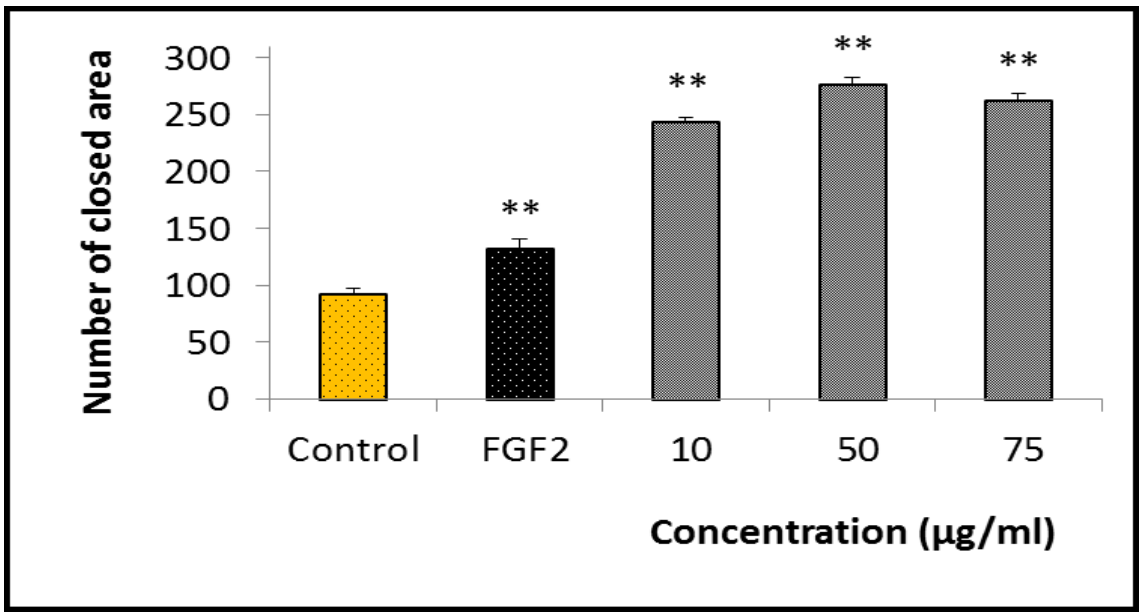

Figure 5.21: Effect of MCF on BAEC tube formation assay. (a) Representative photomicrographs showing the effect of (A) control, (B) FGF2 (25 ng/ml), (C) MCF (10 µg/ml), (D) MCF (50 µg/ml) and (E) MCF (75 µg/ml) on BAEC differentiation (original magnification, 40X). (b) The graph shows the effects of MCF on BAEC tube formation. The bar graph shows the mean ± S.D. $^{**}p < 0.01$.

(a)

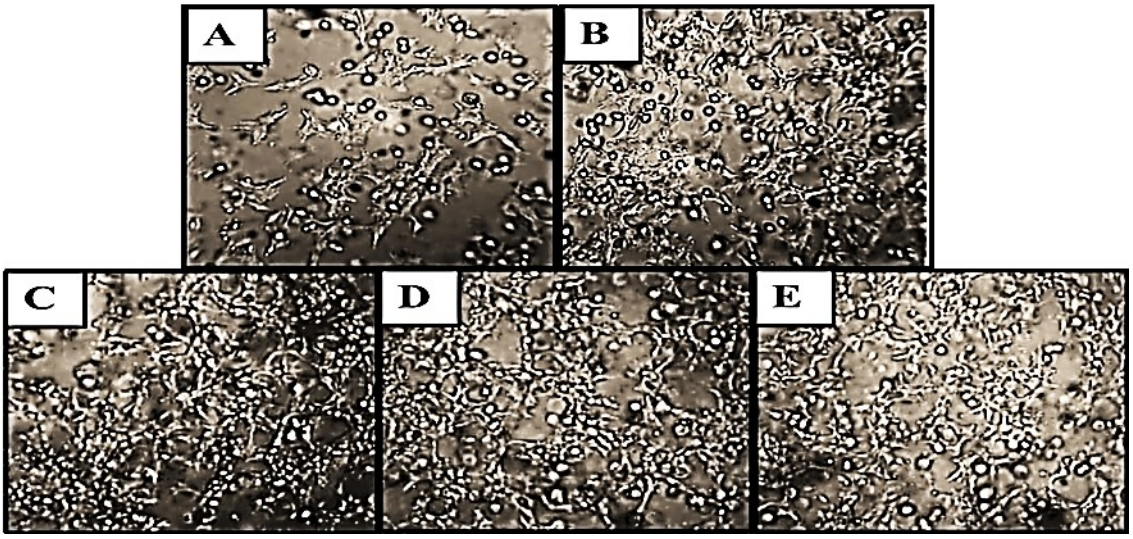

(b)

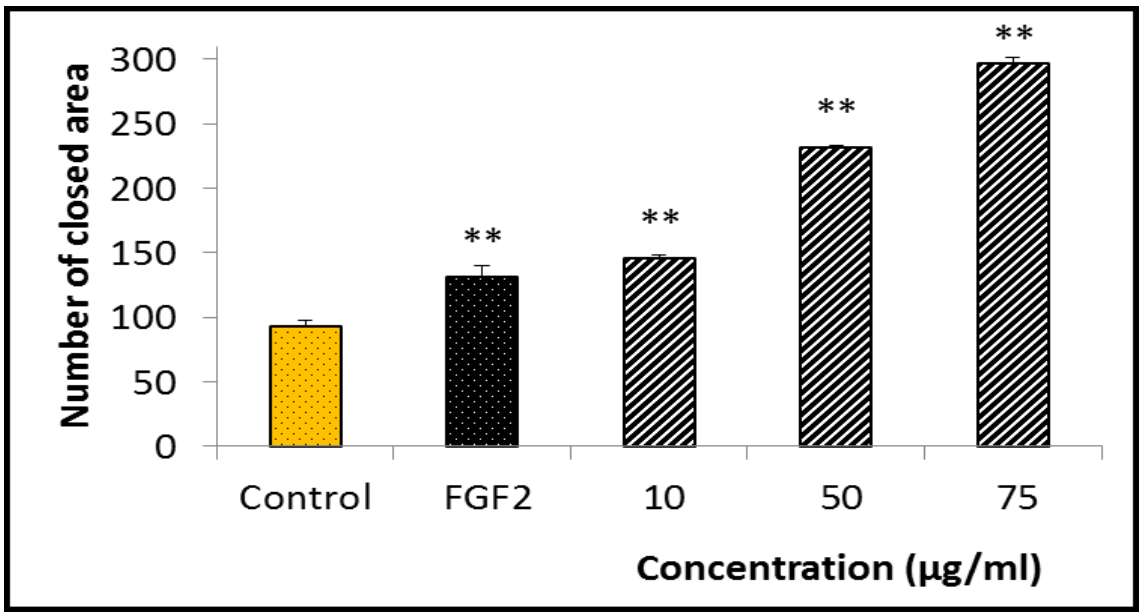

Figure 5.22: Effect of charantin on BAEC tube formation assay. (a) Representative photomicrographs showing the effect of (A) control, (B) FGF2 (25 ng/ml), (C) charantin (10 µg/ml), (D) charantin (50 µg/ml) and (E) charantin (75 µg/ml) on BAEC differentiation (original magnification, 40X). (b) The graph shows the effects of charantin on BAEC tube formation. The bar graph shows the mean ± S.D. $^{**}p < 0.01$.

5.4.7 Effect of MC and charantin extracts on AGE-induced inhibition of endothelial cell tube formation using tri-dimensional Matrigel ™ culture

Endothelial cell differentiation assessed by the tube formation assay was analysed using a 3-D Matrigel™ culture. Within 24 hours of incubation, activated endothelial cells differentiation, aligned to form tubes organized in a capillary-like network (Figure 5.23. a). Representative photomicrographs of tube formation in untreated condition (Figure 5.23, A), or treated conditions either with FGF-2 (Figure 5.23, B), BSA-AGEs (Figure 5.23, C), or BSA-AGEs combined with MCP (Figure 5.23, D), MCF (Figure 5.23, E) or with charantin (Figure 5.23, F) were shown. Treated with FGF-2, the positive control, the stimulated cells formed a capillary-like network with a significant increase of the network density by 2.0-fold (p = 0.001), compared to the untreated control cells which formed a few tube-like structures (Figure 5.23, B). High concentration of BSA-AGEs significantly decreased the tube formation by 0.67-fold (p = 0.014), while native BSA had no effect, compared to the control (Figure 5.23, C). The addition of MC extracts (MCP and MCF) to high concentration BSA-AGEs not only counteracted the inhibitory effect of BSA-AGEs on BAEC tube formation but also significantly increased the tube formation by 2.7-fold ($p < 0.01$), compared to the BSA-AGEs treated cells (Figure 5.23, D and 5.23, E). Charantin reduced the inhibitory effect of BSA-AGEs on tube formation and increased the tubulogenesis process by 1.5-fold (p = 0.013), as compared to the BSA-AGEs treated cells (Figure 5.23, F).

(a)

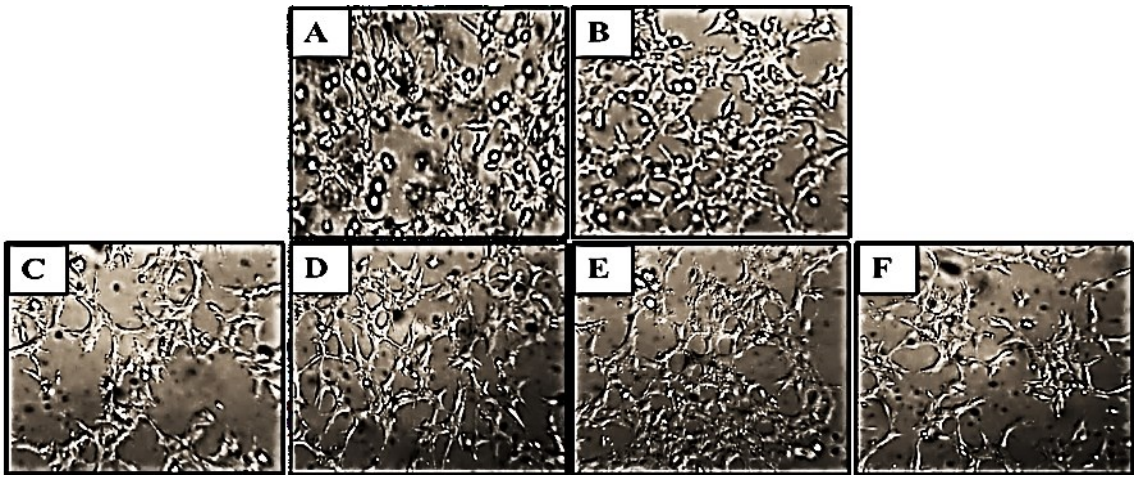

(b)

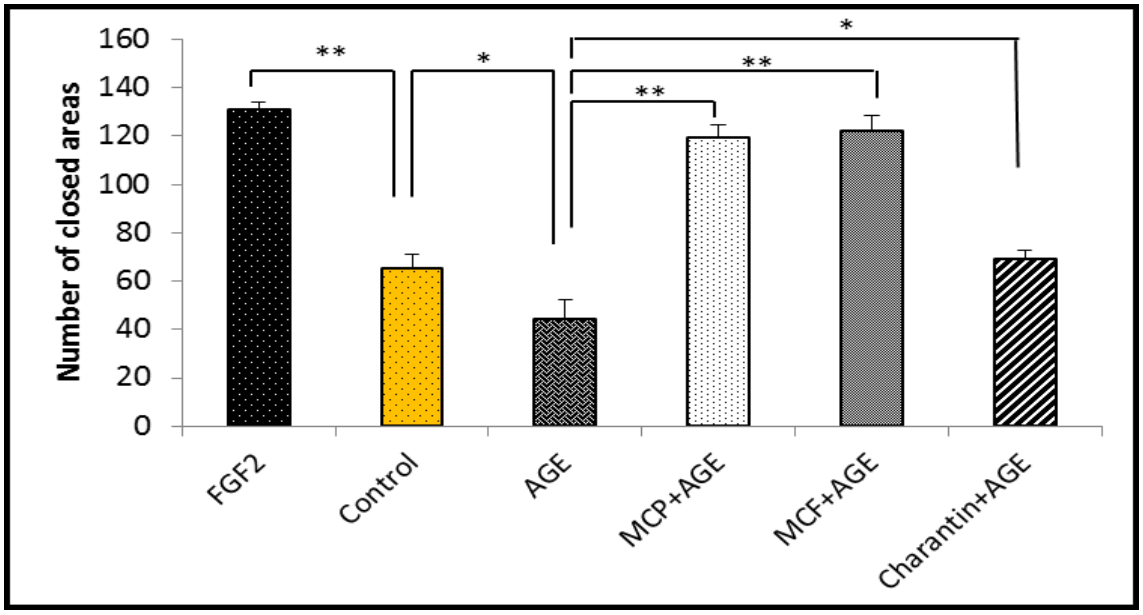

Figure 5.23: Effect of MC and charantin extracts on AGE-induced inhibition of endothelial cell tube formation. (a) Representative photomicrographs showing the effect of (A) control, (B) FGF2 (25 ng/ml), (C) AGE (250 µg/ml), (D) AGE (250 µg/ml) + MCP (10 µg/ml), (E) AGE (250 µg/ml) + MCF (10 µg/ml) and (F) AGE (250 µg/ml) + charantin (10 µg/ml) on BAEC differentiation (40 x). (b) The bar graph shows the effects of AGE (250 µg/ml) combined with *Momordica charantia* extracts (10 µg/ml), FGF-2 (25ng /ml) on BAEC tube formation after 24 hours. The number of closed areas was counted. The bar graph shows the mean ± S.D. (*) and (**) signify a statistically significant difference ($p < 0.05$ and $p < 0.01$) compared with the AGE .Experiments were performed in triplicate wells and repeated at least three times. A representative example is shown.

5.4.8 Effect of *Momordica charantia* extracts on extracellular signal-regulated kinase 1/2 phosphorylation in BAEC.

Since activating ERK1/2 is the key step of angiogenesis (Baek *et al.*, 2012), in this regards, p-ERK1/2 expression in presence of *Momordica charantia* extracts was examined. To optimize the incubation time corresponding to the maximal cell signalling induced by MC extracts, Western blotting was used to determine the expression of p-ERK1/2 in BAEC treated with 10 µg/mL MCP for 10 minutes and 1-3-6 hours incubation along with cells treated with FGF-2 for 10 minutes incubation (Figure 5.24). At 10 minutes incubation, the cell treatment with MCP significantly increased the phosphorylation of ERK1/2 like FGF-2, compared to the basal level of p-ERK1/2 expressed in untreated control cells. The expression of p-ERK1/2 slightly decreased at 1 hour incubation point, and nearly disappeared at 6 hours incubation point (Figure 5.24).

The phosphorylation of ERK was initiated by exogenous addition of different concentrations (10-75 µg/ml) of MC extract and 25 ng/mL FGF-2 for 10-minute. BAEC proteins lysates were subjected to western blotting analysis. As expected, FGF-2 significantly induced p-ERK1/2 over-expression by 5.5-fold increase of p-ERK2 and by 1.9-fold increase of p-ERK1, compared to the basal level of p-ERK1/2 expressed in untreated control cells. The addition of 50 µg/ml of MCP extract (Figure 5.25) significantly (p =0.0075) increased p-ERK1/2 over-expression by 4.7-fold increase of p-ERK2 and by 1.8-fold increase of p-ERK1, compared to the control. At the same concentration, MCF significantly (p =0.0073) induced p-ERK1/2 over-expression by 4.5-fold increase p-ERK2 and by 1.8-fold p-ERK1, compared to the control (Figure 5.26). At the same conditions, charantin significantly increased p-ERK1/2 expression by 3.79-fold (p =0.0075) p-ERK2 and by 1.23-fold p-ERK1, compared to the untreated cells (Figure 5.27).

(a)

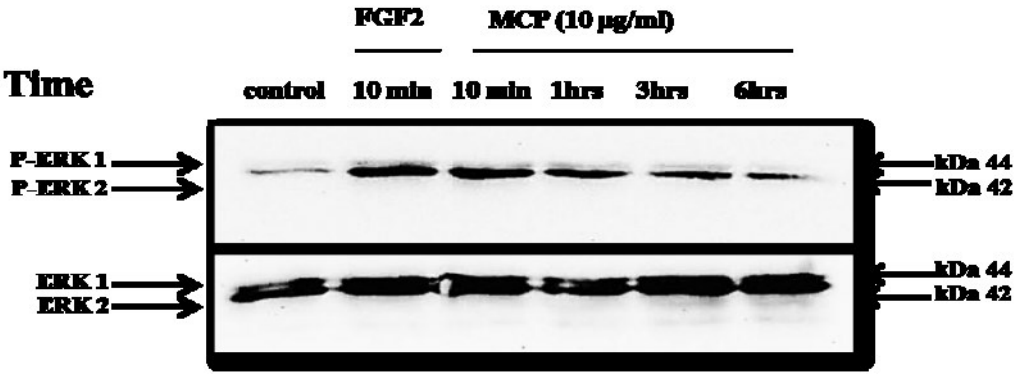

(b)

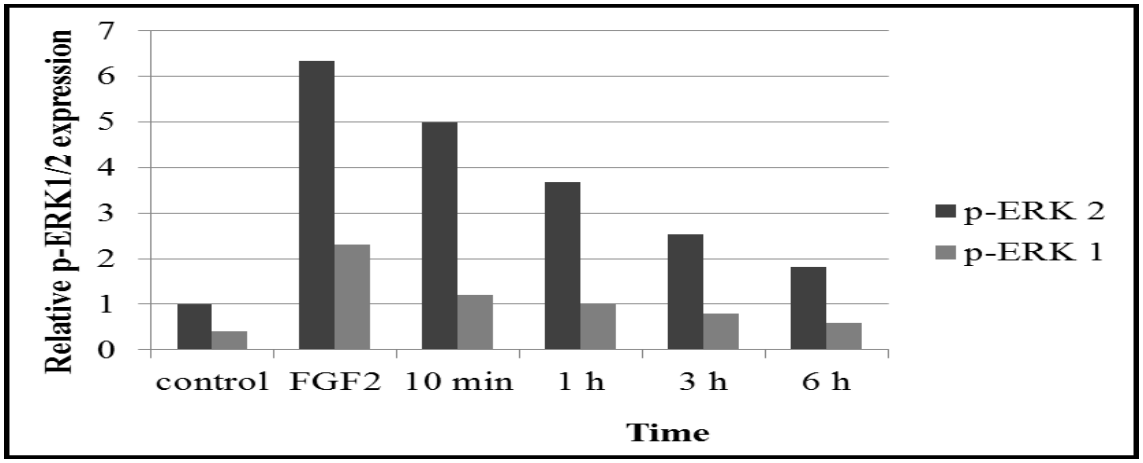

Figure 5.24: Effect of MCP on P-ERK expression in different time. (a) A representative Western blot showing the up regulation of ERK1 / ERK2 phosphorylation by MCP (10 µg/ml) and FGF2 in different time. (b) The bar graph shows the effects of control, FGF2 (25 ng/ml) and MCP (10 µg/ml) in different time (10 minutes, 1 hour, 3 hours and 6 hours). The results expressed are relative to total-ERK1/2 expression. To check the equal loading of proteins, total-ERK1/2 was used as loading control. Each panel was representative of at least three independent experiments.

(a)

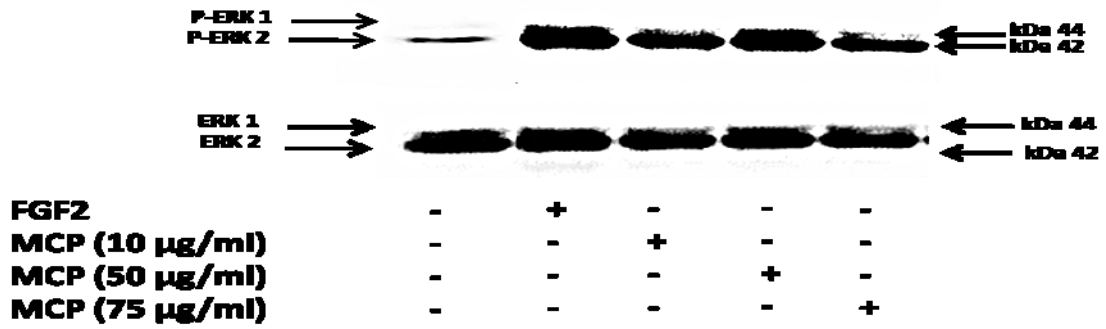

(b)

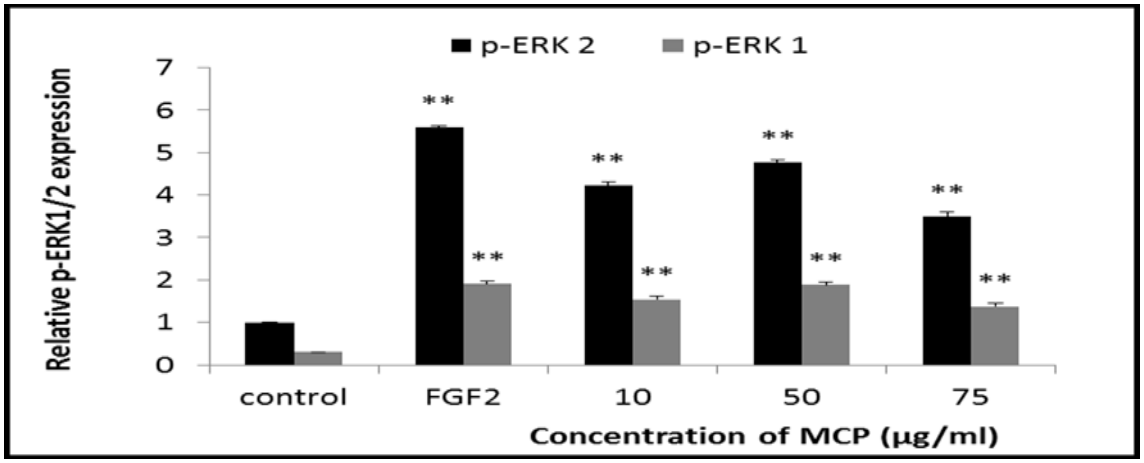

Figure 5.25: Effect of different concentration of MCP on P-ERK expression in 10 minutes. (a) A representative Western blot showing the up regulation of ERK1 / ERK2 phosphorylation by MCP at different concentration (10, 50, 75 µg/ml) in 10 minutes time. (b) The bar graph shows the effects of control, FGF2 (25 ng/ml), MCP (10 µg/ml), MCP (50 µg/ml) and MCP (75 µg/ml) in 10 minutes. The results expressed are relative to total-ERK1/2 expression in control. To check the equal loading of proteins, total-ERK1/2 was used as loading control. Each panel was representative of at least three independent experiments. (**) signify a statistically significant difference ($p < 0.01$) compared with the control.

(a)

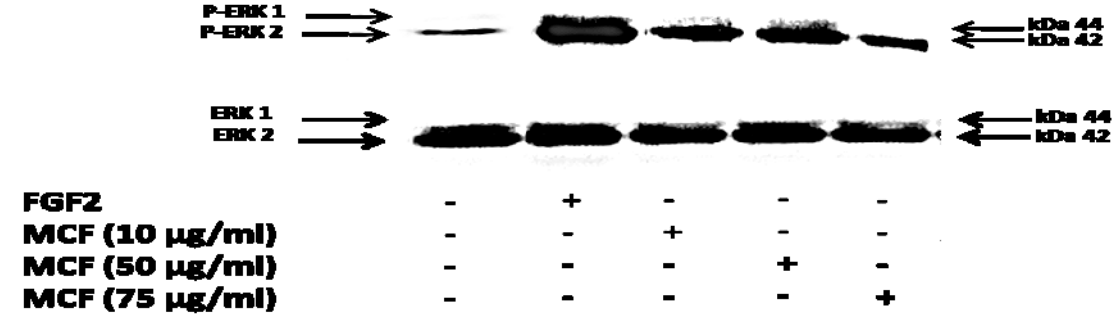

(b)

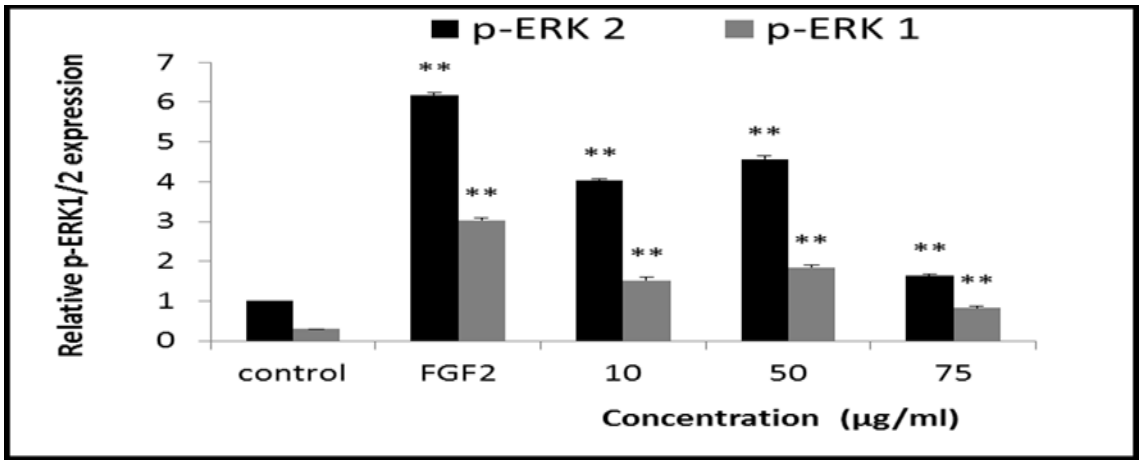

Figure 5.26: Effect of different concentration of MCF on P-ERK expression in 10 minutes. (a) A representative Western blot showing the up regulation of ERK1 / ERK2 phosphorylation by MCF at different concentration (10, 50, 75 µg/ml) in 10 minutes time. (b) The bar graph shows the effects of control, FGF2 (25 ng/ml), MCF (10 µg/ml), MCF (50 µg/ml) and MCF (75 µg/ml) in 10 minutes. The results are expressed as relative to total-ERK1/2 expression. To check the equal loading of proteins, total-ERK1/2 was used as loading control. Each panel was representative of at least three independent experiments. (**) signify a statistically significant difference ($p < 0.01$) compared with the control.

(a)

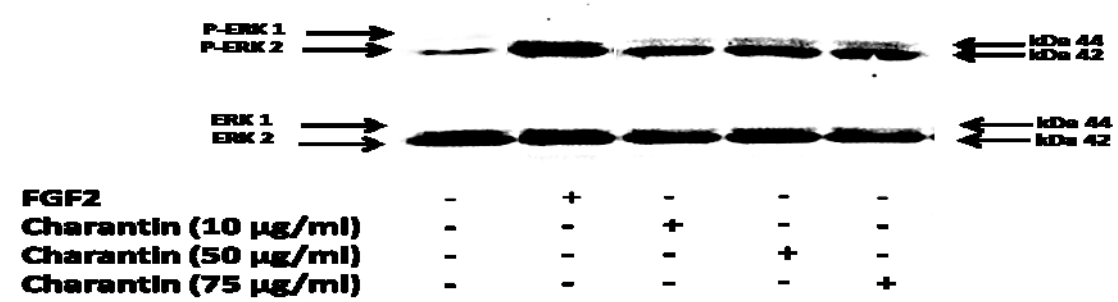

(b)

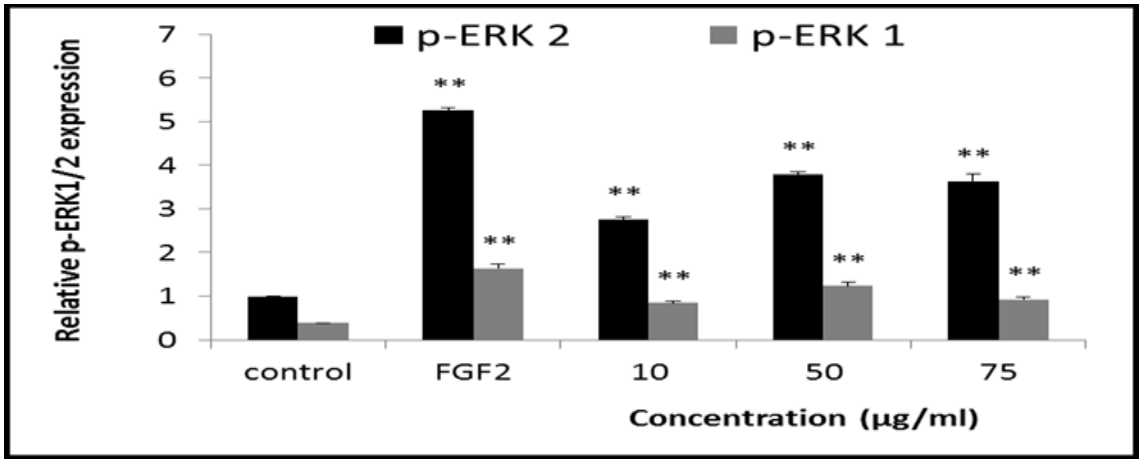

Figure 5.27: The effect of different concentration of charantin on P-ERK expression in 10 minutes. (a) A representative Western blot showing the up regulation of ERK1 / ERK2 phosphorylation by charantin at different concentration (10, 50, 75 µg/ml) in 10 minutes time. (b) The bar graph shows the effects of control, FGF2 (25 ng/ml), charantin (10 µg/ml), charantin (50 µg/ml) and charantin (75 µg/ml) in 10 minutes. The bands and the results are expressed as relative to total-ERK1/2 expression. To check the equal loading of proteins, total-ERK1/2 was used as loading control. Each panel was representative of at least three independent experiments. (**) signify a statistically significant difference ($p < 0.01$) compared with the control.

5.4.10 Effects of AGEs or Momordica charantia extracts on cell differentiation after RAGE neutralization

To understand cellular mechanisms whereby either the *Momordica charantia* extracts or AGE can activate ERK via the receptor of AGEs (RAGE). In this regards, Figure 5.28 shows the effect of MC extracts or AGE on BAEC tube formation when (RAGE) neutralized by RAGE antibody. Isotybic control (IgG) was used as positive control. All extracts and AGE combined with IgG were significantly ($p < 0.05$) increased tube formation compared to untreated cells (control). Furthermore, cells were treated with RAGE (20 μg/ml) showed significant ($p < 0.05$) reduction on tube formation compared with control group. AGE showed a significant inhibition on BAEC tube formation (treated with RAGE) by 92% of control. In addition, MCP, MCF and charantin were showed a significant ($p < 0.05$) inhibition on tube formation by 94%, 93% and 95% of control respectively when cells were neutralized with RAGE antibody (Figure 5.28).

(a)

(b)

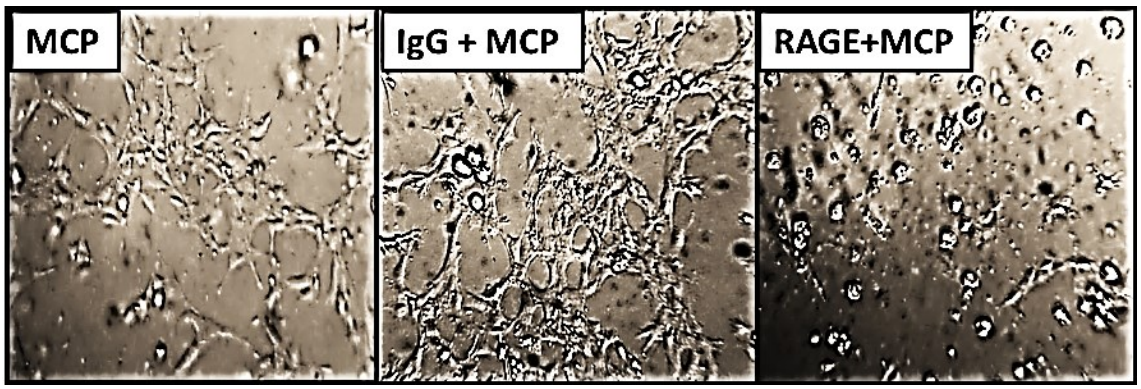

(c)

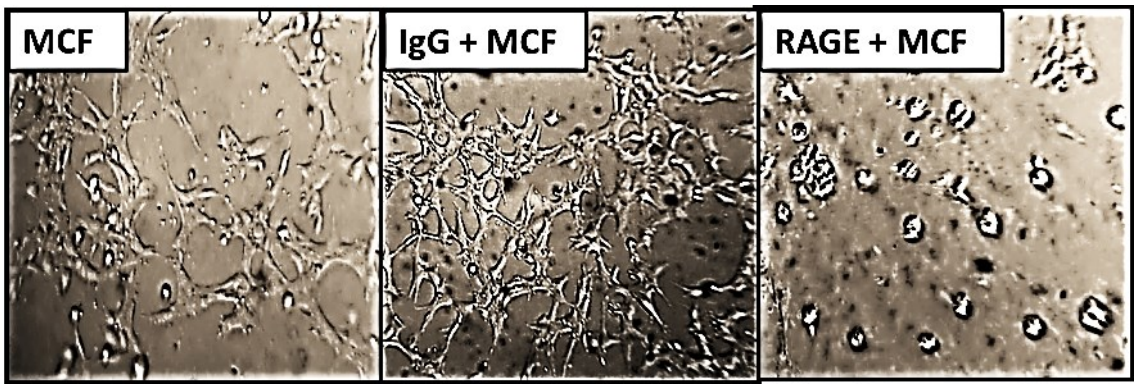

(d)

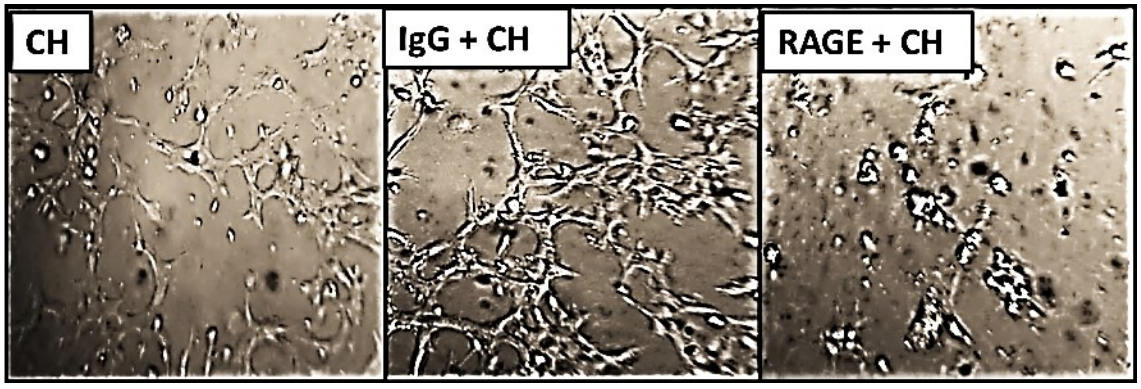

(e)

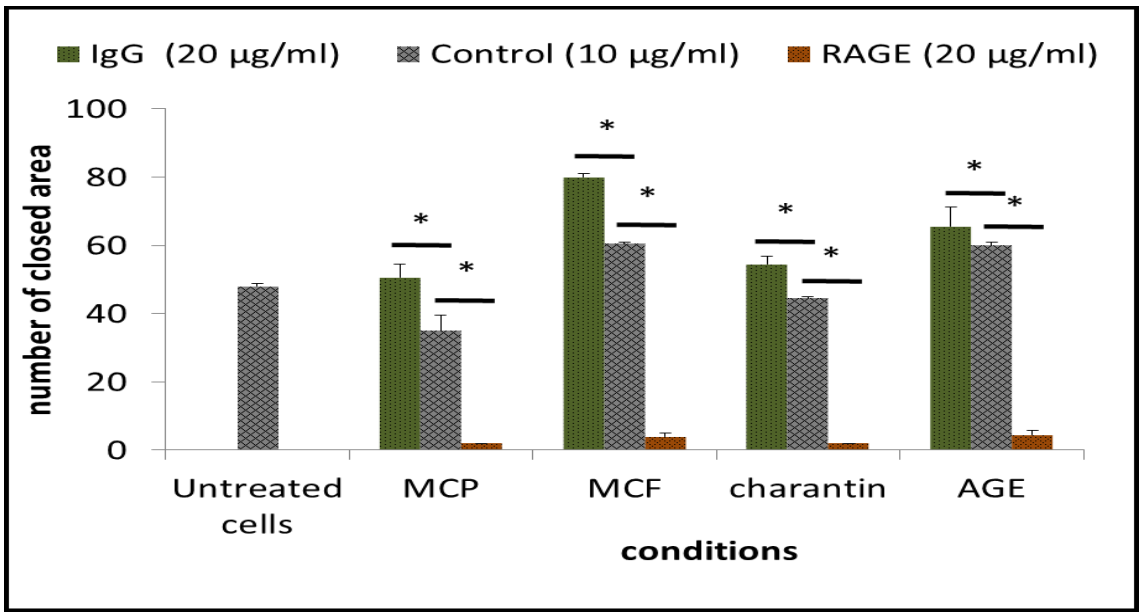

Figure 5.28: Effects of AGEs or *Momordica charantia* extracts on cell differentiation assay after RAGE neutralization. (a) Representative photomicrographs showing the effect of (A) AGE (10 µg/ml), (B) IgG + AGE and (C) RAGE + AGE. (b) Representative photomicrographs showing the effect of (A) MCP (10 µg/ml), (B) IgG + MCP and (C) RAGE + MCP. (c) Representative photomicrographs showing the effect of (A) MCF (10 µg/ml), (B) IgG + MCF and (C) RAGE + MCF. (d) Representative photomicrographs showing the effect of (A) charantin (10 µg/ml), (B) IgG + charantin and (C) RAGE + charantin on BAEC differentiation (40 x). (e) The bar graph shows the effects of all conditions (10µg /ml) ± IgG and RAGE Ab on BAEC tube formation after 24 hours. The number of closed areas was counted. The bar graph shows the mean ± S.D. (*) signify a statistically significant difference ($p < 0.05$) compared with the control. Experiments were performed in triplicate wells and repeated at least three times. A representative example is shown.

5.4.11 Effects of AGEs or *Momordica charantia* extracts on extracellular signal-regulated kinase 1/2 phosphorylation in BAEC after RAGE neutralization

ERK1/2 protein activity characterized as its phosphorylated form is required for EC Proliferation, migration and tube formation in angiogenesis (Slevin *et al.*, 2002). To demonstrate whether MCP, MCF extracts and charantin acted through the receptor for AGEs (RAGE) in the induction of the signal transduction, the cells were treated with anti-RAGE antibody to neutralize the action of the receptors before being stimulated for 10 minutes incubation with 50 µg/ml BSA-AGEs or with 10 µg/ml MC extracts and charantin (Figure 5.30). First, using the isotype control of anti-RAGE antibody, a significant induction of p-ERK1/2 overexpression was observed by the addition of BSA-AGEs, MC extracts and charantin, compared to the basal level of p-ERK1/2 expression in untreated control cells (Figure 5.31). By neutralizing RAGE with anti-RAGE antibody, a significant decrease of BSA-AGE-induced p-ERK1/2 overexpression was observed as expected but also a strong inhibition of p-ERK1/2 overexpression induced by MC extracts and charantin, compared to the control (Figure 5.31).

(a)

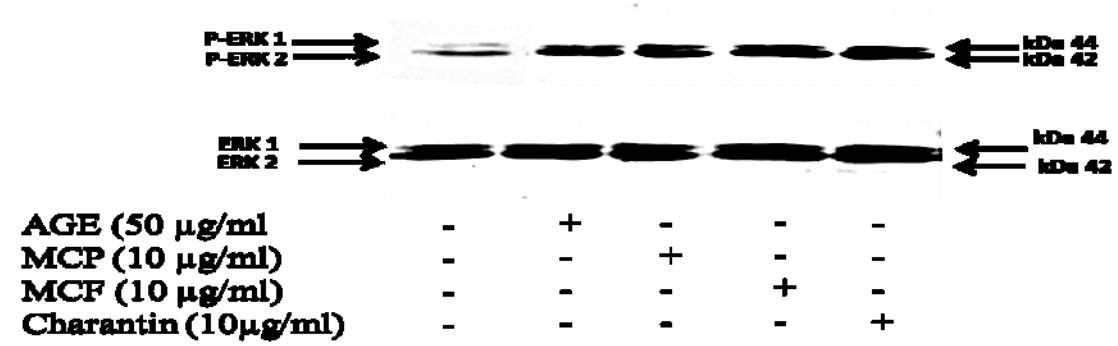

(b)

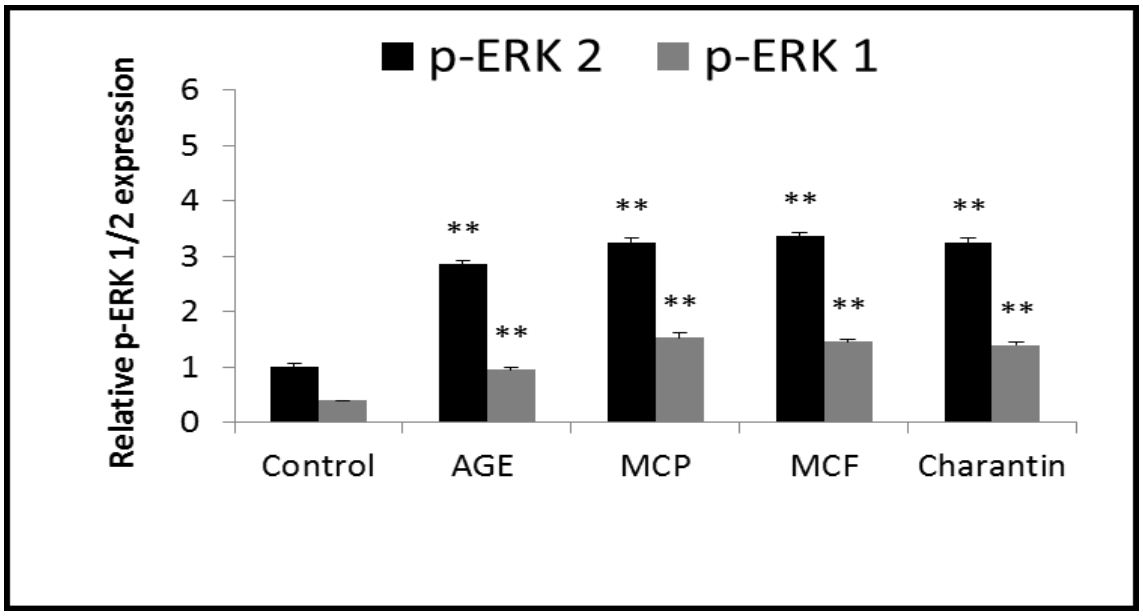

Figure 5.29: Effect of AGE, MCP, MCF and charantin on P-ERK expression in 10 minutes. (a) A representative Western blot showing the up regulation of ERK1 / ERK2 phosphorylation by AGE (50 µg/ml) and MC extracts at the concentration of (10 µg/ml) in 10 minutes time. (b) The bar graph shows the effects of control, AGE (50 µg/ml), MCP (10 µg/ml), MCF (10 µg/ml) and charantin (10 µg/ml) in 10 minutes. The results are expressed as relative to total-ERK1/2 expression. To check the equal loading of proteins, total-ERK1/2 was used as loading control. Each graph was representative of at least three independent experiments. (**) signify a statistically significant difference ($p < 0.01$) compared with the control.

(a)

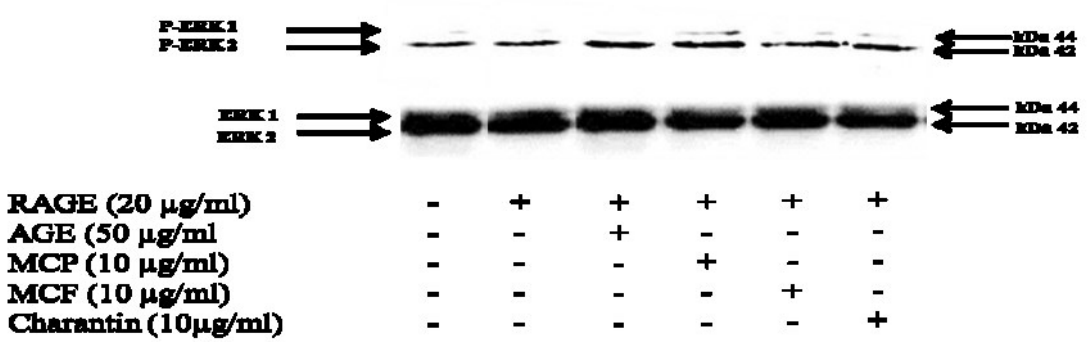

(b)

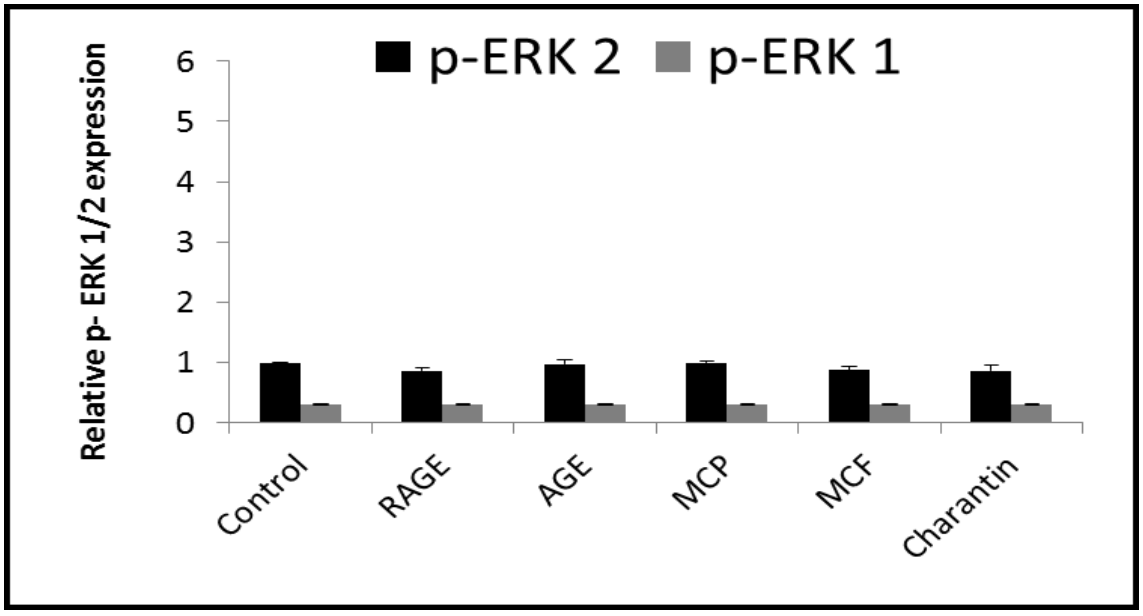

Figure 5.30: The effect of AGE, MCP, MCF and charantin on P-ERK expression in 10 minutes with RAGE Ab. (a) A representative Western blot showing the down regulation of ERK1 / ERK2 phosphorylation by AGE (50 µg/ml) and MC extracts at the concentration of (10 µg/ml) in the presence of RAGE (20 µg/ml). (b) The bar graph shows the effects of control, RAGE (20 µg/ml), AGE (50 µg/ml), MCP (10 µg/ml), MCF (10 µg/ml) and charantin (10 µg/ml) in the presence of RAGE (20 µg/ml) for 10 minutes. The results are expressed as relative to total-ERK1/2 expression. To check the equal loading of proteins, total-ERK1/2 was used as loading control. Each graph was representative of at least three independent experiments.

(a)

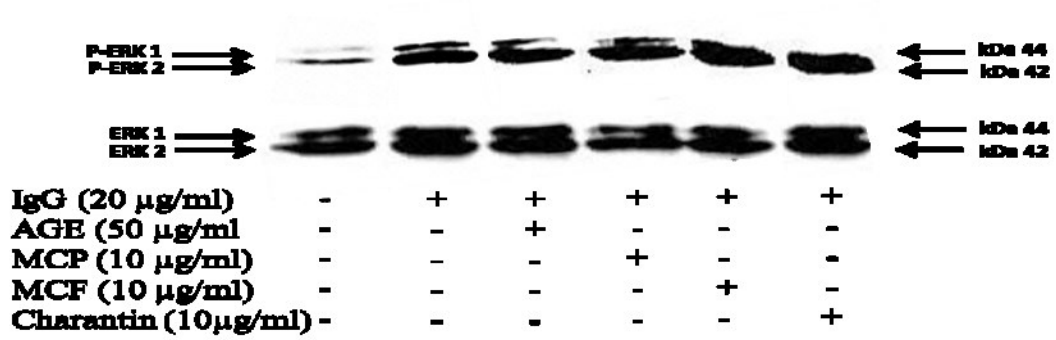

(b)

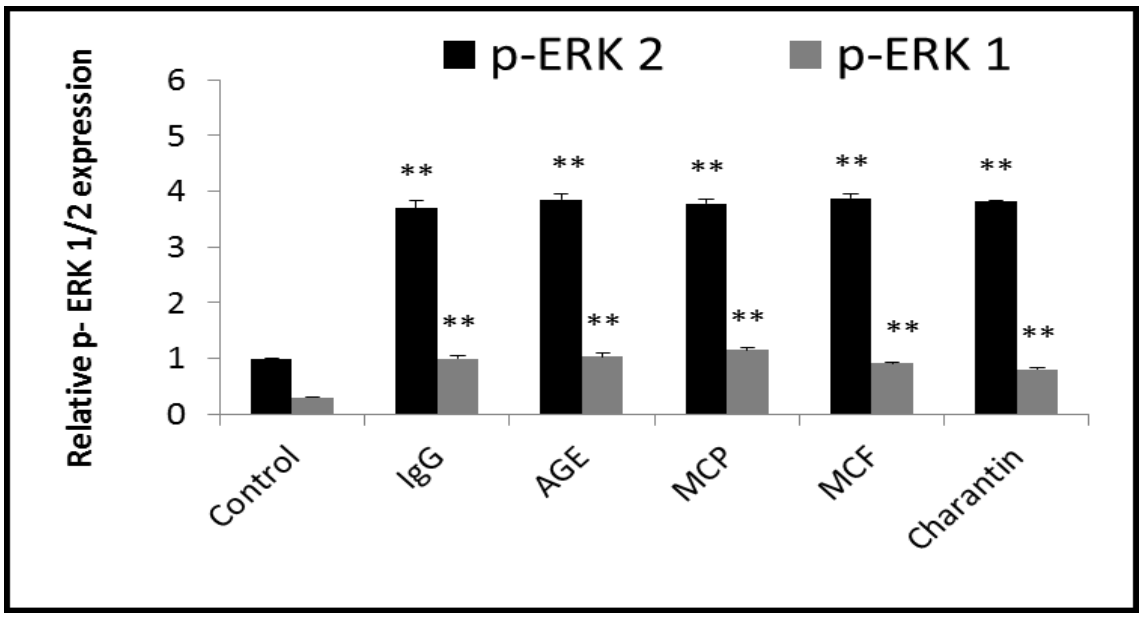

Figure 5.31: The effect of AGE, MCP, MCF and charantin on P-ERK expression in 10 minutes with IgG. (a) A representative Western blot showing the up regulation of ERK1 / ERK2 phosphorylation by AGE (50 µg/ml) and MC extracts at the concentration of (10 µg/ml) in the presence of IgG (20 µg/ml). (b) The bar graph shows the effects of control, IgG (20 µg/ml), AGE (50 µg/ml), MCP (10 µg/ml), MCF (10 µg/ml) and charantin (10 µg/ml) in the presence of IgG (20 µg/ml) for 10 minutes. The results are expressed as relative to total-ERK1/2 expression. To check the equal loading of proteins, total-ERK1/2 was used as loading control. Each graph was representative of at least three independent experiments. (**) signify a statistically significant difference ($p < 0.01$) compared with the control.

5.5 Discussion

Initial development of complications in diabetes like disturbed wound healing, neuropathy, retinopathy and nephropathy have been found to be linked with reduced angiogenesis (Ahmed *et al*., 2008). Studies have determined that migration of endothelial cells proliferation and formation of capillary tube *in vitro* is decreased by hyperglycemia and thereby leads to inadequate angiogenesis (Martin *et al*., 2003). There are several *in vivo* and *in vitro* experiments whose findings provide strong evidence about the development of diabetic complications can caused by accumulation of AGEs, which are formed in diabetic patients due to chronic hyperglycemia (Giardino *et al*., 1994; Goh and Cooper, 2008; Vlassara and Palace, 2002; Yamagishi, 2011; Zheng *et al*., 2002). Consequently, it has been hypothesized that a significant role in angiogenesis is played by protein glycation, through AGE synthesis (Okamoto *et al*., 2002; Stitt *et al*., 2005). BSA-AGEs have been used as glycated proteins in the current study at concentrations between 10 µg/ml and 75 µg/ml. The concentration range 10-50 µg/ml was selected since Xu *et al*. (2003) have reported that it may represent the lowest level of plasma AGEs found in patients suffering from diabetes. Moreover, the 75 µg/ml concentration was used to verify the findings of Chibber *et al*. (1997) which showed that BSA-AGE demonstrates toxicity to BAEC only when its concentration exceeds 62.5 µg/ml. In the present study, BSA-AGE was unable to demonstrate any cytotoxic effect on BAECs when used at concentrations of 10-50 µg/ml; however, significantly optimum increase in cell proliferation, migration and tube formation was caused when concentration of BSA-AGEs was 50 µg/ml i.e. a concentration comparable to the diabetic situation *in vivo* (Chen *et al*., 2009). In addition to these, it was found that BSA-AGEs at high concentrations i.e. 75 µg/ml caused inhibition of cell proliferation, migration and tube formation, this finding is supported by previous research (Chibber *et al*., 1997). Besides this, BSA-AGEs have also been employed for exploring the influence of protein glycation on

various cell lines and tissues (Franke *et al*., 2009; Hirasawa *et al*., 2011; Hung *et al*., 2010; Kowluru, 2005). However, BAECs remained unaffected by unglycated BSA.

This study indicated that all MC extracts (MCF, MCP and charantin) increased endothelial cell proliferation in a dose-response curve. Compared to FGF-2, the lowest and the highest concentrations of MCP and MCF used (i.e. 10 and 75 µg/ml) stimulated cell proliferation reaching the same level than the cell proliferation induced by FGF-2 while a peak of stimulation (higher than FGF-2 effect) was reached by the presence of the intermediary concentration of MC extracts (i.e. 50 µg/ml). The bell-shaped curve is indicative of a bivalent bridging mechanism describing the cell response (i.e. cell proliferation, migration and tube formation) induced by the activation of signal transduction pathways through the dimerization/oligomerization of specific cell-surface receptors after binding with the ligand (Posner *et al*, 1998). The maximal cell response was obtained with 50 µg/ml of all the extracts, which seem to correspond to the optimal oligomerisation of the receptors to induce the maximal activation of the signalling pathways. Among the photochemical components and proteins previously mentioned, MC extracts contain insulin-like proteins that can stimulate endothelial cell proliferation by acting as an insulin-like growth factor (a pro-angiogenic growth factor) bound to two dimers of insulin receptors followed by the activation of the receptor tyrosine kinase. In addition, a recent study has reported that topical insulin accelerates the skin wound healing in diabetic rats (Lima *et al*, 2012). A bell-shaped curve was also observed in response to the mitogenic effect of charantin, which is only composed of the combination of sterol and glucose metabolites. The pro-mitogenic activity of charantin on endothelial cells showed lower effect than FGF-2 at the lowest and highest concentrations of charantin while the maximum stimulation (higher than FGF-2 effect) was reached in the presence of 50 µg/ml charantin. On hydrolysis, charantin gives glucose and a sterol. Glucose is essential, and a vital metabolite for the cell function and its facilitated transport through the

hexose transport (e.g. GLUT1) cannot explain the bell-shaped curve that describes a receptor-dependent mechanism (Young *et al*, 2011). Therefore, the charantin, which can be considered as a glycated phytochemical, could be recognized by a receptor for AGEs, for example. Altogether, these findings suggest that MC extracts and charantin stimulated endothelial cell proliferation through dimerization/oligomerisation of receptors which remain to be identified.

Using the wound-healing assay, this study showed that MC extracts increased endothelial cell migration in a dose-dependent manner. Charantin effect can be justified by the presence of sterol (its hydrolytic metabolite) which induces changes in the contents of membrane cholesterol and alters the micro-viscosity of the plasma membrane, which in turn can regulate endothelial cell migration. These findings suggest that the pro-migratory effects of MC extracts and charantin occurred through a receptor-dependent mechanism and plasma membrane physico-chemical changes.

Tube formation results suggest that MCF extracts contain more insulin-like proteins or other stimulating agents than MCP extracts. In contrast to MCP and MCF extracts, charantin increased tube formation with its concentrations: starting with a stimulatory effect similar than FGF-2 to mostly doubled FGF-2 effect at the highest concentration.

ERK extracellular signal-regulated kinase 1/2 phosphorylation was studied to comprehend the molecular mechanisms behind the action of MC extracts. All of the MC extracts have demonstrated a considerable stimulation on ERK1/2. This finding is supported by other research studies and verifies the pro-angiogenesis action of MC extracts (Ahmed *et al*., 1998; Teoh *et al*., 2009). Moreover, it has been established that AGEs interact with RAGE causing cell death in the presence of reactive oxygen species (Morita *et al*., 2013). Whereas, stimulation of ERK1/2 by MC still needs to be deciphered. The current study proposes for the first time that MC caused activation of ERK1/2 signalling through RAGE, and when RAGE

was made ineffective by using anti-RAGE antibodies, tube formation was not observed in comparison to the control. These findings were confirmed by western blotting.

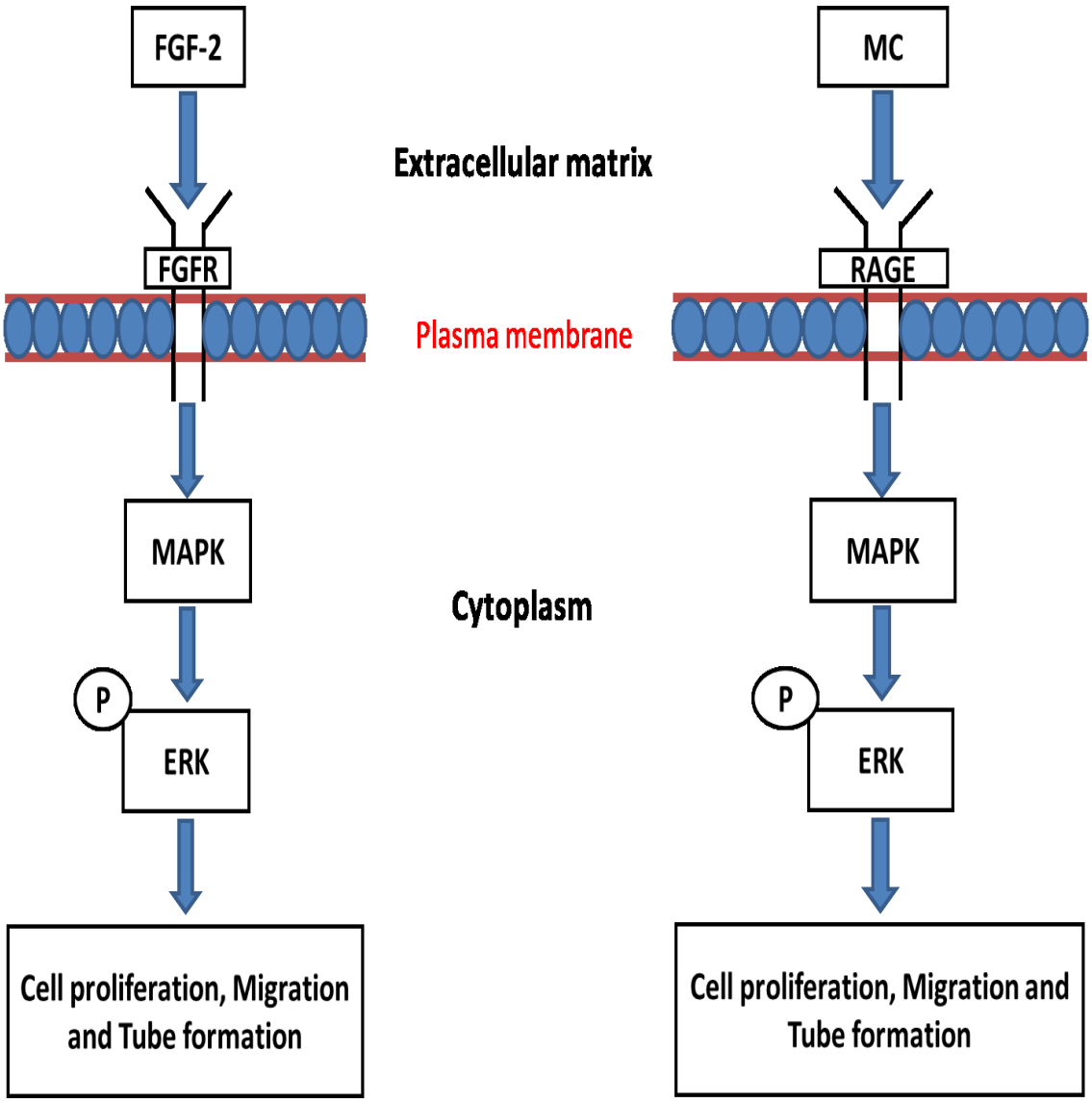

Figure 5.1: Angiogenic signalling pathways induced by FGF-2 and MC in BAEC.

Chapter 6. General discussion

6.1 Novel results

Several important novel results have emerged from this study. MCP, MCF and charantin extracts shows antioxidants properties and antiglycation effect on methylglyoxal-derived AGE formation. Furthermore, MC extracts shows a pro-angiogenic effects on endothelial cell proliferation, migration and differentiation (tube formation) in BAEC. In addition, MC extracts reduce advanced glycation end-products mediated anti-angiogenic effects *in vitro*. This study shows for the first time that MC extracts induced ERK pathway via RAGE.

6.2 General discussion

Protein glycation in diabetes cause protein modifications, including structural and functional impairments and formation of intra- and inter-protein cross-linking resulting in AGE accumulation (Wu *et al*., 2009). The accumulation of cross-linked AGEs in plasma and tissues is thought to account for the long-term risks associated with diabetes and aging (Nishigaki *et al*., 2008). In addition, glycation plays an important role in the pathogenesis of microvascular and macrovascular complications of diabetes (Chen *et al*., 2012). Many researchers have emphasized the advantages of using medicinal plants to reduce AGE formation by their antioxidants activities and may therefore provide protection to alleviate the development of such diabetes-related complications (Tsuji-Naito *et al*., 2009; Wu *et al*., 2009).

The antioxidant as well as radical-scavenging properties of phenolic compounds tends to be generally due to their phenolic hydroxylic groups (Raman and Lau, 1996). The particular free radical-scavenging capacity associated with MC extracts could be caused by their polyphenolic compounds, including flavonoids, flavonols and other phenolics. Several studies have suggested the relation between free radicals-scavenging activity involving

polyphenol substances and their own chemical structure (Aksoy *et al*., 2013; Samak *et al*., 2009). In addition, MC has antioxidant activities probably due to the presence of different contents of vitamins such as ascorbic acid (Vitamin C), Vitamin A and Vitamin E (Ullah, 2011; Senthilkumar, 2012).

Important novel findings have emerged from glycation study, which is discussed in relation to the published literature mentioned in the previous chapters. In this study, it was established for the first time that MCP, MCF extracts and charantin displayed potent inhibitory effects on AGE formation in a dose-dependent manner. Previous research has shown that MC extracts cause a reduction in serum glucose levels and improve glucose tolerance in normal and diabetic humans and animals by increasing insulin sensitivity but without increasing blood insulin levels (Raman and Lau, 1996). Furthermore, the higher amount of phenolic compounds and flavonoids in all extracts may prevent the formation of AGEs. The AGE formation pathway is complex, to understand the inhibition pathway of AGE formation induced by MC extracts, more investigations are needed. In addition, numerous researches have established that MC dose comprises of several amino acids that could decrease the generation of AGEs by the blockage of carbonyl groups (Huang *et al*., 1999; Yuwai *et al*., 1991)

Certainly, to verify the inhibitory outcome of different MC extracts on AGEs, effect of MC on CML contents was investigated. Carboxymethyllysine is one of the most attribute AGE products via glycation and oxidation reactions (Fujiwara *et al*., 2011). Additionally, throughout diabetes, elevated degrees of CML contents have been discovered within the animal along with human tissues (Dyer *et al*., 1993; Kamata *et al*., 2009). These studies

confirm that all extracts show inhibitory effect on CML formation. MCF was also having the most potent inhibitory effect.

AGEs have been implicated in the pathogenesis of diabetic complications including vascular complications arising from angiogenesis. Notably, excessive angiogenesis may play an essential role in diabetic retinopathy and nephropathy, whilst reduced angiogenesis contribute to impaired wound-healing (Martin *et al*., 2003). Specifically, high serum levels of AGEs in diabetics are thought to reduce the formation of granulation tissue during wound-healing (Teixeira *et al*., 1999). The results of the current study indicate that high concentrations of AGEs reduce BAEC proliferation, migration and tube formation, which are believed to play a crucial role in the inhibition of angiogenesis in diabetes. Furthermore, AGE formation may cause changes in biological activities of macrophages (Liu *et al*., 1999), smooth muscle cells and fibroblasts (Okano *et al*., 2002), which are also involved in angiogenesis. On the other hand, MC extracts induced BAEC proliferation, migration and tube formation (Pro-angiogenic activities) which are believed to facilitate the healing of ulcers caused by diabetes-induced atherosclerosis of small arteries. These results were supported by previous studies (Prasad *et al*., 2006; Prashanthi *et al*., 2012). Moreover, in this connection, pro-angiogenic action of MC was explored for the first time in the presence of high concentration of AGEs. The mechanism behind this activity still needs to be explored. AGE/RAGE axis and oxidative stress cause abnormal angiogenesis in wound healing (Chen *et al*., 2012). ERK extracellular signal-regulated kinase 1/2 phosphorylation was studied to investigate the molecular mechanisms behind the action of MC extracts. All of the MC extracts have demonstrated a considerable stimulation of phospho-ERK 1/2 expression. This finding is supported by other research studies and verifies the pro-angiogenesis action of MC extracts (Ahmed *et al*., 1998; Teoh *et al*., 2009). Moreover, it has been established that high concentrations of AGEs interact with RAGE causing programmed cell death (apoptosis) with

the involvement of reactive oxygen species (Morita *et al*., 2013). In addition, stimulation of phospho-ERK1/2 expression through RAGE by MC needs more investigations. The current study proposes for the first time that MC caused activation of ERK1/2 signalling via RAGE. Indeed, after RAGE neutralization using specific antibodies, tube formation was not observed when cells were stimulated by all extracts in comparison to the control. MC extracts and charantin were shown to increase phospho-ERK1/2 expression through RAGE.

6.3 Conclusion

The present results have demonstrated that different MC extracts and charantin can effectively provide protection against methylglyoxal-derived AGE formation *in vitro*. This finding suggests that the daily consumption of MC extracts is considered to be of potential benefit for the prevention of ageing and lifestyle-related diseases. Such protective effects are largely attributed to the antioxidant properties of MC. As MC extracts may be a potentially novel nutrient to delaying diabetic complications, it is of crucial importance to demonstrate that dietary supplementation of MC extract protects against the development of diabetic complications. In addition, all extracts have antioxidant properties and reduce oxidative stress. Moreover, MC extracts have pro-angiogenic action associated with phospho-ERK1/2 over-expression. MC extracts have been shown to counter-act the anti-angiogenic effects of high concentration of AGEs. In addition, MC extracts activate ERK pathway via RAGE. Thus, consumption of MC may not only reduce hyperglycemia but also protect against diabetes-induced complications and deserves more attention.

6.4 Future work

- Wide investigations of the signalling pathways induced by MC extracts and charantin using protein micro-array. The wide investigation of the cytoplasmic proteins is to

increase our understanding of how the stimulated endothelial cells respond leading to angiogenesis.

- Confirmation of *in vitro* angiogenic effects using *in vivo* assays such as CAM assay Confirmation of pro-angiogenic effects using *in vivo* angiogenesis assays such as murine *in vivo* Matrigel-based angiogenesis assay or ex ovo assay such as CAM assay. This study is mandatory to validate the pro-angiogenic effects of MC extracts and charantin. Additional information regarding the structure of the new blood vessels formed can be also examined.

- Conduct an *in vivo* study using patient samples (clinical trial). Further clinical exploration in diabetic patients to validate these experimental findings and to develop MC extracts and charantin as potential wound repair therapy for impairment of the healing of acute and chronic wounds as observed in diabetic foot ulcer.

Chapter 7. References

Ahmad, M. S. and Ahmed, N. (2006). Antiglycation properties of aged garlic extract: possible role in prevention of diabetic complications. *The Journal of nutrition,* **136,** 796S-799S.

Ahmad, M. S., Pischetsrieder, M. and Ahmed, N. (2007). Aged garlic extract and S-allyl cysteine prevent formation of advanced glycation endproducts. *European Journal of Pharmacology,* **561,** 32-38.

Ahmed, I., Adeghate, E., Sharma, A. K., Pallot, D. J. and Singh, J. (1998). Effects of *Momordica charantia* fruit juice on islet morphology in the pancreas of the streptozotocin-diabetic rat. *Diabetes research and clinical practice,* **40,** 145-151.

Ahmed, K. A., Muniandy, S. and Ismail, I. S. (2009). N(epsilon)-(Carboxymethyl)lysine and coronary atherosclerosis-associated low density lipoprotein abnormalities in type 2 diabetes: current status. *Journal of Clinical Biochemistry and Nutrition,* **44,** 14-27.

Ahmed, N. (2005). Advanced glycation endproducts—role in pathology of diabetic complications. *Diabetes Research and Clinical Practice,* **67,** 3-21.

Ahmed, N. and Thornalley, P. J. (2003). Quantitative screening of protein biomarkers of early glycation, advanced glycation, oxidation and nitrosation in cellular and extracellular proteins by tandem mass spectrometry multiple reaction monitoring. *Biochemical Society Transactions,* **31,** 1417-1422.

Ahmed, N. and Thornalley, P. J. (2007). Advanced glycation endproducts: what is their relevance to diabetic complications? *diabetes obesity and metabolism,* **9,** 233-245.

Ahmed, U., Dobler, D., Larkin, S. J., Rabbani, N. and Thornalley, P. J. (2008). Reversal of hyperglycemia-induced angiogenesis deficit of human endothelial cells by overexpression of glyoxalase 1 *In vitro*. *Annals of the New York Academy of Sciences,* **1126,** 262-264.

Aksoy, L., Kolay, E., Agilonu, Y., Aslan, Z. and Kargioglu, M. (2013). Free radical scavenging activity, total phenolic content, total antioxidant status, and total oxidant status of endemic Thermopsis turcica. *Saudi Journal of Biological Sciences,* **20,** 235-239.

Al-Hassan, N. (2003). Definition of diabetes mellitus. *British Journal of General Practice,* **53,** 567-568.

Ali, M. K., Narayan, K. M. and Tandon, N. (2010). Diabetes & coronary heart disease: current perspectives. *Indian Journal of Medical Research,* **132,** 584-597.

American Diabetes Association (2009) Diagnosis and Classification of Diabetes Mellitus. *Diabetes Care.* **32**, S62-S67

American Diabetes Association (2010). Diagnosis and classification of diabetes mellitus. *Diabetes Care,* **33,** S62-S69.

American Diabetes Association (2013). Standards of Medical Care in Diabetes. *Diabetes care,* **36,** S11-S66.

American Diabetes Association (2014). Diagnosis and Classification of Diabetes Mellitus. *Diabetes care,* **37,** S81-S90.

Ames, J. (2008). Determination of N epsilon-(carboxymethyl)lysine in foods and related systems. *Annals of the New York Academy of Sciences,* **1126,** 20-24.

Anitha, B., Sampathkumar, R., Balasubramanyam, M. and Rema, M. (2008). Advanced glycation index and its association with severity of diabetic retinopathy in type 2 diabetic subjects. *Journal of Diabetes and Its Complications,* **22,** 261-266.

Argirova, M., and Argirov, O. (2003) Inhibition of ascorbic acid-induced modifications in lens proteins by peptides. *Journal of Peptide Science*, **9**, 170-176.

Assero, G., Lupo, G., Anfuso, C. D., Ragusa, N. and Alberghina, M. (2001). High glucose and advanced glycation end products induce phospholipid hydrolysis and phospholipid enzyme inhibition in bovine retinal pericytes. *Biochimica et Biophysica Acta,* **1533,** 128-140.

Babu, P. V., Sabitha, K. E. & Shyamaladevi, C. S. (2006) Therapeutic effect of green tea extract on advanced glycation and cross-linking of collagen in the aorta of streptozotocin diabetic rats. *Clinical and Experimental Pharmacology and Physiology*, **33**, 351-357.

Babu, P. V., Sabitha, K. E., Srinivasan, P. and Shyamaladevi, C. S. (2007) Green tea attenuates diabetes induced Maillard-type fluorescence and collagen cross-linking in the heart of streptozotocin diabetic rats. *Pharmacological Research*, **5**, 433-440.

Baby, J. and Jini, D. (2013). Antidiabetic effects of *Momordica charantia* (bitter melon) and its medicinal potency. *Asian Pacific Journal of Tropical Disease,* **3,** 93-102.

Baek, Y.-Y., Cho, D. H., Choe, J., Lee, H., Jeoung, D., Ha, K.-S., Won, M.-H., Kwon, Y.-G. and Kim, Y.-M. (2012). Extracellular taurine induces angiogenesis by activating ERK-, Akt-, and FAK-dependent signal pathways. *European journal of pharmacology,* **674,** 188-199.

Bailey, A. J. (2001). Molecular mechanisms of ageing in connective tissues. *Mechanisms of Ageing and Development,* **122,** 735-755.

Bainbridge, P. (2013). Wound healing and the role of fibroblasts. *Journal of Wound Care,* **22,** 407-8, 410-412.

Balakumar, P., Rohilla, A., Krishan, P., Solairaj, P. and Thangathirupathi, A. (2010). The multifaceted therapeutic potential of benfotiamine. *Pharmacological Research,* **61,** 482-488.

Bao, P., Kodra, A., Tomic-Canic, M., Golinko, M. S., Ehrlich, H. P. and Brem, H. (2009). The role of vascular endothelial growth factor in wound healing. *Journal of Surgical Research,* **153,** 347-358.

Basta, G. (2008). Receptor for advanced glycation endproducts and atherosclerosis: From basic mechanisms to clinical implications. *Atherosclerosis,* **196,** 9-21.

Basta, G., Schmidt, A. and Caterina, R. D. (2004). Advanced glycation end products and vascular inflammation: implications for accelerated atherosclerosis in diabetes. *Cardiovascular research,* **63,** 582 - 592.

Baumgartner-Parzer, S. M., Wagner, L., Pettermann, M., Grillari, J., Gessl, A. and Waldhausl, W. (1995). High-glucose--triggered apoptosis in cultured endothelial cells. *Diabetes,* **44,** 1323-1327.

Baynes, J. W. (2001). The role of AGEs in aging: causation or correlation. *Experimental Gerontology,* **36,** 1527-1537.

Behera, T. K. (2005). Heterosis in Bittergourd. *Journal of New Seeds,* **6,** 217-221.

Beisswenger, P. J., Howell, S. K., Russell, G. B., Miller, M. E., Rich, S. S. and Mauer, M. (2013). Early progression of diabetic nephropathy correlates with methylglyoxal-derived advanced glycation end products. *Diabetes Care,* **36,** 3234-3239.

Berger, M., Monks, D., Wanner, C. and Lindner, T. H. (2003). Diabetic nephropathy: an inherited disease or just a diabetic complication? *Kidney and Blood Pressure Research,* **26,** 143-154.

Boilly, B., Vercoutter-Edouart, A. S., Hondermarck, H., Nurcombe, V. and Le Bourhis, X. (2000). FGF signals for cell proliferation and migration through different pathways. *Cytokine and Growth Factor Reviews,* **11,** 295-302.

Boo, H.-O., Hwang, S.-J., Bae, C.-S., Park, S.-H., Heo, B.-G. and Gorinstein, S. (2012). Extraction and characterization of some natural plant pigments. *Industrial Crops and Products,* **40,** 129-135.

Bousova, I., Vukasovic, D., Juretic, D., Palicka, V. and Drsata, J. (2005). Enzyme activity and AGE formation in a model of AST glycoxidation by D-fructose in vitro. *Acta Pharmaceutica (Zagreb, Croatia),* **55,** 107-114.

Brieger, K., Schiavone, S., Miller, F. J., Jr. and Krause, K. H. (2012). Reactive oxygen species: from health to disease. *Swiss Medical Weekly,* **142,** w13659.

Brown, B. E., Dean, R. T. and Davies, M. J. (2005). Glycation of low-density lipoproteins by methylglyoxal and glycolaldehyde gives rise to the in vitro formation of lipid-laden cells. *Diabetologia,* **48,** 361-369.

Brown, B. E., Nobecourt, E., Zeng, J., Jenkins, A. J., Rye, K. A. and Davies, M. J. (2013). Apolipoprotein A-I glycation by glucose and reactive aldehydes alters phospholipid affinity but not cholesterol export from lipid-laden macrophages. *PloS One,* **8,** e65430.

Brownlee, M. (1992). Glycation products and the pathogenesis of diabetic complications. *Diabetes Care*, **15**, 1835-1843.

Brownlee, M. (2000). Negative consequences of glycation. *Metabolism,* **49,** 9-13.

Brownlee, M. (2005). The Pathobiology of Diabetic Complications: A Unifying Mechanism. *Diabetes,* **54,** 1615-1625.

Brownlee, M. D., Michael (1995). Advanced protein glycosylation in diabetes and aging. *Annual Review of Medicine,* **46,** 223-234.

Brownlee, M., Cerami, A. and Vlassara, H. (1988). Advanced glycosylation end products in tissue and the biochemical basis of diabetic complications. *New England Journal of Medicine,* **318,** 1315-1321.

Bucala, R. and Vlassara, H. (1995). Advanced glycosylation end products in diabetic renal and vascular disease. *American Journal of Kidney Diseases,* **26,** 875-888.

Bucala, R., Makita, Z., Koschinsky, T., Cerami, A. and Vlassara, H. (1993). Lipid advanced glycosylation: pathway for lipid oxidation in vivo. *Proceedings of the National Academy of Sciences,* **90,** 6434-6438.

Bunn, H. F. & Higgins, P. J. (1981) Reaction of monosaccharides with proteins: possible evolutionary significance. *Science*, **213**, 222-224.

Burke, A. P., Kolodgie, F. D., Zieske, A., Fowler, D. R., Weber, D. K., Varghese, P. J., Farb, A. and Virmani, R. (2004). Morphologic findings of coronary atherosclerotic plaques in diabetics: a postmortem study. *Arteriosclerosis, Thrombosis, and Vascular Biology,* **24,** 1266-1271.

Cade, W. T. (2008). Diabetes-related microvascular and macrovascular diseases in the physical therapy setting. *Physical Therapy,* **88,** 1322-1335.

Cai, C. (2012). SIVmac239-Nef Down-regulates Cell Surface Expression of CXCR4 in Tumor Cells and Inhibits Proliferation, Migration and Angiogenesis. *Anticancer research,* **23,** 2759-2758.

Cerami, C., Founds, H., Nicholl, I., Mitsuhashi, T., Giordano, D., Vanpatten, S., Lee, A., Al-Abed, Y., Vlassara, H., Bucala, R. and Cerami, A. (1997). Tobacco smoke is a source of toxic reactive glycation products. *Proceedings of the National Academy of Sciences,* **94,** 13915-13920.

Cervantes-Laurean, D., Schramm, D. D., Jacobson, E. L., Halaweish, I., Bruckner, G. G. and Boissonneault, G. A. (2006) Inhibition of advanced glycation end product formation on collagen by rutin and its metabolites. *The Journal of Nutritional Biochemistry*, **17**, 531-540.

Chang, J.-B., Chu, N.-F., Syu, J.-T., Hsieh, A.-T. and Hung, Y.-R. (2011). Advanced glycation end products (AGEs) in relation to atherosclerotic lipid profiles in middle-aged and elderly diabetic patients. *Lipids in Health and Disease,* **10,** 228-235.

Chang, K. C., Hsu, K. L., Peng, Y. I., Lee, F. C., Tseng, Y. Z. (2003). Aminoguanidine prevents age-related aortic stiffening in Fisher 344 rats: aortic impedance analysis. *British Journal of Pharmacology,* **140**, 107-114.

Chellan, P. & Nagaraj, R. H. (1999) Protein crosslinking by the Maillard reaction: dicarbonyl-derived imidazolium crosslinks in aging and diabetes. *Archives of Biochemistry dysfunction and Biophysics*, **268**, 98-104.

Chen, J. C., Liu, W. Q., Lu, L., Qiu, M. H., Zheng, Y. T., Yang, L. M., Zhang, X. M., Zhou, L. and Li, Z. R. (2009). Kuguacins F-S, cucurbitane triterpenoids from *Momordica charantia*. *Phytochemistry,* **70,** 133-140.

Chen, S.-A., Chen, H.-M., Yao, Y.-D., Hung, C.-F., Tu, C.-S. and Liang, Y.-J. (2012). Topical treatment with anti-oxidants and Au nanoparticles promote healing of diabetic wound through receptor for advance glycation end-products. *European Journal of Pharmaceutical Sciences,* **47,** 875-883.

Cheng, R., Feng, Q. and Ortwerth, B. J. (2006). LC-MS display of the total modified amino acids in cataract lens proteins and in lens proteins glycated by ascorbic acid in vitro. *Biochimica et Biophysica Acta,* **1762,** 533-543.

Cheng, T. L., Cheng, C. M., Chen, B. M., Tsao, D. A., Chuang, K. H., Hsiao, S. W., Lin, Y. H. and Roffler, S. R. (2005). Monoclonal antibody-based quantitation of poly(ethylene glycol)-derivatized proteins, liposomes, and nanoparticles. *Bioconjugate Chemistry,* **16,** 1225-1231.

Chibber, R., Molinatti, P. A., Rosatto, N., Lambourne, B. and Kohner, E. M. (1997). Toxic action of advanced glycation end products on cultured retinal capillary pericytes and endothelial cells: relevance to diabetic retinopathy. *Diabetologia,* **40,** 156-164.

Christian, W. and Heidi, N. (2011). Atherosclerosis: current pathogenesis and therapeutic options. *Nature Medicine,* **17,** 1410-1422.

Chua, M.-T., Tung, Y.-T. and Chang, S.-T. (2008). Antioxidant activities of ethanolic extracts from the twigs of Cinnamomum osmophloeum. *Bioresource technology,* **99,** 1918-1925.

Coughlan, M. T., Cooper, M. E. and Forbes, J. M. (2005). Can advanced glycation end product inhibitors modulate more than one pathway to enhance renoprotection in diabetes? *Annals of the New York Academy of Sciences,* **1043,** 750-758.

Cox, D. J., Kovatchev, B. P., Gonder-Frederick, L. A., Summers, K. H., McCall, A., Grimm, K. J. and Clarke, W. L. (2005). Relationships between hyperglycemia and cognitive performance among adults with type 1 and type 2 diabetes. *Diabetes Care,* **28,** 71-77.

Crabbe, M. J. (1998). Cataract as a conformational disease--the Maillard reaction, alpha-crystallin and chemotherapy. *Cellular and Molecular Biology (Noisy-Le-Grand, France),* **44,** 1047-1050.

Crauwels, H. M., Herman, A. G. and Bult, H. (2000). Local application of advanced glycation endproducts and intimal hyperplasia in the rabbit collared carotid artery. *Cardiovascular research,* **47,** 173-182.

Culav, E. (1999). Connective tissues : Matrix composition and its relevance to physical therapy. *Physical therapy,* **79,** 308-319.

Davies, C. G. A., Netto, F. M., Glassenap, N., Gallaher, C. M., Labuza, T. P. and Gallaher, D. D. (1998). Indication of the Maillard reaction during storage of protein isolates. *Journal of agricultural and food chemistry,* **46,** 2485-2489.

De Nardo, D., De Nardo, C. M. and Latz, E. (2013). New insights into mechanisms controlling the NLRP3 inflammasome and Its role in lung disease. *The American Journal of Pathology*, **1**, 1-13.

Delgado, V. M., Nugnes, L. G., Colombo, L. L., Troncoso, M. F., Fernandez, M. M., Malchiodi, E. L., Frahm, I., Croci, D. O., Compagno, D., Rabinovich, G. A., Wolfenstein-Todel, C. and Elola, M. T. (2011). Modulation of endothelial cell migration and angiogenesis: a novel function for the "tandem-repeat" lectin galectin-8. *Federation of American Societies for Experimental Biology Journal,* **25,** 242-254.

Deng, R. (2012). A review of the hypoglycemic effects of five commonly used herbal food supplements. *Recent Patents on Food, Nutrition and Agriculture.* **4**, 50-60.

Desai, K. and Wu, L. (2008). Free radical generation by methylglyoxal in tissues. *Drug Metabolism,* **23,** 151-173.

Dhar, I. and Desai, K. (2012). Aging: Drugs to Eliminate Methylglyoxal, a Reactive Glucose Metabolite, and Advanced Glycation Endproducts. *In:* Gallelli (ed.) *Pharmacology.* Rijeka: InTech.

Dills, L. (1993). Protein fructosylation: Fructose and the Maillard reaction. *American Journal of Clinical Nutrition,* **58**, 779-787.

Dyer, D. G., Dunn, J. A., Thorpe, S. R., Bailie, K. E., Lyons, T. J., McCance, D. R. and Baynes, J. W. (1993). Accumulation of Maillard reaction products in skin collagen in diabetes and aging. *The Journal of clinical investigation,* **91,** 2463-2469.

Egginton, S. (2010). Angiogenesis - may the force be with you! *Journal of Physiology,* **588,** 4615-4616.

Faist, V. and Erbersdobler, H. (2001). Metabolic transit and *in vivo* effects of melanoidins and precursor compounds deriving from the Maillard reaction. *Annals of Nutrition and Metabolism,* **45,** 1-12.

Ferrara, N. and Kerbel, R. S. (2005). Angiogenesis as a therapeutic target. *Nature,* **438,** 967-974.

Ferreira, A. E., Ponces Freire, A. M. and Voit, E. O. (2003). A quantitative model of the generation of N(epsilon)-(carboxymethyl)lysine in the Maillard reaction between collagen and glucose. *The Biochemical journal,* **376,** 109-121.

Fong, D. S., Aiello, L., Gardner, T. W., King, G. L., Blankenship, G., Cavallerano, J. D., Ferris, F. L. and Klein, R. (2004). Retinopathy in diabetes. *Diabetes Care,* **27,** s84-s87.

Forbes, J. M., Soldatos, G. and Thomas, M. C. (2005). Below the radar: advanced glycation endproducts that detour "around the side". Is HbA1c not an accurate enough predictor of long term progression and glycaemic control in diabetes? *Clinical Biochemist,* **26,** 123-134.

Fowler, M. J. (2008). Microvascular and macrovascular complications of diabetes. *Clinical Diabetes,* **26,** 77-82.

Franke, S., Sommer, M., Rüster, C., Bondeva, T., Marticke, J., Hofmann, G., Hein, G. and Wolf, G. induce cell cycle arrest and proinflammatory changes in osteoarthritic fibroblast-like synovial cells. *Arthritis research & therapy,* **11,** R136-R155.

Franke, S., Dawczynski, J., Strobel, J., Niwa, T., Stahl, P. and Stein, G. (2003). Increased levels of advanced glycation end products in human cataractous lenses. *Journal of Cataract and Refractive Surgery,* **29,** 998-1004.

Fujiwara, Y., Kiyota, N., Tsurushima, K., Yoshitomi, M., Mera, K., Sakashita, N., Takeya, M., Ikeda, T., Araki, T., Nohara, T. and Nagai, R. (2011). Natural compounds containing a catechol group enhance the formation of Nε-(carboxymethyl)lysine of the Maillard reaction. *Free Radical Biology and Medicine,* **50,** 883-891.

Gallicchio, M. A. and Bach, L. A. (2010). Advanced glycation end products inhibit Na+ K+ ATPase in proximal tubule epithelial cells: Role of cytosolic phospholipase A2α and phosphatidylinositol 4-phosphate 5-kinase γ. *Biochimica et Biophysica Acta (BBA) - Molecular Cell Research,* **1803,** 919-930.

Gerhardinger, C., Marion, M. S., Rovner, A., Glomb, M. and Monnier, V. M. (1995). Novel degradation pathway of glycated amino acids into free fructosamine by a Pseudomonas sp. soil strain extract. *The Journal of biological chemistry,* **270,** 218-224.

Giacco, F. and Brownlee, M. (2010). Oxidative stress and diabetic complications. *Circulation Research,* **107,** 1058-1070.

Giardino, I., Edelstein, D. and Brownlee, M. (1994). Nonenzymatic glycosylation in vitro and in bovine endothelial cells alters basic fibroblast growth factor activity. A model for intracellular glycosylation in diabetes. *The Journal of clinical investigation,* **94,** 110-117.

Giardino, I., Edelstein, D. and Brownlee, M. (1996). BCL-2 expression or antioxidants prevent hyperglycemia-induced formation of intracellular advanced glycation endproducts in bovine endothelial cells. *The Journal of clinical investigation,* **97,** 1422-1428.

Giuliano, S. and Pagès, G. (2013). Mechanisms of resistance to anti-angiogenesis therapies. *Biochimie,* **95,** 1110-1119.

Gogi, M. D., Ashfaq, M., Arif, M. J., Sarfraz, R. M. and Nawab, N. N. (2010). Investigating phenotypic structures and allelochemical compounds of the fruits of *Momordica charantia L.* genotypes as sources of resistance against *Bactrocera cucurbitae* (Coquillett) (Diptera: Tephritidae). *Crop Protection,* **29,** 884-890.

Goh, S.-Y. and Cooper, M. E. (2008). The role of advanced glycation endproducts in progression and complications of diabetes. *Journal of Clinical Endocrinology & Metabolism,* **93,** 1143-1152.

Goldberg, T., Cai, W., Peppa, M., Dardaine, V., Baliga, B. S., Uribarri, J. and Vlassara, H. (2004). Advanced glycoxidation end products in commonly consumed foods. *Journal of the American Dietetic Association,* **104,** 1287-1291.

Goldin, A., Beckman, J. A., Schmidt, A. M. and Creager, M. A. (2006). Advanced glycation endproducts: sparking the development of diabetic vascular injury. *Circulation,* **114,** 597-605.

Gomes, R. A., Sousa Silva, M., Vicente Miranda, H., Ferreira, A. E., Cordeiro, C. A. and Freire, A. P. (2005). Protein glycation in Saccharomyces cerevisiae. Argpyrimidine formation and methylglyoxal catabolism. *Federation of American Societies for Experimental Biology Journal,* **272,** 4521-4531.

Groche, D., Hoeno, W., Hoss, G., Vogt, B., Herrmann, Z. and Witzigmann, A. (2003). Standardization of two immunological HbA1c routine assays according to the new IFCC reference method. *Clínical Laboratory,* **49,** 657-661.

Grover, J. K. and Yadav, S. P. (2004). Pharmacological actions and potential uses of *Momordica charantia*: a review. *Journal of Ethnopharmacology,* **93,** 123-132.

Guillausseau, P. J., Charles, M. A., Godard, V., Timsit, J., Chanson, P., Paolaggi, F., Peynet, J., Eschwege, E., Rousselet, F. and Lubetzki, J. (1990). Comparison of fructosamine with glycated hemoglobin as an index of glycemic control in diabetic patients. *Diabetes Research,* **13,** 127-131.

Guo, S. and Dipietro, L. A. (2010). Factors affecting wound healing. *Journal of Dental Research,* **89,** 219-229.

Hallam, K. M., Li, Q., Ananthakrishnan, R., Kalea, A., Zou, Y. S., Vedantham, S., Schmidt, A. M., Yan, S. F. and Ramasamy, R. (2010). Aldose reductase and AGE-RAGE pathways: central roles in the pathogenesis of vascular dysfunction in aging rats. *Aging Cell,* **9,** 776-784.

Hammes, H. P., Brownlee, M., Lin, J., Schleicher, E. and Bretzel, R. G. (1999). Diabetic retinopathy risk correlates with intracellular concentrations of the glycoxidation product Ne-(carboxymethyl) lysine independently of glycohaemoglobin concentrations. *Diabetologia,* **42,** 603-607.

Hartog, J. W. L., Voors, A. A., Bakker, S. J. L., Smit, A. J. and van Veldhuisen, D. J. (2007). Advanced glycation endproducts (AGEs) and heart failure: Pathophysiology and clinical implications. *European Journal of Heart Failure,* **9,** 1146-1155.

Hashimoto, H., Arai, K., Chikuda, M. and Obara, Y. (2010). Relationship between Pentosidine and Pyridinoline Levels in Human Diabetic Cataract Lenses. *Journal of Clinical Biochemistry and Nutrition,* **47,** 233-237.

Hensley, K., Robinson, K. A., Gabbita, S. P., Salsman, S. and Floyd, R. A. (2000). Reactive oxygen species, cell signaling, and cell injury. *Free Radical Biology and Medicine,* **28,** 1456-1462.

Hipkiss, A. R. (2005). Glycation, ageing and carnosine: Are carnivorous diets beneficial? *Mechanisms of Ageing and Development*, **10**, 1034-1039.

Hipkiss, A. R., Michaelis, J. and Syrris, P. (1995). Non-enzymatic glycosylation of the dipeptide L-carnosine, a potential anti-protein-cross-linking agent. *The Federation of European Biochemical Societies Letters*, **371**, 81-85.

Hirasawa, Y., Sakai, T., Ito, M., Yoshimura, H., Feng, Y. and Nagamatsu, T. (2011). Advanced-glycation-endproduct-cholesterol-aggregated-protein accelerates the proliferation of mesangial cells mediated by transforming-growth-factor-beta 1 receptors and the ERK-MAPK pathway. *European journal of pharmacology,* **672,** 159-168.

Hobart, L. J., Seibel, I., Yeargans, G. S. and Seidler, N. W. (2004) Anti-crosslinking properties of cornosine: Significance of histidine. *Life Science*, **11**, 1379-1389

Hogan, M., Cerami, A. and Bucala, R. (1992). Advanced glycosylation endproducts block the antiproliferative effect of nitric oxide. Role in the vascular and renal complications of diabetes mellitus. *Journal of Clinical Investigation,* **90,** 1110-1115.

Hsieh, C.-L., Lin, Y.-C., Ko, W.-S., Peng, C.-H., Huang, C.-N. and Peng, R. Y. (2005). Inhibitory effect of some selected nutraceutic herbs on LDL glycation induced by glucose and glyoxal. *Journal of Ethnopharmacology,* **102,** 357-363.

Hsu, D. and Zimmer, V. (2010). Canadian diabetes association national nutrition committee technical review: Advanced glycation endproducts in diabetes management. *Canadian Journal of Diabetes,* **34,** 136-140.

Huang, B., Ng, T. B., Fong, W. P., Wan, C. C. and Yeung, H. W. (1999). Isolation of a trypsin inhibitor with deletion of N-terminal pentapeptide from the seeds of Momordica cochinchinensis, the Chinese drug mubiezhi. *The international journal of biochemistry & cell biology,* **31,** 707-715.

Hudson, B. and Schmidt, A. (2004). RAGE: A novel target for drug intervention in diabetic vascular disease. *Pharmaceutical Research,* **21,** 1079-1086.

Huebschmann, A. G., Regensteiner, J. G., Vlassara, H. and Reusch, J. E. (2006). Diabetes and advanced glycoxidation end products. *Diabetes Care,* **29,** 1420-1432.

Huggins, T. G., Wells-Knecht, M. C., Detorie, N. A., Baynes, J. W. and Thorpe, S. R. (1993). Formation of o-tyrosine and dityrosine in proteins during radiolytic and metal-catalyzed oxidation. *Journal of Biological Chemistry,* **268,** 12341-12347.

Huijberts, M. S., Schaper, N. C. and Schalkwijk, C. G. (2008). Advanced glycation end products and diabetic foot disease. *Diabetes/metabolism research and reviews,* **24,** S19-S24.

Hung, L.-F., Huang, K.-Y., Yang, D.-H., Chang, D.-M., Lai, J.-H. and Ho, L.-J. (2010). Advanced glycation endproducts induce T cell apoptosis: Involvement of oxidative stress, caspase and the mitochondrial pathway. *Mechanisms of ageing and development,* **131,** 682-691.

Huttunen, H. J., Kuja-Panula, J., Sorci, G., Agneletti, A. L., Donato, R. and Rauvala, H. (2000). Coregulation of neurite outgrowth and cell survival by amphoterin and S100 proteins through receptor for advanced glycation end products (RAGE) activation. *The Journal of biological chemistry,* **275,** 40096-40105.

International Diabetes Federation. (2013). Diabetes Atlas, 6th edn. Brussels, Belgium. Accessed 23 May 2014.

Ikeda, K., Higashi, T., Sano, H., Jinnouchi, Y., Yoshida, M., Araki, T., Ueda, S. & Horiuchi, S. (1996) N (epsilon)-(carboxymethyl)lysine protein adduct is a major immunological epitope in proteins modified with advanced glycation end products of the Maillard *Diabetologia*, **46,** 248-287.

Inagaki, Y., Yamagishi, S., Okamoto, T., Takeuchi, M. and Amano, S. (2003). Pigment epithelium-derived factor prevents advanced glycation end products-induced monocyte chemoattractant protein-1 production in microvascular endothelial cells by suppressing intracellular reactive oxygen species generation. *Diabetologia,* **46,** 284-287.

Jack, M. and Wright, D. (2012). Role of advanced glycation endproducts and glyoxalase I in diabetic peripheral sensory neuropathy. *Translational Research,* **159,** 355-365.

Jaeger, H., Janositz, A. and Knorr, D. (2010). The Maillard reaction and its control during food processing. The potential of emerging technologies. *Pathologie Biologie,* **58,** 207-213.

Jakus, V. and Rietbrock, N. (2004). Advanced glycation endproducts and the progress of diabetic vascular complications. *Physiological Research,* **53,** 131-142.

Jandeleit-Dahm, K. and Cooper, M. E. (2008). The role of AGEs in cardiovascular disease. *Current Pharmaceutical Design,* **14,** 979-986.

Joseph, B. and Jini, D. (2013). Antidiabetic effects of *Momordica charantia* (bitter melon) and its medicinal potency. *Asian Pacific Journal of Tropical Disease,* **3,** 93-102.

Kamata, K., Ozawa, Y., Kobayashi, T. and Matsumoto, T. (2009). Effect of N-epsilon-(carboxymethyl)lysine on coronary vasoconstriction in isolated perfused hearts from control and streptozotocin-induced diabetic rats. *Journal of smooth muscle research,* **45,** 125-137.

Kameswararao, B., Kesavulu, M.M., and Apparao, C., (2003). Evaluation of antidiabetic effect of *Momordica cymbalaria* fruit in alloxan-diabetic rats. *Fitoterapia,* **74**, 7-13.

Karachalias, N., Babaei-Jadidi, R., Ahmed, N. and Thornalley, P. J. (2003). Accumulation of fructosyl-lysine and advanced glycation end products in the kidney, retina and peripheral nerve of streptozotocin-induced diabetic rats. *Biochemical Society Transactions,* **31,** 1423-1425.

Kaur, H. and Halliwell, B. (1994). Detection of hydroxyl radicals by aromatic hydroxylation. *Methods in Enzymology,* **233,** 67-82.

Kerkeni, M., Saïdi, A., Bouzidi, H., Yahya, S. B. and Hammami, M. (2012). Elevated serum levels of AGEs, sRAGE, and pentosidine in Tunisian patients with severity of diabetic retinopathy. *Microvascular Research,* **84,** 378-383.

Keter, L. K. and Mutiso, P. C. (2012). Ethnobotanical studies of medicinal plants used by Traditional Health Practitioners in the management of diabetes in Lower Eastern Province, Kenya. *Journal of Ethnopharmacology,* **139,** 74-80.

Khuhawar, M. Y., Kandhro, A. J. and Khand, F. D. (2006). Liquid Chromatographic Determination of Glyoxal and Methylglyoxal from Serum of Diabetic Patients using Meso-Stilbenediamine as Derivatizing Reagent. *Analytical Letters,* **39,** 2205-2215.

Kiho, T., Usui, S., Hirano, K., Aizawa, K. & Inakuma, T. (2004) Tomato paste fraction inhibiting the formation of advanced glycation end-products. *Bioscience, Biotechnolog and Biochemistry journal*, **68**, 200-205.

Kikuchi, S., Shinpo, K., Takeuchi, M., Yamagishi, S., Makita, Z., Sasaki, N. and Tashiro, K. (2003). Glycation—a sweet tempter for neuronal death. *Brain Research Reviews,* **41,** 306-323.

Kim, Y. K., Hui Xu, Nam Il Park, Hee Ock Boo, Sook Young Lee and Sang Un Park (2009). Amino acid and GABA content in different cultivars of *Momordica charantia L*. *Journal of Medicinal Plants Research,* **3,** 894-897.

Kislinger, T., Humeny, A. and Pischetsrieder, M. (2004). Analysis of protein glycation products by matrix-assisted laser desorption ionization time-of-flight mass spectrometry. *Current Medicinal Chemistry,* **11,** 2185-2193.

Kolluru, G. K., Bir, S. C. and Kevil, C. G. (2012). Endothelial dysfunction and diabetes: dffects on angiogenesis, vascular remodeling, and wound healing. *International journal of vascular medicine.* **2012**, 1-30.

Koschinsky, T., He, C.-J., Mitsuhashi, T., Bucala, R., Liu, C., Buenting, C., Heitmann, K. and Vlassara, H. (1997). Orally absorbed reactive glycation products (glycotoxins): An environmental risk factor in diabetic nephropathy. *Proceedings of the National Academy of Sciences,* **94,** 6474-6479.

Kousar, S., Sheikh, M. A. and Asghar, M. (2012). Antiglycation activity of thiamin-HCl and benfotiamine in diabetic condition. *The Journal of the Pakistan Medical Association,* **62,** 1033-1038.

Kowluru, R. A. (2005). Effect of advanced glycation end products on accelerated apoptosis of retinal capillary cells under in vitro conditions. *Life sciences,* **76,** 1051-1060.

Koyama, H., Yamamoto, H. and Nishizawa, Y. (2007). RAGE and soluble RAGE: potential therapeutic targets for cardiovascular diseases. *Molecular Medicine,* **13,** 625-635.

Krishnaiah, D., Sarbatly, R. and Nithyanandam, R. (2011). A review of the antioxidant potential of medicinal plant species. *Food and Bioproducts Processing,* **89,** 217-233.

Kubola, J. and Siriamornpun, S. (2008). Phenolic contents and antioxidant activities of bitter gourd (*Momordica charantia L*.) leaf, stem and fruit fraction extracts in vitro. *Food Chemistry,* **110,** 881-890.

Kumaran, A. and Karunakaran, R. J. (2007). Antioxidant activity of *Cassia auriculata* flowers. *Fitoterapia,* **78,** 46-47.

Kvietys, P. R. and Granger, D. N. (2012). Role of reactive oxygen and nitrogen species in the vascular responses to inflammation. *Free Radical Biology and Medicine,* **52,** 556-592.

Laakso, M. (2010). Cardiovascular disease in type 2 diabetes from population to man to mechanisms: the Kelly West Award Lecture 2008. *Diabetes Care,* **33,** 442-449.

Laemmli, U. K. (1970) Cleavage of structural proteins during the assembly of the head of bacteriophage T4. *Nature*, **227**, 680-685.

Lai, L. C. (2008). Global standardisation of HbA1c. *Malaysian Journal of Pathology,* **30,** 67-71.

Lamalice, L., Le Boeuf, F. and Huot, J. (2007). Endothelial cell migration during angiogenesis. *Circulation Research,* 100, 782-794.

Lander, H. M., Tauras, J. M., Ogiste, J. S., Hori, O., Moss, R. A. and Schmidt, A. M. (1997). Activation of the receptor for advanced glycation endproducts triggers a p21 ras - dependent Mitogen-activated protein kinase pathway regulated by oxidant stress. *Journal of Biological Chemistry,* **272,** 17810-17814.

Lapolla, A., Molin, L. and Traldi, P. (2013). Protein Glycation in Diabetes as Determined by Mass Spectrometry. *International Journal of Endocrinology,* **2013,** 11.

Lapolla, A., Traldi, P. and Fedele, D. (2005). Importance of measuring products of non-enzymatic glycation of proteins. *Clinical Biochemistry,* **38,** 103-115.

Lee, S., Eom, S., Kim, Y., Park, N., and Park, S. (2009). Cucurbitane-type triterpenoids in *Momordica charantia* Linn. *Journal of Medicinal Plants Research,* **3***,* 1264-1269.

Leonil, J., Molle, D., Fauquant, J., Maubois, J., Pearce, R. and Bouhallab, S. (1997). Characterization by ionization mass spectrometry of lactosyl-b-lactoglobulin conjugates formed during heat treatment of milk and whey identification of one lactose binding site. *Journal of Dairy Science,* **80,** 2270-2281.

Lerman, O. Z., Galiano, R. D., Armour, M., Levine, J. P. and Gurtner, G. C. (2003). Cellular dysfunction in the diabetic fibroblast: impairment in migration, vascular endothelial growth factor production, and response to hypoxia. *The American Jurnal of Pathology,* **162,** 303-312.

Liekens, S., De Clercq, E. and Neyts, J. (2001). Angiogenesis: regulators and clinical applications. *Biochemical Pharmacology,* **61,** 253-270.

Lima M.H., Caricilli A.M., de Abreu L.L., Araujo E.P., Pelegrinelli F.F., Thirone A.C., Tsukumo D.M., Pessoa A.F., dos Santos M.F., de Moraes M.A., Carvalheira J.B., Velloso L.A., Saad M.J. (2012) Topical insulin accelerates wound healing in diabetes by enhancing the AKT and ERK pathways: a double-blind placebo-controlled clinical trial. *PloS One*, **7,** e36974.

Lin, C. Y., Chen, C. S., Shieh, M. S., Wu, C. H. and Lee, H. M. (2002). Development of an automated immunoassay for advanced glycosylation end products in human serum. *Clinical Biochemistry,* **35,** 189-195.

Lin, K.-W., Yang, S.-C. and Lin, C.-N. (2011). Antioxidant constituents from the stems and fruits of *Momordica charantia*. *Food Chemistry,* **127,** 609-614.

Lin, P. P., Barry, R. C., Smith, D. L. and Smith, J. B. (1998). In vivo acetylation identified at lysine 70 of human lens α A-crystallin. *Protein Science,* **7,** 1451-1457.

Linetsky, M., Shipova, E., Cheng, R. and Ortwerth, B. J. (2008). Glycation by ascorbic acid oxidation products leads to the aggregation of lens proteins. *Biochimica et Biophysica Acta,* **1782,** 22-34.

Liu, B. F., Miyata, S., Kojima, H., Uriuhara, A., Kusunoki, H., Suzuki, K. and Kasuga, M. (1999). Low phagocytic activity of resident peritoneal macrophages in diabetic mice: relevance to the formation of advanced glycation end products. *Diabetes,* **48,** 2074-2082.

Loizzo, M. R., Tundis, R., Bonesi, M., Menichini, F., Mastellone, V., Avallone, L. and Menichini, F. (2012). Radical scavenging, antioxidant and metal chelating activities of Annona cherimola Mill. (cherimoya) peel and pulp in relation to their total phenolic and total flavonoid contents. *Journal of Food Composition and Analysis,* **25,** 179-184.

Luevano-Contreras, C., and Chapman-Novakofski, K. (2010). Dietary advanced glycation endproducts and aging. *Nutrients,* **2,** 1247-1265.

Magalhães, P. M., Appell, H. J. and Duarte, J. A. (2008). Involvement of advanced glycation endproducts in the pathogenesis of diabetic complications: the protective role of regular physical activity. *European Review of Aging and Physical Activity,* **5,** 17-29.

Mahomoodally, F., Subratty, A., Gurib-Fakim, A. and Choudhary, M. (2012). Antioxidant, antiglycation and cytotoxicity evaluation of selected medicinal plants of the Mascarene Islands. *BMC complementary and alternative medicine,* **12,** 165-177.

Maillard, L. C. (1912) Action of amino acids on sugars. Formation of melanoidins in a methodical way. *Compte Rendu du roi*, **154**, 66-68.

Malik, S. (2014) Diabetes: Excess risk of stroke in women[mdash]the role of diabetes mellitus. *Nature Reviews Endocrinology*, **10**, 318-320.

Mao, Y., Ootaka, T., Saito, T., Sato, H., Sato, T. and Ito, S. (2003). The involvement of advanced glycation endproducts (AGEs) in renal injury of diabetic glomerulosclerosis: association with phenotypic change in renal cells and infiltration of immune cells. *Clinical and Experimental Nephrology,* **7,** 201-209.

Marchetti, P. (2009). Advanced glycation endproducts (AGEs) and their receptors (RAGEs) in diabetic vascular disease. *Medicographia,* **31,** 257-266.

Martin, A., Komada, M. R. and Sane, D. C. (2003). Abnormal angiogenesis in diabetes mellitus. *Medicinal Research Reviews,* **23,** 117-145.

Mashilipa, C., Wang, Q., Slevin, M. and Ahmed, N. (2011). Antiglycation and antioxidant properties of soy sauces. *Journal of Medicinal Food,* **14,** 1647-1653.

Matsumoto, K., Nagai, R., Masunaga, K., Yoshida, M., Ueda, S., Smedsrød, B. and Horiuchi, S. (2002) Endocytic uptake of advanced glycation endproducts by mouse liver sinusoidal endothelial cells is mediated by a receptor distinct from the class A scavenger receptor. *International congress Series,* **1245**, 157-162.

McCance, D. R., Dyer, D. G., Dunn, J. A., Bailie, K. E., Thorpe, S. R., Baynes, J. W. and Lyons, T. J. (1993). Maillard reaction products and their relation to complications in insulin-dependent diabetes mellitus. *Journal of Clinical Investigation,* **91,** 2470-2480.

Meerwaldt, R., Links, T., Zeebregts, C., Tio, R., Hillebrands, J.-L. and Smit, A. (2008). The clinical relevance of assessing advanced glycation endproducts accumulation in diabetes. *Cardiovascular Diabetology,* **7,** 29-37.

Miliauskas, G., Venskutonis, P. R. and van Beek, T. A. (2004). Screening of radical scavenging activity of some medicinal and aromatic plant extracts. *Food Chemistry,* **85,** 231-237.

Mima, A. (2013). Diabetic nephropathy: protective factors and a new therapeutic paradigm. *Journal of Diabetes and Its Complications,* **27,** 526-530.

Miura, J., Yamagishi, S., Uchigata, Y., Takeuchi, M., Yamamoto, H., Makita, Z. and Iwamoto, Y. (2003). Serum levels of non-carboxymethyllysine advanced glycation endproducts are correlated to severity of microvascular complications in patients with Type 1 diabetes. *Journal of Diabetes and Its Complications,* **17,** 16-21.

Monnier, V. M. (2003). Intervention against the Maillard reaction in vivo. *Archives of Biochemistry and Biophysics,* **419,** 1-15.

Monnier, V. M., Kohn, R. R. and Cerami, A. (1984). Accelerated age-related browning of human collagen in diabetes mellitus. *Proceedings of the National Academy of Sciences of the United States of America,* **81,** 583-587.

Monnier, V. M., Sell, D. R. and Genuth, S. (2005). Glycation products as markers and predictors of the progression of diabetic complications. *Annals of the New York Academy of Sciences,* **1043,** 567-581.

Morimitsu, Y., Yoshida, K., Esaki, S. and Hirota, A. (1995) Protein glycation inhibitors from thyme (Thymus vulgaris). *Bioscience, Biotechnology, and Biochemistry,* **59**, 2015-2021.

Morita, M., Yano, S., Yamaguchi, T. and Sugimoto, T. (2013). Advanced glycation endproducts-induced reactive oxygen species generation is partly through NF-kappa B activation in human aortic endothelial cells. *Journal of Diabetes and its Complications,* **27,** 11-15.

Nakata, B., Ishikawa, T., Amano, R., Kimura, K. and Hirakawa, K. (2013). Impact of preoperative diabetes mellitus on clinical outcome after pancreatectomy. *International Journal of Surgery*.**11,** 757-761

Namiki, M. and Hayashi, T. (1983). A new mechanism of the Maillard reaction involving sugar fragmentation and free radical formation. ACS Symp Series The Maillard reaction in foods and nutrition. *American chemical society symposium*. **215**, 21-46.

Nathan, D. M., Cleary, P. A., Backlund, J. Y., Genuth, S. M., Lachin, J. M., Orchard, T. J., Raskin, P., Zinman, B. and null (2005). Intensive diabetes treatment and cardiovascular disease in patients with type 1 diabetes. *The New England journal of medicine,* **353,** 2643-2653.

Nelson, C. and Chen, C. (2003). VE-cadherin simultaneously stimulates and inhibits cell proliferation by altering cytoskeletal structure and tension. *Journal of Cell Science,* **116,** 3571-3581.

Ni, J., Yuan, X., Gu, J., Yue, X., Gu, X., Nagaraj, R. H. and Crabb, J. W. (2009). Plasma protein pentosidine and carboxymethyllysine, biomarkers for age-related macular degeneration. *Molecular & Cellular Proteomics,* **8,** 1921-1933.

Nimbalkar, V. V., Mandlik, R. V., Naik, S. R. and Maseeh, A. (2012). Nonenzymatic glycosylation: A biochemical link between chronic hyperglycemia and pathophysiologic processes associated with diabetic complications and aging related debilities. *Biomedicine & Aging Pathology,* **2,** 133-142.

Niwa, T. (1999). 3-Deoxyglucosone: metabolism, analysis, biological activity, and clinical implication. *Journal of Chromatography B: Biomedical Sciences,* **731,** 23-36.

Niwa, T. (2006). Mass spectrometry for the study of protein glycation in disease. *Mass Spectrometry Reviews,* **25,** 713-723.

O'Brien, J. and Morrissey, P. (1990). Nutritional and toxicological aspects of the Maillard browning reaction in foods. *Critical Reviews on Food Science and Nutrition,* **28,** 211-248.

Okamoto, T., Tanaka, S., Stan, A. C., Koike, T., Kase, M., Makita, Z., Sawa, H. and Nagashima, K. (2002). Advanced glycation endproducts induce angiogenesis *in vivo*. *Microvascular Research,* **63,** 186-195.

Okano, Y., Masaki, H. and Sakurai, H. (2002). Dysfunction of dermal fibroblasts induced by advanced glycation endproducts (AGEs) and the contribution of a nonspecific interaction with cell membrane and AGEs. *Journal of dermatological science,* **29,** 171-180.

Okayama, J., Ko, S., Kanehiro, H., Kanokogi, H. and Nakajima, Y. (2006). Efficacy of transient treatment with FK506 in the early phase on cyclophosphamide-induced bone marrow chimerism and transplant tolerance across MHC barriers. *Journal of Surgical Research,* **133,** 61-68.

O'Sullivan, E. P. and Dinneen, S. F. (2009). Benefits of early intensive glucose control to prevent diabetes complications were sustained for up to 10 years. *Evidence-Based Medicine,* **14,** 9-10.

Pacher, P., Beckman, J. S. and Liaudet, L. (2007). Nitric oxide and peroxynitrite in health and disease. *Physiological Reviews,* **87,** 315-424.

Pandolfi, A. and De Filippis, E. A. (2007). Chronic hyperglicemia and nitric oxide bioavailability play a pivotal role in pro-atherogenic vascular modifications. *Genes Nutr,* **2,** 195-208.

Patel, D. K., Kumar, R., Laloo, D. and Hemalatha, S. (2012). Diabetes mellitus: An overview on its pharmacological aspects and reported medicinal plants having antidiabetic activity. *Asian Pacific Journal of Tropical Biomedicine,* **2,** 411-420.

Paul, R. G., Avery, N. C., Slatter, D. A., Sims, T. J. and Bailey, A. J. (1998). Isolation and characterization of advanced glycation end products derived from the in vitro reaction of ribose and collagen. *The Biochemical journal,* **330,** 1241-1248.

Peppa, M. and Vlassara, H. (2005). Advanced glycation endproducts and diabetic complications: a general overview. *Hormones (Athens),* **4,** 28-37.

Peppa, M., Uribarri, J. and Vlassara, H. (2003). Glucose, advanced glycation endproducts, and diabetes complications: What is new and what works. *Clinical Diabetes,* **21,** 186-187.

Pitipanapong, J., Chitprasert, S., Goto, M., Jiratchariyakul, W., Sasaki, M. and Shotipruk, A. (2007). New approach for extraction of charantin from *Momordica charantia* with pressurized liquid extraction. *Separation and Purification Technology,* **52,** 416-422.

Popova, E., Mironov, R. and Odjakova, M. (2010). Non-enzymatic glycosylation and deglycating enzymes. *Biotechnology & Biotechnological Equipment,* **24,** 1928-1935.

Posner RG, Bold J, Bernstein Y, Rasor J, Braslow J, Hlavacek WS and Perelson AS (1998) Measurement of receptor crosslinking at the cell surface via multiparameter flow cytometry. *Proceeding of the Royal Society*. **3256**, 132-143.

Prasad, V., Jain, V., Girish, D. and Dorle, A. K. (2006). Wound-healing property of *Momordica charantia L.* fruit powder. *Journal of Herbal Pharmacotherapy,* **6,** 105-115.

Prashanthi, R., Mohan, N. and Siva, G. V. (2012). Wound-healing property of aqueous extract of seed and outer layer of *Momordica Charantia L.* on albino rats. *Indian Journal of Science and Technology,* **5,** 1936-1940.

Rahbar, S. and Figarola, J. (2003). Novel inhibitors of advanced glycation endproducts. *Advances of Biochemistry and Biophysics,* **419,** 63-79.

Rahimi, R., Nikfar, S., Larijani, B. and Abdollahi, M. (2005). A review on the role of antioxidants in the management of diabetes and its complications. *Biomedicine & Pharmacotherapy,* **59,** 365-373.

Rahman, K. (2007). Studies on free radicals, antioxidants, and co-factors. *Clinical Interventions and Aging,* **2,** 219-236.

Rahman, S., Rahman, T., Ismail, A. A. and Rashid, A. R. (2007). Diabetes-associated macrovasculopathy: pathophysiology and pathogenesis. *diabetes obesity and metabolism,* **9,** 767-780.

Rains, J. L. and Jain, S. K. (2011). Oxidative stress, insulin signaling, and diabetes. *Free Radical Biology and Medicine,* **50,** 567-575.

Raman, A. and Lau, C. (1996). Anti-diabetic properties and phytochemistry of *Momordica charantia L.* (Cucurbitaceae). *Phytomedicine : international journal of phytotherapy and phytopharmacology,* **2,** 349-362.

Raposeiras-Roubin, S., Rodino-Janeiro, B. K., Paradela-Dobarro, B., Grigorian-Shamagian, L., Garcia-Acuna, J. M., Aguiar-Souto, P., Jacquet-Hervet, M., Reino-Maceiras, M. V., Gonzalez-Juanatey, J. R. and Alvarez, E. (2013). Fluorescent advanced glycation endproducts and their soluble receptor: the birth of new plasmatic biomarkers for risk stratification of acute coronary syndrome. *PloS one,* **8,** e74302.

Reddy, S., Bichler, J., Wells-Knecht, K. J., Thorpe, S. R. and Baynes, J. W. (1995) N.epsilon.-(Carboxymethyl)lysine is a dominant advanced glycation end product (AGE) antigen in tissue proteins. *Biovhemistry*, **34**, 10872-10878.

Reinke, J. M. and Sorg, H. (2012). Wound repair and regeneration. *European Surgical Research,* **49,** 35-43.

Richard, D. S., Emily, J. N. and Luigi, F. (2010). Does accumulation of advanced glycation endproducts contribute to the aging phenotype? *The Journals of Gerontology Series A: Biological Sciences and Medical Sciences,* **65A,** 963-975.

Romao, I. & Roth, J. (2008). Genetic and environmental interactions in obesity and type 2 diabetes. *Journal of the American Diabetes Association*, **108**, S24-S28.

Roy, M. K., Takenaka, M. and Isobe, S. (2007). Thermal processing enhances anti-radical activity and reduces pro-oxidant activity in water-soluble fraction of selected Allium vegetables. *Journal of the Science of Food and Agriculture,* **87,** 2259-2265.

Sakata, N., Uesugi, N., Takebayashi, S., Nagai, R., Jono, T., Horiuchi, S., Takeya, M., Itabe, H., Takano, T., Myint, T. and Taniguchi, N. (2001). Glycoxidation and lipid peroxidation of low-density lipoprotein can synergistically enhance atherogenesis. *Cardiovascular research,* **49,** 466-475.

Samak, G., Shenoy, R. P., Manjunatha, S. M. and Vinayak, K. S. (2009). Superoxide and hydroxyl radical scavenging actions of botanical extracts of Wagatea spicata. *Food Chemistry,* **115,** 631-634.

Sato, T., Iwaki, M., Shimogaito, N., Wu, X., Yamagishi, S. and Takeuchi, M. (2006). TAGE (toxic AGEs) theory in diabetic complications. *Current Molecular Medicine,* **6,** 351-358.

Schalkwijk, C. G. and Miyata, T. (2012). Early- and advanced non-enzymatic glycation in diabetic vascular complications: the search for therapeutics. *Amino Acids,* **42,** 1193-1204.

Schmidt, A. and Stern, D. (2000). Atherosclerosis and diabetes: The rage connection. *Current Atherosclerosis Reports,* **2,** 430-436.

Sell, D., Nagaraj, R., Sunitha, K., Grandhee, S., Odetti, P., Lapolla, A., Fogarty, J. and Monnier, V. (1999). Pentosidine: A molecular marker for the cumulative damage to proteins in diabetes, aging, and uremia. *Diabetes/Metabolism Reviews,* **7,** 239-251.

Senthilkumar, S., Nithya, N., Ganesan, V., and Chandrakumar, K. (2012). *In vivo* antioxidant potential of *Momordica charantia* against cyclophosphamide induced hepatic damage in rats. *International Journal of Biological Chemistry,* **6,** 89-96.

Shan, B., Xie, J.-H., Zhu, J.-H. and Peng, Y. (2012). Ethanol modified supercritical carbon dioxide extraction of flavonoids from *Momordica charantia L*. and its antioxidant activity. *Food and Bioproducts Processing,* **90,** 579-587.

Shi, X., Chen, Y., Nadeem, L. and Xu, G. (2013). Beneficial effect of TNF-alpha inhibition on diabetic peripheral neuropathy. *Journal of Neuroinflammation,* **10,** 69-79.

Shimoike, T., Inoguchi, T., Umeda, F., Nawata, H., Kawano, K. and Ochi, H. (2000). The meaning of serum levels of advanced glycosylation end products in diabetic nephropathy. *Metabolism: Clinical and Experimental,* **49,** 1030-1035.

Sim, K. H. and Sil, H. Y. (2008). Antioxidant activities of red pepper (Capsicum annuum) pericarp and seed extracts. *International Journal of Food Science & Technology,* **43,** 1813-1823.

Singh, J., Cumming, E., Manoharan, G., Kalasz, H. and Adeghate, E. (2011). Medicinal chemistry of the anti-diabetic effects of *Momordica charantia*: active constituents and modes of actions. *Open Medicinal Chemistry Journal,* **5,** 70-77.

Singh, R., Barden, A., Mori, T. and Beilin, L. (2001). Advanced glycation endproducts: a review. *Diabetologia,* **44,** 129-146.

Slevin, M., Kumar, S. and Gaffney, J. (2002). Angiogenic oligosaccharides of hyaluronan induce multiple signaling pathways affecting vascular endothelial cell mitogenic and wound healing responses. *The Journal of biological chemistry,* **277,** 41046-41059.

Smit, A. J. and Lutgers, H. L. (2004). The clinical relevance of advanced glycation endproducts (AGE) and recent developments in pharmaceutics to reduce AGE accumulation. *Current Medicinal Chemistry,* **11,** 2767-2784.

Spiro, R. G. (2002). Protein glycosylation: nature, distribution, enzymatic formation, and disease implications of glycopeptide bonds. *Glycobiology,* **12,** 43R-56R.

Srikanth, V., Maczurek, A., Phan, T., Steele, M., Westcott, B., Juskiw, D. and Münch, G. (2011). Advanced glycation endproducts and their receptor RAGE in Alzheimer's disease. *Neurobiology of Aging,* **32,** 763-777.

Stevens, A. (1998). The contribution of glycation to cataract formation in diabetes. *Journal of the American Optometric Association,* **69,** 519-530.

Stitt, A. W. and Curtis, T. M. (2005). Advanced glycation and retinal pathology during diabetes. *Pharmacological Reports,* **57,** 156-168.

Stitt, A. W., McGoldrick, C., Rice-McCaldin, A., McCance, D. R., Glenn, J. V., Hsu, D. K., Liu, F.-T., Thorpe, S. R. and Gardiner, T. A. (2005). Impaired retinal angiogenesis in diabetes: role of advanced glycation endproducts and Galectin-3. *Diabetes,* **54,** 785-794.

Sugimoto, K., Yasujima, M. and Yagihashi, S. (2008). Role of advanced glycation end products in diabetic neuropathy. *Current Pharmaceutical Design,* **14,** 953-961.

Szwergold, B. S., Howell, S. and Beisswenger, P. J. (2001). Human fructosamine-3-kinase: purification, sequencing, substrate specificity, and evidence of activity *in vivo*. *Diabetes,* **50,** 2139-2147.

Tabatabaei-Malazy, O., Larijani, B. and Abdollahi, M. (2013). A novel management of diabetes by means of strong antioxidants' combination. *Journal of Medical Hypotheses and Ideas,* **7,** 25-30.

Tan, A. L. Y., Forbes, J. M. and Cooper, M. E. (2007) AGE, RAGE, and ROS in Diabetic Nephropathy. *Seminars in Nephrology,* **2**, 130-143.

Tan, K. C., Chow, W. S., Ai, V. H., Metz, C., Bucala, R. and Lam, K. S. (2002). Advanced glycation endproducts and endothelial dysfunction in type 2 diabetes. *Diabetes Care,* **25,** 1055-1059.

Tang, S. Y., Whiteman, M., Peng, Z. F., Jenner, A., Yong, E. L. and Halliwell, B. (2004). Characterization of antioxidant and antiglycation properties and isolation of active ingredients from traditional chinese medicines. *Free Radical Biology and Medicine,* **36,** 1575-1587.

Teixeira, A. S., Caliari, M. V., Rocha, O. A., Machado, R. D. P. and Andrade, S. P. (1999). Aminoguanidine Prevents Impaired Healing and Deficient Angiogenesis in Diabetic Rats. *Inflammation,* **23,** 569-581.

Teoh, S. L., Latiff, A. A. and Das, S. (2009). The effect of topical extract of *Momordica charantia* (bitter gourd) on wound healing in nondiabetic rats and in rats with diabetes induced by streptozotocin. *Clinical and experimental dermatology,* **34,** 815-822.

Thornalley, P. (1998). Glutathione-dependent detoxification of α-oxoaldehydes by the glyoxalase system: involvement in disease mechanisms and antiproliferative activity of glyoxalase I inhibitors. *Chemico-Biological Interactions,* **111-112,** 137-151.

Thornalley, P. (2003). Use of aminoguanidine (Pimagedine) to prevent the formation of advanced glycation endproducts. *Archives of Biochemistry and Biophysics,* **419,** 31-40.

Thornalley, P., Langborg, A. and Minhas, H. (1999). Formation of glyoxal, methylglyoxal and 3-deoxyglucosone in the glycation of proteins by glucose. *Biochemical Journal,* **344,** 109-116.

Thorpe, S. R. and Baynes, J. W. (1996). Role of the Maillard reaction in diabetes mellitus and discases of aging. *Drugs and Aging,* **9,** 69-77.

Thorpe, S. R. and Baynes, J. W. (2003) Maillard reaction products in tissue proteins: new products and new perspectives. *Amino Acids*, **25**, 275-281.

Tomlinson, D. R. and Gardiner, N. J. (2008). Glucose neurotoxicity. *Nature Reviews: Neuroscience,* **9,** 36-45.

Tsai, S.-Y., Huang, S.-J. and Mau, J.-L. (2006). Antioxidant properties of hot water extracts from Agrocybe cylindracea. *Food Chemistry,* **98,** 670-677.

Tsuji-Naito, K., Saeki, H. and Hamano, M. (2009). Inhibitory effects of Chrysanthemum species extracts on formation of advanced glycation end products. *Food Chemistry,* **116,** 854-859.

Ullah, M., Chy, F., Sarkar, S., Islam, K., and Absar, N. (2011). Nutrient and phytochemical analysis of four varieties of bitter gourd (*Momordica charantia*) grown in chittagong hill tracts, Bangladesh. *Asian Journal of Agricultural Research,* **5,** 186-193.

Ulrich, P. and Cerami, A. (2001). Protein glycation, diabetes, and aging. *Recent Progress in Hormone Research,* **56,** 1-21.

Uribarri, J., Woodruff, S., Goodman, S., Cai, W., Chen, X., Pyzik, R., Yong, A., Striker, G. E. and Vlassara, H. (2010). Advanced glycation endproducts in foods and a practical guide to their reduction in the diet. *Journal of the American Dietetic Association,* **110,** 911-916.

Venkatraman, J., Aggarwal, K. and Balaram, P. (2001). Helical peptide models for protein glycation: proximity effects in catalysis of the Amadori rearrangement. *Chemistry and Biology,* **8,** 611-625.

Vestweber, D. (2007). Endothelial cell contacts in inflammation and angiogenesis. *International Congress Series,* **1302,** 17-25.

Vinik, A. (2011). The question is, my dear watson, why did the dog not bark?: the joslin 50-year medalist study. *Diabetes Care,* **34,** 1060-1063.

Virdi, J., Sivakami, S., Shahani, S., Suthar, A. C., Banavalikar, M. M. and Biyani, M. K. (2003). Antihyperglycemic effects of three extracts from *Momordica charantia*. *Journal of Ethnopharmacology,* **88,** 107-111.

Vlassara, H. and Palace, M. R. (2002). Diabetes and advanced glycation endproducts. *Journal of Internal Medicine,* **251,** 87-101.

Vlassara, H., Brownlee, M. & Cerami, A. (1988) Specific macrophage receptor activity for advanced glycosylation end products inversely correlates with insulin levels *in vivo*. *Diabetes*, **37**, 456-461.

Wada, R. and Yagihashi, S. (2005). Role of advanced glycation endproducts and their receptors in development of diabetic neuropathy. *Annals of the New York Academy of Sciences,* **1043,** 598-604.

Waheed, A., Miana, G. A. and Ahmad, S. I. (2006). Clinical investigation of hypoglycemic effect of seeds of Azadirachta-inidca in type-2 (NIDDM) diabetes mellitus. *Pakistan journal of pharmaceutical sciences,* **19,** 322-325.

Wang, W.-q., Bao, Y.-h. and Chen, Y. (2013). Characteristics and antioxidant activity of water-soluble Maillard reaction products from interactions in a whey protein isolate and sugars system. *Food Chemistry,* **139,** 355-361.

Wautier, J. L. & Schmidt, A. M. (2004) Protein glycation: a firm link to endothelial cell dysfunction. *Circulation Research*, **95**, 233-238.

WHO (2007) The World Health Organization 2007. Diabetes Programme: facts and figures [on line]. Accessed 25 April 2014.

Win, M. T., Yamamoto, Y., Munesue, S., Saito, H., Han, D., Motoyoshi, S., Kamal, T., Ohara, T., Watanabe, T. & Yamamoto, H. (2012). Regulation of RAGE for attenuating progression of diabetic vascular complications. *Experimental Diabetes Research,* **2012,** 1-8.

Wolf, G. (2004). New insights into the pathophysiology of diabetic nephropathy: from haemodynamics to molecular pathology. *European Journal of Clinical Investigation,* **34,** 785-96.

Wolff, S. P. and Dean, R. T. (1987). Glucose autoxidation and protein modification. The potential role of 'autoxidative glycosylation' in diabetes. *Biochemical Journal,* **245,** 243-50.

Wu, J.-W., Hsieh, C.-L., Wang, H.-Y. and Chen, H.-Y. (2009). Inhibitory effects of guava (Psidium guajava L.) leaf extracts and its active compounds on the glycation process of protein. *Food Chemistry,* **113,** 78-84.

Xie, C., Liu, N., Long, J., Tang, C., Li, J., Huo, L., Wang, X., Chen, P. and Liang, S. (2011). Blue native/SDS-PAGE combined with iTRAQ analysis reveals advanced glycation end-product-induced changes of synaptosome proteins in C57 BL/6 mice. *Electrophoresis,* **32,** 2194-205.

Xu, B., Chibber, R., Ruggiero, D., Kohner, E., Ritter, J. & Ferro, A. (2003) Impairment of vascular endothelial nitric oxide synthase activity by advanced glycation end products. *Federation of American Societies for Experimental Biology*, **17**, 1289-1291.

Yamagishi, S., Fukami, K., Ueda, S. and Okuda, S. (2007). Molecular mechanisms of diabetic nephropathy and its therapeutic intervention. *Current Drug Targets,* **8,** 952-959.

Yamagishi, S., Nakamura, K. and Imaizumi, T. (2005). Advanced glycation end products (AGEs) and diabetic vascular complications. *current diabetes reviews,* **1,** 93-106.

Yamagishi, S.-i. (2011). Role of advanced glycation endproducts (AGEs) and receptor for AGEs (RAGE) in vascular damage in diabetes. *Experimental gerontology,* **46,** 217-224.

Yamaguchi, F., Ariga, T., Yoshimura, Y. & Nakazawa, H. (2000) Antioxidative and anti-glycation activity of garcinol from Garcinia indica fruit rind. *Journal of Agricultural and Food Chemistry,* **48**, 180-185.

Yaylayan, V. A., Harty-Majors, S. & Ismail, A. A. (1999). Monitoring carbonyl-amine reaction and enolization of 1-hydroxy-2-propanone (Acetol) by FTIR spectroscopy. *Journal of Agricultural and Food Chemistry*, **47**, 2335-2340.

Yaylayan, V. A., Huyghues-Despointes, A. and Feather, M. S. (1994). Chemistry of Amadori rearrangement products: Analysis, synthesis, kinetics, reactions, and spectroscopic properties. *Critical Reviews in Food Science and Nutrition,* **34,** 321-369.

Yokozawa, T. & Nakagawa, T. (2004) Inhibitory effects of Luobuma tea and its components against glucose-mediated protein damage. *Food and Chemical Toxicology,* **42**, 975-981.

Young C.D., Lewis A.S., Rudolph M.C., Ruehle M.D., Jackman M.R., Yun U.J., Ilkun O., Pereira R., Abel E.D., Anderson S.M. (2011). Modulation of glucose transporter 1 (GLUT1) expression levels alters mouse mammary tumor cell growth in vitro and in vivo. *PloS One,* **6,** e23205

Yuwai, K. E., Rao, K. S., Kaluwin, C., Jones, G. P. and Rivett, D. E. (1991). Chemical composition of *Momordica charantia L*. fruits. *Journal of agricultural and food chemistry,* **39,** 1762-1763.

Zheng, F., He, C., Cai, W., Hattori, M., Steffes, M. and Vlassara, H. (2002). Prevention of diabetic nephropathy in mice by a diet low in glycoxidation products. *Diabetes/metabolism research and reviews,* **18,** 224-237.

Zochodne, D. W. (2007). Diabetes mellitus and the peripheral nervous system: manifestations and mechanisms. *Muscle ad Nerve,* **36,** 144-66.